Wegener Center
SCIENTIFIC REPORT
99 | 2023

Sensitivity and uncertainty analysis of hydro-climatic changes in south-east Alpine foreland catchments

Clara Hohmann

January 2023

Climate Change Graz
Field of Excellence
University of Graz

Wegener Center

UNI GRAZ

The Wegener Center for Climate and Global Change is an interdisciplinary, internationally recognized research and graduate education institute of the University of Graz that is pooling the University's expertise in Climate, Environmental and Global Change. It brings together research teams and scientists from fields such as geophysics and climate physics, meteorology, economics, geography, and social sciences. At the same time, close links are maintained and further developed with many national and international cooperation partners. The research interests range from monitoring, analysis, and modeling of climate and environmental change to the investigation of climate change impacts and the analysis of the human dimensions of these changes related to mitigation, adaptation, and loss & damage. More information at **www.wegcenter.at**.



Alfred Wegener (1880 – 1930), after whom the Wegener Center is named, was founding holder of the University of Graz Geophysics Chair (1924 – 1930). In his work in the fields of geophysics, meteorology, and climatology he was a brilliant scientist and scholar, thinking and acting in an interdisciplinary way, far ahead of his time with this style. The way of his ground-breaking research on continental drift is a shining role model. His sketch on the relations of continents based on traces of an ice age about 300 million years ago (left) as basis for the Wegener Center Logo is thus a continuous encouragement to explore equally innovative ways: paths emerge in that we walk them (motto of the Wegener Center).

This report is the result of a PhD thesis work completed in 2021.

SR 99 | 2023 Sensitivity and uncertainty analysis of hydro-climatic changes in south-east Alpine foreland catchments
ISBN 978-3-9504700-8-6 January 2023

Suggested citation:
Hohmann, C. (2023), Sensitivity and uncertainty analysis of hydro-climatic changes in south-east Alpine foreland catchments, Wegener Center Scientific Report 99-2023, Wegener Center Verlag, University of Graz, Austria, January 2023. ISBN 978-3-9504700-8-6

(c) 2023 Wegener Center Verlag, University of Graz, Austria
The usage of images, tables, or texts of this Scientific Report is permitted for non-commercial purposes if appropriate credit is given.
For any other purposes, please contact: wegcenter@uni-graz.at

Publishing institution:
Wegener Center for Climate and Global Change, University of Graz
Brandhofgasse 5, 8010 Graz, www.wegcenter.at

Contact: Dr. Clara Hohmann
clara.hohmann@gmx.de

Clara HOHMANN

Sensitivity and uncertainty analysis of hydro-climatic changes in south-east Alpine foreland catchments

PhD thesis

to obtain the academic degree
Doctor of Natural Sciences

submitted to the
Faculty of Environmental and Regional Sciences and Education
University of Graz

First referee: Univ.-Prof. Dr. Gottfried Kirchengast
Wegener Center for Climate and Global Change
and Institute of Physics, University of Graz, Austria

Second referee: Univ.-Prof. Dr. Kerstin Stahl
Institute of Hydrology, University of Freiburg, Germany

Third referee: Univ.-Prof. Dr. Steffen Birk
Institute of Earth Sciences, University of Graz, Austria

2021

Supervisor

Univ.-Prof. Dr. Gottfried Kirchengast
University of Graz, Austria

Co-supervisor

Univ.-Prof. Dr. Steffen Birk
University of Graz, Austria

Acknowledgements

"All models are wrong, but some are useful"
George Box

This PhD thesis would not have been possible without the support from many different persons. I am sorry that it is impossible to name all those personally who helped to make this PhD journey successful and enjoyable. My sincere gratitude goes out to all of you!

My sincerest thanks go to my supervisor Gottfried Kirchengast who supported me during all stages of this work. He was always reliable and supportive, and created an encouraging work environment by providing both his support but also by giving me the freedom to work independently. My special thanks also go to my co-supervisor Steffen Birk. On my PhD journey, his scientific knowledge and networks provided great support. I gratefully acknowledge my colleagues from my research stay at TUM in Germany for the fruitful collaboration.

For their support with the WaSiM model, I wanted to thank many persons. The developer Jörg Schulla, Markus Casper who gave me a great introduction, the TUM team and especially Wolfgang Rieger who provided their support and user knowledge, and, last but not least, Stefanie Peßenteiner, my close colleague in the WaSiM jungle at the University of Graz.

I sincerely thank my co-authors for their great support during the whole publication process. I also acknowledge the whole Wegener Center team, and especially Matt and Jürgen for their support. Finally, warm thanks go out to my great office mates (Katha, Lukas, Josef, Hallgeir and Christoph), who made coming into my office every morning much more fun.

I want to thank the whole DK team for demonstrating the true spirit of interdisciplinary work. Thanks to the DK faculty, the DK students and the DK support team, and here especially to the faithful soul Regina.

I also sincerely thank the hydro community. They lent sympathetic ears and their support at the conferences, workshops, and, furthermore, helped me take a very important step in my scientific career.

I am grateful to the Austrian Science Fund (FWF) for giving this international and interdisciplinary group the opportunity to conduct cuttingedge research on climate change (W 1256). I also acknowledge the offices of the Styrian and Burgenland government, the Austrian Hydrographic Service, and the ZAMG for providing data. The partners of the WegenerNet climate station network are thanked for setting up and maintaining this unique data resource.

Last but not least, I thank my family. This was a very special time of my life and, therefore, a huge thank you goes to Vincent. Without you, this work would not have been possible for a hundred reasons. I also wanted to thank my two children, Emil and Finn, who were/are relaxed babies and kids, which made my scientific work possible. They joined me at conferences and gave me time to write my publications. A special thank you goes out to my parents for their devoted and continuous support in all situations.

Abstract

Research on catchment hydrology related to climate change improves the understanding of changes and their impacts on environment and society. Under climate change, extreme events like heavy precipitation events and droughts tend to increase in frequency and intensity. I studied sensitivities and uncertainties of hydro-climatic changes in response to runoff and other water-balance quantities with the hydrological model WaSiM. The thesis work involved: 1) Simulating hydrological responses to changes in climate, land use, and water management (low-flow focus); 2) examining the influence of precipitation station density and interpolation schemes on runoff during heavy rainfall events; and 3) assessing the value of high-resolution climate data sets (ÖKS15) in hydrological impact studies.

The prealpine Raab catchment in southeastern Austria served as the main focal area (complemented by an alpine catchment). The area is well-known for heavy precipitation events and summer dryness, and has a good data availability.

The comprehensive sensitivity and uncertainty analyses yielded the following results: The Raab catchment will be vulnerable to summer dryness in the future. Non-climatic drivers have lower impacts on the water balance than climate drivers, but can counteract other changes. The reliable precipitation station density depends strongly on the event, catchment, and station distribution in heavy precipitation events. The evaluated Austrian ÖKS15 high-resolution climate data sets are suitable for hydrological impact studies with some limitations.

Overall, I could clearly identify how uncertainty affects assessments of climate change and precipitation events. Climate change is a key driver in hydrological changes, but other non-climatic drivers (i.e., land use or water management changes) should also be analyzed. Extreme precipitation events should be studied together with runoff to evaluate the impacts of such events on the environment and society more effectively.

Zusammenfassung

Wissenschaftliche Forschung im Bereich von Hydrologie und Klimawandel trägt zu einem besseren Verständnis von möglichen Veränderungen und deren Einfluss auf Umwelt und Gesellschaft bei. Extremereignisse wie Starkregen und Dürren nehmen im Zuge des Klimawandel tendenziell an Häufigkeit und Intensität zu. Die Sensitivitäten und Unsicherheiten von hydro-klimatischen Veränderungen des Abflusses und anderen Wasserbilanzgliedern untersuchte ich mit Hilfe des hydrologischen Modells WaSiM. Die Schwerpunkte dieser Arbeit wurden gelegt auf: 1) Simulation von Klima-, Landnutzungs- und Wassermanagementänderungen bei Niedrigwasser; 2) Einfluss von Niederschlagsstationsdichte und -Interpolationsverfahren auf den Abfluss bei Starkregen; und 3) der Wert hochaufgelöster Klimadatensätze (ÖKS15) für hydrologische Studien.

Schwerpunktregion ist das voralpine Raab Einzugsgebiet im Südosten Österreichs (ergänzt durch ein alpines Einzugsgebiet). Diese Region ist bekannt für Starkregen und sommerliche Trockenheit und bietet eine gute Datenlage. Die Ergebnisse dieser Sensitivitäts- und Unsicherheitsanalysen beinhalten, dass das Raabtal in Zukunft besonders Trockenheitsgefährdet ist. Auch wenn nichtklimatische Faktoren einen geringeren Einfluss auf die Wasserbilanz haben, sind diese Faktoren auf Grund von Wechselwirkungen nicht zu vernachlässigen. Die notwendige Niederschlagsstationsdichte ist bei Starkregenereignissen stark ereignis-, einzugsgebiets- und stationsabhängig. Die ausgewerteten ÖKS15 Klimadatensätze sind für hydrologische Impaktstudien mit einigen Einschränkungen geeignet.

Insgesamt wurde die Bedeutung von Unsicherheiten in Bezug auf Klimawandel und Niederschlag deutlich. Im Kontext der Hydrologie sollten die klimatischen und nicht klimatischen Treiber (u.a. Landnutzungsänderungen) des Klimawandels zusammen analysiert werden. Extremniederschläge sollten zusammen mit Abflüssen untersucht werden, um deren Auswirkungen auf Umwelt und Gesellschaft besser einschätzen zu können.

Research articles and author contributions

Hohmann, C., G. Kirchengast, and S. Birk (2018), Alpine foreland running drier? Sensitivity of a drought vulnerable catchment to changes in climate, land use, and water management, *Climatic Change*, 147, 179–193, DOI:10.1007/s10584-017-2121-y.

Author contributions: CH acquired the data, conducted the modeling and analysis, produced the results, and wrote the first draft of the paper, mainly advised on all aspects of this work by GK; GK and SB provided the initial conception and jointly contributed while interacting with CH to the study design, the results, discussions, and the writing of the paper. All authors helped shape the analysis and manuscript revisions and gave their final approval of the paper to be published.

Hohmann, C., G. Kirchengast, S. O, W. Rieger, and U. Foelsche (2021), Small catchment runoff sensitivity to station density and spatial interpolation: Hydrological modeling of heavy rainfall using a dense rain gauge network, *Water, 13*, 1381, DOI:10.3390/w13101381.

Author contributions: All authors designed the study, with primary contributions by CH and GK. CH collected the data, performed the modeling and most of the analyses, created the figures, and wrote the first draft of the manuscript. GK provided guidance and advice on all aspects of the study and significantly contributed to the figure design and the text. SO contributed to the data collection, precipitation data analysis, and figure creation. WR supported the model calibration and validation. All authors helped to shape the research and analysis; they provided critical feedback and contributions to the text until its submission and during the review. All authors have read and agreed to the published version of the manuscript.

Peßenteiner, S., C. Hohmann, G. Kirchengast, and W. Schöner (2021), High-resolution climate datasets in hydrological impact studies: Assessing their value in alpine and prealpine catchments in southeastern Austria, *Journal of Hydrology: Regional Studies*, 38, 100962, DOI:10.1016/j.ejrh.2021.100962.

Author contributions: SP: Conceptualization, methodology, data curation, software, validation, formal analysis, writing – original draft, writing – review and editing, visualization; CH: Software, validation, visualization, writing – review and editing; GK: Writing – review and editing, supervision, funding acquisition; WS: Writing – review and editing, supervision, project administration, funding acquisition.

Contents

List of Abbreviations xv

1 Introduction 1

2 Research challenges 5
2.1 Climate change sensitivity 7
2.1.1 Comparison of scenario-neutral and scenario-based approaches 7
2.1.2 Drought vulnerability 10
2.2 Precipitation station density and interpolation 11
2.2.1 Precipitation measurements and interpolation 11
2.2.2 Runoff sensitivity 13
2.3 Evaluation of high-resolution climate data sets 14
2.3.1 Scenario-based approach 14
2.3.2 High-resolution climate data sets 15

3 Data and methods 19
3.1 Study areas 19
3.1.1 The Raab catchment 19
3.1.2 The Wölzerbach catchment 21
3.2 Input data 22
3.2.1 Hydro-meteorological data sets 22
3.2.2 Elevation models, land use, and soil data sets 26
3.3 Hydrological model 29
3.3.1 Model characteristics and setup 29
3.3.2 Input data preprocessing 33
3.3.3 Model calibration and validation 33
3.4 Choice of methods 38

4 Sensitivity and uncertainty analysis of hydro-climatic changes 41
4.1 Research Article 1: Sensitivity of a drought vulnerable catchment to changes in climate, land use, and water management 41
4.2 Research Article 2: Small catchment runoff sensitivity to station density and spatial interpolation 67
4.3 Research Article 3: High-resolution climate data sets in hydrological impact studies 97

5 Summary and conclusions 125
5.1 Main results of the three research articles 125
5.2 Synthesis, conclusions, and prospects 129

List of Figures 134

List of Tables 136

References 137

List of Abbreviations

AHYD	Hydrographischer Dienst Österreich/National Austrian Hydrographic Service
DEM	Digital Elevation Model
EURO-CORDEX	Regional climate model simulations for the European domain
GCM	General Circulation Model
HYDROBOD	Soil and hydrological characteristics with a 100 m x 100 m grid resolution
IAHS	International Association of Hydrological Science
IDW	Inverse Distance Weighting
KGE	Kling-Gupta Efficiency
LBgld	State government offices of the Provinces of Burgenland, Austria
LStmk	State government offices of the Provinces of Styria, Austria
NSE	Nash-Sutcliffe Efficiency
ÖKS15	Austrian high-resolution climate data sets
PBIAS	Percent Bias
RCM	Regional Climate Model
SCE-UA	Shuffled Complex Evolution optimization algorithm developed at the University of Arizona
TANALYS	Topographic Analysis Tool
TP	Thiessen Polygons
WaSiM	Water balance and Simulation Model
Wegener Center	Wegener Center for Climate and Global Change, University of Graz, Austria
WEGN	WegenerNet, a high-resolution climate station network
ZAMG	Zentralanstalt für Meteorologie und Klimatologie/ National Austrian Weather Service

1 Introduction

The hydrological cycle is strongly influenced by climate change. Since the changes might seriously affect society, infrastructure, natural resources, and well being, scientists, water managers, and decision-makers are interested in the hydrological changes that could occur in the future. Knowledge of these changes enables them to deepen their knowledge and set up adaptation strategies.

The hydrological changes can occur in many directions, ranging from more heavy precipitation events and more extreme floods to more droughts and longer low flow periods. If and which extreme events might occur more frequently and/or more intensely differs regionally. An increase in the frequency and intensity of heavy precipitation events over land areas has been recognized by the *IPCC* (2021) with a high confidence. An increase in the intensity and/or duration of droughts is also strongly region-dependent, but in the Mediterranean, southern Europe, and other regions, an increase is likely (*IPCC*, 2021). The scale and focus area are very important, since effects can differ on the regional and local scales as compared to on the global scale.

Turning our attention to Austria, even though this country covers a much smaller scale than the forty-five IPCC land regions assessed for treat heavy precipitation and drought extremes, the regional differences are strongly pronounced (*APCC*, 2014). Especially the more mountainous alpine region is substantially different from the forelands, and here one must differentiate between the northern and southern alpine forelands. The latter is more strongly influenced by the Mediterranean climate conditions. In this area, a decrease in runoff is expected, and especially in the summer months (*APCC*, 2014).

Regarding the relevance of uncertainty, *Blöschl and Montanari* (2010) asked the somewhat provocative question of whether conducting a climate change impact analysis is like throwing the dice. They argue that obtaining a process understanding is more important than simulating future conditions with climate simulations as an input in hydrological models. Although much progress has been made since

then (*IPCC*, 2021), the question about uncertainties is still a fundamental question, especially regarding future projections. A variety of sources of uncertainty are found in the process of climate modeling (e.g., *Knutti and Sedláček*, 2013; *Beevers et al.*, 2020; *Wang et al.*, 2020), downscaling, and bias correction (e.g., *Maraun and Widmann*, 2018; *Maraun et al.*, 2010; *Chen et al.*, 2011; *Sharma et al.*, 2018), hydrological modeling (e.g., *Balin et al.*, 2010; *Gädeke et al.*, 2014; *Joseph et al.*, 2018; *Beevers et al.*, 2020), spatial interpolation of input data (e.g., *Goodrich et al.*, 1995; *Huang et al.*, 2019; *O and Foelsche*, 2019), and observational uncertainty (e.g., *Kidd and Huffman*, 2011; *McMillan*, 2012; *Kotlarski et al.*, 2017). The uncertainty aspects of the whole model chain have also been studied broadly (e.g., *Wilby and Harris*, 2006; *Bosshard et al.*, 2013; *Gädeke et al.*, 2014; *Hattermann et al.*, 2018). These studies often identified larger amounts of uncertainty in the climate modeling part as compared to the hydrological model uncertainty.

When studying aspects of uncertainty and sensitivity in hydrological changes in the context of climate change, the southeastern alpine foreland of Austria offers an especially interesting location. Here, a strong temperature increase was measured in the last decades (*Kabas et al.*, 2011), and the region is vulnerable to extreme events like heavy convective rainfall (*Schroeer and Kirchengast*, 2018) and droughts (*Laaha et al.*, 2016). In addition, the lower part of the Austrian Raab catchment area is especially well-equipped with the highly dense meteorological station network, the Wegener Net (WEGN) (*Kirchengast et al.*, 2014). Therefore, this region was selected as the focus region for this thesis to study sensitivities and uncertainties in the context of climate, hydrology and environmental changes. A complementary small scale alpine catchment, the Wölzerbach, was studied for the high-resolution climate data sets analysis. We used the process-based Water balance and Simulation Model (WaSiM) (*Schulla*, 1997) to conduct the simulations. It appears that this versatile model is suitable for studying hydrological and environmental changes in southeastern Austria under climate change conditions.

The thesis is structured as follows: Chapter 2 describes the research challenges with reference to a state-of-the-art literature review and the derived research questions. In Chapter 3, the data and methods, as well as the study regions are described, the data used are explained in detail, the hydrological modeling is explained, and the main points of the study designs are summarized. The three research articles that constitute the core part of this thesis are provided in Chapter 4. These include:

Research Article 1 *Alpine foreland running drier? Sensitivity of a drought vulnerable catchment to changes in climate, land use, and water management*,

Research Article 2 *Small catchment runoff sensitivity to station density and spatial interpolation: Hydrological modeling of heavy rainfall using a dense rain gauge network*, and

Research Article 3 *High-resolution climate data sets in hydrological impact studies: Assessing their value in alpine and prealpine catchments in southeastern Austria*.

The thesis ends with a summary and discussions part that summarizes the main results of the three research articles, and the provides synthesis conclusions and prospects of the thesis in Chapter 5.

2 Research challenges

Climate change presents an increasing challenge for our society. Due to temperature increases, many places in the world might get hotter and drier (*IPCC*, 2021). Extreme events like heavy precipitation and droughts will also shift in magnitude and frequency worldwide. All of these changes have huge impacts on the hydrological cycle (*IPCC*, 2021). Therefore, studying the hydrological response to such changes is becoming steadily more important. The International Association of Hydrological Science (IAHS) named its science decade from 2013 to 2022 "Panta Rhei-Everything Flows" and have placed a focus on changes in hydrology and society (*Montanari et al.*, 2013; *McMillan et al.*, 2016). They argue that there is an urgent need to understand and predict the interactions between the society and water. It is also important to support the sustainable use of water resources under climate and environmental change conditions (*McMillan et al.*, 2016). *Montanari et al.* (2013) also mentioned the importance of taking interdisciplinary approaches when carrying out scientific research in the future.

A new initiative on the 23 unsolved problems in hydrology (*Blöschl et al.*, 2019) build on this IAHS initiative to update the current topics in the hydrological community. We developed this paper based on a community initiative to identify the major unsolved scientific problems in the hydrological area. The 23 unsolved problems are very broad, as is the hydrological community. The main research challenges presented in this thesis are also covered by these problems.

Since the topic of climate change is a current aspect in the field of hydrology and water management, *Blöschl et al.* (2019) addressed the climate change aspect from different angles. On the one hand, we asked if the hydrological cycle is regionally affected by climate and environmental changes, which is Question 1 in *Blöschl et al.* (2019). This problem corresponds to Research Articles 1 and 2 presented in this thesis. On the other hand, we addressed climate change issues and focused on hydrological modeling (Question 19), which correspond to all three Research Articles presented in this thesis. The aspect of land cover changes and

their impact on water and energy fluxes is also mentioned in Question 4 of *Blöschl et al.* (2019). This problem is addressed in this thesis in Research Article 1. Since many aspects in hydrology are studied in a modeling framework, the model uncertainty also plays an important role. Here, the model input uncertainty is one specific aspect of the 23 unsolved problem in hydrology (Question 20), which is addressed in this thesis in Research Article 2.

This thesis contributes to the above-mentioned unsolved problems in hydrology by contributing hydrological modeling studies on the catchment scale and placing a focus on the different sensitivity and uncertainty aspects of hydro-climatic changes. One focus was placed on low flow and the sensitivity of runoff and evapotranspiration to changes in climate, land use, and water management (Research Article 1). Another focus was directed toward the influence of precipitation station density and interpolation methods used to study runoff/floods of heavy precipitation events (Research Article 2). And, last, a focus was placed on the value of high-resolution climate data sets in hydrological impact studies (Research Article 3).

With these foci, the following main research questions were addressed and its corresponding research challenges, as described in the following sections.

1. How do summer runoff and evapotranspiration respond to changes in a warming climate? This research question is addressed in Research Article 1, where future climatic changes are implemented by a scenario-neutral approach to the drought-vulnerable Raab catchment.

2. How many stations are needed to reliably model runoff in small catchments under heavy precipitation events? This research question is addressed in Research Article 2 by conducting sensitivity and uncertainty analyses related to precipitation station densities and interpolation methods.

3. How well do the Austrian ÖKS15 high-resolution climate data sets perform in hydrological impact studies? This research question is addressed in Research Article 3 in the context of a scenario-based approach and by estimating the high-resolution climate data sets for Austria (ÖKS15).

2.1 Climate change sensitivity of a drought-vulnerable catchment

In Research Article 1, *Hohmann et al.* (2018) we studied the climate and environmental changes to runoff in a drought-vulnerable catchment and answered the first main research question (see above) described in this thesis. In the following section, the scenario-neutral approach is described with reference to recent literature and compared to the scenario-based approaches which are described in Chapter 2.3 in more detail. The aspect of the drought vulnerability of the research area will also be explained in the following section.

2.1.1 Comparison of scenario-neutral and scenario-based approaches

To deal with climate change in the context of hydrology, different approaches like hydrological impact studies are possible. On the one hand, the scenario-based approach is often used, whereby climate projections are downscaled to the focus area. Here, a model chain of future greenhouse gas concentrations which require the use of General Circulation Models (GCMs) are then statistically or dynamically downscaled to Regional Climate Models (RCMs) and sometimes also bias-corrected. These scenarios with possible future options are then used as an input in hydrological models. This approach is also called the "scenario-led" or "top-down" approach.

On the other hand, the "scenario-neutral" approach can be used, which was described in the publication by *Prudhomme et al.* (2010). This approach is based on a vulnerability or sensitivity test like a "stress test" used to detect changes in climate and to identify practical adaptation strategies (*Brown and Wilby*, 2012; *Nazemi and Wheater*, 2014). Here, the water system is in the spotlight, and the GCM projections provide information about possible options, but do not drive the analysis (*Brown and Wilby*, 2012). The same considerations are made when using approaches like the "bottom up" (*Wilby*, 2010; *Nazemi and Wheater*, 2014; *Singh et al.*, 2014), "vulnerability driven" (*Singh et al.*, 2014), "risk-based" (*Steinschneider et al.*, 2015), or "decision scaling" (*Brown and Wilby*, 2012) approaches.

For example, the potential future changes have been analyzed with this approaches in the context of low flow/droughts (*Weiß*, 2011; *Vormoor et al.*, 2017),

high flow/floods (*Prudhomme et al.*, 2010; *Weiß*, 2011; *Vormoor et al.*, 2017; *Kim et al.*, 2018; *Keller et al.*, 2019), flood damage (*Steinschneider et al.*, 2015), and water resources (*Brown and Wilby*, 2012). A further description, including pro and contra arguments for using the scenario-neutral and the scenario led approaches, is given in Table 2.1. The scenario-neutral approach should be seen as complementary to the scenario-based one.

Table 2.1: Comparison of the scenario-neutral and the scenario-based approaches based on a literature review (*Prudhomme et al.*, 2010; *Maraun et al.*, 2010; *Beven*, 2011; *Brown et al.*, 2011; *Mote et al.*, 2011; *Brown and Wilby*, 2012; *Pielke and Wilby*, 2012; *Nazemi and Wheater*, 2014; *Singh et al.*, 2014; *Vormoor et al.*, 2017; *Nathan et al.*, 2019)

	Scenario-neutral approach	**Scenario-based approach**
Focus question	"Is the climate that favors action A more or less likely than the climate that favors action B?" (*Brown and Wilby*, 2012)	"What will the future climate be?" (*Brown and Wilby*, 2012)
Method	1) identification of climate hazards/ thresholds/ management objectives 2) forcing variables and modeling 3) identify vulnerability 4) climate-informed risk estimation/ analysis behavior	1) choose scenarios for future greenhouse gas concentration to force GCMs 2) downscale GCMs to focus region 3) hydrological (impact) model 4) simulate system/ adaptation response
Pro arguments	– focus to the users' needs/ stakeholders' needs – identify practical adaptation strategies – better understand the system – test the robustness of adaption strategies – avoid uncertainty initiated from GCMs – flexible towards new climate data sets – flexible toward new time horizons – flexible towards evolving societal risk attribution	– most widely used strategy – plenty of literature available – climate information for the next 100 years – comprehensive information on possible futures – multi-ensemble scenarios of the future – variability of climate change impact and adaptation under different possible futures – valuable database to study scenario output data
Contra arguments	– methodologically more limited – probability of occurrence is unknown – risk cannot be quantified – challenging to chose adequate parameters which are both sensitive model parameters and sensitive under climate change conditions – challenging to choose a suitable perturbation method for modifying the climate parameters	– computationally intensive – changes require to re-run the whole model chain – large uncertainties sum up in the model cascade – uncertainty in greenhouse gas emissions and uncertain response of climate to these emissions – downscaling is based on assumptions which are not fully justified

2.1.2 Drought vulnerability

The region of the southern alpine foreland of Austria is especially vulnerable to droughts. As seen in *Laaha et al.* (2016), a decreasing trend in low flow already exist in this area. With a slight decrease in precipitation and a strong temperature increase as described in *Kabas et al.* (2011), droughts may occur more frequently in the future (*Cook et al.*, 2018). The human impact also has to be taken into account by analyzing drought-vulnerable regions (*Van Loon et al.*, 2016; *AghaKouchak et al.*, 2021). Many droughts worldwide are largely influenced by human activities, and the natural climate variability is not the only driver (*AghaKouchak et al.*, 2021). Beside the human-induced climate change, urbanization, deforestation, and the extensive use of groundwater and surface water also play important roles (*Schewe et al.*, 2014; *Van Loon et al.*, 2016; *Yuan et al.*, 2017; *Ashraf et al.*, 2019; *AghaKouchak et al.*, 2021).

Therefore, in addition to climate drivers like temperature and precipitation, non-climatic drivers like land use and water management also might change in the future and need to be further analyzed. Many studies have analyzed the influence of land use changes on the water cycle (e.g., *Gupta et al.*, 2015; *Yira et al.*, 2016). In our drought-vulnerable study area, no drastic land use changes have been visible over the last decades. Nevertheless, possible changes in the future might include an increase in sealed areas, due to population growth and the resulting increase in the size of cities and populated areas. The vegetation might also response to the drier conditions in the area, making it more challenging to carry out agricultural activities.

These thoughts led to the development of the following specific research questions which are addressed in Research Article 1.

How does summer runoff and evapotranspiration respond to different changes (drivers) and what are the characteristics of these driver-response relationships?

How do the anthropogenic non-climatic effects, and especially changes in land use and irrigation, interact with climate change in a drought-vulnerable catchment?

2.2 Runoff sensitivity of small catchments to precipitation station density and spatial interpolation

The importance of precipitation to runoff response in the catchment is clear; this is demonstrated in Research Article 1. Therefore, especially in hydrological modeling the precipitation input is the key to reliable model hydrological processes (*Bárdossy and Das*, 2008; *Price et al.*, 2014; *Zeng et al.*, 2018; *Gilewski and Nawalany*, 2018). When the measurement uncertainty increases, the model input uncertainty also increases. Therefore, it is especially challenging to model heavy precipitation events where the importance of spatial and temporal heterogeneity increases (*St-Hilaire et al.*, 2003; *Maier et al.*, 2020).

The study region of the southern alpine forelands is well-known for its heavy convective precipitation events (*Schroeer and Kirchengast*, 2018). Under climate change, these events might even intensify (*Kharin et al.*, 2007; *Chen et al.*, 2012; *Fischer and Knutti*, 2016; *Prein et al.*, 2016; *IPCC*, 2021). Hence, it is especially important to study the sensitivity of precipitation station density in combination with precipitation interpolation to runoff in this area. We developed a second main research question, which addresses the number of stations needed to reliable model runoff under heavy precipitation events. This question is answered in Research Article 2 *Hohmann et al.* (2021).

2.2.1 Precipitation measurements and interpolation

Different measurement strategies for precipitation data sets are known and encompass both direct and indirect measurements. A direct measurement technique is a point measurement, whereby a gauge is used to measure the precipitation amount at one specific location (point). Many measurement uncertainties might exist, because of the gauge construction (e.g. wind-undercatch (*Sevruk et al.*, 2009; *Pollock et al.*, 2018)), placement, or limited spatial coverage (*Kidd and Huffman*, 2011; *McMillan et al.*, 2012; *Gilewski and Nawalany*, 2018).

On the other hand, weather radar provides information about the spatial distribution of the rain field, but cannot be used to measure the precipitation amount itself. This indirect measurement strategy can be used to measure the particle concentrations in the atmosphere with microwave energy that is backscattered, i.e. measuring the radar reflectivity (*Tetzlaff and Uhlenbrook*, 2005; *Kidd and Huffman*,

2011). This information is than converted into precipitation intensities. In this way, the drop size can be measured, but this depends on the precipitation regime, which might introduce errors. Other errors arise by the convention, oration of the beam (e.g. over-shooting), or false returns from ground objects (*Kidd and Huffman*, 2011). To obtain good precipitation information, radar measurements should be calibrated with ground-based station data (*Sun et al.*, 2000; *Tetzlaff and Uhlenbrook*, 2005).

Another indirect measurement are satellite-based precipitation measurements (*Tian and Peters-Lidard*, 2010; *Kirstetter et al.*, 2012; *O et al.*, 2017; *Lasser et al.*, 2019). These data sets provide precipitation data on the global scale with resolutions from around $2.5° \times 2.5°$ to $0.1° \times 0.1°$. This option is often used to make global scale estimates or when the ground-based data source with measurement stations or radar data is not dense or reliable enough.

Due to these aspects of uncertainty and the data availability, ground-based point measurements are still widely used in hydrological modeling (*Price et al.*, 2014; *Lopez et al.*, 2015; *Zeng et al.*, 2018). To cover the full spatial distribution of the precipitation event, such point measurements need to be interpolated in space. Here, another source of uncertainty exists (*Goodrich et al.*, 1995; *McMillan et al.*, 2012; *Huang et al.*, 2019; *O and Foelsche*, 2019).

Different interpolation methods are broadly studied in the context of catchment hydrology (*Zhang and Srinivasan*, 2009; *Ly et al.*, 2013; *Szcześniak and Piniewski*, 2015). The most common interpolation schemes are the Arithmetic Mean (*Andréassian et al.*, 2001; *Dong et al.*, 2005; *Huang et al.*, 2019), Thiessen polygons (TP) (*Kobold and Brilly*, 2006; *Meselhe et al.*, 2009; *Zeng et al.*, 2018), Inverse Distance Weighting (IDW) (*Verworn and Haberlandt*, 2011; *Schwarzak et al.*, 2015; *O and Foelsche*, 2019; *Breinl et al.*, 2020), and Kriging, with Ordinary Kriging (*St-Hilaire et al.*, 2003; *Verworn and Haberlandt*, 2011; *Breinl et al.*, 2020) or External Drift Kriging (*Bárdossy and Das*, 2008; *Verworn and Haberlandt*, 2011; *Xu et al.*, 2013).

The literature is ambiguous regarding the best interpolation method, and using more complex geostatistical methods like Kriging does not add much value, especially for dense station networks (*Dirks et al.*, 1998; *Goovaerts*, 2000; *Syed et al.*, 2003). The method choice depends on different aspects like data availability, topography, as well as the measurement station density, distribution, and reliability (*Lopez et al.*, 2015). Under heavy precipitation events the differences between the

interpolation methods are especially pronounced (*Szcześniak and Piniewski*, 2015). Hence, the selection of interpolation methods has to be made with due care.

2.2.2 Runoff sensitivity

In Research Article 2, we studied the influence of the interpolation scheme on the runoff response and addressed the following research question as one of the specific research questions discussed in this article:

How strongly does the interpolation scheme influence runoff results when the precipitation station density is the same?

Beside the importance of the choice of precipitation interpolation method, the influence of precipitation station density has also been broadly studied (*Obled et al.*, 1994; *Dong et al.*, 2005; *Bárdossy and Das*, 2008; *Meselhe et al.*, 2009; *Xu et al.*, 2013; *Zeng et al.*, 2018; *Huang et al.*, 2019). Previous researchers have mostly focused on the model performance. To find the appropriate number of precipitation stations and to study the influence of station density on model performance, *Dong et al.* (2005) and *Xu et al.* (2013) used a statistical approach and a lumped hydrological model in study areas of around $12\,000\,\mathrm{km}^2/20\,000\,\mathrm{km}^2$. *Huang et al.* (2019) also used a lumped hydrological model, but also a distributed hydrological model. They studied the sensitivity of runoff simulations to the temporal and spatial resolutions of rainfall data in four catchments (basin areas of $417\,\mathrm{km}^2$ to $1300\,\mathrm{km}^2$).

In addition to these large and mesoscale scale catchments, *Meselhe et al.* (2009) studied a small catchment (basin area of $12.4\,\mathrm{km}^2$) with a highly dense station network (30 rain gauges in that area). They used a conceptual and a physically based model to identify the impact of the spatial and temporal distribution of precipitation data on runoff simulations. All studies identified a threshold: The model performance does not significant increase above a specific station density.

Other studies have focused on data quality, such as the mean or extreme precipitation values, by analyzing the station density and interpolation (*Gervais et al.*, 2014; *Avila et al.*, 2015; *Herrera et al.*, 2018).

In Research Article 2, we took the next step and studied the sensitivity of station density and interpolation method to runoff, and especially to runoff peaks. For this, we use the very dense station network, WEGN (*Kirchengast et al.*, 2014). The presence of such dense and well-distributed precipitation station networks

are important for obtaining reliable precipitation information, a fact that has been mentioned by *Lopez et al.* (2015) and *Goovaerts* (2000). By taking this study approach, we answered the following specific research questions presented in Research Article 2:

How many precipitation stations do we need to reliably model runoff during heavy rainfall events over small catchments?

Since we particularly focused on small catchments, we added the research question:

Are there specific features of very small catchments of around $10\,\mathrm{km}^2$ *size to reliably model runoff under heavy rainfall events?*

2.3 Evaluation of high-resolution climate data sets for hydrological impact studies

In 2016, an ensemble of high-resolution national climate data sets for Austria (ÖKS15) was released at a resolution of $1\,\mathrm{km} \times 1\,\mathrm{km}$ grid cells and daily time steps (*Chimani et al.*, 2016). In Research Article 3, *Peßenteiner et al.* (2021) we answered the third main research question of how well these data sets perform in hydrological impact studies. In the following section, the scenario-based approach and the high-resolution Austrian climate data sets are introduced in detail.

2.3.1 Scenario-based approach

Stakeholders and the scientific community are interested to learn whether extreme events, such as floods, droughts, or landslides, will become more frequent in the future. In the scenario-based approach (see also Table 2.1), statistically or dynamically downscaled GCM data are used as input in impact studies. Dynamical downscaling indicates that a RCM is nested into a GCM to model a limited area of interest at a higher resolution (*Maraun et al.*, 2010). Statistical downscaling links the GCM output with regional or local conditions (*Bronstert et al.*, 2007). By combining the two approaches, it is possible to get downscaled information on the point scale, when the gridded RCM output is first statistically corrected (*Maraun et al.*, 2010). The model chain of GCM-RCM combined with bias correction is then used as an input in hydrological impact studies (i.e. *Willkofer et al.*, 2018;

Rössler et al., 2019; *Smiatek and Kunstmann*, 2019; *Pastén-Zapata et al.*, 2020).

This climate-hydrological modeling is still challenging (*Teutschbein and Seibert*, 2010; *Olsson et al.*, 2016; *Reszler et al.*, 2018; *Smiatek and Kunstmann*, 2019), even though the GCMs and RCMs are becoming much more detailed in terms of their temporal and spatial resolution. The RCM simulations now have a typical grid size of around 20 km to 50 km or even down to 5 km (*Maraun et al.*, 2010). One problem with the climate-hydrology model chains is that they poorly represent heavy, and especially convective precipitation events which occur on the sub-daily time scale (*Maraun et al.*, 2010). The spatial distribution of the rainfall fields is also not yet fully covered (*Maraun et al.*, 2010). *Liersch et al.* (2018) ask whether climate simulations are the right fuel to drive hydrological models. They argue that bias correction might deteriorate hydrological extremes, but improve the performance for average rainfall characteristics and for non-extreme discharge conditions (Q20 to Q80). They also suggest that some of the models should be excluded in the regional context.

Different methods to bias correct RCMs exist, ranging from simple scaling to more sophisticated approaches, such as linear scaling, local intensity scaling, power transformation, variance scaling, distribution transfer, the delta-change, quantile mapping, quantile delta mapping, and scaled distribution mapping (*Teutschbein and Seibert*, 2012; *Switanek et al.*, 2017). The bias correction should adjust the RCM (or GCM) output to the regional conditions with reference to observational data. *Hakala et al.* (2018) also mentioned the importance of bias correction. They suggested first ranking the GCM-RCM simulations according to their hydrological model performance and then performing the bias correction as a second step. In this context, we note that models that have shown good performance in the past, where observational data is available, may not necessarily perform robustly in future simulations (*Reifen and Toumi*, 2009; *Huang et al.*, 2015; *Mendlik and Gobiet*, 2016). Nevertheless, the scientific community and especially the stakeholders need robust information to manage water resources, such as offering flood risk protection or ensuring the availability of water.

2.3.2 High-resolution climate data sets

Some countries invest in high-resolution data sets for climate simulations which have been specifically adjusted for their country and regional characteristics. These data sets are used to support decision-makers and stakeholders as they develop

adaptation strategies (*Chimani et al.*, 2016; *Wong et al.*, 2016; *Rössler et al.*, 2019; *Kay et al.*, 2020). The data sets are downscaled and bias-corrected GCM-RCM simulations.

The Climate Scenarios for Switzerland (CH2018) are based on the initiative of RCM simulations for the European domain (EURO-CORDEX), as well as downscaled and bias-corrected with quantile mapping. These climate scenarios were evaluated by *Rössler et al.* (2019) in the context of hydrology for the Thur basin (prealpine catchment, area of 1700 km^2). The authors saw an added value of the new CH2018 data set as compared to the older version from 2011 regarding some points and especially for indices related to extreme weather events.

The UK released climate projections for the UK (UKCP18) on a 12 km × 12 km grid. *Kay et al.* (2020) also compared the new data set to an older version from 2009. *Kay* (2021) used the UKCP18 regional projections with a grid resolution of 12 km with a national-scale, grid-based hydrological model, including a bias correction for only the precipitation data. With this setup, a relatively good agreement between the observation data (1980 to 2010) and the simulations could be shown.

The data products for Norway are gridded 1 km × 1 km climate and hydrological projections (*Wong et al.*, 2016) which use an ensemble of ten EURO-CORDEX GCM-RCM simulations. The bias-correction was performed with empirical quantile mapping. The data set is available from 1971 to 2100. These data where directly used as an input for the hydrological model HBV to generate time series for different hydrological components on a daily basis (*Wong et al.*, 2016).

In Austria, the ensemble of the ÖKS15 data sets (*Chimani et al.*, 2016) is also based on the EURO-CORDEX simulations (12.5 km × 12.5 km) (*Jacob et al.*, 2014), and downscaled and bias-corrected with Scaled Distribution Mapping to create a 1 km × 1 km grid for Austria (*Switanek et al.*, 2017). The Research Article 3 presented in this thesis provides an evaluation of these data in the hydrological context.

Even though the ÖKS15 data sets were released 2016, their usability for hydrological impact studies was not assessed until the study described in Research Article 3 in this thesis. We evaluated the ÖKS15 data sets in combination with the raw RCM simulations, gridded data sets, and station data in a hydrological modeling framework. The study was carried out to assess the value of the ÖKS15 high-resolution climate data sets for hydrological impact studies. A strong focus

was placed on the strength, peculiarities, and potential pitfalls of using such data sets in the context of hydrological impact studies. The study addresses the following specific research questions:

How well do the gridded high-resolution data sets of temperature and precipitation agree with observations at station (gridpoint) scale and also with WaSiM-interpolated observations at subcatchment scale?

How well do long-term statistics of the ÖKS15 temperature and precipitation data sets and related hydro-climatic indicators agree with observations at station (gridpoint) scale and at subcatchment scale?

What is the impact of differences in the various input data sets on the modeled hydrological runoff and how well do modeled long-term statistics runoff agree, for the different input data, to runoff observations?

3 Data and methods

3.1 Study areas

The study areas, which include the prealpine Raab catchment and alpine Wölzerbach catchment, are located in southeast Austria, in the province of Styria (Figure 3.1). This region is located in the mid-latitudes. It falls within the transition zone between the Mediterranean and the Alpine climate zones. This zone is characterized by weather patterns and precipitation, with cyclones approaching from the west/north-west and south. The region is also affected by heavy convective precipitation events, especially during the summer months (*Seibert et al.*, 2007). According to the Köppen climate classification, Styria is mainly classified as Dfb, the warm-summer humid continental climate class.

The main study area described in this thesis is the mesoscale, prealpine Raab catchment area, with a specific focus placed on the lower part of the catchment. For comparison and additional information, the small-scale alpine Wölzerbach catchment area was also included in the analysis of the high-resolution climate data sets.

3.1.1 The Raab catchment

The Raab is a typical example of an alpine foreland river occurring at the mid-latitudes. The source of the river is located in the "Passailer" Alps in Styria, Austria, at an altitude of around 1150 m a.s.l. It flows as a tributary to the Danube River in Hungary. We study the Austrian, and mainly the Styrian part of the Raab catchment, which extends up to gauging station Neumarkt/Raab located in Burgenland, Austria (Figure 3.1). This part has a length of about 95 km and covers a catchment area of 987 km^2. The land use is dominated by agricultural areas 42% and forest 40%. The soil textures are loam (50% silty loam, and 41% loam). The Raab river shows a pluvio-nival runoff regime, with a relatively evenly distributed discharge over the year (*Mader et al.*, 1996).

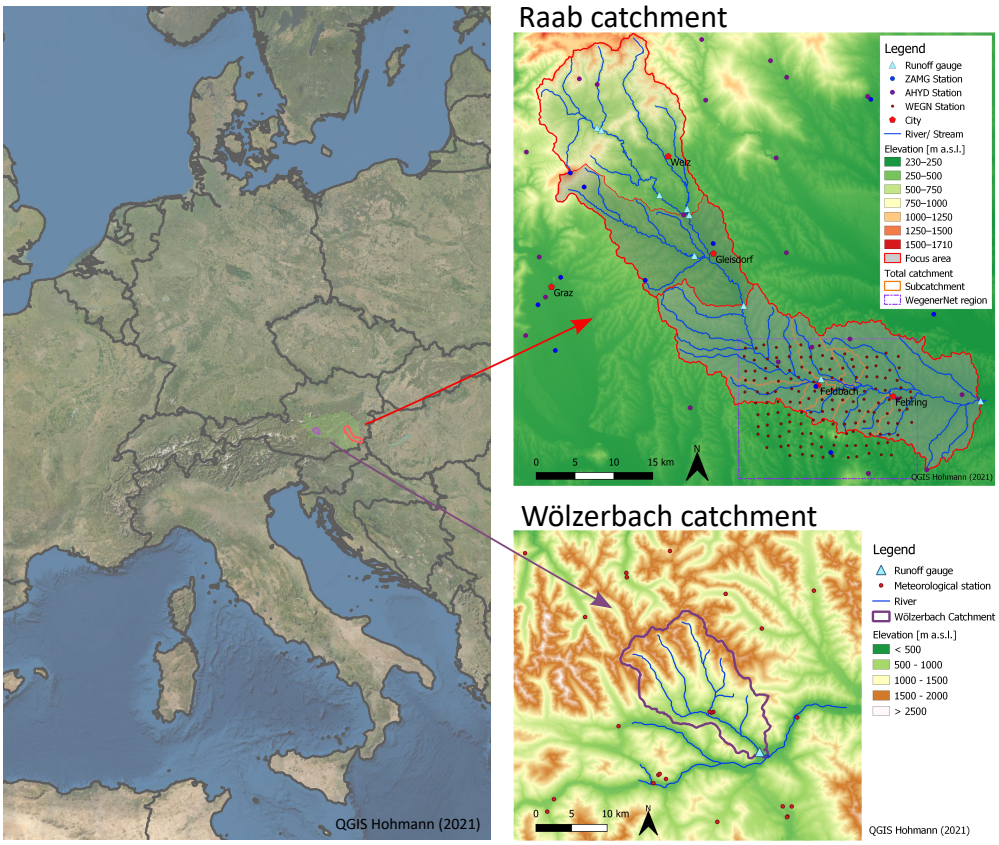


Figure 3.1: Left: Overview map of Europe with Styria (greenish area), with study areas Raab catchment (red line) and Wölzerbach catchment (purple line), the base map of Europe was created with ArcGIS, its source is: Esri, DigitalGlobe, GeoEye, Earthstar, Geographics, CNES/Airbus DS, USDA, USGS, AeroGRID, IGN, and the GIS User Community. Right: Studied catchments Raab (top) and Wölzerbach (bottom) with elevation information as a background, marked station locations, river network and analyzed subcatchments. (Maps created with QGIS, www.qgis.org, 2021)

The Raab catchment can be divided into three parts (Figure 3.1). These are the *upper Raab* which extends up to gauging station St. Ruprecht/Raab, a low mountain area where the land use is dominated by forest; the *middle Raab* range extending from the gauging station St. Ruprecht/Raab to Takern II/Raab, with less hilly areas and land use dominated by agricultural areas and forest patches; and the *lower Raab* stretch extending from the gauging station Takern II/Raab to Neumarkt/Raab, which is also dominated by agricultural areas and patchy forest. The area is moderately hilly with elevations from 230 m to 530 m and anthropogenic influences can be detected. The lower Raab was chosen as the main focus area, which includes the gauging station Feldbach/Raab between the stations Takern

II/Raab and Neumarkt/Raab. In this focus area, small subcatchments that are located here were also studied, namely, the Auersbach, Saazerbach, Giemerbach, Haselbach and Kornbach subcatchments. In this region, the long-term mean annual temperature is about 9.5° and the long-term mean annual precipitation around 850 mm.

This region is especially interesting to study due to the strongly increased summer temperature trend of 0.7° per decade, which has been observed since the 1970s (*Kabas et al.*, 2011), and the tendency of heavy precipitation events to occur here in summer (*Schroeer and Kirchengast*, 2018; *Breinl et al.*, 2020). The data availability, including the dense station network WEGN is also unique (*Kirchengast et al.*, 2014). The Raab catchment has been the focus of other climate change studies in the recent years (*Piringer et al.*, 2019; *Schürz et al.*, 2019).

3.1.2 The Wölzerbach catchment

In addition to the mesoscale prealpine Raab catchment, the small-scale alpine Wölzerbach catchment has been studied. This mountainous alpine catchment has an area of 227 km^2. It is located in the Niedere Tauern range of the Central Eastern Alps in Styria, Austria. The altitude ranges from 740 m a.s.l. up to 2475 m a.s.l. The land use is dominated by forest (48%), alpine dwarf-shrub heath, and grasslands (25%) and includes pastures and rock-ribbed mountain tops. The soil texture is dominated by loam (loam, sandy loam and loamy sand). The mean annual precipitation ranges from around 1700 mm to 700 mm along the north-south elevation gradient. The runoff is dominated by snow melt and shows a moderate nival discharge regime, with the flood peak occurring in May (*Mader et al.*, 1996).

3.2 Input data

To study runoff under conditions of different environmental changes using hydrological model simulations, many different data sets are needed. Beside the direct model input, data for comparing the model simulations are also necessary to calculate efficiencies and for further analyses. These data sets range from meteorological point measurements over gridded data products to geographical information. All hydro-meteorological data sets used are summarized in Table 3.1 and described in Chapter 3.2.1. All constant grid data sets, as well as geographical information, are listed in in Table 3.2 and further described in Chapter 3.2.2. The main data sources/data providers were the National Austrian Weather Service (ZAMG), the National Austrian Hydrographic Service (AHYD), the Wegener Center for Climate and Global Change, University of Graz, Austria (Wegener Center) with its WEGN, and the provincial government offices of the provinces of Styria, Austria (LStmk) and Burgenland, Austria (LBgld). The temporal resolutions range from 5 min to daily time steps. The spatial resolutions range from point measurements to 12.5 km × 12.5 km grids. The data sets, each with a different resolution, are described in detail in the following section.

3.2.1 Hydro-meteorological data sets

Different time series are needed as hydrological model input. Hydrological models minimally require precipitation and temperature data as meteorological input, either as station data or gridded data sets. Additional information about humidity, wind, radiation, and air pressure are also helpful, especially for performing the evapotranspiration calculations. The observed runoff was used for the model calibration and validation. In the following section, first the station data and then the gridded data sets are described together with their sources. A concise overview is provided in Table 3.1.

Hydro-meteorological station data

The meteorological data of the ZAMG are available for researchers at the Wegener Center through a data-sharing agreement. These data are stored in ISQL databases and include both daily data (SYBKLIM) and sub-daily data (TAWES). We inquired the daily data collected at precipitation and temperature stations

for our coarse-resolution setups, which were located in the study area or its surroundings. To perform the fine-resolution setup, we obtained the 10 min data from five measurement stations for precipitation, temperature, relative humidity, wind speed, global radiation, and air pressure. These stations were located close to the study area in the lower Raab catchment or its surroundings. Afterward, we checked the quality of these data and aggregated these time series to a 30 min target time resolution.

The AHYD data sets of quality controlled daily time series for precipitation and runoff data is freely available online (https://ehyd.gv.at/ehyd.gv.at, last access on 2021-07-13) with a delay of a few years. A manual download of the runoff and precipitation station data sets of data collected within the study area and its surroundings was executed. Daily temperature data were also made available via AHYD for the study described in Research Article 3. Higher resolution data (1 min to 15 min) for precipitation, temperature, and runoff were available from AHYD upon request. These data were again checked for their quality and aggregated to the requested 30 min time resolution.

The WEGN, a highly dense meteorological station network of the Wegener Center, was set up for research purposes under a open data policy (www.wegenernet.org, last access on 2021-07-13). In an area of around 23 km × 18 km, 150 meteorological stations have been set up at a density of approximately 1 station per 2 km^2. All of these stations measure precipitation, temperature, and relative humidity at a 5 min interval since 2007. The other data sets, such as those for wind speed, have been acquired at twelve stations, and air pressure, at one station, respectively, at a 5 min interval since 2007. These data are available online for download at a 30 min time resolution. For further information about the WEGN, see *Kirchengast et al.* (2014). In this work, we used the quality-controlled data version 7.1 (*Fuchsberger et al.*, 2021).

Meteorologically gridded data

In addition to point measurements, gridded data products for precipitation and temperature were used as part of this thesis work, which is presented in Research Article 3. The ZAMG provides a 1 km × 1 km precipitation grid for each day from 1961 to 2010, called GPARD (*Hofstätter et al.*, 2015). This grid contains the precipitation sum from 07:00 to 07:00 CET and is spatially interpolated with a gradient-based anisotropic interpolation method using a background-climatology

technique. For further information, see *Hofstätter et al.* (2015). The temperature-gridded data product with a 1 km × 1 km resolution is also available from ZAMG on a daily time scale for the years 1961 to 2010 (*Hiebl and Frei*, 2016). This data set with an average daily temperature (Tmean = (Tmin+Tmax)/2) is called SPARTACUS. It is spatially interpolated by nonlinear profiles and non-Euclidean distances. For further information, see *Hiebl and Frei* (2016).

The high-resolution ÖKS15 data sets were created to provide climate change scenarios for the identification of intervention and adaptation strategies in Austria (*Chimani et al.*, 2016). These have a spatial resolution of 1 km × 1 km and a temporal resolution of one day. These data sets contain 13 GCM-RCM combinations from the EURO-CORDEX ensemble (*Jacob et al.*, 2014). The combinations were statistically down-scaled with Scaled Distribution Mapping (*Switanek et al.*, 2017) for precipitation and air temperature. The data are available from 1951 to 2100 or 1971 to 2100, depending on the GCM-RCM combinations. Further information can be found in *Chimani et al.* (2016). The raw data from the GCM-RCM combination, which have a resolution of 12.5 km × 12.5 km, were also used to compare the ÖKS15 data sets.

Table 3.1: Hydro-meteorological data sets used in this thesis; all data sets are given with their resolutions and data sources.

Data type	**Name**	**No. of stations/ Spatial resolution**	**Time Resolution**	**Source**	**Catchment area**
Precipitation [mm] & Temperature [°C]	WEGN	150 stations	5 min	WEGN[a]	lower Raab
	ZAMG	5 stations	10 min	TAWES data base	lower Raab
	AHYD	3 stations	5 min	AHYD	lower Raab
	ZAMG	18 & 11 stations	daily	SYBKLIM data base	Raab & Wölzerb.
	AHYD	34 & 11 precip. stations	daily	AHYD download[b]	Raab & Wölzerb.
	GPARD	1 km × 1 km grid (precipitation)	daily	ZAMG *Hofstätter et al.* (2015)	Raab & Wölzerbach
	SPARTACUS	1 km × 1 km grid (temperature)	daily	ZAMG *Hiebl and Frei* (2016)	Raab & Wölzerbach
	ÖKS15 ensemble	1 km × 1 km grid	daily	*Chimani et al.* (2016); *Switanek et al.* (2017)	Raab & Wölzerbach
	RAW ensemble	12.5 km × 12.5 km grid	daily	EURO-CORDEX *Jacob et al.* (2014)	Raab & Wölzerbach
Relative humidity [%]	ZAMG	5 stations	10 min	TAWES data base	lower Raab
	AHYD	3 stations	5–10 min	AHYD	lower Raab
	WEGN	150 stations	5 min	WEGN[a]	lower Raab
Wind speed [m/s]	ZAMG	5 stations	10 min	TAWES data base	lower Raab
	WEGN	12 stations	5 min	WEGN[a]	lower Raab
Global radiation [W/m^2]	ZAMG	5 stations	10 min	TAWES data base	lower Raab
Air pressure [hPa]	ZAMG	5 stations	10 min	TAWES data base	lower Raab
	WEGN	1 stations	5 min	WEGN[a]	lower Raab
Runoff [m^3/s]	AHYD	9 & 1 stations	daily	AHYD download[b]	Raab & Wölzerb.
	AHYD	3 stations	15 min	AHYD	lower Raab

[a] quality-controlled data version 7.1 (*Fuchsberger et al.*, 2021)

[b] https://ehyd.gv.at, last access on 2017-12-01

3.2.2 Elevation models, land use, and soil data sets

In addition to time series for hydro-meteorological input data, having constant grids of geographical information, as well as soil and land use information, is important to run a process-based hydrological model. All data sets used are summarized in Table 3.2.

The Digital Elevation Model (DEM) was received by the LStmk and LBgld at a resolution of 10 m × 10 m and 30 m × 30 m, respectively. For the study regions, these data were aggregated to the 1 km × 1 km or the 100 m × 100 m target grid, respectively. The ÖKS15 target grid presented in Research Article 3 was slightly shifted as compared to the 1 km × 1 km setup shown in Research Article 1. Therefore, the 1 km × 1 km DEM was adjusted for the study of Research Article 3 to the shifted origin.

To create the coarse-resolution setups, the land use information was adopted from the CORINE[1] data set. The data set from the year 2006 was selected, since it fits the calibration period of the setup. Furthermore, a cross-check of temporal changes with respect to other CORINE data sets for the years 1990, 2000, and 2012 show few land use changes. For the research areas, the data set was re-sampled to the 1 km × 1 km target grid (Figure 3.2). The fine-resolution study setup used the land use data set presented in *Klebinder et al.* (2017). These authors used the technical strategy of *Sotier et al.* (2010) in the wider Raab area to create a 100 m × 100 m land use information map with 31 classes (Figure 3.2). This data set provides a geometrical and content-dependent map of land use and, therefore, is more detailed than the map based on the CORINE data set (*Klebinder et al.*, 2017).

The soil information used also depends on the resolution and catchment. The coarse-resolution, 1 km × 1 km grid for the Raab catchment relied on soil texture information obtained from the Agricultural Soil map of Austria[2]. This polygon-style map gives information about the soil texture for the agricultural areas. Therefore, the map was assigned to the 1 km × 1 km target grid, with the most dominant soil texture shown in each grid cell (Figure 3.2). The few grid cells which were totally covered by forest and which, therefore, did not have any soil information were interpolated from the surrounding cells, again showing the most dominant soil texture. The soil information for the Wölzerbach at its 1 km × 1 km

[1] https://land.copernicus.eu/pan-european/corine-land-cover, last access on 2021-07-13
[2] https://geometadatensuche.inspire.gv.at, last access on 2021-07-13

resolution were based on the online version of the Austrian soil map (EBOD[3]) and the Austrian Hydrological Atlas (HAÖ[4]).

The fine-resolution setup of the Raab catchment used the soil information created by *Klebinder et al.* (2017) and is named HYDROBOD. HYDROBOD was created for the Raab area such that it was similar to the one in Lower Austria (*Krammer et al.*, 2016). All needed soil parameters, such as soil texture (percentage of sand, silt, and clay), saturated hydraulic conductivity, the Mualem van Genuchten parameters, and soil sickness, are given in separate maps with a 100 m × 100 m spatial resolution (Figure 3.2). These maps are respectively available for three soil layers with depths of 0 cm to 20 cm, 20 cm to 50 cm, and 50 cm to 100 cm, respectively, and different standard deviations. The Mualem van Genuchten parameters are given in different combinations and were calculated using the method described in *Vereecken* (1989).

Table 3.2: Elevation model, land use, and soil data, which are used in this thesis for process-based hydrological modeling. All data sets are given with their resolutions and data sources.

Data type	**Name**	**Resolution**	**Source**	**Catchment area**
Elevation model	DEM	10 m × 10 m (Styria) 30 m × 30 m (Burgenland)	LStmk, LBgld	Raab and Wölzerbach
Land use information	CORINE	100 m × 100 m	Online	Raab and Wölzerbach
	HYDROBOD	100 m × 100 m	*Klebinder et al.* (2017)	Lower Raab
Soil information	Agricultural Soil Map of Austria	Shape file	Online	Raab
	Basis of EBOD and HAÖ	Shape file	Digital	Wölzerbach
	HYDROBOD	100 m × 100 m	*Klebinder et al.* (2017)	lower Raab

[3]https://bodenkarte.at, last access on 2021-07-13

[4]https://info.bmlrt.gv.at/themen/wasser/wasser-oesterreich/hydrographie/der-weg-zu-den-daten/hydrologischer_atlas.html, last access on 2021-07-13

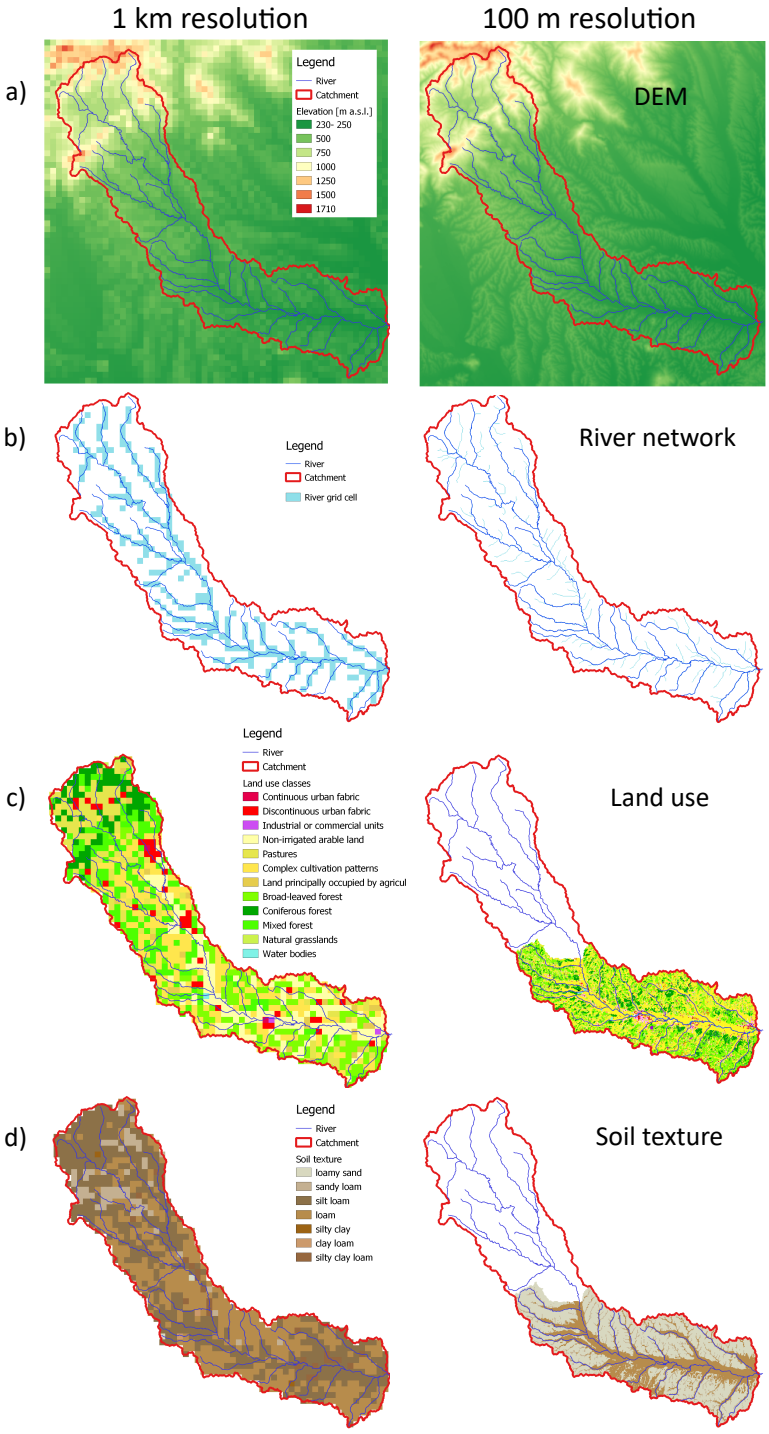


Figure 3.2: Input data maps for the Raab catchment with the coarse-resolution grid of 1 km × 1 km (left) and the fine-resolution grid of 100 m × 100 m (right). a) The digital elevation model (DEM) aggregated to the target grids 1 km (left) or 100 m (right) cell size, b) river network: calculated by TANALYS depending on the above DEMs, c) land use information: left aggregated CORINE data to the 1 km target grid, right land use information created by *Klebinder et al.* (2017), and d) soil texture: left aggregated soil information based on the Agricultural Soil Map of Austria and right soil information by *Klebinder et al.* (2017). (Maps created with QGIS, www.qgis.org, 2021)

3.3 Hydrological model

The process-based hydrological model WaSiM was developed by *Schulla* (1997) at the ETH Zurich in Switzerland and was originally developed for use in climate change studies in the alpine region. Since then, the model has become well-established and been widely used for many studies of climate change (*Bürger et al.*, 2011; *Korck et al.*, 2012; *Rössler et al.*, 2012; *Muerth et al.*, 2013; *Gädeke et al.*, 2014) and land use changes (*Niehoff et al.*, 2002; *Elfert and Bormann*, 2010; *Alaoui et al.*, 2014; *Gharun et al.*, 2014; *Yira et al.*, 2016). It is in current operational use (e.g. BAFU/FOEN, Switzerland).

3.3.1 Model characteristics and setup

WaSiM is a distributed and process-oriented hydrological model. The scales and resolutions are very flexible. Some studies used one single model cell (e.g. *Grigoryan et al.*, 2010) or even large catchments with areas exceeding 100 000 km^2 (e.g. *Kleinn et al.*, 2005), but recalibration is necessary when switching between resolutions (*Cullmann et al.*, 2006; *Schulla*, 2019). The modular structure of WaSiM enables users to use more or less complex setups depending on the available data. The selection of modules as well as choice of temporal and spatial resolution has to be made with due care, depending on the research focus, data availability, and computational power.

In this thesis, two different model setups were used. First, the coarse-resolution 1 km × 1 km – daily, climate change setup and, second, the fine-resolution 100 m × 100 m – 30 min, WEGN setup. All modules used for each setup are listed in Table 3.3. Detailed descriptions of all modules can be found in *Schulla* (1997, 2019). Depending on the modules used and their complexity, more or less input data were required. The minimum meteorological inputs are precipitation and temperature time series. The potential evapotranspiration is then calculated depending on a temperature-only approach (e.g., *Hamon* (1961) or *Haude* (1955)). If the more physically based Penman-Monteith equation (*Montheith*, 1975) is used, the meteorological parameters of relative humidity, wind speed, global radiation, and air pressure are also needed. To calculate the potential evapotranspiration in this thesis, the coarse-resolution setups applied the Hamon approach, and the fine-resolution setup applied the Penman-Monteith equation. The real evapotranspiration is reduced depending on the soil moisture tension. The interception is

calculated by taking a simple bucket approach, whereby its capacity depends on the leaf area index, the vegetation coverage, and the maximum height of water at the leafs (*Schulla*, 2019).

In WaSiM, an internal spatial interpolation of the meteorological point measurements to the target gird is implemented. Possible options are IDW, elevation depending regression, TP, TP combined with a constant lapse rate, bi-linear interpolation, bi-cubic splines, as well as combinations thereof. If grids are available as input files (e.g., of climate change scenarios), these grids can be used directly or be adjusted to the target grid. To adapt to uncertainties in the precipitation data sets, a wind-dependent correction can be used. Here, the correction is performed separately for liquid and solid precipitation input. A shadowing and exposition correction is also possible for radiation and temperature adjustments.

To spatially interpolate meteorological data for the coarse-resolution setup of the Raab catchment, we used a combination of the IDW interpolation (75%) and TP with a constant laps rate (25%) for temperature data and the IDW interpolation for precipitation data. For the Wölzerbach catchment, the temperature data was interpolated with TP with a constant laps rate, and the precipitation data was interpolated as a combination of IDW (70%) and elevation-dependent regression (30%). In the fine-resolution setup, we used the IDW interpolation of all meteorological input data sets in the calibration setup. The correction modules of precipitation and radiation correction were switched on in this fine-resolution setup.

To model snow accumulation and melt, the Temperature Index Snowmelt (degree day method) was used. This rather simple method was chosen due to its data availability for the Raab and Wölzerbach catchment areas. Snow accumulation in WaSiM was modeled with a threshold temperature (T r/s), whereby 50% of the precipitation is falling as snow and this precipitation is combined with a transitional range (T trans) in which solid and liquid precipitation are simulated. Since the Raab catchment is not dominated by snow, these values were set to the default (T r/s 0.5°C and T trans ±1°C). In the snow-dominated Wölzerbach catchment, these values were calibrated to T r/s 2.1°C and T trans ±0.35°C.

The infiltration and soil water modeling can be done with the TOPMODEL or Richards approach. In this thesis, we used the more physically based soil moisture estimations of WaSiM, the Richards' approach, which is used to simulate the vertical water flow in the unsaturated zone. The parametrization of the pF curves

was performed based on *van Genuchten* (1980). The runoff component interflow was generated as lateral flow processes. The baseflow represents the ex-filtration from the groundwater to the (surface) river system.

The groundwater flow can be simulated with a linear storage or the 2D groundwater module. The linear storage approach needs to be calibrated. In the 2D groundwater module, multiple aquifers may be defined. Here, information about the saturated horizontal conductivity, colmation factor, the storage coefficient, and the aquifer thickness were needed. This information was gathered from measurements and the literature and could be adjusted with reference to the baseflow. We used the 2D groundwater module for the fine-resolution setup for the Raab catchment, as well as the coarse-resolution climate change setup for the Wölzerbach, and the linear storage approach for the coarse-resolution setup for the Raab catchment.

The runoff generated is separated into baseflow, interflow, and surface flow. The baseflow is water which exfiltrates into the channel network, although infiltration from the river to the baseflow is also possible. The interflow is the water in the soil layer, and this water can be translated to the sub-basin outlet with the flow time histogram (isochronic methods). The surface runoff is simulated by assuming saturation from above when the precipitation intensity is higher than the hydraulic conductivity or from below when the groundwater rises to the surface. The runoff routing in the channels is performed by taking the kinematic wave approach, based on flow velocities obtained by applying the Manning-Strickler equation.

In addition to these basic, water-balance-related modules, many other features are already implemented in WaSiM. For example, the use of irrigation, a lake module, a glacier module, macropore runoff, or tracer and solute transport. In Table 3.3, all WaSiM modules used and input data for the coarse- and fine-resolution study setups described in this thesis are listed.

Table 3.3: WaSiM setups used, with input and modules for the two setups in the Raab catchment and for the setup in the Wölzerbach catchment.

WaSiM setups	**Research Articles 1 & 3**	**Research Article 2**	**Research Article 3**
Catchment	Raab	Lower Raab and subcatchments	Wölzerbach
Meteorological input	Temperature, precipitation	Temperature, precipitation, relative humidity, wind speed, global radiation, air pressure	Temperature, precipitation
Time steps	Daily	Half-hourly	Daily
Gridded data	1 km × 1 km coarse-resolution DEM, subcatchment, river network, soil, land use, others	100 m × 100 m fine-resolution DEM, subcatchment, river network, soil, land use, groundwater, river with, river depth, others	1 km × 1 km coarse-resolution DEM, subcatchment, river network, soil, land use, groundwater, river with, river depth, others
Interpolation to grid	IDW and TP-lapse rate	IDW	IDW, TP-lapse rate, elevation depending regression
Precipitation corr.	-	Rain/snow temperature	-
Radiation corr.	-	With shadow and temperature correction	With shadow and temperature correction
Pot. evapotranspiration	Hamon approach	Penman-Monteith equation	Hamon approach
Interception	Bucket approach	Bucket approach	Bucket approach
Snow accumulation and snow melt	Temperature index	Temperature index	Temperature index
Unsaturated zone	Richards equation	Richards equation	Richards equation
Saturated zone	Linear storage	2D groundwater module	2D groundwater module
Discharge routing	Kinematic wave approach	Kinematic wave approach	Kinematic wave approach
Irrigation	Partly used	-	-

3.3.2 Input data preprocessing

To setup a new catchment in WaSiM, data pre-processing is necessary. In the WaSiM model, the Topographic Analysis Tool (TANALYS) is provided for the preparation of the required geographical grids (*Schulla*, 2019). TANALYS used the DEM to calculate grids such as slope, aspect, flow direction, flow accumulation, river network with river depth and width, as well as the subbasin structure. The parameter threshold, Manning-Strickler roughness, and specific runoff need to be set to conduct the flow network analysis. As a comparison, the real river network and subcatchment size can be used. See Figure 3.2 for a comparison of the river network with a 1 km gird spacing, a 100 m grid spacing, and the real river network.

To convert the hydro-meteorological time series to the WaSiM format, scripts were written in Python, mostly with the help of the Python package pandas[5]. More information about the specific WaSiM formats can be found in *Schulla* (2019).

3.3.3 Model calibration and validation

The model parameters for which no measured or literature data were available needed to be calibrated. To select the most important calibration parameter, we tested the sensitivity and used literature sources for further reference (*Kunstmann and Stadler*, 2005; *Cullmann et al.*, 2006; *Schulla*, 2019). Based on this information, soil and groundwater parameters were calibrated in our model setups. In Table 3.4, the calibrated parameters with their best fits are listed for each model setup.

To analyze the model performance, many different efficiency measures can be applied. In Table 3.5, the efficiency measures used in this thesis are listed, including the equations and focus targets.

The calibration used in the thesis was performed with an automatic model calibration algorithm, the Shuffled Complex Evolution optimization algorithm, which was developed at the University of Arizona (SCE-UA) (*Duan et al.*, 1992, 1994). This is a frequently used and powerful global optimization algorithm which was developed for use in conceptual rainfall-runoff models. In addition to the traditional trial-and-error calibration methods, different automatic algorithms have been used for WaSiM (*Kunstmann et al.*, 2006; *Cullmann et al.*, 2011; *Singh et al.*, 2012), including the SCE-UA. For this thesis, we scripted the SCE-UA algorithm in Python and adapted it to WaSiM.

[5] a powerful Python data analysis toolkit, https://pandas.pydata.org last access on 2021-07-13

Table 3.4: Calibration parameter of WaSiM used in this thesis, as well as its calibrated values for all three setups (cf. Table 3.3).

Calibration parameter	**Description**	**Influence**	**Unit**	**Best fit setup**		
				coarse-res. Raab	**fine-res. lower Raab**	**coarse-res. Wölzerbach**
krec	Factor controlling decrease of hydraulic conductivity with soil depth	Amount of interflow	-	0.8	0.8	0.6
dr	Drainage density	Linear scaling of interflow	m^{-1}	$13.7^a/11.4^b/9.4^c$	40	$4.5^d/3.9^e/2.2^f$
ki	Storage coefficient flow hydrograph	Shape of interflow hydrograph	h	$20^a/19^b/50^c$	2	$92^d/77^e/87^f$
kd	Storage coefficient runoff hydrograph	Shape of surface flow hydrograph	h	kd = ki	1.5	$34^d/32^e/3.3^f$
Q0	Scaling factor	Baseflow	mm h^{-1}	$0.9^a/0.6^b/0.2^c$	-	-
kb	Storage coefficient	Baseflow	m	$1.3^a/0.2^b/0.9^c$	-	-

[a] Upper Raab catchment until gauge St. Ruprecht/Raab
[b] Middle Raab catchment from gauge St. Ruprecht/Raab until gauge Takern II/Raab
[c] Lower Raab catchment from gauge Takern II/Raab until gauge Neumarkt/Raab
[d] Wölzerbach catchment, area of Hinteregger and Schöttelbach
[e] Wölzerbach catchment, area of Eselsbergbach
[f] Wölzerbach catchment, other areas which are lower in elevation

Table 3.5: Model efficiency metrics used in this thesis, with *obs* as observed discharge, *sim* simulated discharge, μ_{obs} mean observed discharge, μ_{sim} mean simulated discharge, n total number of time steps, r linear correlation between observations and simulations, α a measure of the flow variability error, β a bias term, σ_{obs} standard deviation in observations, and σ_{sim} standard deviation in simulations.

Efficiency	**Equation**		**Focus**	**Source**
NSE	$1 - \frac{\sum_{i=1}^{n}(obs_i - sim_i)^2}{\sum_{i=1}^{n}(obs_i - \mu_{obs})^2}$	(3.1)	Peak flow	*Nash and Sutcliffe* (1970)
NSE_{log}	$1 - \frac{\sum_{i=1}^{n}(\log(obs_i) - \log(sim_i))^2}{\sum_{i=1}^{n}(\log(obs_i) - \log(\overline{obs}))^2}$	(3.2)	Low flow	*Oudin et al.* (2006)
PBIAS	$\frac{\sum_{i=1}^{n}(obs - sim) \cdot 100}{\sum_{i=1}^{n} obs}$	(3.3)	Percent bias	*Moriasi et al.* (2007)
KGE	$1 - \sqrt{(r-1)^2 + (\alpha-1)^2 + (\beta-1)^2}$ i.e.	(3.4)	Correlation, bias and variability of over- and underestimation of discharge	*Gupta et al.* (2009); *Knoben et al.* (2019)
	$1 - \sqrt{(r-1)^2 + (\frac{\sigma_{sim}}{\sigma_{obs}} - 1)^2 + (\frac{\mu_{sim}}{\mu_{obs}} - 1)^2}$	(3.5)		

Coarse-resolution model setup – Raab catchment

The model calibration for the coarse-resolution model setup was performed with the SCE-UA for the Raab catchment. The model performance was determined with the well-known Nash-Sutcliffe Efficiency (NSE) (*Nash and Sutcliffe*, 1970), see Table 3.5 for equations. To include the low flow focus, we also used the logarithmic version of NSE, the NSE_{log} (*Oudin et al.*, 2006). The model efficiency was a combination of NSE and NSE_{log}, both weighted with 50%. To validate the water balance, the Percent Bias (PBIAS) (*Moriasi et al.*, 2007) was also analyzed. PBIAS is used to measure the average tendency to over- or underestimate the simulated runoff as compared to the observed runoff (*Gupta et al.*, 1999). The runoff components were also visually analyzed for validation purposes.

To calibrate the model, three gauging stations were used, one for the upper, middle, and lower Raab catchment areas, respectively. The three stations were weighted with 25% St. Ruprecht/Raab (upper Raab), 25% Takern II/Raab (middle Raab), and Neumarkt/Raab (lower Raab) with 50%, since this is our focus region. The calibration time series of point measurements represents seven years from 2003 to 2009 and seven years for validation from 1995 to 2001. Both time series include specific dry (2003/2001) and wet (2009/1996) years. The classification of the dry and wet years is based on the Standardized Precipitation Evapotranspiration Index (SPEI), calculated with an SPEI-R-package [6].

The calibration parameters for the coarse-resolution model setup of the Raab catchment are given in Table 3.4 together with best-fit parameter set used in this thesis. This setup results in a NSE/NSE_{log} of 0.74/0.76 across the three gauging stations for the calibration period and 0.64/0.74, for the validation period. More detailed information about the model calibration of the coarse-resolution setup in the Raab catchment can be found in the supplementary material for Research Article 1 in Chapter 4.1.

Fine-resolution model setup – lower Raab catchment

To create the fine-resolution model setup, the SCE-UA was used to obtain an initial estimate and a starting point. A trial and error, manual calibration was necessary to consider the right physical parameters underlying the runoff components, such as interflow, baseflow, and surface flow. For example, it is known that in mid-latitudes,

[6] Version 1.6, https://spei.csic.es/tools.html, last access on 2021-07-13

the interflow is the dominant runoff component.

In this setup, the 2D groundwater module was used. The groundwater parameters were separately fitted to represent the baseflow quite well. The saturated horizontal conductivity was split into two areas: Around the river, it was set to $1 \cdot 10^{-3}$ m/s and in the surrounding hilly areas, to $5 \cdot 10^{-4}$ m/s. The calibration period chosen was the summer of 2009 (May to September) and the validation period, the summers of 2010 and 2011 (May to September). In addition to conducting a visual comparison of time series, we calculated the efficiencies NSE, NSE_{log}, PBIAS and Kling-Gupta efficiency (KGE) (*Gupta et al.*, 2009; *Knoben et al.*, 2019) as described in Table 3.5. The distributions of the runoff components were also visually analyzed for specific events.

The calibration parameters for the fine-resolution model setup for the lower Raab catchment are given in Table 3.4 together with best fit parameter set used in this thesis. For the calibration period, this setup results in an NSE of 0.80, an NSE_{log} of 0.76, an KGE of 0.77, and a PBIAS of 8% at the gauging station Neumarkt/Raab, and for the validation period in an NSE of 0.63, an NSE_{log} of 0.56, an KGE of 0.69, and a PBIAS of 19%. More detailed information about the model calibration for the fine-resolution setup can be found in Research Article 2 in Chapter 4.2.

Coarse-resolution model setup – Wölzerbach catchment

For the Wölzerbach catchment, the calibration was performed with a combination of the SCE-UA and a manual recalibration. Especially the 2D groundwater module and snow parameters were adjusted. The performance measure was a linear combination of NSE and NSE_{log}, both weighted with 50%. The calibration period was 2004 to 2007, and the validation period was 2008 to 2010. Beside the model calibrations for the Raab catchment with station data, the Wölzerbach catchment was calibrated with gridded data products, SPARTACUS (*Hiebl and Frei*, 2016) for temperature and GPARD (*Hofstätter et al.*, 2015) for precipitation (see also Table 3.1).

The calibration parameter for the coarse-resolution model setup of the Wölzerbach catchment are given in Table 3.4 together with best fit parameter set used in this thesis. At gauging station Niederwölz/Wölzerbach, this setup results in a NSE/NSE_{log} of 0.70/0.71 for the calibration period and 0.68/0.69 for the validation

period. More detailed information about the model calibration of Wölzerbach can be found in Research Article 3 in Chapter 4.3.

3.4 Choice of methods for the specific studies

The choice of methods used in this thesis was based on sensitivity and uncertainty analyses, but the actual approach was focus-dependent. On the one hand, the climate-change focus of Research Articles 1 and 3 led to simulations of runoff that had a coarse-resolution model setup and long time frames of periods of decades. On the other hand, the precipitation station density study presented in Research Article 2 was carried out to simulate runoff with a fine-resolution model setup and used short, event-based time frames. WaSiM provide this flexibility to study long- and short-term hydrological behavior. Therefore, the temporal and spatial resolution was target-, data-, and computational power-dependent.

In Research Article 1, the scenario-neutral approach was chosen as described in Section 2.1. We analyzed the long summer mean for the years 1982 to 2011. This time frame was chosen due to the data availability (time series of precipitation, temperature, and runoff). The focus was placed on the extended summer (May to September), since the temperature increase in this area is especially pronounced during the summer months (*Kabas et al.*, 2011). We studied the simulated discharge at the gauging stations Neumarkt/Raab and Feldbach/Raab, and the mean actual evapotranspiration. In addition to determining the long-term mean, we also analyzed a time series for a specific dry (2003) and wet year (2009). The time series analysis results show a strong influence of specific drivers in extreme cases. The non-climatic driver like land use changes and irrigation were also specifically pronounced in this daily time series and visible individually on each day.

In Research Article 2, we also simulated the runoff continuously, but studied the output based on events. We chose the three most extreme short- and three long-duration events in the period of 2009 to 2014. This time frame was chosen because of data availability and computation power constraints. The analysis of the precipitation events was again done for the gauging stations Neumarkt/Raab and Feldbach/Raab, but also on a subcatchment level. This subcatchment level analysis was helpful, because it enabled us to see the influence of station density more locally in five small catchments with an area of $10\,\mathrm{km}^2$ to $30\,\mathrm{km}^2$. After performing the analysis of time series and precipitation maps, we focused on

examining the flood peak. To get a more complete picture, we analyzed both the maximum amount of water at the flood peak and the timing of the peak.

In Research Article 3, we studied the recent past from 1961 until 2005 and from 1971 until 2000, respectively, depending on the data availability. Here, not only the pre-alpine Raab catchment with its gauging stations Feldbach/Raab, but also the alpine Wölzerbach catchment with gauging station Niederwölz/Wölzerbach were analyzed. The analysis of the ÖKS15 high-resolution climate data sets, the raw climate simulations, the gridded data sets, as well as the station data of temperature and precipitation were performed on different levels. The analysis was done on the point level with precipitation and temperature station data compared to grid cells. Spatially averaged values of precipitation and temperature were analyzed on the (sub-)catchment level. For both levels the annual cycles, different biases and hydro-meteorological indicators were calculated and compared between the different input data sets. The discharge was studied for (sub-)catchments with a comparison of the calculated flow regimes, efficiency measures, and hydro-meteorological indicators.

The overall goal of this thesis is a sensitivity and uncertainty analysis of hydro-climatic changes, with different foci. In Table 3.6 the study designs of all three studies are summarized. Further description can be found in the respective publications.

Table 3.6: Summarized study design characteristics of the three research articles, including the overall research questions of this thesis.

Publication	**Study design characteristics**
Research Article 1 *Hohmann et al.* (2018)	*How do summer runoff and evapotranspiration respond to changes in a warming climate?* • Sensitivity to changes in climate, land use, and water management • Low flow focus and vulnerability to summer dryness • Austrian Raab catchment • WaSiM: 1 km grid and daily time resolution • Temporal analysis: long-term summer mean (1982–2011) and times series • Analysis of runoff at gauging stations Neumarkt/Raab and Feldbach/Raab, including other water balance components like evapotranspiration
Research Article 2 *Hohmann et al.* (2021)	*How many stations are needed to reliable model runoff in small catchments under heavy precipitation events?* • Sensitivity and uncertainty analysis related to station density and interpolation scheme of extreme precipitation events • Precipitation input and high-flow focus • Lower Raab catchment and small subcatchments (10–30 km^2) • WaSiM: 100 m grid and half-hourly time resolution • Temporal analysis: three short and three long duration heavy precipitation events • Analysis of runoff at gauging station Neumarkt/Raab and Feldbach/Raab and five small subcatchments
Research Article 3 *Peßenteiner et al.* (2021)	*How well do the Austrian ÖKS15 high-resolution climate data sets perform in hydrological impact studies?* • Sensitivity and uncertainty analysis of an ensemble of high-resolution climate data sets, ÖKS15 • low flow and high flow • Wölzerbach and Austrian Raab catchment • WaSiM: 1 km grid and daily time resolution • Temporal analysis: recent past 1961–2005 incl. 1971–2000; i.e., annual cycle, monthly mean, flow regime, different hydro-meteorological indicators • Study of temperature, precipitation, and runoff at different gauging stations with an analysis of point, grid, and sub(catchment) level

4 Sensitivity and uncertainty analysis of hydro-climatic changes

4.1 Research Article 1: Alpine foreland running drier? Sensitivity of a drought vulnerable catchment to changes in climate, land use, and water management

Published as:
Clara Hohmann, Gottfried Kirchengast, and Steffen Birk (2018), Alpine foreland running drier? Sensitivity of a drought vulnerable catchment to changes in climate, land use, and water management, *Climatic Change*, 147, 179–193, DOI:10.1007/s10584-017-2121-y.
Original article and supporting information available at: https://doi.org/10.1007/s10584-017-2121-y

Climatic Change (2018) 147:179–193
https://doi.org/10.1007/s10584-017-2121-y

Alpine foreland running drier? Sensitivity of a drought vulnerable catchment to changes in climate, land use, and water management

Clara Hohmann[1,2] · **Gottfried Kirchengast**[1,2,3] · **Steffen Birk**[2,4]

Received: 29 March 2017 / Accepted: 1 December 2017 / Published online: 23 December 2017
© The Author(s) 2017. This article is an open access publication

Abstract Southeastern Austria as part of the southeastern Alpine forelands experiences an increase of temperature and a tendency of decreasing precipitation. Especially in summer, the temperature strongly increased by about 0.7 °C per decade since the 1970s. Drought vulnerability under climate change is therefore a key question in this region. Here, we address this question by exploring the hydrological sensitivity of the Raab catchment in Austria (area 987 km^2), a typical catchment in these Alpine forelands. Using the process-oriented Water Flow and Balance Simulation Model (WaSiM) over 1982–2011, we focus on low-flow conditions during extended summer (May–September) and analyze the catchment's runoff sensitivity to climate change, but also land use and water management change. We find that climate change drivers dominate the summertime runoff response (decrease > 40/> 70%), based on moderate and strong climate change cases in the region (temperature + 2/+ 4 K, precipitation − 15/− 30%). Land use changes towards more dry and sealed areas enhance surface runoff and thus may lead to somewhat increased flood peaks. In contrast, water withdrawal for irrigation reduces runoff during low-flow periods in the summer when the irrigation demand is high. Although the impact of these non-climatic drivers on runoff generally is lower than that of the climate change considered, their interactive effects may reinforce the catchment's tendency of running drier during summer. While more detailed

Electronic supplementary material The online version of this article (https://doi.org/10.1007/s10584-017-2121-y) contains supplementary material, which is available to authorized users.

✉ Clara Hohmann
clara.hohmann@uni-graz.at

[1] Wegener Center for Climate and Global Change (WEGC), University of Graz, Graz, Austria

[2] FWF-DK Climate Change, University of Graz, Graz, Austria

[3] Institute for Geophysics, Astrophysics, and Meteorology/Institute of Physics, University of Graz, Graz, Austria

[4] Institute of Earth Sciences, NAWI Graz Geocenter, University of Graz, Graz, Austria

scenario-based assessments are needed to further assess drought risks, this initial study provides clear evidence for the vulnerability of Alpine foreland catchments to increasing summer dryness under climate change.

Keywords Catchment hydrology · Climate change · Sensitivity analysis · Environmental changes · Drought vulnerability

1 Introduction

The impact of climate and environmental changes on hydrology is an important aspect of water management and stakeholder decisions. The widely used scenario approach uses different climate projections for the assessment of impacts on water resources (Blöschl and Montanari 2010; Vano and Lettenmaier 2014; Wagner et al. 2017). But especially for precipitation, the input of primary importance for hydrological models, future scenarios are often very uncertain (Mishra et al. 2017; Wagner et al. 2017). A scenario-neutral approach is increasingly used for climate impact studies, since it is independent of climate change projections (Prudhomme et al. 2010; Brown and Wilby 2012). The overall idea is to acquire a better understanding of the uncertainties and to understand the predicted or projected changes (Blöschl and Montanari 2010). A sensitivity-based approach can help to better understand the system, does not need computationally intensive simulations, and is not necessary to update when new climate models are available (Vano and Lettenmaier 2014). As a foundation on physically consistent climate scenarios is lacking, the approach has its own limitations, though, and should be viewed as complementary to the scenario-based approaches.

Hydrological changes may not only result from climatic changes; also, other environmental changes like land use and water management strongly influence the water balance. When focusing on hydrological changes in the future, the distinction between the important drivers like changes of climate, land use, and water management is quite difficult. Especially on a catchment scale, climate changes might trigger land use and water management changes, and also adaptation strategies should be considered. Often, it is hard to distinguish between the effects of different changes. Therefore, we will analyze the different changes separately and in various combinations to achieve a better understanding of the hydrologic effects of different environmental changes.

For this study, the Raab catchment in southeastern Styria/Austria suits very well, since it is located within the southeastern Alpine forelands, a transition zone between the Alpine and the Mediterranean region which is especially vulnerable to climate change (Section 2). One of the effects of the warming summers might be a stronger vulnerability to drought. Laaha et al. (2016) recognized for this region a decreasing trend of low-flow runoffs, which means the catchments become drier. The Styrian Raab catchment was already affected by drought years in the recent past (e.g., 1992, 2001, 2003). With the temperature increase and a potential decline of precipitation amount in the future, droughts may occur more frequently especially in summer. In the present time, the human activities also have a significant influence on droughts and should be co-considered (Van Loon et al. 2016). For our analysis, we focus on low flow in the summer months to get a better understanding of the drought vulnerability of the Raab catchment.

Streamflow data of the recent past are used to calibrate and validate a process-oriented hydrological model (Section 3.1). The model provides the opportunity to investigate the possible effects of different long-term changes, which are normally slow processes with evolving interactions, by a sensitivity analysis. This study focuses on the hydrological sensitivity of the Raab catchment to climate, land use, and water management changes (Section 3.2), thus providing valuable information about possible low-flow hydrological futures within this and similar vulnerable catchments (Section 4). In particular, the results help to answer two questions (Section 5): (1) How does summer runoff and evapotranspiration respond to the different changes (drivers) and what are the characteristics of these driver-response relationships? (2) How do the anthropogenic non-climatic effects, i.e., changes in land use and irrigation, interact with climate change in a drought-vulnerable catchment? We close the paper with giving the main conclusions (Section 6).

2 Study region

The Raab is a typical southeastern Alpine foreland river, originating in the uplands of the eastern-most Alpine ridges in Austria (see the map in Fig. 1). The Raab's source is located in the "Passailer" Alps in the state of Styria, at a height of around 1150 m a.s.l. The Raab flows towards the southeast through Austria (states of Styria and Burgenland) and continues through Hungary where it ends as a tributary of the Danube. We focus on the Styrian Raab catchment (Fig. 1) up to gauging station Neumarkt (including a small part of Burgenland), with a river length of about 95 km and a catchment size of 987 km^2. The land use is dominated by agriculture (42%) and forest (40%), and the main soil texture is loam (50% silty loam and 41% loam) (Supplementary Fig. S1).

The region is especially interesting to study, since regional climate change is already clearly measurable, potentially because the global warming trend is regionally amplified by a simultaneous increase in solar irradiation related to a reduction of aerosols over the last few decades (Auer et al. 2007; Folini and Wild 2011; Nabat et al. 2014). The temperature in this Alpine foreland region, including the Raab catchment from about the City of Weiz southward, shows a strong summer temperature trend with an increase of near 0.7 °C per decade from 1971 to 2016 (Fig. 1, lower left panel; cf. also Kabas et al. 2011). Compared to the recent global warming trend of near 0.2 °C per decade since the 1970s (Willett et al. 2016; GISTEMP Team 2017), this change is more than three times as strong; compared to near 0.5 °C per decade over the European Alpine region (Gobiet et al. 2014), it is still almost 50% stronger. The precipitation trend is not distinct; the summer precipitation only shows a slight decrease near 1% per decade from 1971 to 2016 (Fig. 1, lower right panel). Yet, climate projections suggest that decreases in the order of 10–20% within the twenty-first century are realistic (Gobiet et al. 2014). Likewise, the river Raab exhibits only slightly decreasing summer streamflow (approximately 3% per decade; see Supplementary Fig. S2). Nevertheless, potential future decreases in precipitation bear the risk of amplifying the reduction of summertime streamflow resulting from enhanced evapotranspiration in a warming climate. This is the drought vulnerability narrative that we explore in this study.

The catchment can be split up into three parts (color tones in the map of Fig. 1): the *upper Raab* down to gauging station St. Ruprecht, with more forest and mountainous areas; the *middle Raab* from St. Ruprecht down to station Takern II, with less hilly areas

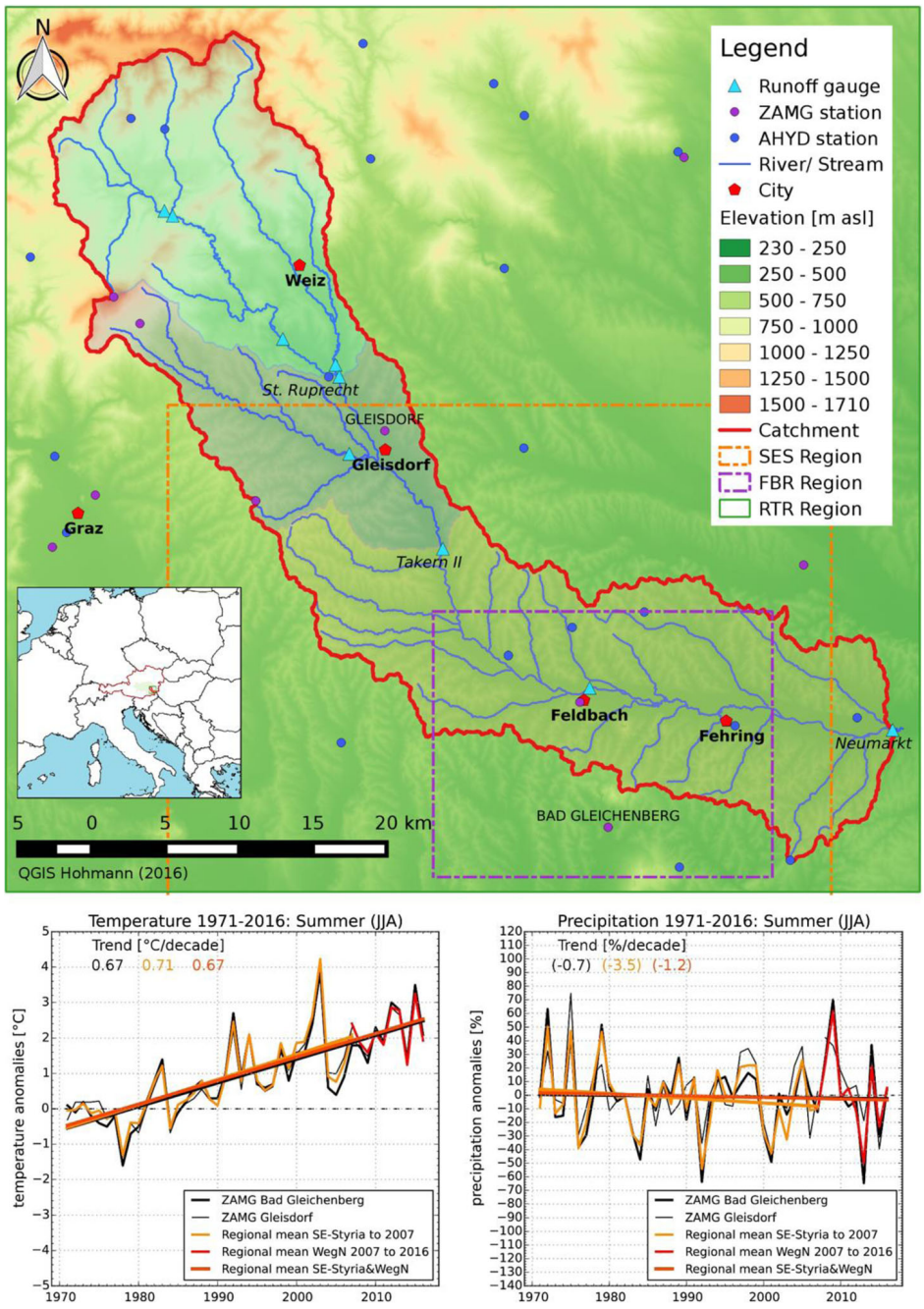


Fig. 1 Upper panel: map of the Raabtal region (RTR) located in southeastern Austria (see lower left inset), including the Styrian Raab catchment (red; with upper, middle, and lower sub-basins in different colors). Digital elevation model topography and other information elements such as station locations are shown as background and complementary information (see legend; southeastern Styria (SES) and Feldbach region (FBR, WegenerNet) are intensively studied sub-regions; Kabas et al. 2011; Kirchengast et al. 2014). Lower panels: summer (JJA) temperature (left) and precipitation (right) anomaly time series (relative to the 1971–1990 average) and corresponding trends over 1971 to 2016, for different sub-regions and climate-quality stations in the catchment region

dominated by agriculture and forest patches; and the *lower Raab* from Takern II down to station Neumarkt, with agriculture-dominated areas and patchy forests. We adopt the lower Raab as the focus region of this study, exhibiting the strongest anthropogenic imprints of the whole catchment. It includes the gauging station Feldbach, located between Takern II and Neumarkt, as interim station for runoff diagnostics.

3 Data and methods

3.1 Hydrological model and input data

We use the Water Flow and Balance Simulation Model (WaSiM), which was developed for climate change analysis in Alpine catchments by Schulla (1997). WaSiM is a well-established, distributed, deterministic, mainly physics-based and process-oriented hydrological model. The model was extensively used already and is thus well tested for climate change studies (e.g., Bürger et al. 2011; Gädeke et al. 2014) as well as for land use change studies (Alaoui et al. 2014; Yira et al. 2016). For our sensitivity analysis, we choose a reasonably simple model setup with WaSiM (Richards), version 9.09.08, with a daily time step (meteorological input, temperature, and precipitation) and a spatial resolution of 1 km × 1 km for the grids (digital elevation model, land use, soil). The input data, resolution, and sources are summarized and illustrated in Supplementary Table S1 and Fig. S1.

The unsaturated zone is modeled by the Richards approach with a Van Genuchten parametrization after Carsel and Parrish (1988). The potential evapotranspiration is calculated using a parsimonious temperature approach after Hamon (1960), in order to keep the meteorological data requirements as simple as possible. The Hamon approach was also used in other climate change studies (Bürger et al. 2011; Wanders and Wada 2015) and showed a good performance in studies comparing different evapotranspiration models (Oudin et al. 2005; Bormann 2011). For an overview of all WaSiM modules used in this study, see Fig. 2, where also the processes affected by land use and water management changes are indicated. A detailed WaSiM description can be found in Schulla (2015).

The model was calibrated to runoff time series from 2003 to 2009 at three Raab stations (St. Ruprecht, Takern II, Neumarkt) using the shuffled complex evolution optimization algorithm developed at the University of Arizona (SCE-UA) (Duan et al. 1994). The time series from 1995 to 2001 was used for validation. Beside the total discharge, also the runoff components (direct flow, interflow, baseflow) were visually analyzed for validation purposes.

The model performance was assessed using the Nash-Sutcliffe efficiency (NSE) (Nash and Sutcliffe 1970) in its standard form and, to account for the low flow focus, its logarithmic version (log NSE; see Section S2 in the supplementary material). The mean NSE over the three stations is 0.74 for the calibration period and 0.64 for the validation, and the log NSE is 0.76 for the calibration and 0.74 for the validation period. After Moriasi et al. (2007), the model has a *good* NSE model performance. This indicates that this model setup is well suitable for the targeted sensitivity simulations of the Raab catchment. We note that a more process-based model setup (e.g., for evapotranspiration and groundwater) as well as further improved input fields (e.g., for land use and soil) could be used for a more detailed follow-on study, but this is beyond the scope of this initial study. See the supplementary material (Sect. S2) for further information about the model setup and calibration.

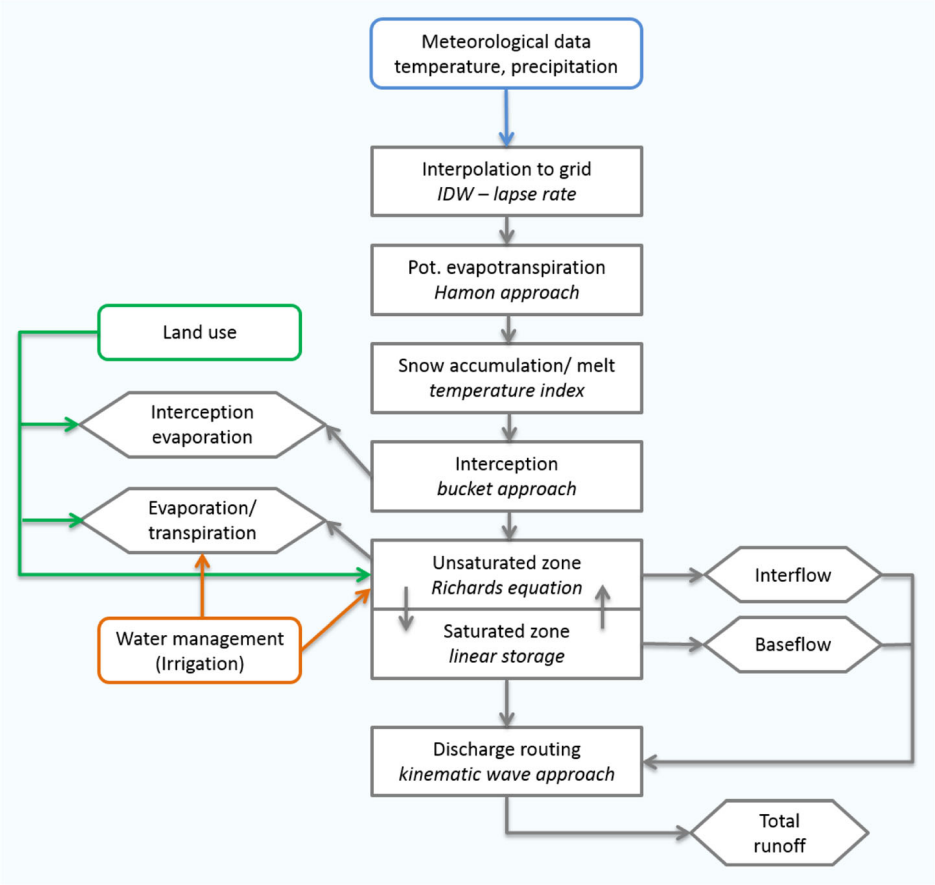


Fig. 2 WaSiM model structure used for the study; after Schulla (2015) and adding information on the chosen modeling approaches for specific main processes as well as indicating the driving influences focused on by the sensitivity analysis, climate change (blue, top), land use change (green, left), and water management change (orange, bottom left)

3.2 Drought sensitivity analysis

In order to analyze the sensitivity of the Raab catchment's hydrological response to possible future changes, different environmental changes are simulated. In the following, these different changes are described in detail (Table 1) and their implementation in WaSiM is specified (Fig. 2).

The temperature and precipitation changes (TC and PC, respectively) are based on the station time series of the recent past from 1982 to 2011 and applied to all days of the summer period. That is, every daily value of the extended summer season (May to September) is changed with an increase in temperature and/or a decrease in precipitation. We included moderate changes (temperature + 2 K, precipitation − 15%) and strong changes (temperature + 4 K, precipitation − 30%), which roughly reflect regional climate projections near the end of the century (e.g., Gobiet et al. 2014). A transition to less frequent but more intense rainfall, which has been suggested by climate models (e.g., Ban et al. 2015), is not considered here. Yet, the changes are only applied over the extended summer because climate change in the

Table 1 Environmental change cases simulated and investigated in the low-flow sensitivity analysis

Type of change	Temperature		Precipitation		Land use		Water management	
	Moderate (K)	Strong (K)	Moderate (%)	Strong (%)	Moderate	Strong	Moderate	Strong
TC	+2	+4						
PC			−15	−30				
LUC					→ sealed	→ sealed and → extensive agriculture		
WMC							Irrigation threshold 0.5	Irrigation threshold 0.8
TP	+2	+4	−15	−30				
TPL	+2	+4	−15	−30	→ sealed	→ sealed and → extensive agriculture		
TPLW	+2	+4	−15	−30	→ sealed	→ sealed and → extensive agriculture	Irrigation threshold 0.5	Irrigation threshold 0.8

TC temperature change, *PC* precipitation change, *LUC* land use change, *WMC* water management change, *TP* combined temperature and precipitation change, *TPL* TP change and, in addition, land use change, *TPLW* TPL change and, in addition, water management change

recent past was especially distinct in the summer months (Kabas et al. 2011). These modified station data are then used as meteorological input to WaSiM, where the data are internally interpolated to grids (Schulla 2015).

Land use changes (LUCs) are implemented as variations of land use classes in WaSiM. For our LUC cases, we changed the input grid of the land use classes in two respects to create a moderate and a strong case. Because of population growth, the cities and populated areas likely become bigger, so our moderate LUC case includes the change of all *partly sealed* grid cells to *sealed* ones. With more dryness experienced over the coming decades, the vegetation will likely change into drier vegetation, challenging agricultural activities; our strong LUC case therefore includes, in addition, the change of 50% *intensive agriculture* and 100% *complex cultivation pattern* grid cells to *extensive agriculture* cells, i.e., a shift to less-water-demanding crops.

Water management changes (WMCs) are considered by introducing irrigation, which is not included in the baseline model setup. We assume irrigation with surface water and its actual use controlled by a demand-driven approach available in WaSiM. If the ratio of actual evapotranspiration to potential evapotranspiration is higher than a specific threshold, all grid cells in a specific class (land use dependent) are irrigated (Fuhrer and Jasper 2012). As limitations in water availability, the available financial resources, or other constraints are not considered, this approach potentially results in irrigation schemes that require unrealistic amounts of water. To examine the effect of different extents of irrigation, we consider two possible irrigation setups that differ in the threshold ratio of actual evapotranspiration to potential evapotranspiration. We assign all intensive agriculture and complex cultivation pattern cells for possible irrigation and use a threshold of 0.5 for the moderate WMC case and of 0.8 for the strong WMC case, respectively, like used by Fuhrer and Jasper (2012).

Beside the individual change cases described above, also combinations are simulated to get an idea how these different human-induced environmental changes interact. In order to see the effect of total meteorological changes, temperature and precipitation are changed together (TP), with a moderate TP change of + 2 K temperature and − 15% precipitation and strong change of + 4 K temperature and − 30% precipitation (Table 1). As the next step, the land use changes are added (TPL) and, finally, the water management change is also included (TPLW).

4 Sensitivity simulation results

For instructive display and interpretation of the various environmental changes of the sensitivity study, diverse foci and formats to visualize the data are chosen (Figs. 3, 4, and 5).

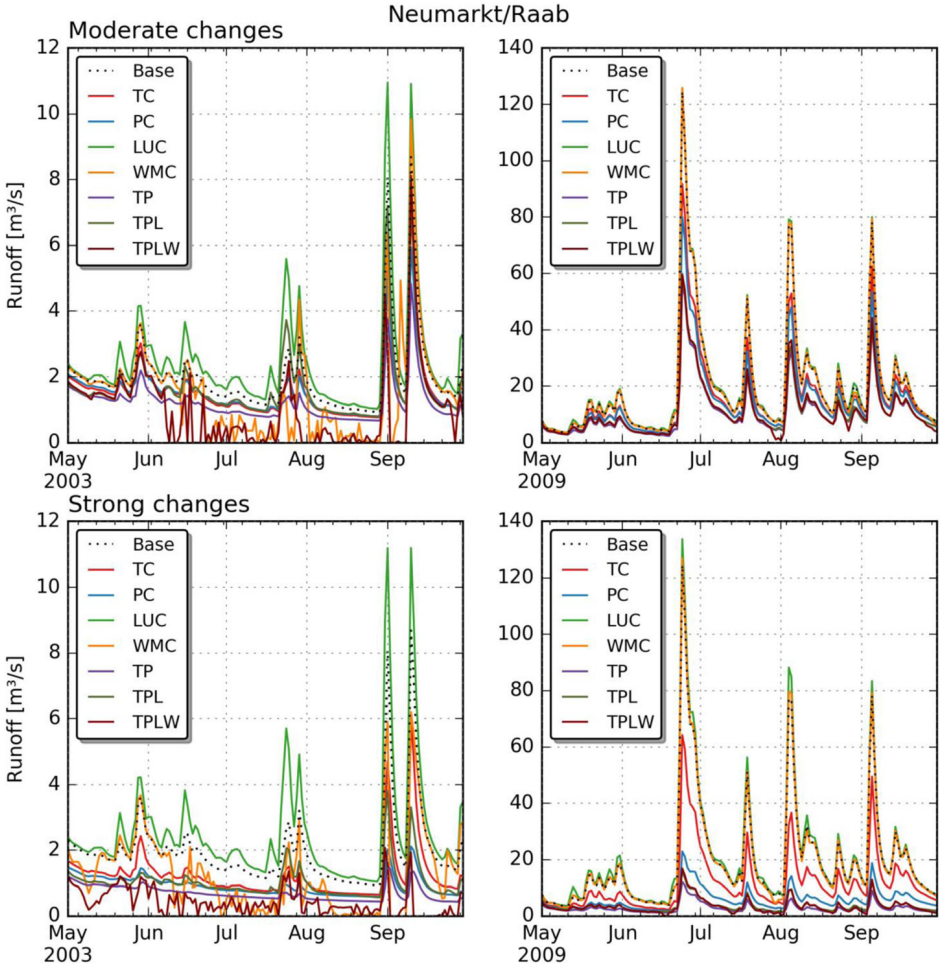


Fig. 3 Daily time series of the runoff at station Neumarkt, for the specific dry year 2003 (left) and the specific wet year 2009 (right), respectively, for both moderate (top panels) and strong (bottom panels) environmental changes

Supplement S3 (Table S5) provides the water budget terms of the entire catchment for all considered cases.

All the environmental changes influence the daily runoff differently in various years (e.g., in specific dry/wet years such as 2003/2009) and in comparison between moderate and strong changes (Fig. 3). Especially noticeable are the WMC and TPLW cases, which clearly show the irrigation influence on the summer runoff of 2003 (Fig. 3, left panels). The moderate WMC

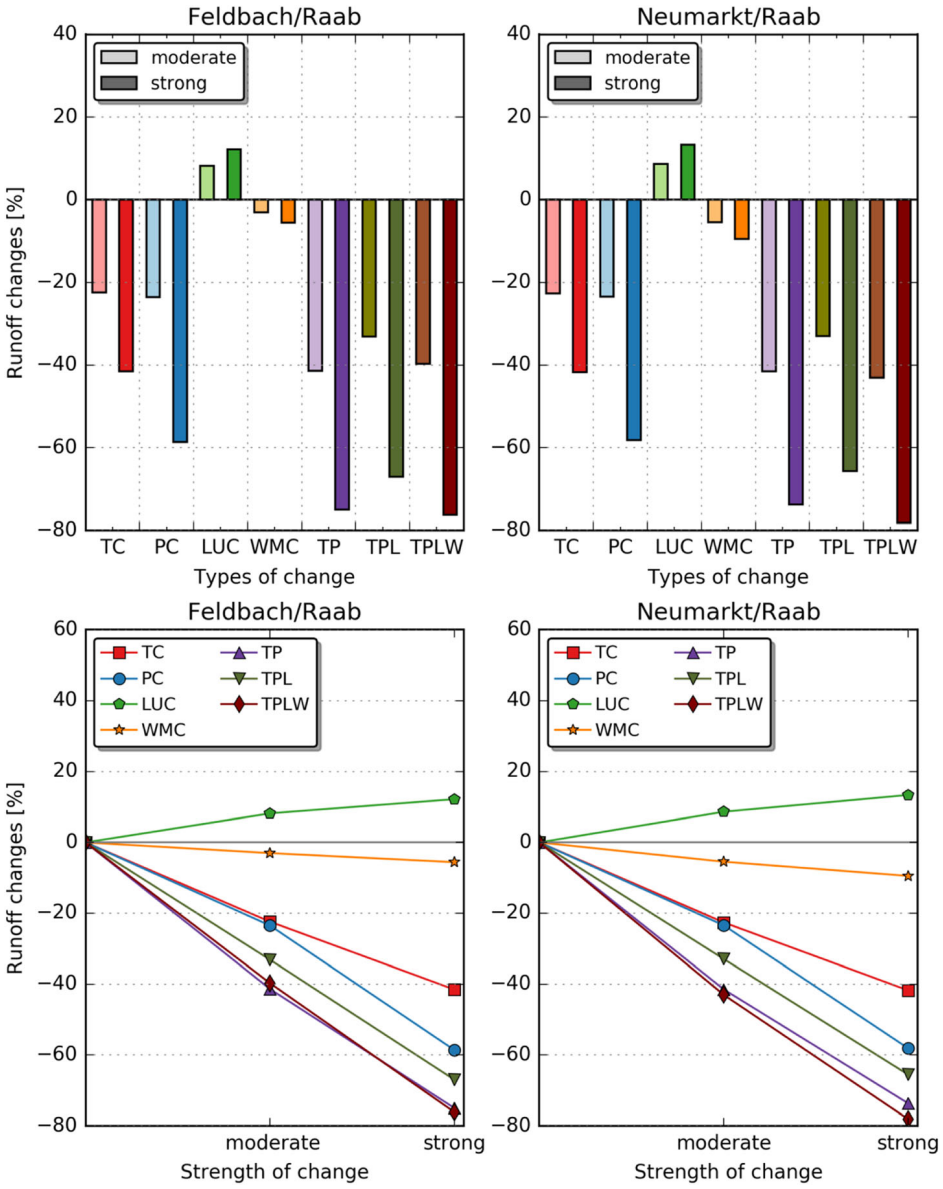


Fig. 4 Average (1982–2011) summertime (MJJAS) runoff changes for the station Feldbach (left) and Neumarkt (right), estimated for the seven sensitivity cases (types of change) for both moderate and strong changes, shown in type-based (top) and strength-based (bottom) views

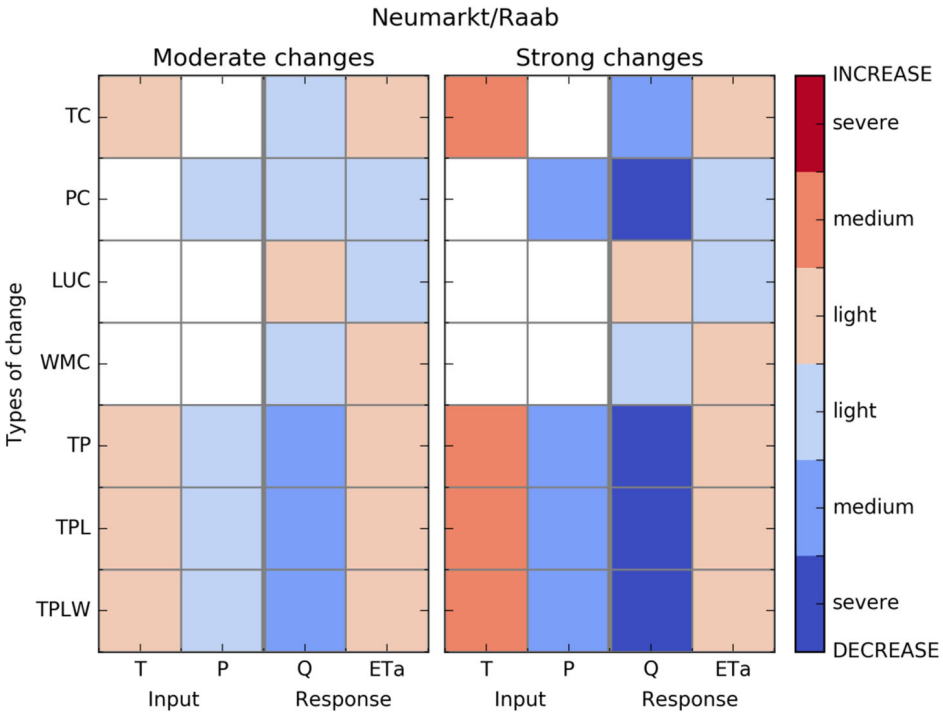


Fig. 5 Severity and direction (increase or decrease) of average (1982–2011) summertime (MJJAS) changes of the input variables temperature (T) and precipitation (P) as well as the response variables runoff (Q) and actual evapotranspiration (ETa) over the whole catchment, illustrated using three severity classes (color bar at the right; light < 2.5 K, < 25%; medium 2.5–5 K, 25–50%; severe > 5 K, > 50%; white = no change) for the seven sensitivity cases (types of change)

and TPLW cases are not that distinct as the strong one. For example, in May 2003, the moderate WMC does not lead to a runoff reduction as marked as the strong WMC. Between mid of August and beginning of September, the strong WMC leads to almost no water in the river for that period, under the moderate WMC only at some days. In May 2003, under moderate changes, the TP, TPL, and TPLW cases are almost the same, but by the end of May, under TPL and TPLW, more runoff is simulated. In June, the irrigation came into account and runoff in the TPLW case becomes very small.

The year 2009 is quite wet, that is why not much irrigation occurs and the discharge is mostly the same as the base run (Fig. 3, right panels). This is also the case with the effects of the LUC, which are also more distinct in the dry year 2003 compared to the wet year 2009. The meteorological changes (TC and PC) are pronounced in all years, with a much stronger runoff reduction under strong changes (Fig. 3).

The sensitivities in terms of the mean percentage runoff changes of the extended summers of the whole period of 30 years (1982–2011), for all different environmental change cases, are inspected for the lower Raab catchment stations Feldbach/Raab and Neumarkt/Raab (Fig. 4). As expected, the discharge is less sensitive to the moderate changes than to the strong changes, but the direction of the diverse environmental changes is different. The meteorological changes (TC and PC) lead to a runoff reduction, as well as the WMC, while the LUC leads to more runoff. The combined changes (TP, TPL, TPLW) always lead to negative sensitivities, towards summer dryness. The combination of all changes (TPLW) leads to the most severe runoff

decrease (of near 80% in the strong case) in our study, directly followed by TP where only the climatic changes are acting. The runoff changes at station Feldbach/Raab (Fig. 4, left panels) compared to Neumarkt/Raab (Fig. 4, right panels) show the same general pattern, with slightly stronger runoff changes at Neumarkt/Raab.

The characteristics of model input variables temperature (T) and precipitation (P) as well as model response variables runoff (Q) and actual evapotranspiration (ETa) are finally visualized in a box diagram to better understand the input-response relationships (Fig. 5). Temperature and precipitation changes always trigger a clear reaction (TC/PC). When the changes are moderate, the combined changes (TP, TPL, TPLW) have the heaviest influence on runoff (Fig. 5, left panel). Under the strongly changing conditions, the combined changes (TP, TPL, TPLW) again influence the runoff the most, but also the strong reduction of precipitation (PC) exerts a strong negative response (Fig. 5, right panel). In total, the reaction is most visible in the runoff response, but also the actual evapotranspiration shows a light reaction up to 25%. The latter exhibits a positive response to most of the changes, i.e., increased actual evapotranspiration, except for PC and LUC, which lead to decreased actual evapotranspiration.

5 Discussion of the drought sensitivities

The results summarized in the previous section help to analyze relative changes of runoff in response to changes of environmental conditions within the Raab catchment. Here, we provide an interpretation and discuss important implications.

Precipitation is the most important input factor in hydrological models (e.g., McCabe and Wolock 2011). In our study, the effects observed for the PC cases are also more pronounced than those for the TC cases (Fig. 4). The sensitivity study revealed a non-additive behavior of temperature and precipitation. Runoff is somewhat less reduced in the combined TP case than the additive change from the TC and the PC case (Fig. 4). This results from water availability limitations, since a higher temperature leads to more evapotranspiration only if sufficient water is available (Laaha et al. 2016). Especially for the strong changes, assuming 30% less rainfall, the water is limited on many days of the year, which leads to less actual evapotranspiration (Fig. 5).

Runoff appears less sensitive to LUC than to PC (Fig. 4) as was also found by Deshmukh and Singh (2016) who noted the land use changes as a second order control on mean annual streamflow in most of their analyzed catchments in the USA. Also, other studies show that precipitation is more important to explain changes in the runoff than land use changes (e.g., Gupta et al. 2015). In our study, the moderate LUC with more sealed areas leads to increased runoff (Fig. 4) and a reduction of actual evapotranspiration (Fig. 5). This is caused by increased surface runoff because the water has fewer areas to infiltrate into the soil and reaches the river much faster. The strong LUC, with more sealed areas plus less intensive agriculture, further strengthened the increased runoff and decreased actual evapotranspiration, because extensive agriculture needs less water than intensive one (Fig. 5).

The actual evapotranspiration is slightly increased under the WMC cases (Fig. 5), because with irrigation, more water is available for plants, especially on dry days. The water management also influences the runoff. The WMC cases use surface water for irrigation and therefore lead to decreased runoff (Figs. 3 and 4). The mean changes over the 30-year period analyzed are quite small compared to other individual changes. However, especially in dry years (such as 2003), the irrigation plays an important role since the river might fall dry if the irrigation

water is withdrawn from the surface waters within the catchment (Fig. 3). It should thus be questioned how sustainable and realistic this irrigation scheme is.

Fuhrer and Jasper (2012) already noted that the limitation of water will be an important point in the climate change—agriculture production discussion. The irrigation demand in the future is very uncertain and region dependent (Woznicki et al. 2015). Ferguson and Maxwell (2012), for example, analyzed a semi-arid catchment in the USA under climate change versus irrigation and pumping. They conclude that climate change impacts and water management impacts on stream discharge are nearly equivalent in their study area and under their scenarios. In contrast, Tang et al. (2008) found for the Yellow River in China that human activities dominated streamflow changes only in the lower reaches of the river, whereas climate change was the dominant driver in the upper and middle reaches.

Our study additionally provides insight into the interactive effects of different human activities, namely land use change and irrigation. The TP and TPLW cases almost show the same mean runoff changes (Fig. 4). Thus, over the whole time period, the water use for irrigation compensates for the increased runoff due to the LUC, which is seen for the TPL case (Fig. 4). The evapotranspiration deficit from the LUC (Fig. 5) seems to be compensated by the irrigation water as well. Inspecting the daily runoff time series, it becomes clear, however, that TP and TPLW do not show the same behavior (Fig. 3). The example of moderate changes in 2003 at station Neumarkt/Raab (Fig. 3) shows that even with the same hydrological starting conditions for the TP, TPL, and TPLW cases at the beginning of May 2003, TPL and TPLW simulate increased runoff at the end of May, caused by the land use changes. In June, the irrigation comes into play and the runoff is hence strongly reduced under the TPLW case. Thus, within particularly dry periods, the TPLW simulates less runoff because of the water withdrawal for irrigation and, when it is wetter, the LUC dominates with more runoff.

Although these effects nearly compensate the total mean over the whole period (compare TP and TPLW in Fig. 4), the tendency to more pronounced peak flows (due to enhanced surface runoff) and reduced low flows (due to irrigation withdrawals) suggests that the runoff regime tends to more extremes (floods and droughts). Such interactive effects of land use change and irrigation thus would amplify a climate-driven increase in hydrological extremes, which may result from the expected increase in extreme precipitation (e.g., Ban et al. 2015). This might be indicated by the observed tendency towards lower minimum and higher maximum summer runoff of the river Raab (see Supplementary Fig. S2).

In order to analyze additional factors which are influenced by the environmental changes imposed, we used the actual evapotranspiration. In our model setup, the potential evapotranspiration was controlled by temperature. Also, the strong dependency, therefore, of actual evapotranspiration on the temperature is clearly visible, since changes of actual evapotranspiration are mostly combined with an alteration of temperature (Fig. 5). Our sensitivity study suggests that the enhanced evapotranspiration resulting from a warming of 2 °C causes a runoff decrease of 20%.

In the Raab catchment, a temperature increase of about this size was observed within the last three decades (see Fig. 1), but the tendency towards lower runoff (Supplementary Fig. S2) appears to be weaker than suggested by the model. This might indicate that the simplified temperature-based approach causes an overestimation of evapotranspiration (Sheffield et al. 2012). Relative to the variance of the runoff time series, however, the observed tendency is not very distinct and thus highly uncertain. In addition, the Raab runoff likely is affected by direct human impacts such as river regulation, which are not explicitly considered by the model. The impacts of these simplifications on the simulated runoff thus deserve further investigation.

Our results, nevertheless, give an initial idea how non-climatic anthropogenic changes might co-affect the runoff in our southeastern Alpine foreland catchment. We found this clearly dominated by the climatic changes that the future may hold for this region. In addition, land use changes and water use for irrigation need to be co-considered for future water resources management and its impact on runoff in the Raab catchment. The intensity of the actual runoff changes is dependent on how the forcings (environmental changes) actually unfold over time and the sensitivity of the catchment (Berghuijs et al. 2016). In this context, our sensitivity study provides valuable initial information about the potential effects of environmental changes in this and similar drought-vulnerable catchments.

6 Conclusions

This hydrological sensitivity study provided initial quantifications and insights to the runoff sensitivity to different environmental changes of the Raab catchment in the southeastern Alpine foreland region of Europe. We used the process-oriented Water Flow and Balance Simulation Model (WaSiM) for the analysis.

The possible future climatic changes in the region, based on trends over the recent decades and climate model projections, may include increased summer temperature and decreased precipitation, which may be accompanied by increased water use for irrigation. All these drivers lead to a runoff reduction that may be substantial in combination. Anthropogenic land use changes, including those of more sealed areas and less intensive agriculture, result in more surface runoff and less actual evapotranspiration, thus partially counteracting the runoff reduction.

More specifically, based on moderate and strong climate change cases in the catchment (temperature + 2/+ 4 K, precipitation − 15/− 30%), optionally combined with human-induced more dry and sealed areas as well as more water use for irrigation, we found the summertime runoff response dominated by climate change. The most important single climatic driver is the precipitation change. The moderate/strong precipitation decrease was estimated to lead to more than 20/50% runoff decrease, together with temperature increase to more than 40/70% decrease (all estimates as an average decrease over a 30-year period).

The combined changes of temperature and precipitation did not lead to an exactly additive decrease of the runoff but to a somewhat less decrease, due to limited water availability. Changes in land use and irrigation were found relevant but minor contributors on average. All changes together lead to the strongest runoff decrease by nearly 80%. However, analysis of the daily time series in specific dry years (such as 2003) and wet years (such as 2009) showed that the runoff evolution in individual years can be drastically different from the average estimate and that irrigation and land use change can play key roles for low flow in individual years. The expected land use changes may help reduce the overall tendency towards decreases in river runoff. However, they tend to enhance surface runoff and peak flows, thus reducing groundwater recharge and baseflow.

The actual evapotranspiration showed less distinct responses to the environmental changes than the runoff. An increase of temperature generally results in an increase of actual evapotranspiration; however, particularly in drought periods, this increase is limited by the low availability of water in the soil. In addition, irrigation leads to an increase of actual evapotranspiration, since more water is available for the vegetation in this case.

This initial study provided clear evidence for the vulnerability of Alpine foreland catchments in this type of setting to increased summer dryness under future climate change. It furthermore showed that it is important to also include non-climatic aspects because of interactions and compensation effects of such changes. More detailed scenario-based assessments are needed as the next step to improve our understanding of how strongly the southeastern Alpine forelands are at risk of drought at the local scale of individual catchments.

Acknowledgements We thank T. Kabas (WEGC) for providing the long-term trend results, included in Fig. 1, and M. Switanek (WEGC) for the support regarding the SCE-UA algorithm used for calibration. The interdisciplinary faculty and students of the FWF-DK are thanked for the discussion and comments. The Austrian Hydrographic Service and the National Weather Service ZAMG provided the hydrometeorological station data; further auxiliary data sources (topography, land cover, soil) are summarized in Table S1. The WaSiM model was obtained via http://www.wasim.ch, and we thank J. Schulla (Zurich, CH) and W. Rieger (TU Munich, DE) for their helpful advice.

Funding information This work was funded by the FWF-DK Climate Change of the Austrian Science Fund (Doctoral Program No. W1256-G15; http://dk-climate-change.uni-graz.at) and co-funded by the University of Graz. Open access funding provided by Austrian Science Fund (FWF).

Open Access This article is distributed under the terms of the Creative Commons Attribution 4.0 International License (http://creativecommons.org/licenses/by/4.0/), which permits unrestricted use, distribution, and reproduction in any medium, provided you give appropriate credit to the original author(s) and the source, provide a link to the Creative Commons license, and indicate if changes were made.

References

Alaoui A, Willimann E, Jasper K et al (2014) Modelling the effects of land use and climate changes on hydrology in the Ursern Valley, Switzerland. Hydrol Process 28:3602–3614. https://doi.org/10.1002/hyp.9895

Auer I, Böhm R, Jurkovic A et al (2007) HISTALP—historical instrumental climatological surface time series of the Greater Alpine Region. Int J Climatol 27:17–46. https://doi.org/10.1002/joc.1377

Ban N, Schmidli J, Schär C (2015) Heavy precipitation in a changing climate: does short-term summer precipitation increase faster? Geophys Res Lett 42:1165–1172. https://doi.org/10.1002/2014GL062588

Berghuijs WR, Hartmann A, Woods RA (2016) Streamflow sensitivity to water storage changes across Europe. Geophys Res Lett 43:1980–1987. https://doi.org/10.1002/2016GL067927

Blöschl G, Montanari A (2010) Climate change impacts—throwing the dice? Hydrol Process 24:374–381. https://doi.org/10.1002/hyp

Bormann H (2011) Sensitivity analysis of 18 different potential evapotranspiration models to observed climatic change at German climate stations. Clim Chang 104:729–753. https://doi.org/10.1007/s10584-010-9869-7

Brown C, Wilby RL (2012) An alternate approach to assessing climate risks. EOS Trans Am Geophys Union 93: 401–412. https://doi.org/10.1029/2012EO410001

Bürger G, Schulla J, Werner AT (2011) Estimates of future flow, including extremes, of the Columbia River headwaters. Water Resour Res 47:1–18. https://doi.org/10.1029/2010WR009716

Carsel RF, Parrish RS (1988) Developing joint probability distributions of soil water retention characteristics. Water Resour Res 24:755–769. https://doi.org/10.1029/WR024i005p00755

Deshmukh A, Singh R (2016) Physio-climatic controls on vulnerability of watersheds to climate and land use change across the U. S. Water Resour Res 52:8775–8793. https://doi.org/10.1002/2016WR019189

Duan Q, Sorooshian S, Gupta VK (1994) Optimal use of the SCE-UA global optimization method for calibrating watershed models. J Hydrol 158:265–284. https://doi.org/10.1016/0022-1694(94)90057-4

Ferguson IM, Maxwell RM (2012) Human impacts on terrestrial hydrology: climate change versus pumping and irrigation. Environ Res Lett 7(1–8):44022. https://doi.org/10.1088/1748-9326/7/4/044022

Folini D, Wild M (2011) Aerosol emissions and dimming/brightening in Europe: sensitivity studies with ECHAM5-HAM. J Geophys Res Atmos. https://doi.org/10.1029/2011JD016227

Fuhrer J, Jasper K (2012) Demand and supply of water for agriculture: influence of topography and climate in pre-Alpine, mesoscale catchments. Nat Resour 3:145–155. https://doi.org/10.4236/nr.2012.33019

Gädeke A, Hölzel H, Koch H et al (2014) Analysis of uncertainties in the hydrological response of a model-based climate change impact assessment in a subcatchment of the Spree River, Germany. Hydrol Process 28:3978–3998. https://doi.org/10.1002/hyp.9933

GISTEMP Team, 2017: GISS Surface Temperature Analysis (GISTEMP). NASA Goddard Institute for Space Studies. Dataset accessed 2017-03-10 at https://data.giss.nasa.gov/gistemp/

Gobiet A, Kotlarski S, Beniston M et al (2014) 21st century climate change in the European Alps—a review. Sci Total Environ 493:1138–1151. https://doi.org/10.1016/j.scitotenv.2013.07.050

Gupta SC, Kessler AC, Brown MK, Zvomuya F (2015) Climate and agricultural land use change impacts on streamflow in the upper Midwestern United States. Water Resour Res 51:5301–5317. https://doi.org/10.1002/2015WR017323

Hamon WR (1960) Estimating potential evapotranspiration. Department of Civil and Sanitary Engineering, Massachusetts Institute of Technology, Cambridge

Kabas T, Foelsche U, Kirchengast G (2011) Seasonal and annual trends of temperature and precipitation within 1951/1971–2007 in south-eastern Styria, Austria. Meteorol Zeitschrift 20:277–289. https://doi.org/10.1127/0941-2948/2011/0233

Kirchengast G, Kabas T, Leuprecht A et al (2014) WegenerNet: a pioneering high-resolution network for monitoring weather and climate. Bull Am Meteorol Soc 95:227–242. https://doi.org/10.1175/BAMS-D-11-00161.1

Laaha G, Parajka J, Viglione A et al (2016) A three-pillar approach to assessing climate impacts on low flows. Hydrol Earth Syst Sci 20:3967–3985. https://doi.org/10.5194/hess-20-3967-2016

McCabe GJ, Wolock DM (2011) Independent effects of temperature and precipitation on modeled runoff in the conterminous United States. Water Resour Res 47(1–11):W11522. https://doi.org/10.1029/2011WR010630

Mishra V, Shah HL, Kumar R et al (2017) Multimodel assessment of sensitivity and uncertainty of water availability under climate change. Clim Chang 141:451–465. https://doi.org/10.1007/s10584-016-1886-8

Moriasi DN, Arnold JG, Van Liew MW et al (2007) Model evaluation guidelines for systematic quantification of accuracy in watershed simulations. Trans ASABE 50:885–900. 10.13031/2013.23153

Nabat P, Somot S, Mallet M et al (2014) Contribution of anthropogenic sulfate aerosols to the changing Euro-Mediterranean climate since 1980. Geophys Res Lett 41:5605–5611. https://doi.org/10.1002/2014GL060798

Nash JE, Sutcliffe JV (1970) River flow forecasting through conceptual models. Part I—a discussion of principles. J Hydrol 10:282–290. https://doi.org/10.1016/0022-1694(70)90255-6

Oudin L, Hervieu F, Michel C et al (2005) Which potential evapotranspiration input for a lumped rainfall-runoff model? Part 2—towards a simple and efficient potential evapotranspiration model for rainfall-runoff modelling. J Hydrol 303:290–306. https://doi.org/10.1016/j.jhydrol.2004.08.026

Prudhomme C, Wilby RL, Crooks S et al (2010) Scenario-neutral approach to climate change impact studies: application to flood risk. J Hydrol 390:198–209. https://doi.org/10.1016/j.jhydrol.2010.06.043

Schulla J (1997) Hydrologische Modellierung von Flussgebieten zur Abschätzung der Folgen von Klimaänderungen. Geogr. Inst., Eidg. Tech. Hochsch., Zurich

Schulla J (2015) Model description WaSiM. Technical report, www.wasim.ch (09.03.2016)

Sheffield J, Wood EF, Roderick ML (2012) Little change in global drought over the past 60 years. Nature 491:435–438. https://doi.org/10.1038/nature11575

Tang Q, Oki T, Kanae S et al (2008) Hydrological cycles change in the Yellow River basin during the last half of the twentieth century. J Clim 21:1790–1806. https://doi.org/10.1175/2007JCLI1854.1

Van Loon AF, Gleeson T, Clark J et al (2016) Drought in the Anthropocene. Nat Geosci 9:89–91. https://doi.org/10.1038/ngeo2646

Vano JA, Lettenmaier DP (2014) A sensitivity-based approach to evaluating future changes in Colorado River discharge. Clim Chang 122:621–634. https://doi.org/10.1007/s10584-013-1023-x

Wagner T, Themeßl M, Schüppel A et al (2017) Impacts of climate change on stream flow and hydro power generation in the Alpine region. Environ Earth Sci 76:1–22. https://doi.org/10.1007/s12665-016-6318-6

Wanders N, Wada Y (2015) Human and climate impacts on the 21st century hydrological drought. J Hydrol 526:208–220. https://doi.org/10.1016/j.jhydrol.2014.10.047

Willett KM, Hurst DF, Dunn RJH, Dolman AJ (eds) (2016) Global climate [in "state of the climate in 2015"]. Bull Amer Meteor Soc 97:S7–S62. https://doi.org/10.1175/2016BAMSStateoftheClimate.1

Woznicki SA, Nejadhashemi AP, Parsinejad M (2015) Climate change and irrigation demand: uncertainty and adaptation. J Hydrol Reg Stud 3:247–264. https://doi.org/10.1016/j.ejrh.2014.12.003

Yira Y, Diekkrüger B, Steup G, Bossa AY (2016) Modeling land use change impacts on water resources in a tropical West African catchment (Dano, Burkina Faso). J Hydrol 537:187–199. https://doi.org/10.1016/j.jhydrol.2016.03.052

Electronic Supplementary Material—Hohmann et al. Paper "Alpine foreland running drier? Sensitivity of a drought vulnerable catchment to changes in climate, land use, and water management"

S1 Input Data

The input data for the WaSiM model setup as well as their sources are summarized in Table S1 and briefly described below.

The meteorological input for temperature and precipitation is based on daily station data. The data were received from the Austrian Hydrographic Service and the Austrian National Weather Service (ZAMG) in quality-controlled form and were visually quality controlled as a cross-check. In WaSiM the station data are internally interpolated to a target grid (1 km x 1 km in our study), for which different interpolation options are available. For the interpolation of temperature, we used the method of Inverse Distance Interpolation (IDW), weighted in with 75%, employed together with a combination of nearest neighbor selection and constant lapse rate (Thiessen laps rate), weighted in with 25%. For precipitation interpolation we used 100% IDW. Illustrative results showing climatologically averaged interpolated fields for the period 2003 to 2009 are depicted in the lower panels of Fig. S1, exhibiting the average of the annual mean temperatures (left) and the average of the annual precipitation amounts (right).

The runoff data are also available as daily data from gauging stations in the catchment and were received from the Austrian Hydrographic Service. We indirectly used them for the WaSiM modeling only, for comparison of simulated and observed runoff as part of model calibration and validation.

The digital elevation model (DEM), received from the state of Styria and state of Burgenland geographic information services as a 10 m/30 m DEM, was aggregated to the 1 km target grid.

The land use type dataset adopted is the CORINE data set from 2006, because this fits best for the calibration period (2003-2009). We cross-checked for temporal change but no drastic changes are found in the catchment of interest from inter-comparing the CORINE data sets for 1990, 2000, 2006, and 2012. As part of the modeling preparation, the land use data were as well resampled from the 100 m CORINE resolution to the 1 km target grid. The dataset is illustrated in the upper left panel of Fig. S1.

The soil texture data are based on the Agricultural Soil Map of Austria provided by the Austrian forest research center (BFW) as a free online dataset (https://geometadaten.lfrz.at Agricultural Soil Map of Austria). The soil information was only available for agricultural areas. We also aggregated the soil data to the 1 km target grid, with soil texture in the forest areas computed by stretching them in from the surrounding agricultural areas. The data are illustrated in the upper right panel of Fig. S1.

Because of a lack of detailed information about different soil layers, the same soil texture, combined with the hydraulic parameters, was assumed to be applicable for the total soil depth. For numerical reasons the model resolution of the soil layers, to solve the Richards equation, is separated into different soil layers: we divided the upper soil part with a thickness of 40 cm in 10 cm layers, the middle part of 60 cm in 15 cm layers, and the lower part with a thickness of 9 m in 0.3 m layers. In the unsaturated zone module in WaSiM the parameter with the Van Genuchten parametrization are based on literature (Carsel and Parrish 1988; Schulla 2015). These settings were found robust and adequate from extensive sensitivity tests on how various soil discretization setups influence the modeling performance.

Table S1 Raw data sets for the Raab catchment used as a model input to WaSiM (ZAMG … Austrian Meteorological Service; AHYD … Austrian Hydrographic Service; Land Stmk & Land Bgld … Government departments on water resources of the Austrian States of Styria and Burgenland)

Data type	No. stations/ Data set	Resolution	Source
Precipitation	32	daily (within 1982-2011)	ZAMG and AHYD
Temperature	9	daily (within 1982-2011)	ZAMG
Runoff	9	daily (within 1982-2011)	AHYD
Topography	Digital elevation model	10 m → 1 km grid	Land Stmk and Land Bgld
Land cover	CORINE (2006) data	100 m → 1 km grid	http://land.copernicus.eu/pan-european/corine-land-cover
Soil	Soil texture map	polygon agricultural areas → 1 km grid	https://geometadaten.lfrz.at Agricultural Soil Map of Austria

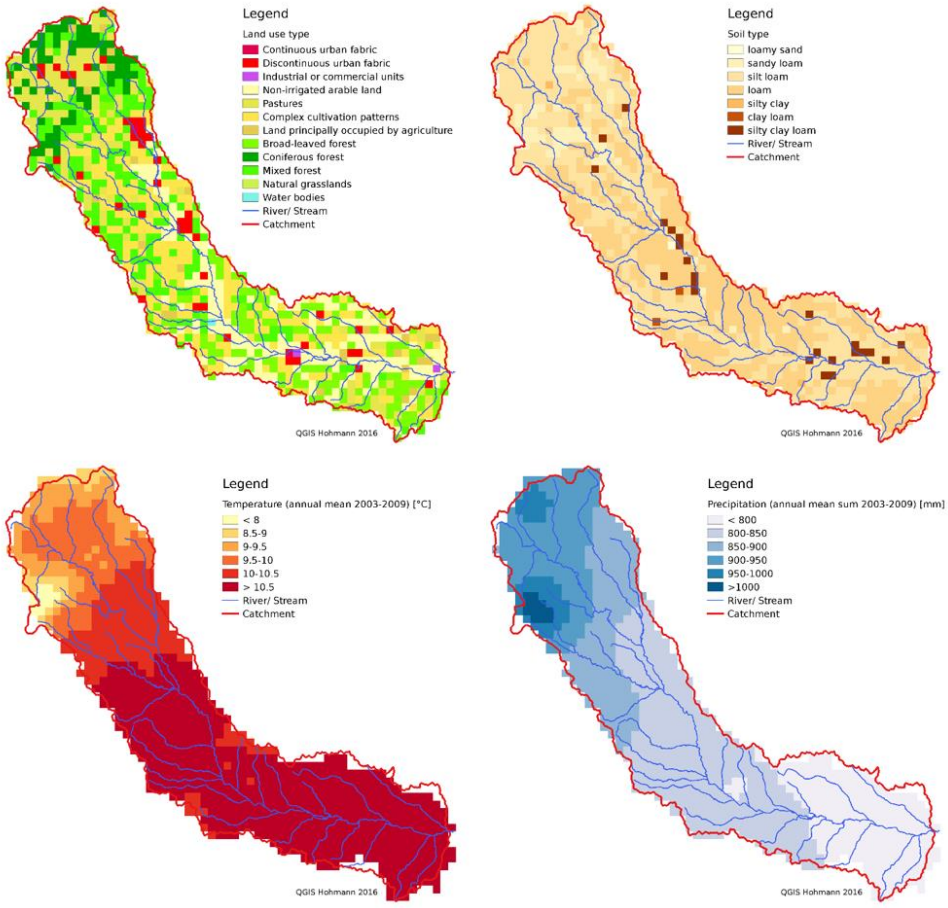


Fig. S1 Illustration of gridded input data to WaSiM. At the top the land use grid (left) and soil grid (right) are shown. The lower panels show the average annual-mean temperature (left) and the average annual precipitation a (right) over the calibration period from 2003 to 2009, calculated within WaSiM.

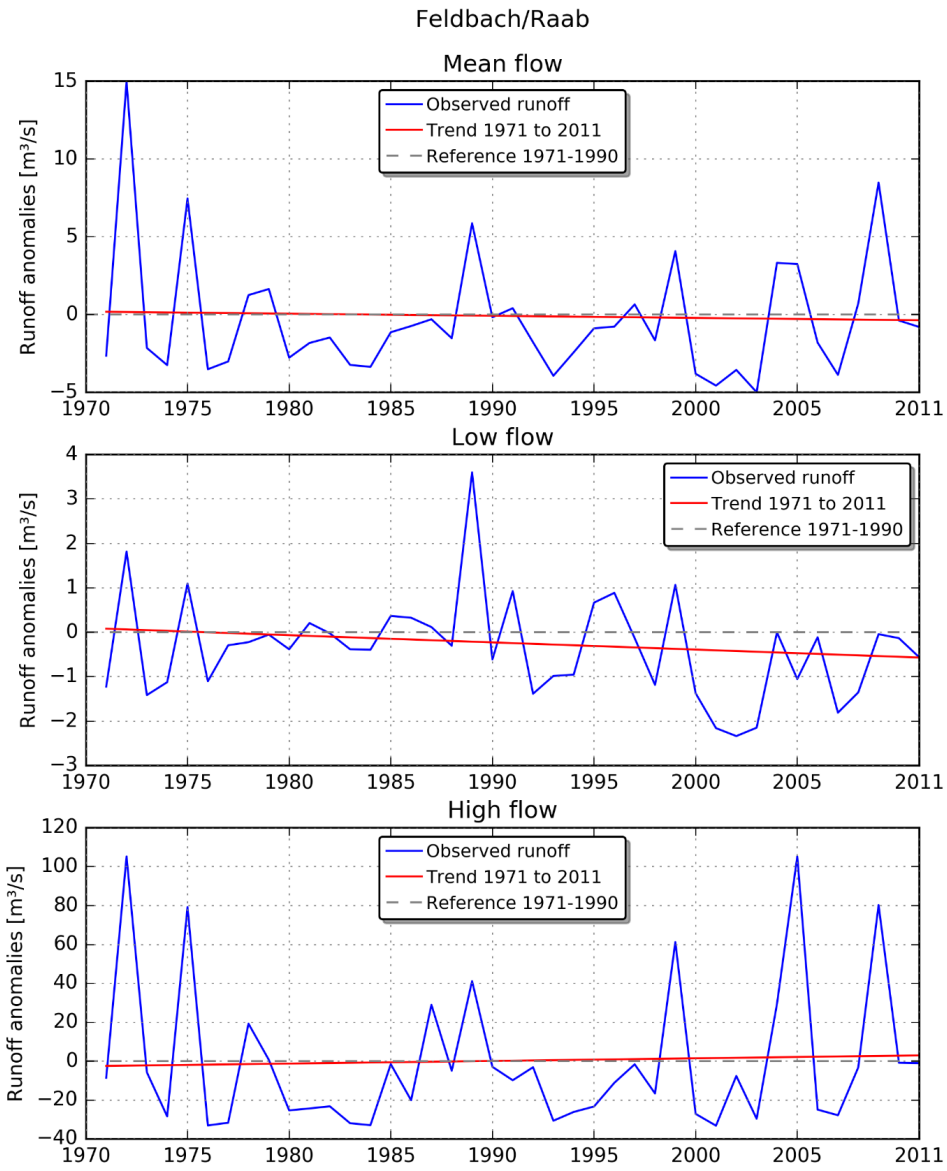


Fig. S2 Runoff anomalies at gauge station Feldbach/Raab from 1971 to 2011 to the reference period 1971 to 1990 for the extended summer month (Mai to September) with mean, low and high flows of each year.

S2 Model Calibration and Validation

S2.1 Calibration and Validation Setup

For the model calibration we used the runoff time series of three gauging stations, namely for the *upper*, *middle* and *lower* Styrian Raab catchment, and employed the shuffled complex evolution optimization algorithm developed at the University of Arizona (SCE-UA) (Duan et al. 1992; Duan et al. 1994) (as described in Sect. 2 of the main paper). The weighting of the three gauging station in the calibration process was set to 25% St. Ruprecht, 25% Takern II and 50% Neumarkt, respectively, because our focus region is the lower Raab valley between Takern II and Neumarkt.

We used the times series from 2003 to 2009 as a calibration period, complemented by an independent validation period from 1995 to 2001. Each of these periods was preceded by a five years warm up period for WaSiM. Both time periods include specific dry (2003/2001) and wet (2009/1996) years. The evaluation and classification related to dry and wet years was based on the Standardized Precipitation Evapotranspiration Index (SPEI) which we calculated with the R-package "SPEI" (Version 1.6, http://sac.csic.es/spei). We performed this SPEI evaluation to inform our choice of adequate calibration and validation periods.

We chose the set of calibration parameters and their range based on the WaSiM model description (Schulla 2015) and a literature review (e.g., Cullmann et al. 2006; Kunstmann and Stadler 2005). The chosen set of five parameters, together with their physical units and allowed ranges, is summarized in Table S2 (a sixth parameter ki is set to always adopt the value of kd).

Table S2 Set of calibration parameters used for the WaSiM calibration for the Styrian Raab catchment, given by parameter name (WaSiM acronym), description, unit, reference area, and value range allowed within the calibration algorithm's optimization procedure.

Parameter	Description	Unit	Area	Permissible Range
krec	recession constant for sat. hydr. conductivity	1	total catchment	0.01-1.0
dr	drainage density for interflow	m^{-1}	sub-basin	1-30
kd	storage coefficient direct flow	h	sub-basin	1-60
ki	storage coefficient interflow	h	sub-basin	ki = kd
Q0	scaling factor for baseflow	mm h^{-1}	sub-basin	0.2-1.5 (St. Ruprecht) 0.1-1.0 (Takern II, Neumarkt)
kb	storage coefficient for baseflow	m	sub-basin	0.2-1.5 (St. Ruprecht) 0.0001-1.0 (Takern II, Neumarkt)

To estimate the model performance in the calibration process we used the Nash-Sutcliffe Efficiency (*NSE*) (Nash and Sutcliffe 1970), which ranges from -∞ to 1. To emphasize more on the low flow, we also weighted in the logarithmic version of *NSE*, NSE_{log}. For the algorithm's optimization runs, the model efficiency targeted by the maximization procedure was chosen as a weighted sum of 50% *NSE* and 50% NSE_{log}. These efficiency measures are defined as

$$NSE = 1 - \frac{\sum_{i=1}^{n}(obs_i - sim_i)^2}{\sum_{i=1}^{n}\left(obs_i - \overline{obs}\right)^2},$$

$$NSE_{log} = 1 - \frac{\sum_{i=1}^{n}(\log(obs_i) - \log(sim_i))^2}{\sum_{i=1}^{n}\left(\log(obs_i) - \log\left(\overline{obs}\right)\right)^2},$$

where *i* is the index for individual days in the period, *n* the total number of days, and *sim* denotes the simulated runoff, *obs* the observed runoff, and $\overline{obs}$ the mean observed runoff averaged over the period.

Regarding the validation of the calibrated model, beside the validation being based on a different time period (1995-2001) the runoff components (direct flow, interflow, baseflow) where visually analyzed. Another important aspect with hydrological models is the water balance, which was validated by assessing in addition to *NSE* and NSE_{log} also the relative bias (in percent) of the model-simulated runoff against the observations, *PBIAS* (Moriasi et al. 2007),

$$PBIAS = 100 \cdot \frac{\sum_{i=1}^{n}(sim_i - obs_i)}{\sum_{i=1}^{n}(obs_i)},$$

where the meaning of the symbols is the same as in the equations above.

S2.2 Calibration and Validation Results

Fig. S3 shows the results over the calibration and validation period for the gauging station Neumarkt, as a representative example. The other calibration stations St. Ruprecht and Takern II exhibit similar results (thus not shown). As an overall indication of the performance, the *NSE*, NSE_{log}, and *PBIAS* values of the calibrated model at the three calibration stations are summarized in Table S3. The corresponding parameter values of the calibrated model are listed in Table S4.

The validation-period results are in general very similar and essentially as good as the calibration-period ones, except for the *NSE* values of the middle and lower Raab valley, reflected by the Takern II and Neumarkt results. This somewhat decreased *NSE* performance is probably caused by the simple model setup and non-modeled human influences like for example small hydro-power stations along the Raab. The NSE_{log} values still score at 0.7 or higher and the *PBIAS* stays within about 20%.

We also carried out careful visual analysis of time series of observed and simulated runoff, which is another important element of quality evaluation, and found reasonable and good overall agreement of the observed and simulated runoff curve characteristics. In addition, besides the total runoff as the formal calibration variable, the components of the runoff (cf. Fig. 2 in the main paper) were visually inspected as part of assessing the performance. The inspection showed that the runoff is dominated by interflow and the high runoff peaks are also fed by direct runoff. The base flow in the middle and lower Raab is quite small, but also shows a realistic behavior. Overall we found that a physically realistic distribution of the components base flow, interflow and direct runoff was simulated.

To conclude, the calibration and validation results show a sufficient model performance to use this model setup for the sensitivity analysis of the drought vulnerable Raab catchment.

Table S3 WaSiM runoff modeling performance measures Nash-Sutcliffe efficiency (NSE), logarithmic NSE (NSE_{log}), and relative simulation bias vs. observations (PBIAS, in percent), for the calibrated model. Results for both the calibration (2003-2009) and validation (1995-2001) period are listed, for the stations St. Ruprecht, Takern II, and Neumarkt.

Gauging Station	Calibration period			Validation period		
	NSE	NSE_{log}	*PBIAS*	*NSE*	NSE_{log}	*PBIAS*
St. Ruprecht	0.72	0.76	11.8	0.76	0.77	15.6
Takern II	0.76	0.77	15.2	0.59	0.75	20.9
Neumarkt	0.75	0.75	19.5	0.59	0.70	17.3

Table S4 Parameter values obtained for the calibrated model, which was then chosen as the basis for the sensitivity analysis. All values except the recession constant for saturated hydraulic conductivity (krec) depend on characteristics of the sub-basin (see Table S2), including the upper (St. Ruprecht), middle (Takern II), and lower (Neumarkt) Raab basins.

Parameter	St. Ruprecht	Takern II	Neumarkt
krec	0.80	0.80	0.80
dr	13.7	11.4	9.4
kd & ki	19.9	19.0	50.4
Q0	0.88	0.63	0.17
kb	1.34	0.21	0.94

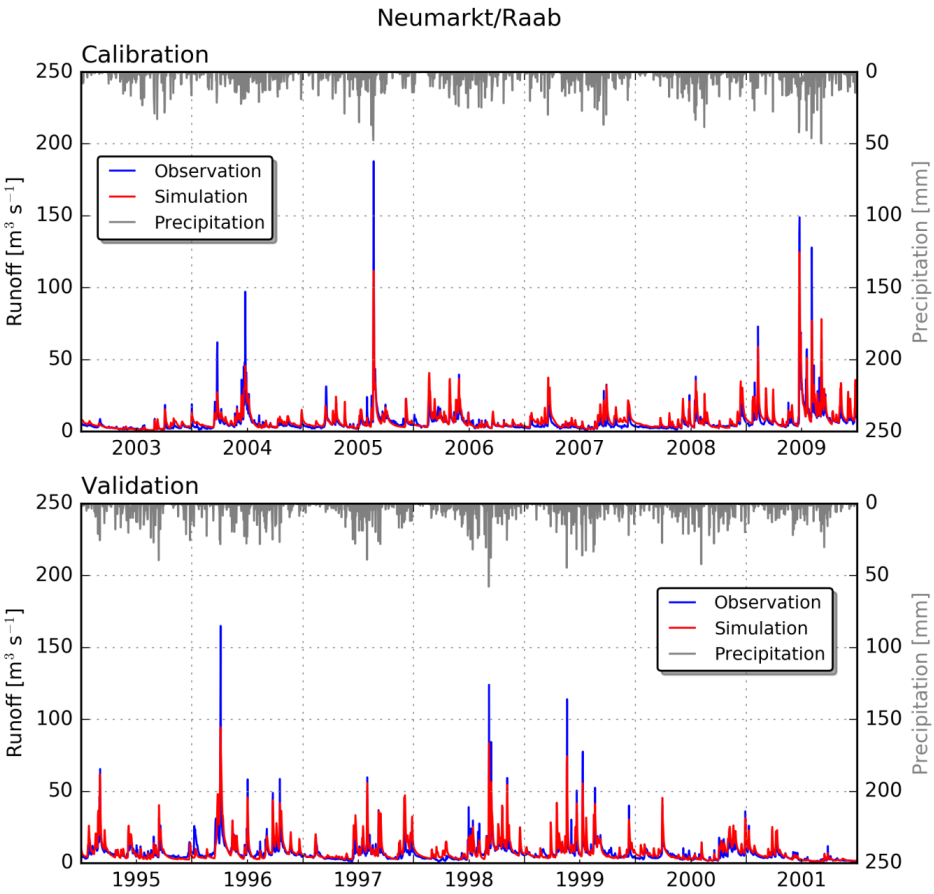


Fig. S3 Runoff time series over the calibration (top) and validation (bottom) period, of the observations (blue) and the calibrated model (red), for the entire Styrian Raab catchment at station Neumarkt. The precipitation time series (grey) are co-visualized in the panels from top downward (right-hand-side y axis).

S3 Water Budgets of Sensitivity Study Cases

Table S5 shows the water budget terms obtained for the entire catchment in response to the various types of changes. The residual ΔS (Precipitation – Runoff – actual Evapotranspiration) corresponds to the change in storage within the catchment. While this is negligible for the entire year (Table S5, right part), it can be seen that a reduction in precipitation and/or an increase in evapotranspiration during the summer (Table S5, left part), in general, is partly compensated by an increased drainage from the storage, which mitigates the effect on the summer river runoff.

Table S5 Water balance with mean values from 1982 to 2011 for the extended summer months May to September (Summer), used in this paper, and all months of the year (Total year) for comparison. P denotes precipitation, Q runoff, ETa actual evapotranspiration, and ΔS the balance P-Q-ETa.

Types of change		Summer				Total year			
		P [mm]	Q [mm]	ETa [mm]	ΔS [mm]	P [mm]	Q [mm]	ETa [mm]	ΔS [mm]
	Base	512	106	435	-29	824	264	562	-2
moderate	**TC**	512	80	484	-52	824	214	611	-1
	PC	461	77	433	-49	773	214	560	-1
	LUC	512	112	429	-29	824	272	554	-2
	WMC	512	105	436	-29	824	263	563	-2
	TP	461	57	479	-75	773	169	606	-2
	TPL	461	63	472	-74	773	178	597	-2
	TPLW	461	60	474	-73	773	176	599	-2
strong	**TC**	512	59	532	-79	824	167	659	-2
	PC	358	36	421	-99	671	125	548	-2
	LUC	512	118	420	-26	824	282	544	-2
	WMC	512	104	436	-28	824	263	563	-2
	TP	358	21	473	-136	671	79	597	-5
	TPL	358	28	462	-132	671	93	583	-5
	TPLW	358	22	466	-130	671	89	588	-6

Supplementary References

Carsel RF, Parrish RS (1988) Developing Joint Probability Distributions of Soil Water Retention Characteristics. Water Resour Res 24:755–769. doi: 10.1029/WR024i005p00755

Cullmann J, Mishra V, Peters R (2006) Flow analysis with WaSiM-ETH - model parameter sensitivity at different scales. Adv Geosci 9:73–77. doi: 10.5194/adgeo-9-73-2006

Duan Q, Sorooshian S, Gupta V (1992) Effective and efficient global optimization for conceptual rainfall-runoff models. Water Resour Res 28:1015–1031. doi: 10.1029/91WR02985

Duan Q, Sorooshian S, Gupta VK (1994) Optimal use of the SCE-UA global optimization method for calibrating watershed models. J Hydrol 158:265–284. doi: 10.1016/0022-1694(94)90057-4

Kunstmann H, Stadler C (2005) High resolution distributed atmospheric-hydrological modelling for Alpine catchments. J Hydrol 314:105–124. doi: 10.1016/j.jhydrol.2005.03.033

Moriasi DN, Arnold JG, Van Liew MW, et al (2007) Model evaluation guidelines for systematic quantification of accuracy in watershed simulations. Trans ASABE 50:885–900. doi: 10.13031/2013.23153

Nash JE, Sutcliffe JV (1970) River flow forecasting through conceptual models part I — A discussion of principles. J Hydrol 10:282–290. doi: 10.1016/0022-1694(70)90255-6

Schulla J (2015) Model Description WaSiM. Technical Report, www.wasim.ch (09.03.2016)

4.2 Research Article 2: Small catchment runoff sensitivity to station density and spatial interpolation: Hydrological modeling of heavy rainfall using a dense rain gauge network

Published as:
Clara Hohmann, Gottfried Kirchengast, Sungmin O, Wolfgang Rieger, and Ulrich Foelsche (2021), Small catchment runoff sensitivity to station density and spatial interpolation: Hydrological modeling of heavy rainfall using a dense rain gauge network, *Water*, 13, 1381, DOI:10.3390/w13101381.
Original article available at: https://doi.org/10.3390/w13101381

water

MDPI

Article

Small Catchment Runoff Sensitivity to Station Density and Spatial Interpolation: Hydrological Modeling of Heavy Rainfall Using a Dense Rain Gauge Network

Clara Hohmann [1,2,*], Gottfried Kirchengast [1,2,3], Sungmin O [2,3,4], Wolfgang Rieger [5] and Ulrich Foelsche [1,2,3]

[1] Wegener Center for Climate and Global Change (WEGC), University of Graz, 8010 Graz, Austria; gottfried.kirchengast@uni-graz.at (G.K.); ulrich.foelsche@uni-graz.at (U.F.)
[2] FWF-DK Climate Change, University of Graz, 8010 Graz, Austria; sungmin.o@bgc-jena.mpg.de
[3] Institute for Geophysics, Astrophysics, and Meteorology/Institute of Physics, University of Graz, 8010 Graz, Austria
[4] Department of Biogeochemical Integration, Max Planck Institute for Biogeochemistry, 07745 Jena, Germany
[5] Bavarian Environment Agency, 86179 Augsburg, Germany; wolfgang.rieger@lfu.bayern.de
* Correspondence: clara.hohmann@uni-graz.at

Abstract: Precipitation is the most important input to hydrological models, and its spatial variability can strongly influence modeled runoff. The highly dense station network WegenerNet (0.5 stations per km^2) in southeastern Austria offers the opportunity to study the sensitivity of modeled runoff to precipitation input. We performed a large set of runoff simulations (WaSiM model) using 16 subnetworks with varying station densities and two interpolation schemes (inverse distance weighting, Thiessen polygons). Six representative heavy precipitation events were analyzed, placing a focus on small subcatchments (10–30 km^2) and different event durations. We found that the modeling performance generally improved when the station density was increased up to a certain resolution: a mean nearest neighbor distance of around 6 km for long-duration events and about 2.5 km for short-duration events. However, this is not always true for small subcatchments. The sufficient station density is clearly dependent on the catchment area, event type, and station distribution. When the network is very dense (mean distance < 1.7 km), any reasonable interpolation choice is suitable. Overall, the station density is much more important than the interpolation scheme. Our findings highlight the need to study extreme precipitation characteristics in combination with runoff modeling to decompose precipitation uncertainties more comprehensively.

Keywords: precipitation variability; extreme events; rain gauge network; hydrological modeling; sensitivity analysis; spatial rainfall resolution; precipitation interpolation

check for updates

Citation: Hohmann, C.; Kirchengast, G.; O, S.; Rieger, W.; Foelsche, U. Small Catchment Runoff Sensitivity to Station Density and Spatial Interpolation: Hydrological Modeling of Heavy Rainfall Using a Dense Rain Gauge Network. *Water* **2021**, *13*, 1381. https://doi.org/10.3390/w13101381

Academic Editor: Scott Curtis

Received: 26 March 2021
Accepted: 11 May 2021
Published: 15 May 2021

Publisher's Note: MDPI stays neutral with regard to jurisdictional claims in published maps and institutional affiliations.

Copyright: © 2021 by the authors. Licensee MDPI, Basel, Switzerland. This article is an open access article distributed under the terms and conditions of the Creative Commons Attribution (CC BY) license (https://creativecommons.org/licenses/by/4.0/).

1. Introduction

Heavy precipitation events can have significant impacts on society and ecosystems by causing severe floods and landslides. Moreover, such events are intensifying due to climate change in many areas [1–4]. Hydrological models have served as an important tool to assess the impacts of heavy precipitation events on runoff and other hydrological processes. Since precipitation is the most important input in hydrological models [5–7], it is crucial to understand its uncertainty and how this uncertainty affects the simulated runoff. Assessing the spatial and temporal heterogeneity of precipitation is becoming increasingly important, especially with respect to heavy precipitation events [8,9]. Convective storm cells with large volumes of precipitation can easily trigger hazards, but the limited spatial and temporal extent of these cells is associated with huge levels of measurement uncertainty [10]. In addition to the measurement uncertainty of rain gauges, considerable uncertainty can arise when point-level measurements are spatially interpolated to obtain final gridded products [10–13]. Such gridded datasets are crucial in that they allow researchers to collect areal precipitation information within catchment and subcatchment areas, which can then

especially be used in spatially distributed hydrological models. Areal precipitation data can also be derived from radar and satellite-based observations. However, all measurements come with their own uncertainty levels and pros and cons [7,14]. On the one hand, the point measurements are most reliable for quantitatively measuring amounts of precipitation, whereas such measurements often do not provide reliable information about the spatial patterns of heavy precipitation because of the sparse distribution of point measurement sites. On the other hand, radar systems and satellites provide higher spatial resolution data, but the indirect precipitation estimates they provide do not allow the quantitation of specific precipitation amounts [15–21].

Despite the availability of remote-sensing data, ground-based precipitation measurement tools are still widely used in hydrological modeling [6,22]. Many studies, such as those by Lopez et al. [22], Goovaerts [23], and Zeng et al. [6], pointed out the advantages of dense and regularly distributed precipitation station networks. For many years, researchers have analyzed the effect of precipitation station density on hydrological model performance [5,6,12,24–27]. Dong et al. [25] and Xu et al. [27] used a statistical approach to identify the appropriate number of precipitation gauges and the influence of gauge density on the model performance of a lumped model. Both studies found a threshold above which an increase in station density does not lead to better model performance. Such a threshold can also be seen in many other studies [5,6]. Meselhe et al. [26] applied a conceptual and a physically based model to identify the impact of temporally and spatially sampling precipitation on runoff predictions (using a highly dense station network). The physically based model was more sensitive to changes in the spatial and temporal resolution of rainfall. A threshold with no significant increase in model performance can also be seen in this case for both models. Huang et al. [12] used a lumped and a distributed hydrological model to study the sensitivity of model performance to spatial rainfall resolution. They identified temporal resolution as the most important aspect, observing better model performance at higher temporal resolutions. Many of these studies placed a focus on the model performance and used lumped hydrological models. Here, we focus on the sensitivity of runoff in small subcatchments and report results of a process-based model.

When using station data as rainfall input for hydrological models, the spatial interpolation schemes must also be considered. Many different interpolation options and possibilities have been broadly studied [28–30] including arithmetic mean [12,25,31], Thiessen polygons (TP) [6,26,32], inverse distance weighting (IDW) [13,33–35], and different types of kriging, such as ordinary kriging [8,33,35] or external drift kriging [5,27,33]. The differences between the interpolation schemes are especially pronounced when extreme values are included [30]. Therefore, the selection of interpolation schemes can affect hydrological simulations, especially under heavy rainfall events. Given that our study area has a moderate topography with regularly distributed stations [36], we did not expect to obtain added value by using more complex geostatistical methods such as kriging. Therefore, we decided to focus on the two most widely used deterministic interpolation schemes, TP and IDW. We further analyzed the weighting power parameter of the IDW interpolation, which indicates the weight of the surrounding stations. A weighting power of 2 is normally used for IDW interpolations [37] but without making any further considerations [38]. Only a few studies have analyzed the influence of the weighting power on hydrological model simulations [38,39], while some other studies have focused only on the interpolated precipitation [37,40].

To counteract the uncertainty with respect to spatial and temporal resolution, it is possible to take ground-based measurements from a highly dense station network. In this study, the following research questions were addressed: How many precipitation stations do we need to reliably model runoff during heavy rainfall events? Are there specific features of small subcatchments to reliably model runoff under heavy rainfall events? How strongly does the interpolation scheme influence runoff results when the precipitation station density is the same? The highly dense station network WegenerNet (WEGN) (about 0.5 station per 1 km^2 over an area of around 300 km^2) in the southeastern Alpine

forelands of Austria was used to ask these questions as applied to the Raab catchment and its subcatchment areas. The region is well known for its heavy precipitation events [35,41]. Because of the exceptionally dense data coverage, it was possible to analyze the influence of precipitation station densities on runoff in detail. Therefore, we set up the widely used, physically based "Water Flow and Balance Simulation Model" WaSiM [42] and simulated runoff with varying station densities. All subnetworks were simulated using different precipitation interpolation schemes, namely, one TP scheme and three IDW schemes with a weighting power of 1 (IDW1), of 2 (IDW2), and of 3 (IDW3). Previous studies have assessed the impact of the station density and interpolation on precipitation data quality, such as mean and extreme rainfall values [43–45]. We go one step further, applying our initial study approach and focus to study the impact of such precipitation uncertainty on hydrologic simulation results, and especially on runoff peaks, using a combination of station densities and interpolation methods.

2. Study Area and Data

2.1. Study Area

The study area is part of the Raab catchment, an area of southeastern Alpine foreland draining into the Raab river. The Raab river flows from the "Passailer" Alps in the province of Styria, Austria, at an altitude of around 1150 m.a.s.l. until it joins the Danube river in Hungary. The area covered in this study ranges from the gauging station Takern II/Raab to Neumarkt/Raab, including a total area of around 500 km^2 (Figure 1). The gauging station Feldbach/Raab is located between these two stations. Beside the main river Raab, we analyzed five subcatchments (Table 1, Figure 1) with areas of around 10 to 30 km^2, all of which are covered by the WEGN. Two subcatchments are located on the northern side of the Raab and three on the southern. Since we did not have measured runoff data for these subcatchments, we implemented pour points in the model directly before they flowed into the Raab river.

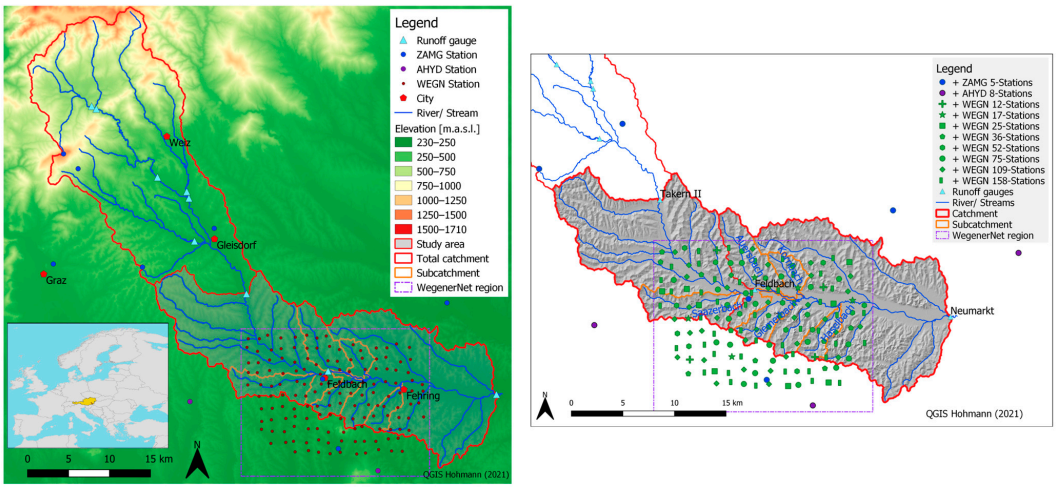


Figure 1. Map of the Raab catchment area in southeastern Austria (**left**), including the full catchment area extending down to the runoff gauge Neumarkt/Raab (red line), the focus area (grey area), the subcatchments (orange line), the WegenerNet region (violet box), the locations of rain gauge stations (dot symbols), and the runoff gauges (triangle symbols). Inset shows a map of Europe; Austria is shown in yellow and the Raab catchment, in red. An enlarged view of the study area (**right**) shows the station subnetworks and subcatchments used in this study.

Table 1. Characteristics of the study catchment area and representative subcatchment areas with the total basin area of the latter extending up to the gauging station/pour point into the river Raab.

Catchment	Area (km^2)	Location from Raab
Neumarkt/Raab (total catchment)	987	-
Neumarkt/Raab (focus area)	488	-
Feldbach/Raab (total catchment)	689	-
Feldbach/Raab (focus area)	190	-
Subcatchment	**Area (km^2)**	**Location from Raab**
Auersbach	28.9	north
Saazerbach	27.2	south
Giemerbach	16.0	south
Haselbach	12.3	south
Kornbach	12.2	north

The total study area is moderately hilly with elevations ranging from 230 to 530 m. The land use is predominately agricultural with some patchy forest areas. The dominant soil texture is sandy loam. The mean annual precipitation is around 850 mm, and the mean annual temperature about 9.5 °C. The study area was chosen because of its vulnerability to heavy/convective precipitation events [41] and climate change [46], as well as the data availability. Since the region has a very dense climate network, the WEGN, which is operated by the Wegener Center for Climate and Global Change, University of Graz, Austria [36]. The WEGN has been used to measure precipitation, temperature, humidity, and other variables since early 2007 and includes 150 stations within an area of around 23 × 18 km. All data are quality controlled by the WEGN QC system [36], and additional bias correction is implemented for precipitation data [47].

2.2. Data

To perform hydrological modeling with WaSiM, we need meteorological data for precipitation, temperature, relative humidity, wind speed, global radiation, and air pressure aggregated at a 30-min time resolution. Table 2 provides an overview of the maximum available number of stations for each parameter, as well as the station source. The WEGN has a dense station network and a 5-min time resolution, forming a rectangular grid due to the comparability to climate models. It is located in the middle of the focus area around the Feldbach/Raab gauging station, but does not cover the total Raab catchment area. Therefore, we also needed to include data from the Austrian Weather Service (ZAMG), which has a 15-min time resolution, and from the Austrian Hydrographic Service (AHYD), which has a 1- to 15-min time resolution to properly simulate runoff (Table 2). In order to run the model only for the focus area, the Takern II/Raab gauging station was used as an inflow point. Runoff data from the Neumarkt/Raab gauging station were used for calibration and from the Feldbach/Raab gauging station for cross checks and further analysis. For precipitation event identification, the Integrated Nowcasting through Comprehensive Analysis (INCA) system developed by Haiden et al. [48] was used, which is a multivariable analysis and nowcasting system developed at the ZAMG.

Table 2. Catchment attributes and hydrometeorological data used for hydrological modeling with WaSiM with the following sources: HYDROBOD—homogeneous soil and land use grids by Klebinder et al. [49]; LStmk/LBgld—state government offices of the provinces of Styria and Burgenland; TANALYS—pre-processing tool of the hydrological model WaSiM [42]; WEGN—highly dense station network data version 7.1 [50]; ZAMG—data from the Austrian Weather Service; AHYD—data from the Austrian Hydrographic Service.

Catchment Attributes	Source	Resolution
Land use types	HYDROBOD	100 m
Soil information	HYDROBOD	100 m
DEM	LStmk, LBgld	10 m
River network	LStmk, LBgld	-
Geological information	LStmk, LBgld	-
Subcatchments, slope, river width and depth, other information	TANALYS output	100 m
Meteorological Data	**Source**	**Number of Stations**
Precipitation	WEGN	150
	ZAMG	5
	AHYD	3
Temperature	WEGN	150
	ZAMG	5
	AHYD	3
Relative humidity	WEGN	150
	ZAMG	5
	AHYD	3
Wind speed	WEGN	12
	ZAMG	5
Air pressure	WEGN	1
	ZAMG	5
Global radiation	ZAMG	5
Runoff	AHYD	3

Static attributes are needed in addition to hydrometeorological station data. The digital elevation model (DEM), river network, and geological information were provided by the Austrian state government offices of Styria and Burgenland. The topographic analysis tool (TANALYS) of WaSiM uses the DEM to calculate other required grids, such as flowtime, subcatchments, slope, river width, and depth [42]. Homogeneous soil and land use grids (HYDROBOD) were provided by Klebinder et al. [49] with a resolution of 100 × 100 m in our research area. The HYDROBOD maps were created using the methods cited in Krammer et al. [51]. Maps for every single soil layer (0–20, 20–50, 50–100 cm) and parameters such as soil texture (percentage of sand, silt, and clay), saturated hydraulic conductivity, Mualem van Genuchten parameters (combinations of residual water content and saturation water content), and soil thickness were used.

3. Modeling Approach

3.1. Model Setup and Calibration

We used the hydrological model WaSiM, which was developed by Schulla [42], at the ETH Zurich in Switzerland for studying climate change in Alpine catchments. WaSiM is a well-established, widely used, distributed, and process-oriented hydrological model. It has been used in similar catchments and for many different purposes, such as to perform climate change studies [46,52,53], land use change studies [54,55], and measure operational uses (e.g., at FOEN Switzerland). We focused on a process-oriented model to keep the model uncertainty as small as possible as compared to conceptual models, which are often used for similar precipitation runoff studies [6,12,25]. Using this type of model also allowed us to study ungauged subcatchments within our calibrated catchment area. Furthermore,

WaSiM had already been successfully applied by Hohmann et al. [46] in the study area to perform a climate change sensitivity study with a low-flow focus.

In this study, we used the WaSiM-Richards Version 10.04.07. All modules of WaSiM used are shown in Figure 2. For more information about the modules, see Schulla [42] or the WaSiM user guide by Schulla [56]. The model was set up with a spatial resolution of 100 × 100 m and a temporal resolution of 30 min. WaSiM allows the option to internally interpolate the meteorological station data to grids. The evapotranspiration was estimated with the Penman–Monteith equation [57], and the unsaturated zone with the Richards equation, parameterized after van Genuchten [58]. The soil was split up into four calculation layers (0–20, 20–50, 50–100 cm, 1–20 m) with a total depth of 20 m, including the first groundwater layer. By including the data from Klebinder et al. [49], we could include a total of 416 soil parameter combinations in the soil table of WaSiM for our study domain. The final groundwater parameters of the 2D groundwater module were fitted to represent the baseflow quite accurately during the calibration period. Therefore, the saturated horizontal conductivity was split up into areas around the river with 1×10^{-3} m s^{-1} and the surrounding hilly areas with 5×10^{-4} m s^{-1}. Adopting reasonable values, the colmation factor was set to 5×10^{-5}, and the unitless specific storage coefficient to 0.2. In addition to the gridded groundwater parameters, WaSiM was calibrated using four soil module parameters, which influence the shape and volume of the simulated runoff hydrograph when no measured or literature data were available [56]: these were the storage coefficient of the surface runoff *kd* (shape of the surface runoff hydrograph) and interflow *ki* (shape of the interflow hydrograph), the drainage density for interflow *dr*, and a recession constant of the soil *krec* (both of which influence the amount of interflow).

The model calibration period was from 1 May to 30 September 2009 with a model spin-up period from 1 November 2007 to 30 April 2009. We calibrated the model only for the extended summer months (May to September), since most of the heavy rainfall events occur during these months in southeastern Styria. The validation periods were the extended summers of 2010 and 2011. The model performance was assessed with the Nash–Sutcliffe model efficiency coefficient (NSE) [59], logarithmic Nash–Sutcliffe efficiency (logNSE), Kling–Gupta efficiency (KGE) [60], and percent bias (PBIAS) [61]. NSE is the most frequently used performance measure in hydrological modelling and places a focus on peak flow [62]. To collect information about the overall flow and especially about the low-flow periods, logNSE was included [46]. KGE provides information about the correlation, bias, and variability between the simulations and observed discharge [62]. PBIAS provides the average tendency of the over- and underestimation of the discharge [61].

The calibration was mostly performed manually. To obtain a first best-guess of the model parameters, the shuffled complex evolution optimization algorithm developed at the University of Arizona (SCE-UA) [63] was used. The manual calibration was first performed with a focus on the efficiency measures and by carrying out a visual comparison of the time series of measured and simulated runoff. Second, since the runoff components such as base flow, interflow, and surface runoff are important in process-based modelling, we visually analyzed the distribution of the runoff components for specific events. Because manual calibration steps were necessary, the model was calibrated with the IDW2 interpolation and 158 precipitation stations and was not recalibrated with all different precipitation inputs and interpolation schemes. This approach is considered as appropriate, because the deviation between the efficiency measures for all studied cases from those observed in the calibration run was found to be negligible. The deviations observed in the calibration/validation period exhibited a maximum deviation of 0.04/0.02 in NSE, 0.07/0.13 in logNSE, 0.08/0.04 in KGE, and 11/14% for PBIAS, respectively.

The best model performance was obtained with the parameter set of *krec* = 0.8, *dr* = 40, *kd* = 1.5, and *ki* = 2. This setup resulted in a model performance for the river runoff in the calibration period of summer 2009 with an NSE of 0.80, logNSE of 0.76, KGE of 0.77, and PBIAS of 8%. The validation period of summer 2010 and 2011 resulted in an NSE of 0.63,

logNSE of 0.56, KGE of 0.69, and PBIAS of 19%. The observed and simulated runoff for the calibration and validation periods are plotted in Figure A2 in Appendix A.

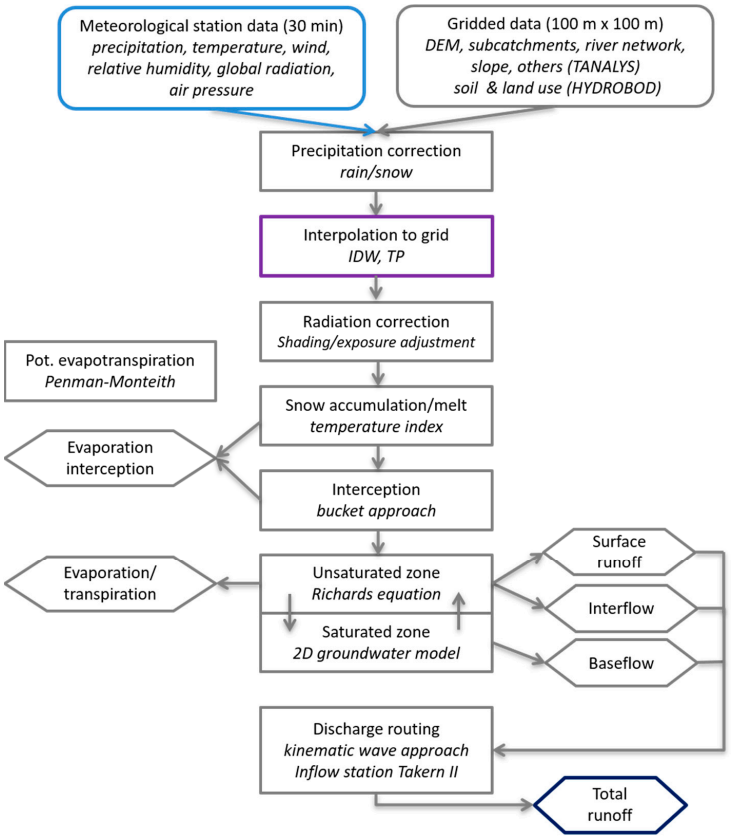


Figure 2. WaSiM model setup, including modules and input datasets used in this study (created after scheme of Schulla [56]). The focus of this study was to evaluate runoff output data (box marked in dark blue) as simulated by WaSiM with various precipitation data resolutions at input (blue box), and using different interpolation schemes (violet box) IDW—inverse distance weighting and TP—Thiessen polygons.

3.2. Experimental Design

Our study design is visualized in Figure 3 and described in the following sections.

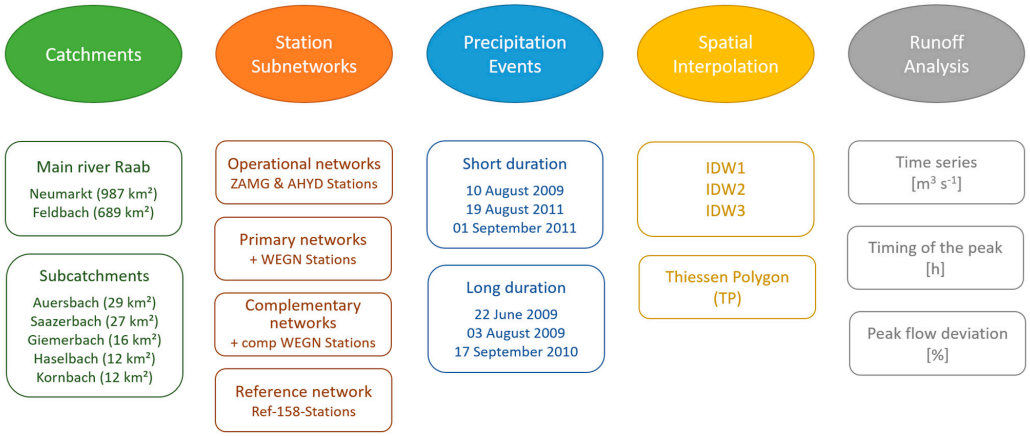


Figure 3. Overview of the study design with total catchment and subcatchment areas, gauge station subnetworks (ZAMG—data from the Austrian Weather Service; AHYD—data from the Austrian Hydrographic Service; WEGN—highly dense station network), and full precipitation network (Ref-158-Stations), analyzed short-duration and long-duration events, spatial interpolation schemes (inverse distance weighting with power of 1 (IDW1), power of 2 (IDW2) and power of 3 (IDW3); Thiessen polygons (TP)) for precipitation input data, and the key runoff output data analyzed.

3.2.1. Selection of Precipitation Station Network Densities

To obtain precipitation input data at various spatial resolutions, we defined subnetworks (Table 3 and Figure 3) using the 158 stations. The lowest-density network includes only the five ZAMG stations (5-Stations); the mean nearest neighbor distance is 11.0 km. This corresponds to an operational meteorological monitoring setup in Austria. The next subnetwork includes three more stations from the AHYD network (8-Stations). This would be a typical setup for the operational use of hydrological models.

In addition to the operational setup, precipitation stations from the WEGN are included for higher resolution subnetworks. For the main analyses, we defined seven evenly distributed subnetworks consisting of rain gauges ranging from 12–109 stations (primary subnetworks in Table 3 and Figure 1). In addition, we defined six complementary subnetwork cases ranging from 12–75 stations with different actual WEGN stations (Table 3 and Figure A1 in Appendix A). The spatial uncertainty of the precipitation depends not only on the number of gauges or station density, but also on their spatial configuration [13]. Therefore, these complementary subnetworks were considered to further investigate the uncertainty that was related to a given number of pre-defined subnetworks.

All available precipitation stations, 158 in total, served as our reference (Ref-158-Stations) with a mean nearest neighbor distance of 1.4 km. We assumed that the most accurate areal precipitation information could be obtained from Ref-158-Stations, and therefore, we calibrated the model using this setup.

Table 3. Precipitation stations of the operational subnetwork cases, the primary subnetwork cases, the complementary subnetwork cases, and the reference subnetwork with the total number of stations per subnetwork, together with the specific station data source (Z: ZAMG, A: AHYD, W: WEGN) and the estimated mean nearest neighbor distance. The distance estimates were calculated with an ArcGIS software tool.

Subnetworks	Gauge Subnetwork Case	Number of Stations (Z/A/W)	Mean Nearest Neighbor Distance (km)
Operational	5-Stations	5 (5/-/-)	11.0
	8-Stations	8 (5/3/-)	10.5
Primary	12-Stations	12 (5/3/4)	7.2
	17-Stations	17 (5/3/9)	5.9
	25-Stations	25 (5/3/17)	4.0
	36-Stations	36 (5/3/28)	3.2
	52-Stations	52 (5/3/44)	2.6
	75-Stations	75 (5/3/67)	2.0
	109-Stations	109 (5/3/101)	1.7
Complementary	12-comp-Stations	12 (5/3/4 comp)	8.3
	17-comp-Stations	17 (5/3/9 comp)	5.4
	25-comp-Stations	25 (5/3/17 comp)	4.1
	36-comp-Stations	36 (5/3/28 comp)	3.0
	52-comp-Stations	52 (5/3/44 comp)	2.4
	75-comp-Stations	75 (5/3/67 comp)	2.0
Reference	Ref-158-Stations	158 (5/3/150)	1.4

3.2.2. Selection of Precipitation Events

We selected heavy precipitation events observed with the WEGN during the extended summer (May–September) period in 2009–2014 (see also [11]). We first defined rain events with a minimum inter-event time of 6 h [64,65] and then selected the top 10% of the heaviest rainfall events. Finally, for the case studies, the three most extreme, small-scale, short-duration and the three most extreme, large-scale, long-duration events were selected (see also Figure A3 in Appendix A). The short-duration events were identified as the three events with the strongest peak hour during our study period. The long-duration events were selected as those with the largest total precipitation amount. We additionally conducted a visual inspection of the INCA data across the study area (Figure 4) to check the spatial scales of the selected rainfall events. Table 4 shows a description of the six rainfall events considered in this study.

Table 4. Precipitation events selected for this study and associated key characteristics. The precipitation information indicated for the events was estimated from WEGN data. The runoff information included the measured peak runoff at the total catchment outlet, the Neumarkt/Raab gauging station. The HQ gives a rating if the peak runoff was statistically reached or exceeded once per year (HQ_1) or once per ten years (HQ_{10}).

Event	Start Date	Duration (h)	Total Precipitation (mm)	Peak Hourly Precipitation (mm)	Peak Runoff ($m^3\ s^{-1}$)	HQ
short-1	10 August 2009	4	34	19	107	HQ_1
short-2	19 August 2011	2	23	18	36	$<HQ_1$
short-3	01 September 2011	4	28	26	26	$<HQ_1$
long-1	22 June 2009	66	121	10	244	$>HQ_{10}$
long-2	03 August 2009	25	106	10	213	HQ_{10}
long-3	17 September 2010	54	60	5	55	$<HQ_1$

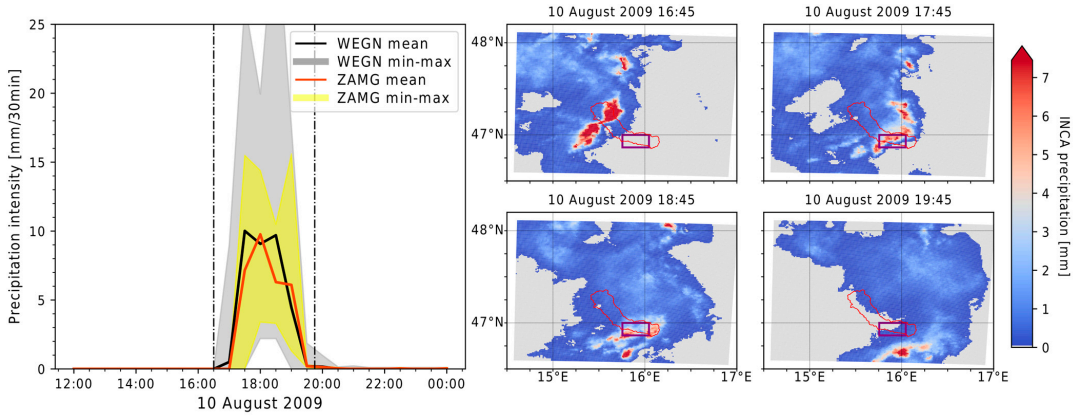


Figure 4. Precipitation time series of the "short-1 event" measured at WEGN and ZAMG stations (left panel) throughout the WEGN network area (purple box in the four panels on the right). In the panel on the left, "WEGN" shows mean areal precipitation computed from the 150 stations (black line) with a min–max range among the stations (gray shaded), while "ZAMG" shows mean precipitation (red line) obtained from the 3 ZAMG stations with a min–max range across the stations (yellow-shaded). The map sequence in the four panels on the right shows the evolution of the precipitation event as revealed by the gridded INCA analysis across the WEGN network (purple box) and the Raab catchment area (red line).

3.2.3. Spatial Interpolation Schemes

In this work, we employed three different IDW setups and the TP interpolation. We decided to use these methods for several reasons: IDW and TP are both widely used interpolation methods in hydrological studies [30,66]. Our network is fairly dense, with regularly distributed stations in a landscape with moderate topography; therefore, we do not expect to obtain additional value from taking more complex geostatistical measures. The literature is ambiguous regarding which interpolation method is the best, and especially for high-resolution station networks, more complex geostatistical methods do not provide additional value [40,67]. The important influence of the weighting power of IDW on modeling results has not yet been studied broadly, nor has it been studied for such a dense station network [38,39]. The methods of IDW and TP are implemented in WaSiM and, therefore, widely used by the model users. Additional altitude information was not included, because the elevation differences in the area are fairly small (altitude differences are no more than about 300 m).

IDW is the sum of all contributing station data with specific weights [42]. It is calculated as follows:

$$\hat{z}(u) = \sum_j \left(w_j \cdot z\left(u_j\right)\right) \quad (1)$$

$$\text{with } w_j = \frac{1}{d\left(u,u_j\right)^p} \cdot \frac{1}{C} \text{ and } C = \sum_j \frac{1}{d\left(u,u_j\right)^p} \text{ follows } \sum_j w_j = 1 \quad (2)$$

$\hat{z}(u)$ interpolated value at location u.
w_j weight of the observed value at the station j.
$z\left(u_j\right)$ observed value at the station j.
$d\left(u,u_j\right)$ distance to the station j.
p weighting-power exponent of the inverse-distance scheme.

In our study, we used the standard weighting power p of 2 (IDW2) as well as the weighting power p of 1 (IDW1) and of 3 (IDW3) for comparison. The search radius was set differently for the core WEGN region and the surrounding stations. Since our focus region was the WEGN region itself, and we do not have such a dense network throughout the entire catchment area, we maintained a fixed precipitation input for the surrounding

area. So, for the 12-Stations case and onwards, the IDW2 interpolation case with the five ZAMG and three AHYD stations and a 60 km radius of influence was maintained for the surrounding area.

The WEGN region (23 × 18 km) was then interpolated with each subnetwork and interpolation scheme, respectively. A smoothing buffer of 3 km was set, between the WEGN region and its surroundings. This setup enabled us to change the radius of influence for the WEGN stations individually without losing important information from the supporting weather stations. The radius of influence was subsequently set to 20 km for the 12- and 17-Stations cases and to 10 km for the 25-Stations case and onward so that we could include all supporting information and still obtain proper information for all locations.

Using the TP interpolation, the precipitation data collected at the nearest station were always taken. Each grid cell of the model received information from the nearest station, and the polygons formed (Thiessen polygons) represent lines of equal distance between two stations [42]. Hence, TP is a simpler method to apply than IDW, but the former is still widely used in hydrological modeling [6,26,32].

3.2.4. Runoff Analysis Approach

In our study, we analyzed an event-specific time series of runoff and peak flow deviations. The time series are visualized for all events individually, but are combined with different station network densities and interpolation schemes. For each catchment, interpolation method, and event, the peak flow deviation was calculated individually as a percent of the total value. For this purpose, the maximum runoff value was calculated using the simulation results from every subnetwork case (MAX value); this value was then compared to the maximum runoff value from the full-network reference case (MAX Ref-158-Stations), which best captures the "true" spatial variability of precipitation in the study area. This deviation metric is computed as follows:

$$\text{peak flow deviation } [\%] = \frac{(\text{MAX value}) - (\text{MAX Ref-158-Stations})}{(\text{MAX Ref-158-Stations})} \times 100 \quad (3)$$

The timing of the maximum peak flow was also calculated. Therefore, the difference between the earliest and the latest peak flows with all station densities (including the complementary subnetworks) of every single event and each catchment was calculated separately.

4. Results

4.1. Results for Individual Example Events

In this section, we focus on individual precipitation events. Figure 5 shows exemplary maps of the interpolated precipitation data, as well as the resulting runoff in the representative small subcatchment of Haselbach (12 km^2) for the short-1 event. With the 12-Stations case, the maps of the two interpolation schemes and the resulting runoffs at Haselbach are very different. In the case of the Ref-158-Stations, the interpolation schemes have a smaller impact on the areal precipitation estimation as compared to the 12-Stations case. In the Haselbach subcatchment at this short-1 event, the difference between the IDW2 and TP interpolation in the 12-Stations case is more pronounced than the difference between the 12-Stations and Ref-158-Stations cases.

In Figure 6, the runoff time series of the short-1 event and the long-1 event for the interpolation schemes of IDW2 and TP are visualized for three subcatchments.

The short-1 event in the Haselbach subcatchment shows very little runoff for the 8-Stations case under the IDW2 interpolation as compared to the other cases. When examining the range of gauge densities, no systematic variation of simulated runoff peaks is observed. For instance, while the lowest runoff is simulated from 8-Stations with IDW2, the highest runoff was seen from 36-Stations with the same interpolation scheme. In the Giemerbach subcatchment, the lowest runoff is seen in the 5- and 8-Stations cases, and the highest runoff with the 36-Stations case (both TP interpolation). Applying the IDW2

interpolation, the 36-Stations case also shows the highest value, but the 8- and 12-Stations cases show the lowest. In the Auersbach subcatchment, the IDW2 interpolation shows the lowest values with 5- and 8-Stations cases, and the highest runoff with the 52-Stations case. Applying the TP interpolation, the 5- and 8-Stations cases produce the same minimum runoff results. The maximum runoff is seen in the 52-Stations case.

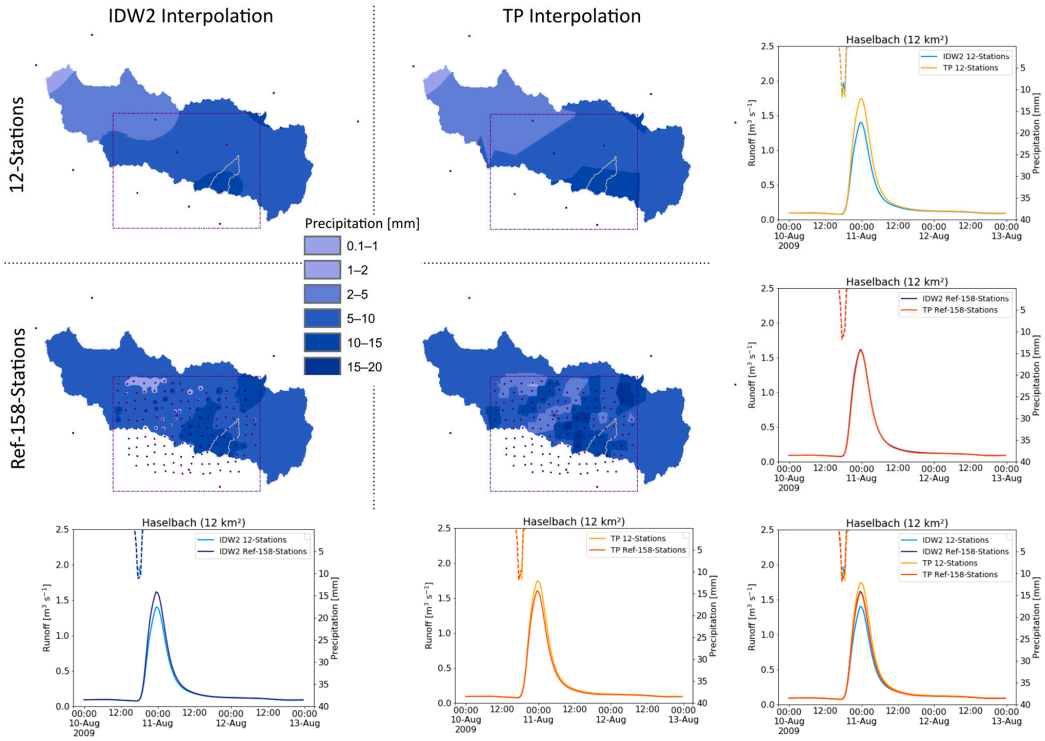


Figure 5. Exemplary precipitation maps using the WaSiM interpolation schemes of inverse distance weighting with power of 2 (IDW2) and Thiessen polygons (TP) for the short-1 event (10 August 2009 at 17:30), for the 12-Stations and Ref-158-Stations subnetwork cases (four panels on the upper-left). The time series (bottom row and right column panels) show the precipitation (dashed, from top) and the modeled runoff (solid) of this event in the representative small subcatchment of Haselbach (12 km^2).

The runoff results obtained for the long-1 event are almost ten times higher than that of the short-1 event. The order, maxima, and minima also differ greatly between the two. The IDW2 and TP interpolation schemes lead to a different runoff curve order and even different curve shapes. This becomes visible in the Haselbach runoff curves, which have different shapes in the two interpolation schemes and different minima and maxima. In the Giemerbach subcatchment, the highest value is simulated for the 12-Stations case with the TP interpolation and for the 5-Stations case under IDW2. In the Auersbach subcatchment, the lowest runoff is seen in the 12-Stations case with both interpolation schemes. The highest values are modelled in the 8-Stations cases when using IDW2, and in the 5- and 8-Stations cases when using TP interpolation.

These are examples of one short- and one long-duration event for three subcatchments, but they do not cover the total range of setups and results. Therefore, the combined figures are shown in Section 4.2.

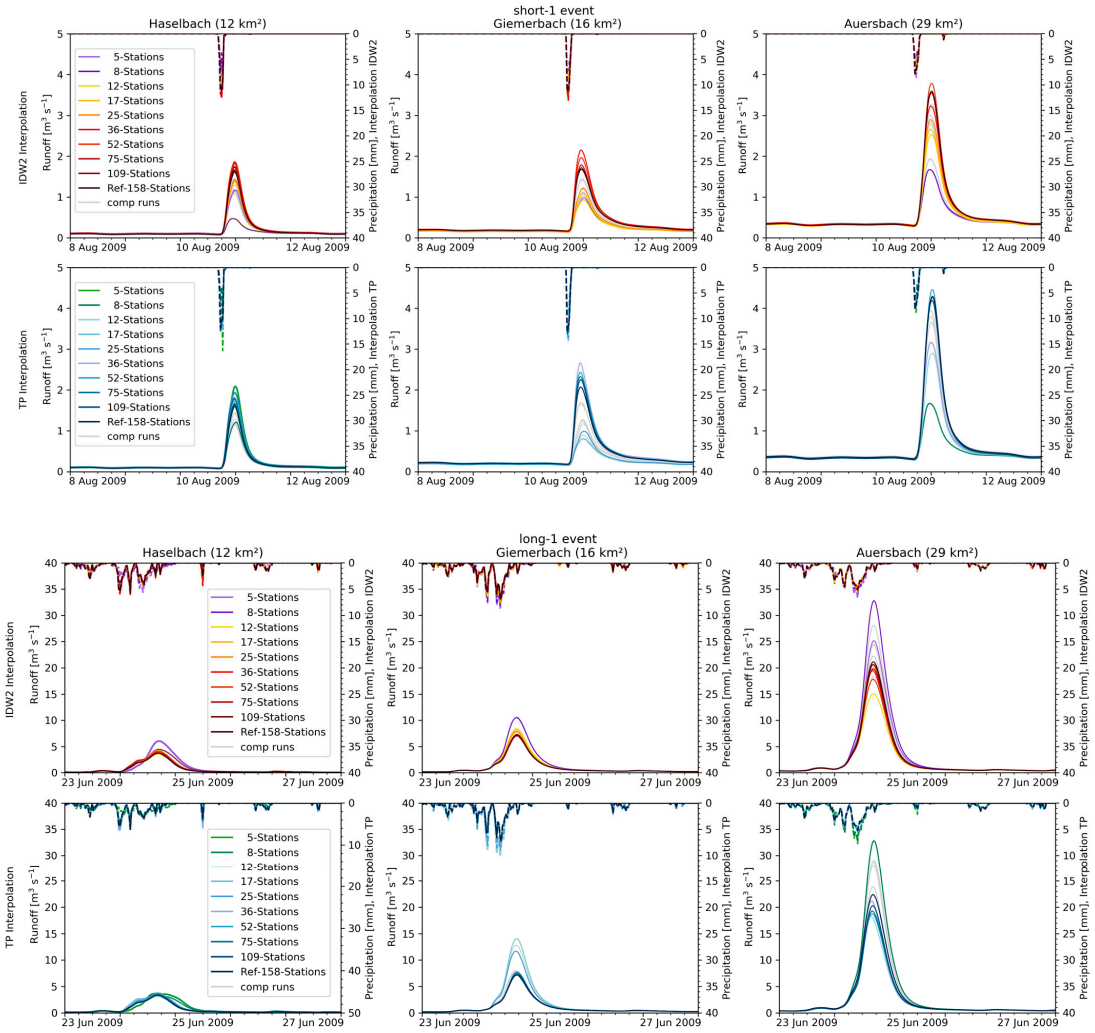


Figure 6. Precipitation and associated runoff time series for the short-1 event (top six-panel plate) and long-1 event (**bottom** six-panel plate), respectively, for all subnetwork cases and the full Ref-158-Stations network; the complementary runs (comp runs) for the 12-comp-Stations to 75-comp-Stations subnetworks are depicted in gray. Results are shown for the inverse distance weighting with power of 2 (IDW2) and Thiessen polygons (TP) interpolation schemes (**top** and **bottom** rows per plate), for the Haselbach (**left**), Giemerbach (**middle**), and Auersbach (**right**) subcatchments.

4.2. Combined Results for All Events

4.2.1. Timing of Peak Flow

We calculated the differences in the timing of the runoff peak using all densities and interpolation schemes for all (sub)catchments (Table 5). The deviations range mostly between 0 and 3.5 h, with the exception of the long-3 event. The long-3 event shows huge timing differences, with up to 31 h in the Saazerbach subcatchment. Here, the first peak flow was measured on 17 September 2010 at 23:30 and the last on 19 September 2010 at 6:30. Haselbach shows a similar timing of the runoff peaks, with the exception of the 8-Stations case, when applying all interpolation schemes. In this case, the timing of the runoff peak

is also one day later than in the other cases. At Neumarkt/Raab gauging station, the difference is mostly just 3 h, but the TP 8-Stations case has a maximum peak flow that is around 15 h later than the other cases.

When examining the short-1 event, we see that the runoff peaks at the Neumarkt/Raab and Feldbach/Raab gauging station were always at the same time. For the short-2 event at station Neumarkt/Raab, the timing of the peak runoff is mostly the same, but the two cases show a half-hour difference. This event also shows the smallest deviations in the peak timing, i.e., just 1.5 h. The short-3 event shows no specifically noticeable cases, whereby the timing differences at Neumarkt/Raab gauging station are up to 3 h; in the Saazerbach subcatchment up to 3.5 h; 1.5 h or less for the other catchments. When examining the long-1 and long-2 events, no specifically noticeable cases are visible, and the timing differences are just between 0.5 and 2/2.5 h.

Table 5. Calculated differences in the timing of the runoff peak for all subnetwork station densities and interpolation schemes separately for all (sub)catchments.

Event	Neumarkt/Raab	Feldbach/Raab	Kornbach	Haselbach	Saazerbach	Auersbach	Giemerbach
short-1	0 h	0 h	0.5 h	2 h	3.5 h	1 h	2 h
short-2	0.5 h	0.5 h	1.5 h	1 h	1.5 h	0.5 h	0.5 h
short-3	3 h	0.5 h	1.5 h	1.5 h	3.5 h	1 h	1.5 h
long-1	1 h	1 h	0.5 h	2 h	2 h	1.5 h	0.5 h
long-2	1.5 h	0.5 h	2.5 h	2 h	1.5 h	1 h	1 h
long-3	15.5 h	1.5 h	1 h	28.5 h	31 h	1 h	1 h

4.2.2. Peak Flow Deviation

Figure 7 shows the peak flow deviations as calculated with Equation (3) for all analyzed station cases and for the IDW and TP interpolations, respectively. The interpolation schemes of IDW1 and IDW3, as well as all results of the complementary subnetworks, are plotted in Appendix A (Figure A4). We can see that the different short- and long-duration rainfall events lead to a significantly different runoff picture, while the interpolation schemes and different catchments are much more similar. Lower station densities (<12-Stations) mostly show larger deviations from the Ref-158-Stations full network case (darker colors) than cases with more stations (lighter colors).

The three short events show more extreme differences between the station densities than the three long events. When a comparison was made between the (sub)catchments, no single (sub)catchment was especially noticeable. Using the TP interpolation generally results in more extreme values than using IDW2. Differences between the results obtained with three IDW interpolation schemes are less pronounced than differences seen between the results from IDW and TP interpolation (Figures 7 and A4).

If we take a look at the short-1 event under all interpolation schemes and for all (sub)catchments, we see that the 8-Stations subnetwork shows the strongest negative peak flow deviation as compared to the Ref-158-Stations case. This sums up to nearly –70% at Saazerbach when using the IDW2 interpolation. The Saazerbach subcatchment modeling results also show slightly different behavior than the others, with a positive peak flow deviation being seen for the 5-Stations case when using the TP interpolation. Haselbach shows the most positive value of around +50% with the 36-Stations subnetwork and the IDW1 interpolation conditions.

The short-2 event reveals a similar picture as the short-1 event, with pronounced negative peak flow deviations also seen for the less dense networks. Again, the most negative deviation appears in the Saazerbach subcatchment in the 8-Stations case (IDW2) with nearly –65%. The most positive values are obtained when TP interpolation is used for the Saazerbach, Giemerbach, and Haselbach subcatchments.

The short-3 event shows a more positive peak flow deviation pattern as compared to those obtained in the short-1 and short-2 events. Especially Auersbach shows positive

deviations, with more simulated runoff seen than in the Ref-158-Stations cases for almost all interpolations and station density cases. Including data from the complementary network, but also the primary networks, results in quite extreme values for the short-3 event. The runoff gauges at the main river stations of Neumarkt/Raab and Feldbach/Raab seem to reflect the mix of extreme positive and extreme negative peak flow deviations with maximum values of around +15% and −30%.

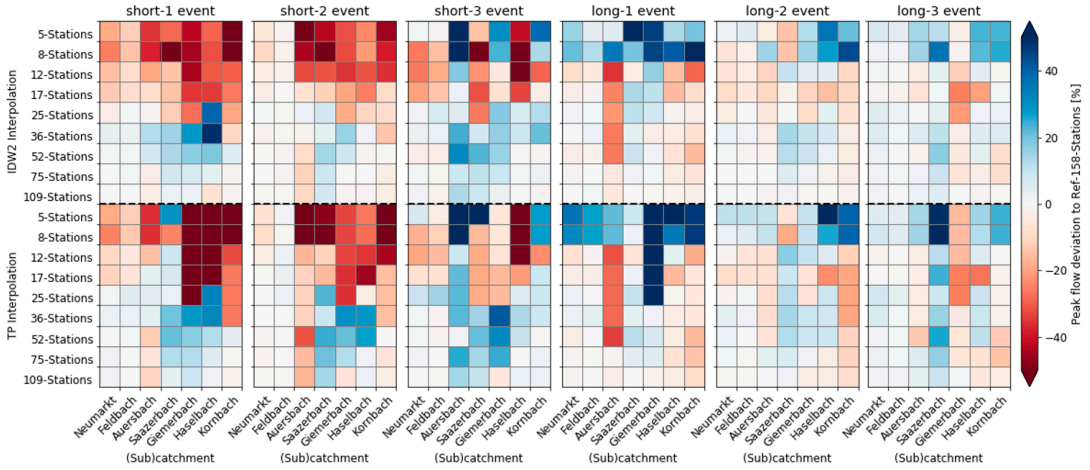


Figure 7. Peak flow deviation from the Ref-158-Stations case as a grid-cell plot with each cell indicating the magnitude of the deviation on a color scale. The cases of all six events (one event per panel), all (sub)catchments (columns within each panel), two interpolation schemes IDW2—inverse distance weighting with power of 2 and TP—Thiessen polygons (stacked subpanels in each panel), and all subnetwork cases (rows per subpanel) are shown.

The long-1 event shows the strongest peak flow deviations among the long duration events. Giemerbach shows especially high positive values when TP interpolation is used, deviating from the Ref-158-Stations case by up to 90%. Auersbach shows different behavior, with the most negative values observed for the 12- to 52-Stations cases and deviations of up to –35%. The 5- and 8-Stations cases result in positive peak flow deviations in all catchments.

The long-2 event shows less pronounced peak flow deviations than the long-1 event. Haselbach and Kornbach show the most positive deviations with up to +60% seen in the 5- and 8-Stations cases.

The long-3 event appears to be very similar to the long-2 event, showing little peak flow deviations in most of the cases. Here, Saazerbach shows the most positive peak flow deviation in the 8-Stations case when TP interpolation is used, i.e., +75%.

By comparing all events together, some results can be summarized for individual (sub)catchments. For the Raab river gauging stations of Feldbach/Raab and Neumarkt/Raab, the peak flow deviation starting from the 25-Stations subnetwork is almost the same as the Ref-158-Stations full network (less than 10%). This implies that data from the 25-Stations network would be sufficient to adequately simulate the Raab river runoff. However, the complementary network shows deviations of up to 14% for the gauge at Neumarkt/Raab in the 25-Stations case, and here, using only the 36-comp-Stations case would be sufficient, as it shows deviations below 10%. At the Feldbach/Raab gauging station, using the 36-Stations case of the primary subnetwork results in deviations below 10%, but using only the complementary subnetwork is not sufficient, even with 75-comp-Stations.

Auersbach and Saazerbach show a deviation of more than 10% at least for one event, where even the 109-Stations case does not result in the same runoff as the 158-Ref-Stations case. Giemerbach and Kornbach show a threshold at the 109-Stations case, after which

no large improvement in the accuracy of the simulated runoff is seen, compared to the Ref-158-Stations case. Haselbach already shows such a threshold in the 75-Stations case.

On the one hand, the inclusion of data from a specific number of stations leads to large changes in simulated runoff in many subcatchments. Giemerbach shows such a large step/change from the 25- to the 36-Stations case (e.g., in the short-1 event when using the TP interpolation, the value for the 25-Stations case is around −50%, and for the 36-Stations case +30%). These large steps are especially noticeable for the short-duration events, but are also measurable for the long-duration ones. The Haselbach subcatchment also shows this behavior, but between the 17- and 25-Stations cases.

On the other hand, no changes between some subnetworks are visible in some subcatchments, especially when using the TP interpolation. The northern catchments Auersbach and Kornbach almost do not show differences if we simulate runoff using data from 5- or 8-Stations subnetworks and all interpolation schemes (<1%). If we use the TP interpolation, the analysis of data from the 17-, 25-, and 36-Stations subnetworks lead to the same peak flow results in these northern catchments. Giemerbach shows almost the same runoff in all events in the 5-, 8-, and 12-Stations, and also between the 17- and 25-Stations cases.

In Figure 8, we summarize the results for peak flow deviations as a function of all station subnetworks for the primary and the complementary subnetworks. These results highlight the fact that the direction of biases (overestimation vs. underestimation) is affected primarily by the gauge network density rather than the interpolation scheme used. For long-duration heavy precipitation events, assessing a mean value over all catchments, we find that the biases decrease more rapidly when the number of gauges in the network increases. The long-duration heavy precipitation events as a mean over all (sub)networks show a threshold behavior with 17 regularly distributed stations, yielding satisfactory performance for all interpolation schemes. From the 17-Stations case and onward, the bias is less than about 10% and converges with higher subnetwork densities.

Note that our subnetworks represent a quite regularly distributed gauge configuration, and therefore, the uncertainty in the runoff simulations can be somewhat greater than for more irregular gauge location configurations, which is visible in the complementary station case. Here, the 25-comp-Stations case would be sufficient, after which no large improvement in the runoff accuracy compared to the Ref-158-Stations case becomes visible.

The short-duration heavy precipitation events show such a threshold behavior in the 52-Stations case, within the 10% range. Above this threshold, the values converge with higher subnetwork densities. In the complementary network, 75-comp-Stations are also below the 10% deviation, so this case would be as good as the Ref-158-Stations case if data are averaged across all (sub)catchments.

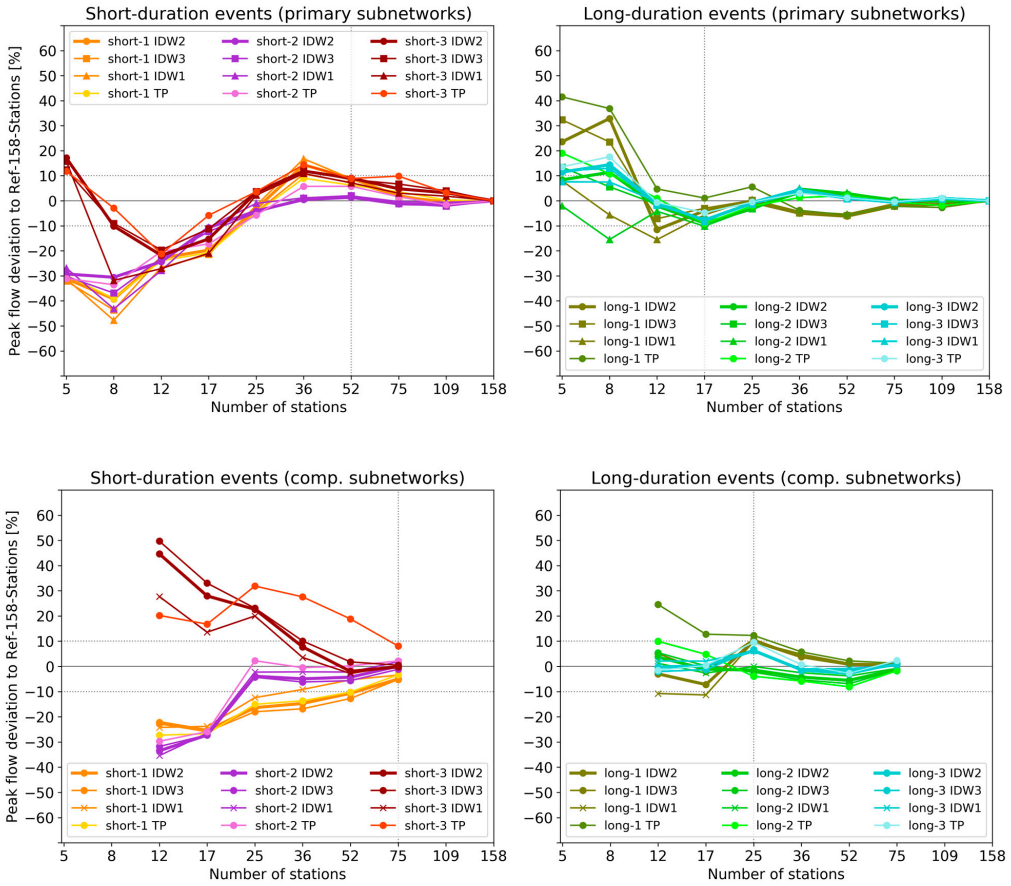


Figure 8. Peak flow deviation between the Ref-158-Stations case and the mean across all (sub)catchments for all subnetwork cases (*x*-axis of panels) and interpolation schemes (different line styles, see legend) IDW2, IDW3, and IDW1—inverse distance weighting with powers of 2, 3, and 1, TP—Thiessen polygons, respectively, for the three short events (**left**) and the three long events (**right**). The data shown in the upper panels were calculated based on the ten primary subnetwork cases (5- to 158-Stations) and in the lower panels, for the six complementary ones (12-comp- to 75-comp-Stations).

5. Discussion

In our event-based study, we chose the three most extreme short- and long-duration events. Significant differences in peak runoff among these six events were observed at the Neumarkt/Raab gauging station, in part due to different preconditions: the short-1 event, with over 100 $m^3\ s^{-1}$ peak flow, was influenced by the long-2 event that had occurred a few days before, and the other two short events in 2011 had drier preconditions and consequently smaller peak flows with 26 to 36 $m^3\ s^{-1}$.

5.1. Threshold Behavior

The mean over all catchments and events (Figure 8) shows a "sufficiency threshold"; above this density, only small runoff changes of about 10% can be observed, which converge when higher subnetwork densities are used. For the long-duration events, this threshold occurs in the 17-Stations case using a regularly distributed subnetwork. This corresponds to a mean nearest neighbor distance of 5.9 km or around 30 stations per 1000 km^2. The short-duration events only show such threshold when the 52-Stations case is analyzed

using the primary subnetwork (mean distance of around 2.6 km or around 150 stations per 1000 km^2). Such thresholds have also been reported in the literature, where no better performances after crossing specific station densities are seen [5,22,25,27]. For example, Lopez et al. [22] mentioned a threshold of 24 gauges per 1000 km^2 for the Thur basin (area 1700 km^2), and Xu et al. [27] of around 1 rain gauge per 1000 km^2 for the Xiangjiang River catchment (area 94,660 km^2). Evidently these studies focused on large catchments and larger scales. By comparing the results of the primary network with the results obtained from the complementary networks (i.e., irregularly distributed stations), we found that collecting data from a regularly distributed network requires the use of fewer stations to properly simulate runoff.

In contrast to these "sufficiency thresholds", the individually fairly small subcatchments do not always show such a sufficient density in our high-resolution case, where the results are both catchment- and event-dependent (Figure 7). Compared to the Ref-158-Stations cases, a sufficient density can only be reached in the Giemerbach and Kornbach subcatchments using a high density with the 109-Stations. In the Auersbach and Saazerbach subcatchments, this is not possible even with 109-Stations. In the Haselbach subcatchment, using the 75 stations of the primary subnetwork are sufficient, but not using the 75 complementary stations. For this, a much denser and well-targeted network is needed to obtain peak flow deviations that are lower than 10% as compared to the Ref-158-Stations case in small subcatchments.

5.2. Influence of Station Location

Adding four WEGN stations to the operational subnetworks (5- and 8-Stations cases), we noticed that including data from the first four WEGN stations in the primary subnetwork (12-Stations cases) consistently resulted in much lower peak flow deviations from the Ref-158-Stations case, but including data from the first four complementary stations (12-comp-Stations) led to much higher peak flow deviations. Therefore, in catchments where station numbers are still sparse, the location of the stations is very important for mitigating the under-sampling problem. Watson et al. [62] pointed out that not only the density of precipitation measurements has a significant impact, but also that the stations needed to be positioned in critical areas.

The effect of the station location is clear within the operational setup when comparing the 5- and 8-Stations cases. In the Auersbach and Kornbach subcatchments, the peak flow under all interpolation schemes in these cases is the same for subcatchments on the northern side of the Raab river. These two catchments are not influenced by the AHYD stations located to the west, south, and farther east of the Raab river. However, the precipitation input of the Saazerbach subcatchment is often strongly influenced by AHYD stations to the west of the river that supply meteorological information. This information is especially important, since many storms come into the area from the west or north-west.

In some cases, the simulated runoff did not change, even when more stations were included. Using TP interpolation in Giemerbach, Kornbach, and Auerbach subcatchments, it did not matter whether we used 5-, 8-, or 12-Stations or the 17- and 25-Stations case. The peak flow deviation always stayed the same for the primary subnetwork, because the supporting stations are too far away to be included when using the TP interpolation. These effects were not as pronounced when IDW interpolation schemes were used, since the influence radius here also included information from weather stations that are within the larger surrounding area.

Due to the "right" location change, the simulated runoff differed strongly from one subnetwork to the other in some cases. In the Haselbach subcatchment in the 17- to the 25-Stations case (IDW2), a change of around −30 to +40% peak flow deviation occurred. This is because one WEGN station of the 25-Stations case is very close to the subcatchment. In the Giemerbach subcatchment, changes from −50 to +30% were observed (25- to 36-Stations case), because two WEGN stations were added, and these are located directly in

the catchment. Therefore, we observed that the location of the gauging stations is highly crucial in areas where the sampling densities are basically still insufficient.

By placing our focus on small catchments, we can clearly point out that the station density has a larger influence on small subcatchments than on the total Raab catchment. The specific spatial location of precipitation stations is much more important when analyzing data for small catchments. It has already been noted in other studies that the location of precipitation measurements is important on all scales [22,24,68]. Using the highly dense WEGN, we could show new empirical evidence that again underlines the importance of these locations in small catchments, i.e., in the 10 to 30 km^2 area class.

5.3. Effect of Timing of Peak Flow

By analyzing the timing of peak flow (Table 5), we see that the differences are mostly quite small as compared to the model time resolution of 30 min. Nevertheless, a difference of three hours can make substantial difference regarding (flash) flood prevention, especially in small catchments. This difference is most profound when the time difference arises only from the station network density in combination with the station locations. In the special case of the long-3 event with a precipitation event duration of 54 h, the absolute peak runoff occurs even on different days. The total rainfall of 60 mm fell over a long time period, and depending on the station density and location, different amounts were simulated in the area. This result is especially important with respect to small catchments, where the influence of specific stations is even more pronounced. As seen before, the total Raab catchment at station Neumarkt/Raab is also influenced by this effect, and a time difference up to 9 h can occur.

5.4. Comparison of Interpolation Schemes IDW and TP

Turning specifically to examine the characteristic influences of the interpolation scheme, several aspects are salient, including the special properties of TP interpolation. Precipitation maps of interpolated gridded rainfall are generally very different when different IDW and TP interpolations are used with stiff borders between the TP polygons (Figure 5). These lead to sharp differences in simulated precipitation amounts between two adjacent polygons, especially in cases of high spatial rainfall variability. Therefore, the greatly pronounced peak flow deviation is also due to this reason (Figure 7).

Compared to using the different IDW interpolation schemes, the effect of using the TP interpolation is much stronger. However, by comparing the three IDW interpolation schemes, we see that the differences among them are not negligible. Peak flow deviations of up to 50% from the IDW2 to the IDW1 case are possible (e.g., short-3 event, 5-Stations, Saazerbach). The influence of the interpolation scheme is highly event-dependent and especially pronounced in small catchments with a low subnetwork number. For the total catchment area of Neumarkt/Raab and Feldbach/Raab, the differences are below a 5% deviation. In this case, it does not make a difference which IDW scheme is used, but the choice between IDW and TP is distinct.

Among the IDW interpolation schemes, the peak flow deviations of IDW3 tend to be the closest ones yielded by using the TP interpolation. This result is expected, since the higher IDW3 weighting power gives less weight to the surrounding stations than IDW2 or IDW1. Dirks et al. [40] suggested using the power values of 2 for daily and monthly, 3 for hourly, and 1 for yearly precipitation interpolations to minimize the interpolation error. Kurtzman et al. [39] mentioned that the influence of weighting power depended on spatial pattern, specifically referring to the location of the catchment in their Mediterranean study area. Large power values of 3 are more effective closer to the coast line, whereas smaller power values such as 1 are more effective closer to the mountains. Our study area is close to the mountains, which seems to support the observations of Kurtzman et al. [39] regarding the IDW1 interpolation, but we use half-hourly time steps, which is more similar to the use of the IDW3 method in Dirks et al. [40]. Our results do not suggest that there is a certain IDW weighting power value for performing optimal hydrological modelling in the Rabb

catchment. We used the IDW2 as reference, as it is also the most widely used [37]. In other studies in the WEGN region, the weighting power of 2 was also set for the precipitation interpolation [69,70] based on performance tests such as leave-one-station-out verifications on small-scale rainfall events. Nevertheless, if we use many stations, we see no relevant difference between the different weighting power of the IDW interpolations from about from the 52-Stations case onward (mean distance of around 2.5 km).

Overall, if only a few stations are available, the IDW interpolations, and in particular IDW2, are preferable for analyzing data from regions with moderate topography. The TP interpolation is not recommended for areas with complex topography and low station densities, as also stated by Kobold and Brilly [32]. Dirks et al. [40] also do not recommend the TP interpolation, because of its unrealistic discontinuous rain fields, although the interpolation errors between TP and IDW are comparable. Only when the network is highly dense, as in our cases with at least 350 station per 1000 km^2 or more, the TP method might be an option, since it is computationally the least expensive. Nevertheless, precipitation maps with sharp differences that are still unrealistic will exist that could adversely impact runoff results in very small catchments.

In summary, our results clearly show the influence of the interpolation scheme on modelling, especially for few-station networks. Nonetheless, the impact of station network density is clearly much more significant for runoff simulations than the impact of the interpolation scheme.

6. Conclusions

We used the highly dense WEGN station network in the southeastern Alpine foreland of Styria, Austria, to analyze the influence of rain gauge network density and interpolation schemes on simulated runoff, placing a focus on small subcatchments (10 to 30 km^2).

Our first key question was "How many precipitation stations do we need to reliably model runoff during heavy rainfall events?" This question cannot be answered in general due to the complex spatiotemporal characteristics of the events, and especially of the short-duration convective events. Although our results show that the influence of the station network density is specifically catchment-, (station) location-, and event-dependent, we were able to derive average, guideline results.

For long-duration stratiform-type events (lasting typically longer than a day) and averaging over all catchments, a station density with a mean nearest neighbor distance of around 6 km (17-Stations) is found to be sufficiently dense to perform robust runoff modeling, including reliable peak runoff estimations. To obtain an average for all catchments from the short-duration heavy convective rainfall events (lasting typically a few hours only), at least a mean nearest neighbor distance of around 2.6 km (52-Stations, regularly distributed subnetwork) is needed for runoff modeling. Our simulations with data from the complementary subnetworks show that not only the density of stations but also their spatial configuration is crucial.

The second research question "Are there specific features of small subcatchments to reliably model runoff under heavy rainfall events?" can be answered with a clear "Yes". By focusing on subcatchments in the 10 km^2 size class, our results show that sufficient station density is mostly higher with 109-Stations (mean distance 1.7 km) or not even reached at numbers lower than the reference case. Therefore, especially in small subcatchments, both the station density and the actual station locations are crucial. Here, the influence of station location also depends on typical storm tracks across the catchment.

Furthermore, the radius of influence of each station plays an important role for precipitation interpolations. The third key research question "How strongly does the interpolation scheme influence runoff results when the precipitation station density is the same?" is related to this. The answer to this question depends on the station density. For very dense station networks (in our case 109 to 158 stations, mean distance of 1.7 km to 1.4 km), the specific interpolation scheme is not relevant. The simpler TP interpolation is already sufficient in these cases, although it can provide unrealistic rainfall fields. Overall,

the interpolation scheme is found to be clearly less influential than the gauge network density on simulated runoff. Hence, when analyzing and interpreting modeled runoff based on rainfall input data, station network density will most importantly influence the results as long as a reasonable interpolation is chosen.

We emphasize that it is important to carry out an explicit study of the hydrological response to different precipitation events. Many earlier studies have evaluated the "accuracy" of (remote-sensing) gridded rainfall event data by making direct comparison with ground gauge measurements [18,19,71]. Our study findings highlight the fact that it is also important to evaluate the performance of precipitation datasets at various resolutions to measure hydrological runoff response. Such evaluations will provide broader practical guidance both to rainfall data providers as well as to hydrological model users.

The dependence on specific rainfall event characteristics and station network density is mitigated in the main river runoff. However, regarding local-scale hazards that can occur, such as severe overland flooding, flashfloods, and hillslope landslides that are triggered by short-duration convective events, it is necessary to obtain more dense observations to perform reliable hydrological modeling and estimate the risks of these hazards and suggest protective action. While the WEGN is a unique, long-term research facility with sufficiently high station density, it is quite limited in terms of area. The densification and expansion of runoff and rainfall gauge networks in this and many other risk-prone areas, therefore, would be a great and much needed improvement on top of existing observations. An alternative would be to tap other data sources, enabling suitable data products to be obtained at high spatiotemporal resolutions, such as well-calibrated, high-quality precipitation radar data.

In deploying new stations, selected station locations have a strong effect on gridded precipitation fields and, therefore, also on runoff results, especially in small catchments. In this study, we selected two subnetwork ensembles, the primary and the complementary subnetwork with gauges from the WEGN. The primary subnetwork contained stations with a quite regular distribution, and the complementary subnetwork contained different WEGN stations. Performing a more detailed analysis, whereby the influences of irregular distributions are examined by randomly picking and evaluating stations more closely on the basis of catchment characteristics, may be a useful design step for determining new station placements in other areas. This would help us to arrive at an optimal rain gauge network design for hydrological purposes in the specific catchment.

Since such dense networks are available in virtually no other place worldwide, the runoff impact results derived here for the Raab catchment and its subcatchments in south-eastern Austria need to be "transferred" to other regions with due care, examining the comparability of weather, hydrology, and landscape characteristics [36,41,72]. With such due care, we consider the essential results and conclusions to be transferable to many other mid-latitude land regions. For the majority of ungauged or extremely sparsely observed small catchments, the awareness of both the level of skill and limitations of rainfall–runoff modeling, as reported here, will be particularly crucial.

Author Contributions: All authors designed the study, with primary contributions by C.H. and G.K. C.H. collected the data, performed the modeling and most of the analysis, created the figures, and wrote the first draft of the manuscript. G.K. provided guidance and advice on all aspects of the study and significantly contributed to the figure design and the text. S.O. contributed to the data collection, precipitation data analysis, and figure creation. W.R. supported the model calibration and validation. All authors helped to shape the research and analysis; they provided critical feedback and contributions to the text until submission and during review. All authors have read and agreed to the published version of the manuscript.

Funding: This research has been supported by the Austrian Science Fund (FWF) Doctoral Programme Climate Change—Uncertainties, Thresholds and Coping Strategies (grant no. W1256) and the University of Graz.

Institutional Review Board Statement: Not applicable.

Informed Consent Statement: Not applicable.

Data Availability Statement: The hydrological model WaSiM is available via http://wasim.ch (accessed on 25 March 2021) (version used: WaSiM-Richards 10.04.07). The WegenerNet data are available at https://doi.org/10.25364/WEGC/WPS7.1:2021.1 (Fuchsberger et al. [50]: WegenerNet climate station network Level 2 data version 7.1 (2007–2020); Wegener Center, Univ. of Graz, Austria). ZAMG data are available from the Austrian Weather Service (www.zamg.ac.at, accessed on 25 March 2021) and AHYD data from the Austrian Hydrographic Service (https://ehyd.gv.at, accessed on 25 March 2021). HYDROBOD data are used from Klebinder et al. [49] and are available on request from these authors. Geoinformation data are from state government offices of Styria and Burgenland and are available from the respective GIS services (www.gis.steiermark.at; https://geodaten.bgld.gv.at, accessed on 25 March 2021).

Acknowledgments: The authors thank J. Fuchsberger (Wegener Center, Univ. of Graz) for support and advice on the WegenerNet data, S. Birk (Inst. for Earth Sciences, Univ. of Graz) for discussions and advice on the water balance and groundwater characteristics of the catchment, and V. Hess (DK Climate Change, Univ. of Graz) for several fruitful discussions and support during the study work. We also thank the anonymous reviewers for their helpful comments. Furthermore, we acknowledge the data providers at the Austrian Weather Service (ZAMG), the Austrian Hydrographic Service (AHYD), the state government offices of Styria and Burgenland, and the Wegener Center regarding the WegenerNet data. WegenerNet funding is provided by the Austrian Ministry for Science and Research, the University of Graz, the Styrian Provincial Government (which also included European Union regional development funds), and the city of Graz; detailed information can be found online (www.wegcenter.at/wegenernet, last access: 25 March 2021). This research project has been funded by the Austrian Science Fund (FWF) Doctoral Programme Climate Change—Uncertainties, Thresholds and Coping Strategies (grant no. W1256) and the University of Graz. Open Access Funding by the Austrian Science Fund (FWF).

Conflicts of Interest: The authors declare no conflict of interest.

Appendix A

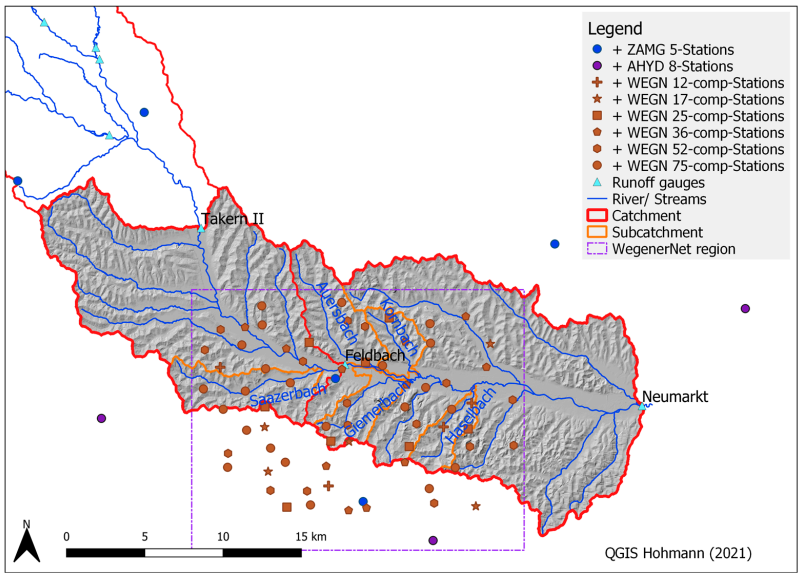


Figure A1. Enlarged view of the study area, as in Figure 1, indicating the complementary subnetwork setups and subcatchments used in the study.

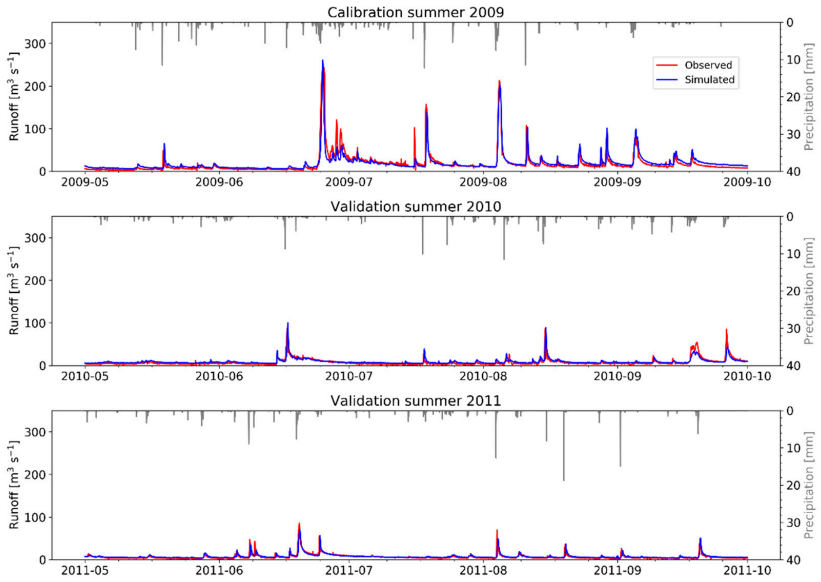


Figure A2. Simulated (blue line) and observed runoff (red line) at the Neumarkt/Raab gauging station for the calibration period of May to September 2009 (top) and the validation period of May to September 2010 (middle) and 2011 (bottom). From the top of each panel, the interpolated precipitation (grey line) is co-visualized over the same extended summer periods.

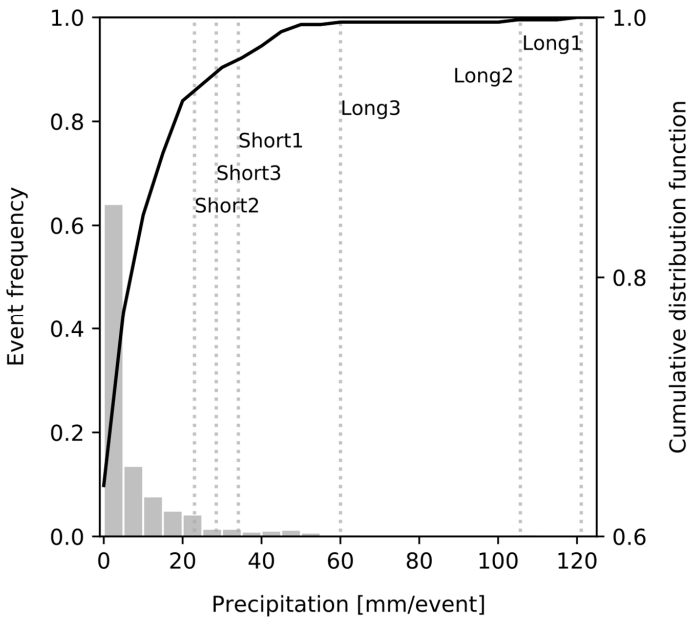


Figure A3. Classification of the selected most extreme three short-duration and three long-duration events within our study time frame over the extended summer months (May to September) in 2009–2014.

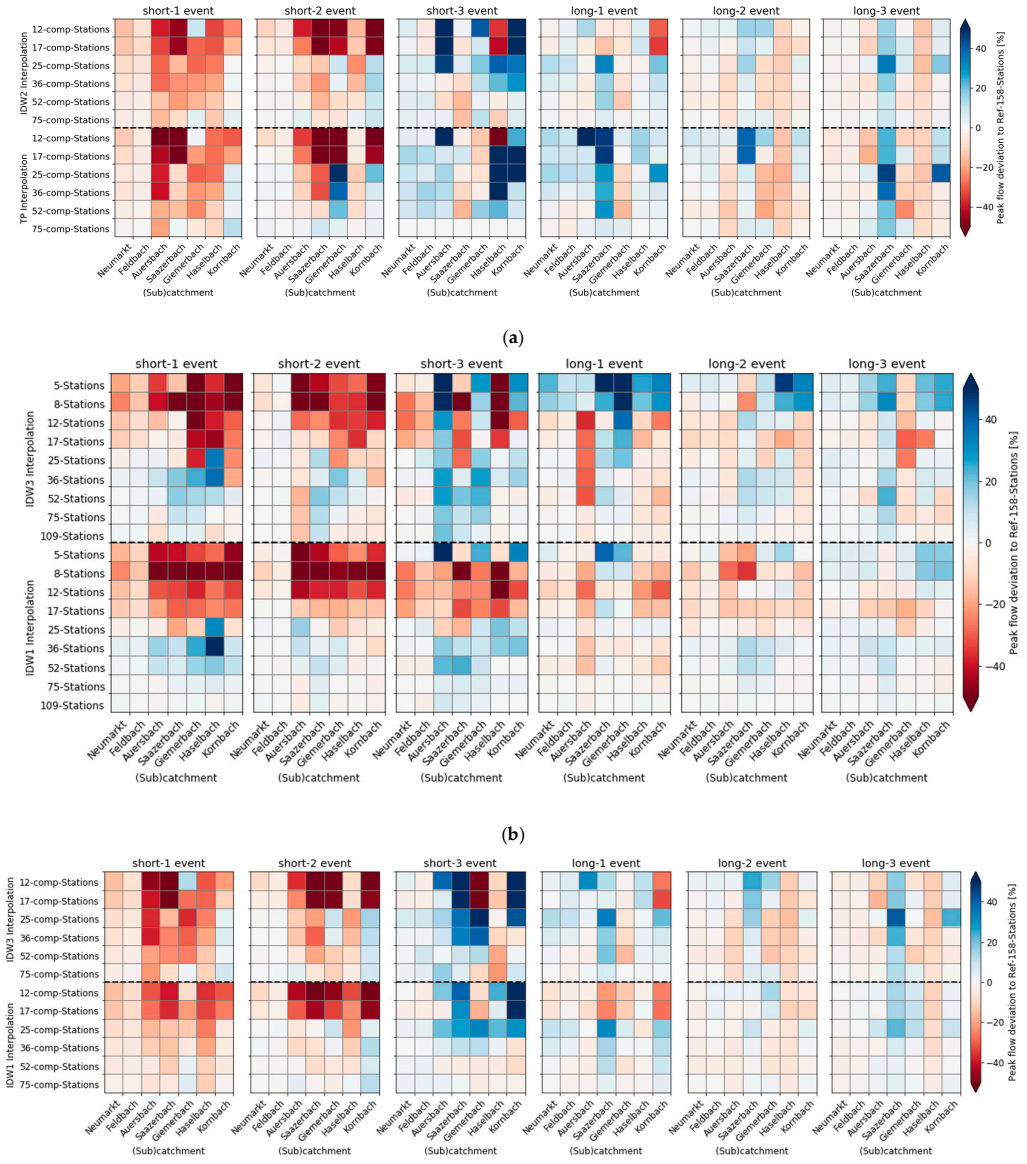


Figure A4. Complementary to Figure 7. Peak flow deviation to Ref-158-Stations case as a grid-cell plot with each cell indicating the magnitude of the deviation on a color-scale, for the cases of all six events (one event per panel), all (sub)catchments (columns per panel), the four interpolation schemes inverse distance weighting with power of 2 (IDW2), power of 3 (IDW3), power of 1 (IDW1), and Thiessen polygons (TP)) (stacked subpanels per panel), and all subnetwork cases (rows per subpanel). (**a**) depicts the results of the complementary subnetwork of IDW2 and TP interpolation; (**b**) the results for the primary subnetworks for IDW3 and IDW1; (**c**) the ones of the complementary subnetworks (IDW3 and IDW1) analyzed in this study.

References

1. Kharin, V.V.; Zwiers, F.W.; Zhang, X.; Hegerl, G.C. Changes in temperature and precipitation extremes in the IPCC ensemble of global coupled model simulations. *J. Clim.* **2007**, *20*, 1419–1444. [CrossRef]
2. Chen, H.; Sun, J.; Chen, X.; Zhou, W. CGCM projections of heavy rainfall events in China. *Int. J. Climatol.* **2012**, *32*, 441–450. [CrossRef]
3. Fischer, E.M.; Knutti, R. Observed heavy precipitation increase confirms theory and early models. *Nat. Clim. Chang.* **2016**, *6*, 986–991. [CrossRef]
4. Prein, A.F.; Rasmussen, R.M.; Ikeda, K.; Liu, C.; Clark, M.P.; Holland, G.J. The future intensification of hourly precipitation extremes. *Nat. Clim. Chang.* **2016**, *7*, 48–52. [CrossRef]
5. Bárdossy, A.; Das, T. Influence of rainfall observation network on model calibration and application. *Hydrol. Earth Syst. Sci.* **2008**, *12*, 77–89. [CrossRef]
6. Zeng, Q.; Chen, H.; Xu, C.-Y.; Jie, M.-X.; Chen, J.; Guo, S.-L.; Liu, J. The effect of rain gauge density and distribution on runoff simulation using a lumped hydrological modelling approach. *J. Hydrol.* **2018**, *563*, 106–122. [CrossRef]
7. Gilewski, P.; Nawalany, M. Inter-Comparison of Rain-Gauge, Radar, and Satellite (IMERG GPM) Precipitation Estimates Performance for Rainfall-Runoff Modeling in a Mountainous Catchment in Poland. *Water* **2018**, *10*, 1665. [CrossRef]
8. St-Hilaire, A.; Ouarda, T.B.M.J.; Lachance, M.; Bobée, B.; Gaudet, J.; Gignac, C. Assessment of the impact of meteorological network density on the estimation of basin precipitation and runoff: A case study. *Hydrol. Process.* **2003**, *17*, 3561–3580. [CrossRef]
9. Maier, R.; Krebs, G.; Pichler, M.; Muschalla, D.; Gruber, G. Spatial Rainfall Variability in Urban Environments—High-Density Precipitation Measurements on a City-Scale. *Water* **2020**, *12*, 1157. [CrossRef]
10. McMillan, H.K. Effect of spatial variability and seasonality in soil moisture on drainage thresholds and fluxes in a conceptual hydrological model. *Hydrol. Process.* **2012**, *26*, 2838–2844. [CrossRef]
11. Goodrich, D.C.; Faurès, J.-M.; Woolhiser, D.A.; Lane, L.J.; Sorooshian, S. Measurement and analysis of small-scale convective storm rainfall variability. *J. Hydrol.* **1995**, *173*, 283–308. [CrossRef]
12. Huang, Y.; Bárdossy, A.; Zhang, K. Sensitivity of hydrological models to temporal and spatial resolutions of rainfall data. *Hydrol. Earth Syst. Sci.* **2019**, *23*, 2647–2663. [CrossRef]
13. O, S.; Foelsche, U. Assessment of spatial uncertainty of heavy rainfall at catchment scale using a dense gauge network. *Hydrol. Earth Syst. Sci.* **2019**, *23*, 2863–2875. [CrossRef]
14. Kidd, C.; Huffman, G. Review Global precipitation measurement. *Meteorol. Appl.* **2011**, *18*, 334–353. [CrossRef]
15. Sun, X.; Mein, R.G.; Keenan, T.D.; Elliott, J.F. Flood estimation using radar and raingauge data. *J. Hydrol.* **2000**, *239*, 4–18. [CrossRef]
16. Tetzlaff, D.; Uhlenbrook, S. Significance of spatial variability in precipitation for process-oriented modelling: Results from two nested catchments using radar and ground station data. *Hydrol. Earth Syst. Sci.* **2005**, *9*, 29–41. [CrossRef]
17. Tian, Y.; Peters-Lidard, C.D. A global map of uncertainties in satellite-based precipitation measurements. *Geophys. Res. Lett.* **2010**, *37*, L24407. [CrossRef]
18. Kirstetter, P.-E.; Hong, Y.; Gourley, J.J.; Chen, S.; Flamig, Z.; Zhang, J.; Schwaller, M.; Petersen, W.; Amitai, E. Toward a framework for systematic error modeling of spaceborne precipitation radar with NOAA/NSSL ground radar–based national mosaic QPE. *J. Hydrometeorol.* **2012**, *13*, 1285–1300. [CrossRef]
19. O, S.; Foelsche, U.; Kirchengast, G.; Fuchsberger, J.; Tan, J.; Petersen, W.A. Evaluation of GPM IMERG Early, Late, and Final rainfall estimates using WegenerNet gauge data in southeastern Austria. *Hydrol. Earth Syst. Sci.* **2017**, *21*, 6559–6572. [CrossRef]
20. Lasser, M.; O, S.; Foelsche, U. Evaluation of GPM-DPR precipitation estimates with WegenerNet gauge data. *Atmos. Meas. Tech.* **2019**, *12*, 5055–5070. [CrossRef]
21. Ghaemi, E.; Foelsche, U.; Kann, A.; Fuchsberger, J. Evaluation of INCA precipitation analysis using a very dense rain gauge network in southeast Austria. *Hydrol. Earth Syst. Sci. Discuss.* **2021**, in review. [CrossRef]
22. Lopez, M.G.; Wennerström, H.; Nordén, L.; Seibert, J. Location and density of rain gauges for the estimation of spatial varying precipitation. *Geogr. Ann. Ser. A Phys. Geogr.* **2015**, *97*, 167–179. [CrossRef]
23. Goovaerts, P. Geostatistical approaches for incorporating elevation into the spatial interpolation of rainfall. *J. Hydrol.* **2000**, *228*, 113–129. [CrossRef]
24. Obled, C.; Wendling, J.; Beven, K.J. The sensitivity of hydrological models to spatial rainfall patterns: An evaluation using observed data. *J. Hydrol.* **1994**, *159*, 305–333. [CrossRef]
25. Dong, X.; Dohmen-Janssen, C.M.; Booij, M.J. Appropriate spatial sampling of rainfall or flow simulation. *Hydrol. Sci. J.* **2005**, *50*, 279–298. [CrossRef]
26. Meselhe, E.A.; Habib, E.H.; Oche, O.C.; Gautam, S. Sensitivity of conceptual and physically based hydrologic models to temporal and spatial rainfall sampling. *J. Hydrol. Eng.* **2009**, *14*, 711–720. [CrossRef]
27. Xu, H.; Xu, C.-Y.; Chen, H.; Zhang, Z.; Li, L. Assessing the influence of rain gauge density and distribution on hydrological model performance in a humid region of China. *J. Hydrol.* **2013**, *505*, 1–12. [CrossRef]
28. Zhang, X.; Srinivasan, R. Gis-based spatial precipitation estimation: A comparison of geostatistical approaches. *J. Am. Water Resour. Assoc.* **2009**, *45*, 894–906. [CrossRef]
29. Ly, S.; Charles, C.; Degré, A.; Sarann Ly, C.C.A.D. Different methods for spatial interpolation of rainfall data for operational hydrology and hydrological modeling at watershed scale. A review. *Biotechnol. Agron. Société Environ.* **2013**, *17*, 392–406.

30. Szcześniak, M.; Piniewski, M. Improvement of Hydrological Simulations by Applying Daily Precipitation Interpolation Schemes in Meso-Scale Catchments. *Water* **2015**, *7*, 747–779. [CrossRef]
31. Andréassian, V.; Perrin, C.; Michel, C.; Usart-Sanchez, I.; Lavabre, J. Impact of imperfect rainfall knowledge on the efficiency and the parameters of watershed models. *J. Hydrol.* **2001**, *250*, 206–223. [CrossRef]
32. Kobold, M.; Brilly, M. The use of HBV model for flash flood forecasting. *Nat. Hazards Earth Syst. Sci.* **2006**, *6*, 407–417. [CrossRef]
33. Verworn, A.; Haberlandt, U. Spatial interpolation of hourly rainfall-effect of additional information, variogram inference and storm properties. *Hydrol. Earth Syst. Sci.* **2011**, *15*, 569–584. [CrossRef]
34. Schwarzak, S.; Hänsel, S.; Matschullat, J. Projected changes in extreme precipitation characteristics for Central Eastern Germany (21st century, model-based analysis). *Int. J. Climatol.* **2015**, *35*, 2724–2734. [CrossRef]
35. Breinl, K.; Müller-Thomy, H.; Blöschl, G. Space–time characteristics of areal reduction factors and rainfall processes. *J. Hydrometeorol.* **2020**, *21*, 671–689. [CrossRef]
36. Kirchengast, G.; Kabas, T.; Leuprecht, A.; Bichler, C.; Truhetz, H. WegenerNet: A pioneering high-resolution network for monitoring weather and climate. *Bull. Am. Meteorol. Soc.* **2014**, *95*, 227–242. [CrossRef]
37. Chen, F.W.; Liu, C.W. Estimation of the spatial rainfall distribution using inverse distance weighting (IDW) in the middle of Taiwan. *Paddy Water Environ.* **2012**, *10*, 209–222. [CrossRef]
38. Gilewski, P. Impact of the Grid Resolution and Deterministic Interpolation of Precipitation on Rainfall-Runoff Modeling in a Sparsely Gauged Mountainous Catchment. *Water* **2021**, *13*, 230. [CrossRef]
39. Kurtzman, D.; Navon, S.; Morin, E. Improving interpolation of daily precipitation for hydrologic modelling: Spatial patterns of preferred interpolators. *Hydrol. Process.* **2009**, *23*, 3281–3291. [CrossRef]
40. Dirks, K.N.; Hay, J.E.; Stow, C.D.; Harris, D. High-resolution studies of rainfall on Norfolk Island Part II: Interpolation of rainfall data. *J. Hydrol.* **1998**, *208*, 187–193. [CrossRef]
41. Schroeer, K.; Kirchengast, G. Sensitivity of extreme precipitation to temperature: The variability of scaling factors from a regional to local perspective. *Clim. Dyn.* **2018**, *50*, 3981–3994. [CrossRef]
42. Schulla, J. Hydrologische Modellierung von Flussgebieten zur Abschätzung der Folgen von Klimaänderungen. Ph.D. Thesis, ETH Zurich, Zurich, Switzerland, 1997.
43. Gervais, M.; Tremblay, L.B.; Gyakum, J.R.; Atallah, E. Representing extremes in a daily gridded precipitation analysis over the United States: impacts of station density, resolution, and gridding methods. *J. Clim.* **2014**, *27*, 5201–5218. [CrossRef]
44. Avila, F.B.; Dong, S.; Menang, K.P.; Rajczak, J.; Renom, M.; Donat, M.G.; Alexander, L.V. Systematic investigation of gridding-related scaling effects on annual statistics of daily temperature and precipitation maxima: A case study for south-east Australia. *Weather Clim. Extrem.* **2015**, *9*, 6–16. [CrossRef]
45. Herrera, S.; Kotlarski, S.; Soares, P.M.M.M.; Cardoso, R.M.; Jaczewski, A.; Gutiérrez, J.M.; Maraun, D. Uncertainty in gridded precipitation products: Influence of station density, interpolation method and grid resolution. *Int. J. Climatol.* **2018**, *39*, 3717–3729. [CrossRef]
46. Hohmann, C.; Kirchengast, G.; Birk, S. Alpine foreland running drier? Sensitivity of a drought vulnerable catchment to changes in climate, land use, and water management. *Clim. Chang.* **2018**, *147*, 179–193. [CrossRef]
47. O, S.; Foelsche, U.; Kirchengast, G.; Fuchsberger, J. Validation and correction of rainfall data from the WegenerNet high density network in southeast Austria. *J. Hydrol.* **2018**, *556*, 1110–1122. [CrossRef]
48. Haiden, T.; Kann, A.; Wittmann, C.; Pistotnik, G.; Bica, B.; Gruber, C. The integrated nowcasting through comprehensive analysis (INCA) system and its validation over the Eastern Alpine region. *Weather Forecast.* **2011**, *26*, 166–183. [CrossRef]
49. Klebinder, K.; Sotier, B.; Lechner, V.; Strauss, P. *Hydrologische und hydropedologische Kenndaten Raabgebiet und Region Südoststeiermark*; Department of Natural Hazards, Austrian Research Center for Forests (BFW): Innsbruck, Austria, 2017.
50. Fuchsberger, J.; Kirchengast, G.; Bichler, C.; Leuprecht, A.; Kabas, T. WegenerNet climate station network Level 2 data version 7.1 (2007–2020). In *Wegener Center for Climate and Global Change*; University of Graz: Graz, Austria, 2021. [CrossRef]
51. Krammer, C.; Klebinder, K.; Eder, A.; Sotier, B.; Strauss, P.; Bauer, T. HYDROBOD: Obtaining a GIS-based hydrological soil database and a runoff coefficient calculator for Lower Austria. *Forum Geogr.* **2016**, *XV*, 100–104. [CrossRef]
52. Bürger, G.; Schulla, J.; Werner, A.T. Estimates of future flow, including extremes, of the Columbia River headwaters. *Water Resour. Res.* **2011**, *47*, 1–18. [CrossRef]
53. Gädeke, A.; Hölzel, H.; Koch, H.; Pohle, I.; Grünewald, U. Analysis of uncertainties in the hydrological response of a model-based climate change impact assessment in a subcatchment of the Spree River, Germany. *Hydrol. Process.* **2014**, *28*, 3978–3998. [CrossRef]
54. Alaoui, A.; Willimann, E.; Jasper, K.; Felder, G.; Herger, F.; Magnusson, J.; Weingartner, R. Modelling the effects of land use and climate changes on hydrology in the Ursern Valley, Switzerland. *Hydrol. Process.* **2014**, *28*, 3602–3614. [CrossRef]
55. Yira, Y.; Diekkrüger, B.; Steup, G.; Bossa, A.Y. Modeling land use change impacts on water resources in a tropical West African catchment (Dano, Burkina Faso). *J. Hydrol.* **2016**, *537*, 187–199. [CrossRef]
56. Schulla, J. Model Description WaSiM (Water Balance Simulation Model); Hydrology Software Consulting J. Schulla, Zurich, Switzerland 2019. Available online: www.wasim.ch (accessed on 25 March 2021).
57. Monteith, J.L. Evaporation and environment. *Symp. Soc. Exp. Biol.* **1965**, *19*, 205–234. [PubMed]
58. van Genuchten, M.T. Closed-form equation for predicting the hydraulic conductivity of unsaturated soils. *Soil Sci. Soc. Am. J.* **1980**, *44*, 892–898. [CrossRef]

59. Nash, J.E.; Sutcliffe, J.V. River flow forecasting through conceptual models part I—A discussion of principles. *J. Hydrol.* **1970**, *10*, 282–290. [CrossRef]
60. Gupta, H.V.; Kling, H.; Yilmaz, K.K.; Martinez, G.F. Decomposition of the mean squared error and NSE performance criteria: Implications for improving hydrological modelling. *J. Hydrol.* **2009**, *377*, 80–91. [CrossRef]
61. Moriasi, D.N.; Arnold, J.G.; Van Liew, M.W.; Bingner, R.L.; Harmel, R.D.; Veith, T.L. Model evaluation guidelines for systematic quantification of accuracy in watershed simulations. *Trans. ASABE* **2007**, *50*, 885–900. [CrossRef]
62. Watson, A.; Kralisch, S.; Künne, A.; Fink, M.; Miller, J. Impact of precipitation data density and duration on simulated flow dynamics and implications for ecohydrological modelling in semi-arid catchments in Southern Africa. *J. Hydrol.* **2020**, *590*, 125280. [CrossRef]
63. Duan, Q.; Sorooshian, S.; Gupta, V.K. Optimal use of the SCE-UA global optimization method for calibrating watershed models. *J. Hydrol.* **1994**, *158*, 265–284. [CrossRef]
64. Schroeer, K.; Tye, M.R. Quantifying damage contributions from convective and stratiform weather types: How well do precipitation and discharge data indicate the risk? *J. Flood Risk Manag.* **2018**. [CrossRef]
65. Dunkerley, D. Identifying individual rain events from pluviograph records: A review with analysis of data from an Australian dryland site. *Hydrol. Process.* **2008**, *22*, 5024–5036. [CrossRef]
66. Cheng, M.; Wang, Y.; Engel, B.; Zhang, W.; Peng, H.; Chen, X.; Xia, H.; Cheng, M.; Wang, Y.; Engel, B.; et al. Performance Assessment of Spatial Interpolation of Precipitation for Hydrological Process Simulation in the Three Gorges Basin. *Water* **2017**, *9*, 838. [CrossRef]
67. Syed, K.H.; Goodrich, D.C.; Myers, D.E.; Sorooshian, S. Spatial characteristics of thunderstorm rainfall fields and their relation to runoff. *J. Hydrol.* **2003**, *271*, 1–21. [CrossRef]
68. Beven, K.J.; Hornberger, G.M. Assessing the effect of spatial pattern of precipitation in modeling stream flow hydrographs. *J. Am. Water Resour. Assoc.* **1982**, *18*, 823–829. [CrossRef]
69. Fuchsberger, J.; Kirchengast, G.; Kabas, T. WegenerNet high-resolution weather and climate data from 2007 to 2020. *Earth Syst. Sci. Data* **2021**, *13*, 1307–1334. [CrossRef]
70. Kabas, T. WegenerNet climate station network region Feldbach: Experimental setup and high- resolution data for weather and climate research (in German). *Wegener Cent. Sci. Rep.* **2012**, *47*, 177.
71. Lamptey, B.L. Comparison of gridded multisatellite rainfall estimates with gridded gauge rainfall over West Africa. *J. Appl. Meteorol. Climatol.* **2008**, *47*, 185–205. [CrossRef]
72. Schroeer, K.; Kirchengast, G.; O, S. Strong dependence of extreme convective precipitation intensities on gauge network density. *Geophys. Res. Lett.* **2018**, *45*, 8253–8263. [CrossRef]

4.3 Research Article 3: High-resolution climate data sets in hydrological impact studies: Assessing their value in alpine and prealpine catchments in southeastern Austria

Published as:
Stefanie Peßenteiner, **Clara Hohmann**, Gottfried Kirchengast, and Wolfgang Schöner (2021), High-resolution climate datasets in hydrological impact studies: Assessing their value in alpine and prealpine catchments in southeastern Austria, *Journal of Hydrology: Regional Studies*, 38, 100962, DOI:10.1016/j.ejrh.2021.100962.
Original article available at: https://doi.org/10.1016/j.ejrh.2021.100962.

Journal of Hydrology: Regional Studies 38 (2021) 100962

Contents lists available at ScienceDirect

Journal of Hydrology: Regional Studies

journal homepage: www.elsevier.com/locate/ejrh

High-resolution climate datasets in hydrological impact studies: Assessing their value in alpine and pre-alpine catchments in southeastern Austria

Stefanie Peßenteiner [a,*], Clara Hohmann [b,c], Gottfried Kirchengast [b,c,d], Wolfgang Schöner [a]

[a] Department of Geography and Regional Science, University of Graz, Heinrichstraße 36, 8010 Graz, Austria
[b] Wegener Center for Climate and Global Change (WEGC), University of Graz, Brandhofgasse 5, 8010 Graz, Austria
[c] FWF-DK Climate Change, University of Graz, Glacisstraße 27/1, 8010 Graz, Austria
[d] Institute for Geophysics, Astrophysics, and Meteorology/Institute of Physics, University of Graz, Universitätsplatz 5, 8010 Graz, Austria

ARTICLE INFO

Keywords:
ÖKS15
Climate datasets
Bias correction
Hydrological impacts
Hydrological modeling

ABSTRACT

Study region: Catchments: Wölzerbach, Raab; Styria; Austria.
Study focus: The study was carried out to investigate the fitness for purpose of the high-resolution Austrian National Climate datasets (ÖKS15) in hydrological applications. Provided as a standard for climate impact studies in Austria in 2016, the potential of the ÖKS15 data for hydrological impact studies has not previously been assessed. To fill this research gap, we evaluated the ÖKS15 datasets for the recent climate period (1961–2005) to determine their suitability for hydrological analyses. Hydro-meteorological indicators of the ÖKS15 datasets, as well as of the data used to obtain them by bias correcting and downscaling the EURO-CORDEX models, were assessed at different spatio-temporal scales and compared to the raw EURO-CORDEX data. The hydrological model WaSiM was driven with the different datasets to generate the hydrological simulations used for validation against long-term observations.
New hydrological insights for the region: Hydro-meteorological indicators obtained from ÖKS15 models are comparable to observations and associated with less uncertainty than the raw EURO-CORDEX data. We thus consider the ÖKS15 dataset basically appropriate for hydrological impact studies. However, despite bias correction, some biases in the ÖKS15 data remain and differences in timing, magnitude and spatial characteristics lead to deviations in hydrological indicators at different scales.

1. Introduction

Regional Climate Model (RCM) projections provide essential information for hydrological climate change impact assessments. These are commonly used as input in hydrological models (e.g., Pastén-Zapata et al., 2020; Rössler et al., 2019; Smiatek and Kunstmann, 2019; Willkofer et al., 2018). However, the application of climate-hydrology modelling chains, specifically for smaller sized basins (< 100 km^2), remains challenging. For this reason, such an application has been subject to numerous studies (Smiatek and

* Corresponding author.
E-mail address: stefanie.pessenteiner@uni-graz.at (S. Peßenteiner).

https://doi.org/10.1016/j.ejrh.2021.100962
Received 11 June 2021; Received in revised form 1 November 2021; Accepted 1 November 2021
Available online 26 November 2021
2214-5818/© 2021 The Authors. Published by Elsevier B.V. This is an open access article under the CC BY license (http://creativecommons.org/licenses/by/4.0/).

Kunstmann, 2019; Reszler et al., 2018; Olsson et al., 2016; Teutschbein and Seibert, 2010).

Among others Maraun et al. (2010) identified "major gaps" between dynamic climate models and the end users' needs: The poor representation of heavy localized convective precipitation and the spatial precipitation distribution in these models, as well as problems in the correct reproduction of sub-daily rainfall, are particularly challenging aspects for hydrologic applications. Liersch et al. (2018) posed a valid question when they asked if climate model simulations are the right fuel to drive hydrological models. They showed that bias correction may enhance the validity of climate simulations for driving hydrological models, but it can also deteriorate hydrological extremes. They concluded that it might be reasonable to select a climate model subset instead of full ensembles in a regional context. Hakala et al. (2018) confirmed the importance of bias correcting RCMs driven by General Circulation Models (GCMs), which improved discharge simulations in most cases in their study. They proposed using hydrological models to rank GCM-RCM simulations (i.e., simulations from RCMs forced by GCMs) according to their performance of discharge simulations before applying bias correction, which would allow the user to evaluate their output in a process-oriented framework.

Although a good performance in the past does not guarantee a robust model performance in the future (Mendlik and Gobiet, 2016; Huang et al., 2015; Reifen and Toumi, 2009), users must assess the fitness for purpose of climate and hydrological model data to meet stakeholders' increasing demands for robust information about water availability and flood risk.

In Austria, the ÖKS15 study (Austrian national climate datasets study; Chimani et al., 2016) provided high-resolution GCM-RCM simulations for researchers and practitioners. It was also carried out to implement a robust climate database and thus enable intervention measures and climate change adaptation strategies. To achieve this goal, the high-resolution ÖKS15 simulations were derived by downscaling and bias correcting projections from the EURO-CORDEX ensemble (Jacob et al., 2014). For additional information regarding the EURO-CORDEX climate modelling initiative, including numerous studies that have evaluated the EURO-CORDEX data in various settings, we refer to the overview article of Jacob et al. (2020).

The approach of the ÖKS15 project followed a general idea of several similar projects that are being conducted to generate and provide national reference climate projections for climate change impact assessment. These projects include *CH2018* (CH2018, 2018) in Switzerland, *UKCP18* (Lowe and Bernie, 2018) in the United Kingdom and the *Gridded 1 km x 1 km climate and hydrological projections* (Wong et al., 2016) in Norway. In order to evaluate the added value for hydrology in Switzerland, Rössler et al. (2019) presented a scheme to compare two Swiss climate scenario datasets *CH2011* (CH2011, 2011) and *CH2018* (CH2018, 2018), which are based on different climate model chains and postprocessing methods. They analyzed the hydrological consequences of the different postprocessing procedures (e.g., delta change approach, quantile mapping, weather generator). The authors identified an added value for quantile mapping, and particularly for extremes (compared to averages), and emphasized the benefit of using numerous realizations from a weather generator.

In this paper, we argue that the climate scenario data that is initially available for hydrological impact research in Austria can be effectively compared with data from other regions, despite apparent differences in national climate projections (e.g., from different reference datasets, bias correction methods, underlying model chains). However, as in other regions worldwide, Austrian researchers are still uncertain how best to use such datasets in hydrological impact studies to generate robust hydrological findings, e.g. useful for climate adaptation. In particular, the spatial and temporal scales at which the climate input data provide robust hydrological information is still uncertain. To address this gap, we explored the potential of the Austrian ÖKS15 dataset for hydrological climate impact assessment, using it as exemplary study for other regions. Two different catchments (alpine, pre-alpine) were defined as case study regions. We applied the following sequence of data analyses:

- We quantified the uncertainty of the meteorological dataset (air temperature and precipitation) that was used to construct the ÖKS15 dataset by bias correcting and downscaling the raw EURO-CORDEX GCM-RCM data (using data inter-comparison statistics such as mean absolute error, bias, and correlation coefficient)
- We then compared the uncertainty associated with these observational data with that of the bias-corrected ÖKS15 and the raw EURO-CORDEX dataset, respectively
- We applied the hydrological model WaSiM to perform discharge simulations for all meteorological input data (observational and climate model data)
- Next, we evaluated the robustness of the simulated hydrological output for the individual input datasets by using selected hydro-meteorological indicators

Finally, we condensed our results in order to enable their transfer to other regions and to guide the use of ÖKS15 and similar datasets in (but not limited to) hydrological impact studies.

2. Study areas, data and methods

2.1. Study areas

In this study, we examined two hydrologically diverse basins, an alpine and a pre-alpine catchment, located in the federal state of Styria in southeastern Austria. Styria is located in a transition zone between the Alpine and the Mediterranean climate regions, an area characterized by specific weather patterns and related precipitation distribution due to the interaction among cyclones approaching from the west/northwest and the south. The warm and dry southeastern parts of Styria experienced a temperature increase of near 0.7 °C per decade from 1971 to 2016 (Hohmann et al., 2018; Kabas et al., 2011) and thus are considered as particularly sensitive to climate change.

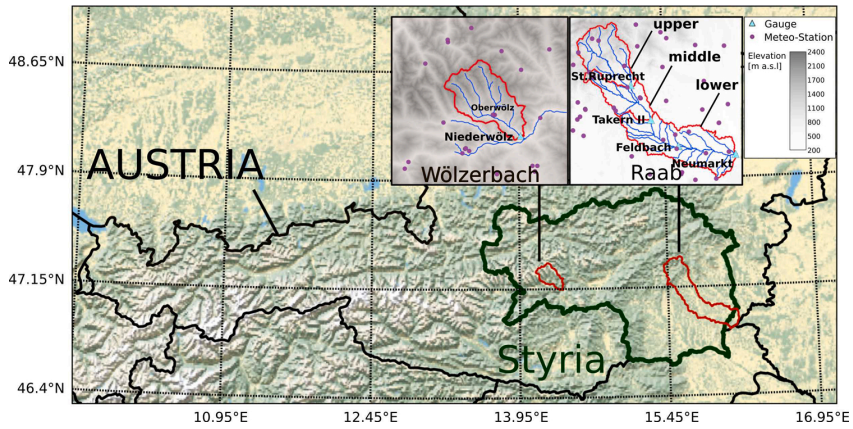


Fig. 1. Location of the study areas in Styria, southeastern Austria. The alpine Wölzerbach (227 km^2) and the pre-alpine Raab (987 km^2) serve as test catchments.

The case study catchments (Fig. 1) differ in size, orographic complexity, climatic setting, data availability, hydro-economic vulnerability and hydrological regimes. This makes them ideal contrasting examples of small catchments within the Greater Alpine Region.

2.1.1. Wölzerbach catchment

The Wölzerbach, a tributary of the Mur, is a medium-sized (227 km^2) mountainous catchment located in the Niedere Tauern range of the Central Eastern Alps. It covers an altitudinal range of more than 1700 m, from 740 m a.s.l. at the stream gauge in the southeast to the highest peak in the northwestern part of the catchment at 2475 m a.s.l. The Wölzerbach basin is mainly covered by forest (48%), alpine dwarf-shrub heath and grasslands (25%) as well as pastures and rock-ribbed mountain tops. The northern parts of the catchment are characterized by a steep mountainous topography. The geology is mainly dominated by mica schist and gneiss, with some enclosures of limestone, dolomite and amphibolite. The three main tributaries cut into highly erodible quaternary unconsolidated sediments, making them vulnerable to torrential floods that carry huge amounts of bedload. Due to its elevation range, snow accumulation and snow melt play a relevant role in the catchment hydrology. Major precipitation events can mainly be attributed to convective summer precipitation. Mean precipitation sums in the Wölzerbach catchment range from around 1800–700 mm following the north-south elevation gradient. With snow melt as the main driver, the Wölzerbach is characterized by a moderate nival discharge regime with a peak in May (c.f. Mader et al., 1996).

2.1.2. Raab catchment

The Raab, being a typical southeastern pre-alpine river, flows from the eastern-most Alpine ridges toward the southeast, through Hungary and ends as a tributary of the Danube. The Austrian part of the catchment covers an area of about 1000 km^2 with the outlet at an altitude of 230 m a.s.l. and the highest elevations at 1545 m a.s.l. in the northern part of the area. The mean annual precipitation sums range from around 1050 mm in the north to around 750 mm in the southeast. Agriculture (42%) and forest areas (40%) dominate the land use of the catchment. Loam represents the main soil texture. Due to its location in a transition zone between the sensitive Alpine and Mediterranean climate regions, the catchment of the Styrian Raab has been a key focus of climate change studies in Austria (Schürz et al., 2019; Piringer et al., 2019; Hohmann et al., 2018). The Raab exhibits a pluvio-nival discharge regime type (c.f. Mader et al., 1996), in which the discharge is relatively evenly distributed over the year.

2.2. Data

Several different hydro-meteorological datasets have been incorporated in this study (Table 1). Station temperature and precipitation data have been provided by the Austrian Central Institution for Meteorology and Geodynamics (ZAMG) and the Austrian Hydrographic Service (AHYD), whereby the latter also provided discharge data. In the alpine Wölzerbach catchment, a total of 18 temperature and 22 precipitation stations were used as direct data sources and as the basis for the spatial internal interpolation by the hydrological model (Section 2.3.2).

In the Raab catchment, measurements were available from 27 temperature and 70 precipitation stations. Stations which underwent a relocation were considered as separate stations in the analysis and interpolation procedure. In order to compare station values and gridpoint values, potential elevation differences, which are particularly prevalent in mountainous parts of the study region, were corrected by applying a simple annual average lapse rate approach (0.5 K per 100 m; c.f. Prettenthaler et al., 2010). In addition to the station data, we used gridded observational datasets for precipitation (GPARD1; Hofstätter et al., 2015) and temperature

Table 1
Meteorological and hydrological data used in the study.

Name/Notation in this Paper	Source	Type	Period	Variables	Interpolation	References
STATION	ZAMG	Point observation	1961–2010 (or shorter, dependent on station)	Precipitation [mm], Air Temperature [°C]	Temporal: Precipitation - Day sum 07:00–07:00 CET; Temperature: before 1971: Tm = (T7 + T14 + T21)/3; after 1971: $T_{mean} = (T_{min}+T_{max})/2$	
STATION	AHYD	Point observation	1961–2010 (or shorter, dependent on station)	Precipitation [mm], Air Temperature [°C]	Temporal: Precipitation - Day sum 07:00–07:00 CET; Temperature: Tm = (T7 + T14 + T21 + T21)/4	
GRID (GPARD1)	ÖKS15 (ZAMG)	Grid 1 km x 1 km	1961–2010	Precipitation [mm]	Temporal: Day sum 07:00–07:00 CET, Spatial: Gradient-based anisotropic Interpolation using a Background-Climatology	Hofstätter et al., 2015
GRID (SPARTACUS)	ÖKS15 (ZAMG)	Grid 1 km x 1 km	1961–2010	Air Temperature [°C]	Temporal: $T_{mean} = (T_{min}+T_{max})/2$; Spatial: Interpolation using nonlinear profiles and non-Euclidean distances	Hiebl and Frei, 2016
ÖKS15	ÖKS15	13 GCM-RCM combinations, Grid 1 km x 1 km	Dependent on GCM-RCM chain 1961–2005 or 1971–2005 (RCA model combinations)	Precipitation [mm], Air Temperature [°C]	Statistical Downscaling with Scaled Distribution Mapping (SDM)	Chimani et al., 2016; Switanek et al., 2017; Leuprecht et al., 2017
RAW	EURO-CORDEX	13 GCM-RCM combinations, Grid 12.5 km x 12.5 km	Dependent on GCM-RCM chain, 1961–2005 or 1971–2005 (RCA model combinations)	Precipitation [mm], Air Temperature [°C]	Bilinear Regridding from 12.5 km x 12.5 km to 1 km x 1 km	Jacob et al., 2014
Gauge	AHYD	Observation	Dependent on Gauge	Discharge [m^3/s]		

(SPARTACUS; Hiebl and Frei, 2016) which are based on some but not all of the station data examined within this study.

Gridded high-resolution climate datasets were provided by the ÖKS15 project (Leuprecht et al., 2017). The ÖKS15 dataset is based on the results of 13 RCMs (12.5-km grid spacing) by downscaling and bias-correcting simulations from the EURO-CORDEX ensemble (Jacob et al., 2014) to a 1-km grid over the entire region of Austria. Bias correction with scaled-distribution mapping (Switanek et al., 2017) was performed for the period 1961–2005 with reference datasets GPARD1 and SPARTACUS. Data from only 1971 and on are available, however, in five out of the thirteen ÖKS15 datasets (all of which are combinations with the regional climate model RCA). A detailed description of the ÖKS15 data is given in Chimani et al. (2016), and an overview of the GCM-RCM combinations is listed in the Appendix (Table A.1). In addition to the bias-corrected ÖKS15 data, we also investigated the raw EURO-CORDEX model data, regridded bilinearly to the 1-km x 1-km grid of the ÖKS15 data. An overview of the datasets and parameters used in our study is given in Table 1.

2.3. Methodology

Fig. 2 provides an overview of the applied methodological steps. To find out how the different input data affect hydrological simulations, we first analyzed the meteorological STATION, GRID, ÖKS15 and RAW data (step 1). In the context of our study, we define uncertainty as differences between the different meteorological input datasets:

1a) GRID to STATION: Uncertainties associated with the interpolation method, the inclusion/exclusion of different stations, and measurement errors associated with those.

1b) GRID to ÖKS15: Uncertainty related to the bias correction.

1c) GRID to RAW: Uncertainty related to the GCM-RCM climate model realization.

We then calibrated the hydrological model with one of the observed datasets (STATION in the Raab catchment, GRID in the Wölzerbach catchment; see Section 2.3.2), and forced the calibrated model with the remaining other dataset, GRID/STATION, ÖKS15 and RAW (step 2).

In step 3 we analyzed the influence of this input uncertainty on discharge and simulated hydro-meteorological indicators. The uncertainty associated with the hydrological model is assessed within the STATION-to-OBSERVED comparison. GRID-to-STATION uncertainty is originating in uncertainty of station interpolation. Comparisons STATION/GRID-to-ÖKS15 assess the performance of the model chain using bias-corrected input whereas comparisons STATION/GRID-to-RAW analyze the uncertainty originating in the climate models. Analyzing differences of ÖKS15 and RAW finally allows to assess the difference between uncorrected and corrected model input.

This methodology is similar to the one described in Hakala et al. (2019) who give a detailed introduction to hydrological modeling of climate change impacts, including a discussion on the different sources of uncertainty.

2.3.1. Evaluation methods and criteria

We examine the meteorological STATION, GRID, ÖKS15 and RAW data at the gridpoint and catchment levels. To evaluate STATION data at the gridpoint level, we contrast station time series with the collocated data matching the STATION location. In addition to visually examining the distribution functions of the identified differences (i.e., of gridpoint-minus-station statistics) and their temporal evolution, we inter-compare cumulative distribution functions (CDFs), and statistics derived from these that serve to indicate performance, for the variables of interest. In particular, Mean Absolute Error (MAE), Bias (BIAS), Percent Bias (PBIAS), and Pearson's Correlation Coefficient (CORR), respectively, serve as the main evaluation indicators. To acknowledge the fact that the nominal 1-km spatial data sampling method used for the gridded datasets does not need to correspond to the actually resolved spatial patterns ("skillful scale") or to the effective resolution of the STATION network (on average approximately 10-km inter-station distance), we apply the same evaluation procedure for temperature and precipitation at the sub-catchment and catchment scales. In this context, it should be noted that Chimani et al. (2019) recommend a meaningful interpretation of spatial precipitation patterns for a resolution coarser than 40 km x 40 km (particularly for extreme precipitation over short time scales).

To validate the hydrological variables, a similar approach in terms of efficiency criteria is chosen. Discharges simulated by WaSiM using the different input datasets are compared with each other and contrasted with the observed discharges. The Nash-Sutcliffe Efficiency (NSE) and logarithmic Nash-Sutcliffe Efficiency (NSElog) (c.f. Krause et al., 2005; Moriasi et al., 2007; Nash and Sutcliffe, 1970) are used for evaluation. In addition, mean annual hydrographs and long-term flow duration curves (FDCs) are assessed, which describe the variability of the flow and thereby provide information about the water regime (c.f. Ridolfi et al., 2020). Table 2 presents an overview of the different spatial scales at which the evaluation of meteorological and hydrological variables is performed.

Finally, we investigate the impact of the various input datasets on simulated hydro-climatic conditions by analyzing different hydro-meteorological indicators (Table 3), which have been suggested as relevant by a variety of studies with a hydrological impact focus (Ekström et al., 2018). We perform our evaluation for different climate reference periods (i.e., 1961–2005, 1971–2000) or, where observational records are shorter, for the longest possible period.

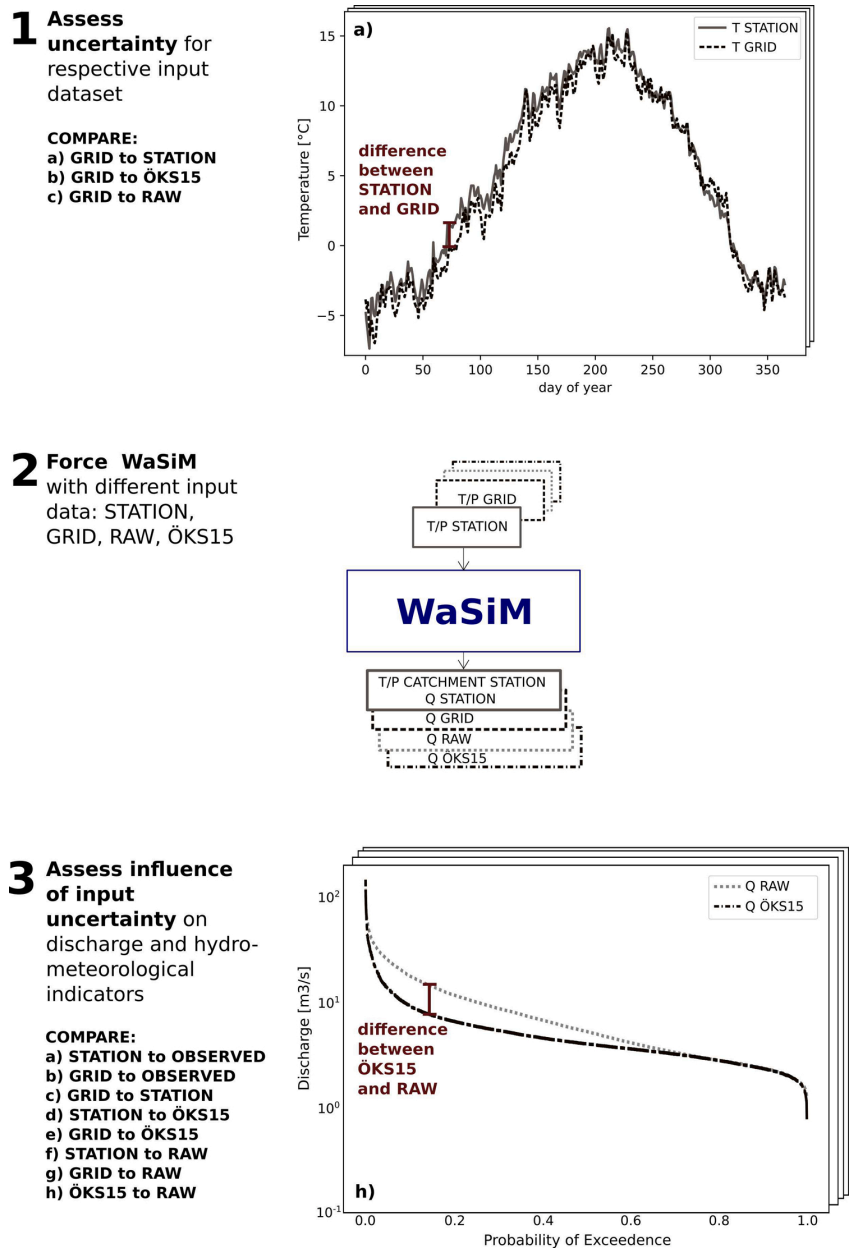


Fig. 2. Methodological approach applied within this study. We start by analyzing differences between the meteorological input data (STATION, GRID, ÖKS15 and RAW) to assess the uncertainties associated with them (step 1). The comparisons (letters a-c) refer to the analyses of the different sources of uncertainty, as described in section 2.3. 1a) Uncertainties associated with station measurements and interpolation method. 1b) Uncertainty related to bias correction. 1c) Uncertainty associated with model realization. In step (2) we apply the hydrological model WaSiM to perform discharge simulations for all input datasets. Finally, we assess the uncertainty of the simulated hydrological output for the individual input datasets by using selected hydro-meteorological indicators (step 3). Steps 1a) and 3h) are shown as examples.

Table 2
Datasets, indicators and variables used for evaluating meteorological and hydrological variables.

Scale	Dataset	Variables	Evaluation Method/ Indicator
Gridpoint	ZAMG/ AHYD, GPARD1, SPARTACUS	Precipitation [mm], Temperature [°C]	Annual cycle, CDFs, MAE, BIAS, PBIAS, CORR, Hydro-meteorological Indicators (see Table 3)
(Sub-) Catchment	GPARD1, SPARTACUS, ÖKS15, RAW	Spatial averages of Precipitation [mm], Temperature [°C]	Annual cycle, CDFs, MAE, BIAS, PBIAS, CORR, Hydro-meteorological Indicators (see Table 3)
(Sub-) Catchment	GPARD1, SPARTACUS, ÖKS15, RAW	Discharge [m^3/s]	Flow Regime (mean annual hydrograph), FDCs, NSE, NSElog, MAE, PBIAS, Hydro-meteorological Indicators (see Table 3)

Table 3
List of hydro-meteorological indicators used for comparing and evaluating different input datasets.

Indicator	Category	Unit	Description	Reference
S_{frac}	Climate: Temperature, Precipitation	%	Snowfall fraction: Ratio of snowfall to precipitation (Percentage of total snowfall on total precipitation)	
$DSPD_{mean}$	Precipitation	days	Mean dry spell duration: Mean number of consecutive dry days (precipitation < 1 mm)	Beyer et al., 2016
$WSPD_{mean}$	Precipitation	days	Mean wet spell duration: Mean number of consecutive wet days (precipitation ≥ 1 mm)	Beyer et al., 2016
Low75, Low95, Low99	Discharge magnitude	m^3/s	Low flow discharge (75th, 95th and 99th percentile)	Zhang et al., 2016
Hig01, Hig05, Hig25	Discharge magnitude	m^3/s	High flow discharge ($>$ 1st, 5th and 25th percentile)	Zhang et al., 2016
S95, S10	Seasonal discharge extremes	days	Number of days in summer in the top fifth percentile annual flows; number of days in the summer in which flows were less than 10% of mean annual flow	Wenger et al., 2010
Peak frequency	Discharge variability	-	Frequency of peaks above three times the monthly median flow	Pennino et al., 2016

2.3.2. Hydrological simulations with the WaSiM model

In order to quantify impacts from the use of the ÖKS15 data on simulated hydrological variables and to extend the discharge timeseries beyond observations, we used the *Richards–10–02–04* version of the hydrological model WaSiM (Schulla, 2017). The spatially distributed, deterministic model incorporates physical-based as well as conceptual approaches and is widely used in climate change studies (e.g., Rössler et al., 2019; Smiatek and Kunstmann, 2019, Willkofer et al., 2018; Gädeke et al., 2014). The WaSiM model was previously applied in the Raab region by Hohmann et al., 2018, 2021 and the same model setting of Hohmann et al. (2018) is used in this study, except for minor modifications due to an altered time frame, a slightly changed digital elevation model (to assure conformity with the GRID input data) and data availability.

For both catchments we chose a reasonably simple model setup with Temperature Index Snowmelt and Hamon evapotranspiration (Hamon, 1961), a daily time step and a spatial resolution of 1 km $\times$ 1 km in accordance with data availability. To perform precipitation interpolation in the STATION runs, we used Inverse Distance Weighting (IDW) in the pre-alpine Raab and a combination of IDW (70%) and altitude dependent regression (30%) in the alpine Wölzerbach. Temperature was interpolated using a combination of IDW (75%) and nearest neighbor combined with a constant lapse rate (25%) in the Raab and nearest neighbor combined with a constant lapse rate (0.5 K per 100 m; c.f. Prettenthaler et al., 2010) in the Wölzerbach catchment.

Snow accumulation is modelled by WaSiM using a threshold temperature $T_{R/S}$ at which 50% of the precipitation falls as snow and a transitional range T_{trans} within which both liquid and solid precipitation occur. The values of $T_{R/S} = 2.1$ °C, $T_{trans} = \pm 0.35$ °C were determined from calibration for the Wölzerbach, and these values were set to $T_{R/S} = 0.75$ °C, $T_{trans} = \pm 1$ °C by default for the Raab catchment.

We chose two different calibration-validation strategies. A combination of manual calibration and the SCE-UA algorithm (Duan et al., 1994) was used for both catchments to choose optimal parameter sets by maximizing the linear combination of the ordinary and the logarithmic NSE (c.f. Moriasi et al., 2007; Nash and Sutcliffe, 1970; Section 2.3.2). Both measures were weighted with 0.5, using a split sample approach (Appendix Table A.2). Although the model was calibrated using meteorological input from STATION data (internally interpolated in WaSiM) for the Raab catchment, the model was calibrated for the Wölzerbach catchment by using the externally interpolated GRID datasets. The performance based on the respective alternative input datasets (i.e., those not used in the calibration procedure) then serves as indicator for the model robustness and reveals differences, strengths and weaknesses in the various input datasets.

3. Results

The hydrological models for the Raab and the Wölzerbach catchments were driven by observational, uncorrected and bias-corrected climate model data to assess the utility of the high-resolution ÖKS15 datasets in hydrological applications. Therefore, the uncertainties in the forcing data from climate models were compared with the uncertainties in the observational data. Our results are presented separately for atmospheric drivers (structured by separate comparisons at point and catchment scale) and hydrological characteristics.

3.1. Uncertainty in atmospheric driving data – observational data vs. model-based datasets

3.1.1. Temperature data consistency at gridpoint level

We found an average MAE of 1.3 °C between the STATION and GRID daily temperature values for gridpoints in the alpine catchment for the period 1961–2005, with a positive bias for GRID temperatures observed in 12 out of 17 locations (statistics for individual gridpoints/stations are found in the Appendix Table A.3). Elevation differences between STATION and GRID pixel height are particularly pronounced in the partly steep Wölzerbach. The GRID dataset can be used to capture inversions, which the simple annual lapse rate correction (Section 2.2) does not consider. Thus, temperatures in autumn and winter often exhibit larger differences between STATION and GRID data in the alpine catchment. The smaller overall MAE of 0.5 °C for the pre-alpine Raab catchment is

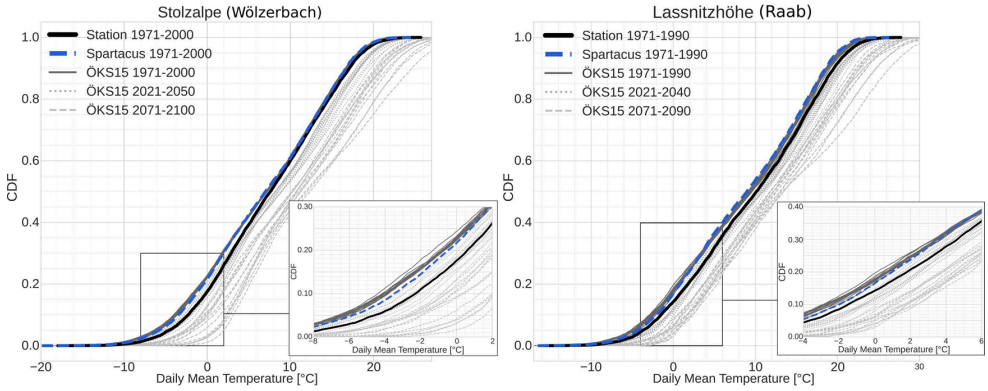


Fig. 3. Modelled versus observed distributions (CDFs) of temperature for historic and future periods. Left: Stolzalpe – a station south of the Wölzerbach catchment. Right: Lassnitzhöhe in the Raab catchment. CDFs of the bias-corrected ÖKS15 models align well with those of the GRID dataset. For both stations, the GRID dataset at least partly underestimates temperatures in the past. As a consequence, bias-corrected low temperatures in the ÖKS15 dataset in the near future partially remain below the observed ones in the past. Due to data availability, the reference period for the Station Lassnitzhöhe is only 20 years.

believed to be an effect of the gentler orography and the higher number of stations used in the creation of the GRID dataset. More than half of the stations show a negative bias (Appendix Table A.3), but this remains predominantly small (average bias −0.1 °C).

Whereas the majority of RAW models underestimate temperature, the cumulative distribution functions of the bias-corrected ÖKS15 models align well with the function of the GRID temperatures for almost all the gridpoint locations, models and temperature ranges (data not shown).

Fig. 3 compares CDFs of modelled and observed temperatures at one location in each catchment. ÖKS15 historic CDFs (solid lines) agree closely with the corresponding GRID distribution functions. The two stations demonstrate locations with over-represented colder-than-observed temperature ranges in the GRID dataset (i.e., a negative temperature bias). Although future scenarios are not the subject of this paper, we would like to point out that the temperature bias affects simulated future temperature distributions; the simulated average daily temperatures of the two stations for the near future (i.e., 2021–2050 at station Stolzalpe, and 2021–2040 at station Lassnitzhöhe) remain below those of the recent reference period.

When comparing the annual cycles of temperatures between ÖKS15 and GRID data (not shown), correspondence is best for the reference period that is also used for the bias correction (i.e., 1961–2005). For periods shorter than that, the level of agreement decreases. This results in temperature differences of up to 0.5 °C for long-term monthly averages for specific models and months, as described in Section 3.1.2.

3.1.2. Temperature data consistency at the catchment level

Table 4 compares the seasonal mean temperatures of GRID, STATION, RAW and bias-corrected ÖKS15 models with each other for two different periods. Positive values indicate warmer GRID temperatures. The GRID temperatures are higher than STATION temperatures for most locations in the Wölzerbach catchment, resulting in a catchment-wide overestimation of about 1 °C for the period of 1961–2005.

The RAW models generally underestimate temperatures in autumn, winter and spring in the Wölzerbach catchment as compared to

Table 4
Catchment-wide seasonal mean temperature differences between GRID and STATION, ÖKS15 and RAW datasets, respectively (positive values indicating "warmer" GRID temperatures). For the ÖKS15 and the RAW models, differences in the ensemble minimum, median and maximum are shown. The two periods correspond to the reference period of 1961–2005 used for bias correction and the exemplary climate period of 1971–2000.

	Wölzerbach			**Raab**		
1961–2005	STATION	ÖKS15 min | med | max	RAW min | med | max	STATION	ÖKS15 min | med | max	RAW min | med | max
DJF	2.5	0.1 | **-0.0** | −0.1	4.8 | **2.9** | 1.7	0.4	0.1 | **-0.0** | −0.2	2.4 | **0.3** | −1.6
MAM	0.3	0.1 | **-0.0** | −0.1	5.0 | **3.5** | 2.1	0.4	0.1 | **-0.0** | −0.1	3.9 | **1.9** | 0.5
JJA	0.6	0.0 | **-0.0** | −0.1	3.8 | **2.1** | −0.2	0.5	0.0 | **-0.0** | −0.1	2.6 | **0.2** | −2.4
SON	1.6	0.1 | **-0.0** | −0.1	5.0 | **2.9** | 1.4	0.1	0.1 | **-0.0** | −0.0	3.1 | **0.7** | −0.2
1971–2000						
DJF	2.0	0.7 | **0.4** | 0.2	5.1 | **3.1** | 2.3	-0.1	0.8 | **0.4** | −0.0	2.8 | **0.7** | −1.6
MAM	0.3	0.1 | **-0.0** | −0.2	5.0 | **3.4** | 2.1	0.3	0.1 | **0.0** | −0.1	3.8 | **1.8** | 0.5
JJA	0.5	0.1 | **-0.0** | −0.2	3.7 | **2.2** | −0.2	0.4	0.1 | **-0.0** | −0.2	2.5 | **0.2** | −2.4
SON	1.6	0.1 | **-0.1** | −0.4	4.7 | **2.8** | 1.3	0.2	-0.0 | **-0.1** | −0.4	2.9 | **0.5** | −0.2

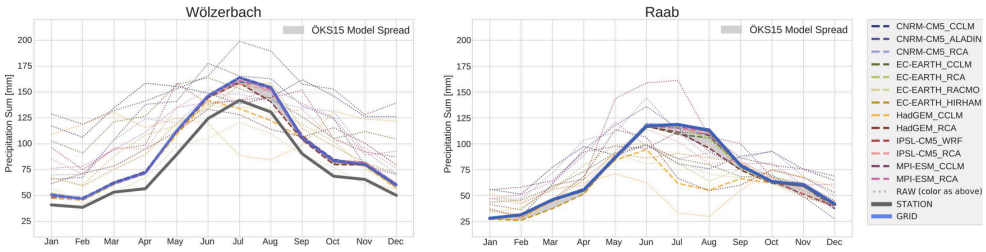


Fig. 4. Annual cycle of catchment average monthly precipitation from non-corrected RCM simulations (RAW) and bias-corrected RCM simulations (ÖKS15) as compared to observations (GRID and STATION). Left: For the alpine Wölzerbach catchment, RAW models highly overestimate precipitation, whereas ÖKS15 align generally well with the GRID dataset. Right: For the pre-alpine Raab catchment, the difference between RAW and ÖKS15 models is less than in the alpine catchment. The HadGEM CCLM model is considered an outlier, underestimating precipitation in both catchments. The underestimation is particularly striking in the southeastern part of the catchment (Raab).

the bias-corrected ÖKS15 models. This effect is less pronounced for the Raab catchment, where only the minority of the RAW models overestimates summer and winter temperatures.

The rather high level of agreement seen between GRID and ÖKS15 data at the gridpoint level is also reflected at the catchment level. The differences between the RAW (multi-model median) and GRID data for the Wölzerbach catchment are much larger than those for the Raab catchment. Both catchments show the lowest level of agreement in spring. One caveat is that, for reference periods different from the one used for bias correction, both the multi-model spread and differences between the ÖKS15 multi-model median and GRID data increase. However, these differences remain below the range of temperature differences between the GRID and STATION datasets (overestimation by GRID temperatures) as discussed previously. This finding is valid for all seasons and both catchments except for the winter season in the pre-alpine Raab catchment (Table 4).

3.1.3. Precipitation data consistency at gridpoint level

Precipitation is overestimated by the GRID data (> 70% of all station/gridpoint locations, see Appendix Table A.4). This is more pronounced for the Wölzerbach catchment, where the average PBIAS is 14% (period 1961–2005) for gridpoints located in the center of the catchment, corresponding to stations not included in the creation of the GRID dataset. With a correlation of 0.92 between the STATION and GRID timeseries, the MAE is smaller equal to 2.0 mm/day. The Raab catchment shows a more similar picture (MAE of 0.7 mm/day, CORR = 0.93), but displays a smaller station-average PBIAS of 3% over the same period of 1961–2005.

Interestingly, the station introducing the largest positive bias in the Raab catchment, as well as the two stations introducing the largest negative bias in the Wölzerbach catchment, are the ones on the opposite sides of the catchment-delineating mountain ridge. We argue that the different precipitation climate north of the mountain ridge explains this finding. In general, datasets from the ZAMG stations correspond more closely with the GRID dataset (although not all of the stations were used for the creation of GRID data) than stations from AHYD. Differences between STATION and GRID data are largest in summer when the major precipitation events (heavy, convective precipitation) usually occur in the study catchments.

3.1.4. Precipitation data consistency at the catchment level

While the GRID exceeds STATION precipitation in all months and sub-catchments over the period of 1961–2005 (more apparent for larger monthly precipitation) for the alpine Wölzerbach catchment, as would be expected from the station level results, the findings are more spatially and temporally diverse for the Raab catchment (Fig. 4 and Appendix Fig. A.1).

An overestimation of GRID as compared to STATION precipitation in the upper part of the Raab catchment opposes the underestimation of precipitation seen in the middle part for both the reference period (1961–2005) and the period of 1971–2000. In the lower part, GRID precipitation underestimates precipitation in the long-term and slightly overestimates it for the period of 1971–2000. This is a result of the accrual and discontinuation of individual stations as well as the partially alternating positive and negative biases for individual years. Interestingly, these spatial and temporal features of under/overestimation result in an almost perfect fit between GRID and STATION precipitation for the entire Raab catchment in the period of 1961–2005.

As shown in Fig. 4, the bias-corrected ÖKS15 precipitation also agrees closely with that of the GRID data, which is also justified by the use of the GRID data in the creation of the ÖKS15 data. However, almost all RAW models, serving as the base data for the bias correction of ÖKS15, significantly overestimate precipitation in both catchments except for the summer period.

Comparing the bias-corrected ÖKS15 model data (Appendix Table A.1) with their reference GRID dataset for the reference period of 1961–2005 (Fig. 5, upper panel), the largest and generally most positive differences are found in the second half of the year (July to December). However, the majority of the bias-corrected models tend to underestimate precipitation for most months. It is noteworthy that the HadGEM CCLM shows a much weaker seasonality than all other models in the warm period of the year and only about half of the precipitation observed in July and August. Chimani et al. (2019) also identified and described this model behavior, i.e., the underestimation of precipitation particularly in Eastern Austria together with the overestimation of cyclone frequency.

When considering the annual cycle of precipitation in a climate period other than the reference period used for bias correction, monthly differences between the GRID and the ÖKS15 runs increase (up to around 18% in August in the alpine catchment). A

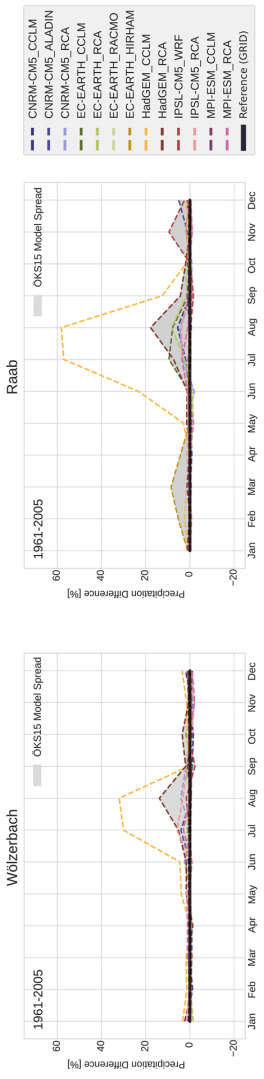


Fig. 5. Annual cycle of percentual differences of precipitation between the GRID reference dataset and the ÖKS15 models (GRID minus ÖKS15 models) for different periods of analysis (upper panel: 1961–2005, lower panel: 1971–2000) and in the Wölzerbach catchment (left column) and the Raab catchment (right column).

Table 5
Performance of the hydrological model WaSiM in the Wölzerbach and the Raab catchments.

Catchment	Gauge	Meteo input used for parameter calibration	Period	NSE STATION input	NSElog STATION input	PBIAS STATION input	NSE GRID input	NSElog GRID input	PBIAS GRID input
Wölzerbach	Niederwölz	GRID	Calibration 2004–2007	0.81	0.81	5.5	0.69	0.71	18.1
Wölzerbach	Niederwölz	GRID	Validation 2008–2010	0.83	0.87	-4.1	0.68	0.69	19.4
Raab	St. Ruprecht	STATION	Calibration 2003–2009	0.66	0.73	7.4	0.7	0.55	18.9
Raab	St. Ruprecht	STATION	Validation 1995–2001	0.78	0.8	4.1	0.4	0.59	33.8
Raab	St. Ruprecht	STATION	LONG-TERM, 1984–2010	0.66	0.79	1.5	0.46	0.62	21.3
Raab	Takern II	STATION	Calibration 2003–2009	0.75	0.79	8.1	0.77	0.74	12.8
Raab	Takern II	STATION	Validation 1995–2001	0.61	0.77	7.2	0.41	0.58	25.0
Raab	Takern II	STATION	LONG-TERM, 1968–2010	0.59	0.77	6.8	0.54	0.73	15.2
Raab	Neumarkt	STATION	Calibration 2003–2009	0.74	0.79	6.4	0.76	0.76	7.4
Raab	Neumarkt	STATION	Validation 1995–2001	0.62	0.65	4.1	0.58	0.59	10.3
Raab	Neumarkt	STATION	LONG-TERM, 1991–2010	0.72	0.80	4.7	0.7	0.77	9.0
Raab	Feldbach	STATION	LONG-TERM, 1961–2010	0.61	0.74	10.4	0.62	0.73	13.4

consistent evaluation of all ÖKS15 models, however, fails because data from 1971 and on is available in only five out of thirteen models.

3.1.5. Analysis under conditions of wet and dry spells

While extended periods of consecutive dry days (i.e., dry spells) may cause droughts and water shortages, long sequences of days with precipitation above 1 mm (i.e., wet spells) can influence the flood risk. An accurate representation of wet and dry spells, therefore, is important in hydrological impact studies. In the long-term mean (1961–2005), the catchment-average monthly dry spell duration in the Wölzerbach is highest for the STATION run (Appendix Figure A.2). The GRID and ÖKS15 model medians align generally well with noticeable differences in October and November, when the average dry spell length is longer for the GRID run.

As seen for the overall precipitation, the wet spell durations of the GRID run surpass the STATION run in the alpine catchment in all months. The GRID and ÖKS15 model median align slightly less closely for the wet than for the dry spell duration. As compared to the GRID run, ÖKS15 models show a shorter wet spell duration in spring and a longer one in the summer season. The RAW model median displays a weaker annual cycle in terms of the dry spell duration, with the lowest differences from the ÖKS15 median seen in summer. Median RAW wet spell lengths are overestimated in all months.

In the Raab catchment, the average dry spell length of STATION and GRID runs align more closely than those of GRID and ÖKS15 runs, where we again find the largest differences in October and November. Interestingly, the wet spell duration in the Raab catchment is similar for all analyzed input variants. The largest differences between the GRID and ÖKS15 model median are found in late spring and summer, and a greater deviation between RAW and the bias-corrected model median is observed in May.

3.1.6. Analysis under snowfall conditions

Snow accumulation and snow-melt play an important role for runoff, and specifically in the alpine Wölzerbach catchment. To assess the combined effect of temperature and precipitation, we analyzed the snowfall fraction (i.e., the percentage of snowfall on total precipitation).

For the mountainous Wölzerbach catchment, the STATION and GRID data agree well for snowfall fractions of 31% and 32%, respectively, (1970–2000 catchment-average). The ÖKS15 model median, however, adds up to only 26% of the snowfall fraction. Except for HadGEM CCLM (which shows a precipitation deficit in summer), the snowfall fraction is underestimated by all ÖKS15 models for all sub-catchments (not shown). RAW models highly overestimate the snowfall fraction with a median of 46% (ranging from 40% to 60%).

In the Raab catchment, the observation-based datasets (STATION and GRID) both give a catchment-average snowfall fraction of 9% and 10%, respectively (reference period 1971–2000). The median ÖKS15 model gives a share of 7% of snow with respect to total precipitation. The RAW model median yields a similar result with a snowfall fraction of 12%. As seen with the precipitation results, the RAW models have a huge spread of 7–22% of snowfall fraction with respect to total precipitation.

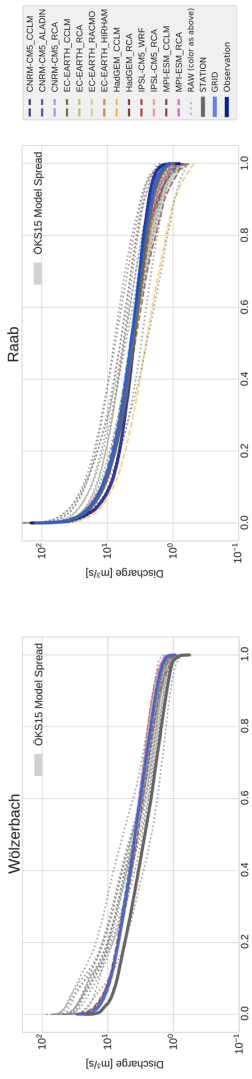


Fig. 6. Flow duration curves of WaSiM-simulated discharges driven either with STATION, GRID, or ÖKS15 data. Left: Niederwölz (Wölzerbach) gauge. Right: Feldbach (Raab) gauge. Only Feldbach covers the full period from 1971 to 2000 and, thus, the FDC of observations is only shown here. For both catchments, the FDCs of GRID and ÖKS15 discharges align well (with the main exception of the HadGEM models in Raab catchment). While the overestimation of GRID vs. STATION discharges is visible across the whole spectrum of discharges for the Wölzerbach, overestimation mainly affects high to medium discharges in the Raab catchment.

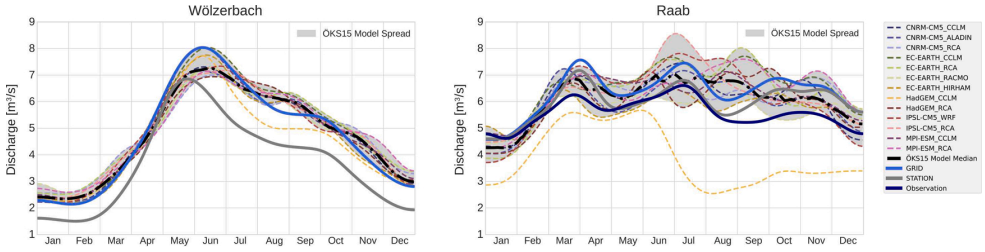


Fig. 7. Flow regimes simulated by WaSiM in the period of 1971–2000 (daily values smoothed by a Gaussian filter with $\sigma = 15$ days). Left: Niederwölz gauge (Wölzerbach). Right: Feldbach gauge (Raab). For Feldbach, covering the full period from 1971 to 2000, observations are shown as well. The HadGEM CCLM model is not able to capture the flow regime due to a vast precipitation underestimation, mainly in the second part of the year. The bias is particularly extreme in the Raab catchment (Feldbach) with an underestimation of discharge up to 50%.

3.2. Uncertainty in simulated discharge and hydrological performance

3.2.1. Consistency of discharge simulations

In addition to the uncertainty in the atmospheric forcing data, uncertainty in the simulated discharges also results from hydrological model uncertainty. A discussion on how much of the uncertainty comes from either source goes beyond the scope of this study, but we consider the bulk effect for discharge and hydrological indicators that have been identified as relevant in hydrology. In order to identify the effect of alternative observational input data (STATION and GRID) and reference periods on simulated discharge, Table 5 lists discharge performance indicators for those input data and periods of analysis. GRID data were used for the Wölzerbach and STATION data were used for the Raab to calibrate WaSiM, and both models show a satisfactory representation of observed discharges (NSE $>$ 0.6, NSElog $>$ 0.65, PBIAS $<$ 20% for all sub-catchments considered). The performance increases for the Wölzerbach catchment when the GRID-calibrated model is used with STATION data as the driving input data (Table 5), which can be explained by including stations not considered in the creation of the GRID dataset. However, the timeseries of discharge was rather short for the Wölzerbach (from the hydrological year 2004 and on).

Regarding the Raab catchment, the model performance in the northern-upper and middle sub-catchments decreases considerably when the GRID input is used as driving data (with NSE-values of 0.4 and 0.46 and PBIAS of more than 33% and 25%, respectively, in the validation period), although the model still performed well in the calibration period. This appears to be mainly a result of significant precipitation-overestimation by GRID data in the northernmost sub-catchments. Whereas overall differences between STATION and GRID precipitation at the pixel level are larger for the calibration period, the over- and underestimations counterbalance each other at the sub-catchment level, leading to similar discharges and efficiencies. Decreasing performance in the validation period for the northern part of the area is increasingly compensated in the lower parts of the Raab valley, leaving the lowest gauge (Neumarkt) almost unaffected. Long-term runs (Table 5) show a picture similar to that of the shorter periods, although the efficiency recovers a bit for the two upper sub-catchments (St. Ruprecht, Takern II), whereby the precipitation over- and underestimation between the GRID and STATION inputs become more balanced.

Due to the rather short period of measured discharge in the Wölzerbach catchment, we considered only simulated discharges to construct FDCs at the gauge Niederwölz (Fig. 6). Overestimation in the GRID precipitation as compared to STATION data (shown in Section 3.1.4) results in an overestimation of the respective modelled discharges, which particularly affects medium to low discharges (50th to 100th percentile). When using the RAW data as the driving data, WaSiM tends to vastly overestimate high flows. Bias correction improves the simulation of overall flow characteristics considerably and, apart from the high-end extremes, the ÖKS15 runs align quite well with the GRID long-term FDCs. HadGEM model results are slightly more disparate than the other GCM-RCM combinations.

Compared to observations, the long-term discharge simulations for the Feldbach gauge in the Raab catchment have a positive bias (i.e., an overestimation) for the high to medium (5th to 50th percentile) daily average discharges for both the STATION and the GRID runs, while the low flows (75th to are 99th percentile) are underestimated. Exceptions to this are the extreme ends (exceedance probability $<$ 0.01 and $>$ 0.995). The result of the analysis using FDCs for ÖKS15 indicates rather good agreement with the GRID run for high to medium discharges; however, these deviate considerably in some cases for low flows (Fig. 6, right panel). The improvement from bias correcting the RAW models is evident. Again, the unrealistic behavior of the HadGEM CCLM model data and the related FDCs must be pointed out. For the Raab catchment, the discharge in all probability segments simulated by HadGEM CCLM are more than 25% lower than those predicted by the other models, and the median to low flows are 40% lower than those seen in the GRID run. The shape of the FDC suggests a higher variance in the daily discharge for HadGEM CCLM and reflects the model's vast underestimation of precipitation in the summer season.

If we examine these datasets at higher temporal resolution, the monthly FDCs (not shown) already shown considerably, pointing out some difficulties with runoff timing, even if the ÖKS15 models are generally able to reproduce the overall flow regimes in both catchments (Fig. 7).

The overestimation of GRID as compared to STATION precipitation results in corresponding discharge overestimation for the Wölzerbach. Furthermore, the discharge peak is shifted from May in the STATION run to June in the GRID run. This can at least partly

Table 6
Discharge indicators for the gauges Niederwölz (Wölzerbach) and Feldbach (Raab) for the different input datasets and two different periods. The model median is given for the ÖKS15 runs, the reduced ÖKS15 ensembles (non-RCA-models only, ensemble without HadGEM CCLM) and the RAW runs.

Catchment/ Period	**Wölzerbach/Niederwölz 1961–2005**						**Raab/Feldbach 1961–2005**						
Indicator	Station	Grid	ÖKS15 (med)	ÖKS15 (med non- RCA)	ÖKS15 (med without HadGEM CCLM)	RAW (med)	Station	Grid	ÖKS15 (med)	ÖKS15 (med non- RCA)	ÖKS15 (med without HadGEM CCLM)	RAW (med)	Measured
Low75	1.7	2.4	2.5	2.5	2.5	2.1	2.8	3.0	2.6	2.6	2.6	3.1	2.9
Hig25	4.8	6.3	6.2	6.3	6.2	8.4	7.0	7.2	7.2	7.2	7.2	9.2	6.1
Low95	1.1	1.6	1.7	1.7	1.7	1.4	1.6	1.8	1.3	1.3	1.4	1.7	1.8
Hig05	8.9	11.6	11.4	11.4	11.4	24.9	17.9	17.8	18.2	18.0	18.5	20.5	14.6
Low99	0.9	1.3	1.3	1.3	1.3	1.2	1.1	1.3	0.9	0.9	0.9	1.3	1.0
Hig01	12.7	16.5	17.0	16.8	17.0	34.2	36.0	35.3	38.4	36.0	38.1	37.9	34.1
meanS10	2.9	1.6	3.6	2.7	3.1	0.0	14.5	13.4	11.1	12.0	11.6	8.1	11.2
meanS95	9.2	11.2	10.3	10.4	10.2	15.9	5.6	5.8	6.2	6.2	6.3	2.8	5.8
meanPeakFrequency	2.9	2.6	2.6	2.7	2.6	3.7	13.4	11.6	10.3	11.3	10.3	7.5	15.4
	Wölzerbach/Niederwölz 1971–2000						**Raab/Feldbach 1971–2000**						
Low75	1.7	2.4	2.5	2.5	2.5	2.0	2.7	3.0	2.5	2.6	2.6	3.3	3.0
Hig25	4.9	6.2	6.2	6.2	6.2	8.3	6.6	7.1	7.0	7.0	7.0	9.3	5.9
Low95	1.1	1.6	1.6	1.5	1.6	1.4	1.7	1.9	1.3	1.3	1.3	1.8	2.1
Hig05	8.8	11.4	11.3	11.2	11.3	24.8	16.9	17.4	17.5	17.0	17.7	20.4	13.6
Low99	0.9	1.3	1.3	1.3	1.3	1.2	1.3	1.4	0.9	0.9	0.9	1.3	1.6
Hig01	12.7	16.2	16.4	16.2	16.5	34.4	35.1	35.2	36.7	34.2	36.0	38.2	31.5
meanS10	1.7	0.9	2.8	2.8	2.8	0.0	15.3	13.7	10.8	12.2	11.5	8.0	11.0
meanS95	9.5	10.6	10.5	10.6	10.4	16.6	4.7	5.0	6.0	6.0	6.4	3.1	5.7
meanPeakFrequency	2.7	2.4	2.6	2.6	2.5	3.7	13.4	11.6	11.2	11.0	11.4	9.3	14.7

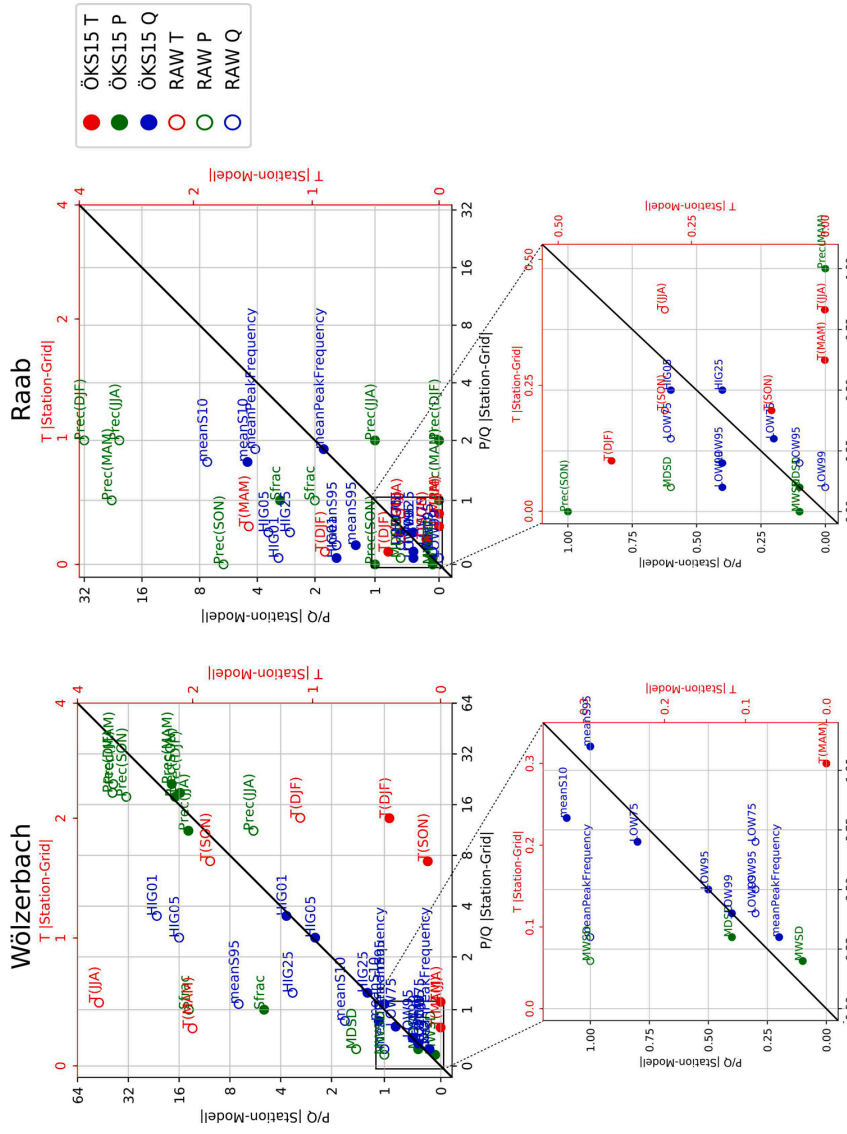


Fig. 8. Overview of uncertainties for different meteorological and hydrological indicators for the Wölzerbach (left) and the Raab catchments (right) for the period of 1971–2000. Differences in simulated variables from observations (STATION minus GRID) on the *x*-axis are opposed to differences from observations to models (STATION minus ÖKS15/RAW respectively) on the *y*-axis. Indicators linked to precipitation are colored in green, discharge indicators in blue and temperature indicators in red. A logarithmic scale is applied for better readability with different axis limits for the two catchments. Temperature indicators are related to the upper and the right axis. Units differ for the different indicators (see Table 3), temperature differences are given in Kelvin, and precipitation differences are expressed as percentages. Differences similar to (close to the 1:1 line) or lower than differences in observations (below the 1:1 line) indicate lower levels of uncertainty and robust model simulations.

be attributed to temperature differences between the two datasets (warm bias of GRID as compared to station temperatures described in Section 3.1.1), which affect snow accumulation and melt. Keeping in mind that the Wölzerbach model was calibrated with the "warmer" GRID dataset, this leads (due to higher melt and accumulation temperatures) to earlier snow accumulation as well as melt, prevailing later in the year for the STATION run. However, these temperature effects are merged with the overestimation of GRID precipitation, resulting in a delayed, higher discharge peak for the GRID run.

Results for the Raab catchment are similar, even if the impact of the slight temperature underestimation (GRID compared to STATION) and precipitation overestimation remains lower than for the alpine Wölzerbach.

Generally, the pluvio-méridional regime of the pre-alpine Raab catchment is reproduced well by both input datasets, but the spring and autumn peaks are overestimated by the models as compared to the observations. Interestingly, ÖKS15-driven models result in a clear peak in September which is neither simulated by the other forcing data nor is visible in the observations. This could indicate the higher relevance of precipitation associated with cyclones coming from the south. Comparing the inter-model spread of ÖKS15-driven WaSiM simulations between Raab and Wölzerbach clearly indicates the higher spread for the Raab catchment. This finding may be related to the impact of snow melt on runoff, which, in turn, is highly related to temperature and thus associated with a lower spread in the alpine catchment. As seen for the Wölzerbach, the HadGEM CCLM vastly underestimates the discharge for the Raab catchment, particularly in the second half of the year. When comparing different periods of time, the small positive bias of discharge between STATION and GRID runs in the reference period of 1961–2005 (not shown) becomes larger for the period 1971–2000 (climate normal).

3.2.2. Hydrological performance indicators

In order to inspect results beyond mean annual hydrographs and probabilities, several discharge indicators were computed to show the characteristics of flow magnitude, extremes and variability. Again, this is presented for different input datasets and periods of time (Table 6). To acknowledge the fact that RCA model runs only start in 1971, the analysis was also carried out with a smaller ensemble excluding GCM-RCM combinations with RCA as the RCM (c.f. Appendix Table A.1). Furthermore, we analyzed a reduced ensemble, excluding the peculiar HadGEM CCLM realization.

We find a diverse picture for the different input data, indicators and catchments. In the Wölzerbach, the overestimation of GRID precipitation is reflected in the magnitude-related discharge indicators, with the STATION simulations yielding the respectively lowest values. However, for low flow indicators, differences between the other input data (GRID, ÖKS15, RAW) are of the same order of magnitude in both catchments. Also, in the pre-alpine Raab catchment, the highest discharges (Hig01) do not differ considerably between the input datasets (including RAW). For the other high flow indicators (Hig25 and Hig95 in both catchments, Hig01 in the alpine catchment; Table 3), the deviation between the RAW model median is more distinct and particularly pronounced in the alpine catchment, whereas differences in other input data remain comparable.

As far as the number of days in summer which are in the top fifth percentile annual flows (S95) are concerned, different input datasets show a greater divergence. For the number of days in summer with flows less than 10% of the mean annual flow (S10), differences between ÖKS15 and their reference GRID data are higher than for other indicators. In both catchments, the RAW models yield the lowest values (zero in the Wölzerbach), reflecting precipitation overestimation in the uncorrected data. Whereas days with high flows (S95 and PeakFrequency; Table 3) as indicated by the RAW models are inflated in the Wölzerbach, they are underrepresented in the Raab catchment. However, when considering observations as the baseline (Raab catchment), differences among the different input data are again of the same order of magnitude, particularly for low flow indicators. The reduced ensembles leave the multi-model median barely unaffected and do not stand out in our analyses.

4. Discussion

Departures of climate model simulations from observations for an identical past represent a significant source of uncertainty in scenario studies, and especially for precipitation. The bias correction method attempts to minimize this problem with empirical methods. Obviously, bias-corrected data can only be as good as the reference data used for bias correction, and these data are also prone to errors (e.g., Gampe et al., 2019; Prein and Gobiet, 2017; Iizumi et al., 2017). The question of how credible the bias-corrected data are for the future remains to be addressed. This credibility generally increases when simulations with a hydrological model, forced by uncorrected model data, can already represent certain basic hydrological mechanisms.

4.1. Uncertainty in input data

Our overall line of reasoning here is that, if the uncertainties inherent in the observations are as large as or similar to the differences between the observational and the model data, a useful application in hydrological scenario modelling should be possible. However, with regard to climate impact studies, a significantly large climate signal is needed to move beyond the zone of uncertainty. In our case, the differences between the two observational datasets, as well as between the model datasets (ÖKS15 and RAW) and observations are discussed in the following against this methodical background.

- Differences between STATION and GRID meteorological input data:
  At the gridpoint level, we found a positive bias for GRID temperatures in the alpine catchment and an overestimation of GRID as compared to STATION precipitation for two-thirds (both catchments) of the locations. The differences are particularly pronounced in the alpine catchment, resulting in a GRID temperature overestimation of about 1 °C and precipitation overestimation of almost 20% at the catchment level.

Calibrating the hydrological model WaSiM with GRID data in the Wölzerbach, the performance increases, when STATION input is used. However, driving STATION-calibrated WaSiM-Raab with the GRID dataset leads to a dramatic decline in model performance in the validation period. Yet, differences in the pre-alpine catchment spatially and temporally compensate each other, leaving the simulated discharge at the most downstream outlet relatively unaffected in the long-term, whereas precipitation overestimation leads to continuous discharge overestimation in the alpine catchment. Overall, timing (i.e., inter-seasonal variation) of hydrological variables differs to a much lesser extent than magnitude (volume).

- Differences between ÖKS15 and GRID meteorological input data:

  Seasonal cycles of wet spells and discharges of the ÖKS15 models diverge from those of the GRID input, even if annual cycles of precipitation and temperature of both input data align well (exception: RCMs driven by the HadGEM GCM). In the alpine catchment, ÖKS15 models (with HadGEM CCLM as single exception) significantly underestimate the snowfall fraction, which is probably related to errors in the combined occurrence of temperature and precipitation for snowfall. This translates to some overestimation of discharge in winter and an underestimation of the meltwater peak in May. The lack of overlap between the analysis period and bias-correction reference period results in deviations in the temperature and precipitation distributions. Their impact on hydrological quantities, however, is equivocal. Significantly shorter periods (e.g., 10 years of analysis) lead to higher discrepancies due to natural variability.
- Differences between bias-corrected ÖKS15 and RAW EURO-CORDEX input data:

  Unlike the bias-corrected simulations, the temperatures obtained from RAW models are generally underestimated, while precipitation is overestimated. This leads to higher snowfall fractions from the RAW model input. Although this effect is present in both catchments, it is particularly pronounced in the alpine catchment. Whereas discharges simulated with the RAW model input are overestimated in the alpine catchment, the highest discharges seen in the pre-alpine catchment do not differ considerably regardless of the input data used. Differences in low flow discharges are of the same order of magnitude for all inputs in both catchments.

Fig. 8 compares these differences as uncertainty in the observed data with the uncertainties from the model data (ÖKS15, RAW) for different meteorological and hydrological variables. This gives a clear picture of the robustness of the model simulations as a relative position to the uncertainty in the observed data. Indicators located close to the 1:1 line (similar differences; please note the logarithmic scaling) or below the 1:1 line (differences lower than those from observations) indicate lower levels of uncertainty and a higher level of model robustness. The differences in the temperature and precipitation indicators are generally higher in the Wölzerbach catchment for both observations and models (ÖKS15 as well as RAW) and are presumably related to the complex orography of the catchment.

Whereas our analyses identify the bias-corrected ÖKS15 models as suitable (robust) for most of the indicators, the uncorrected RAW models are associated with high levels of uncertainty, as indicated by their location high above the 1:1 line. Interestingly, some exceptions exist. In the Wölzerbach, winter temperatures and summer precipitation, as well as low flow indicators are reasonably captured by the RAW models. In the Raab catchment, the RAW models simulate summer temperatures, autumn temperatures and precipitation as well as low flows to a moderate degree. Thus, in less complex settings, and particularly when studying low flows, using the RAW input data might still be an interesting option.

4.2. Remaining uncertainty in bias-corrected input data

The bias-corrected ÖKS15 models do not fully capture the timing of discharge characteristics, leading to slight mismatches in the simulation of past mean annual hydrographs. Furthermore, even when the bias correction improved precipitation simulations in the alpine catchment, due to precipitation overestimation in the reference data, a percent bias of almost 20% persisted.

As seen with the snowfall fraction, the univariate bias correction does not account for inter-variable dependencies and the often-used approach of evaluating climate model variables independently fosters overlooking disparities arising from it. Differences in the long-term monthly average dry spell duration could further explain the temporal mismatches to some extent. This highlights the fact that an adequate representation of temperature and precipitation cycles, and individual flood-/drought-related meteorological indicators of climate models do not necessarily translate into an accurate representation of average runoff conditions, which might be specifically problematic when investigating possible changes in the timing of discharge in the future.

Potential remaining biases, as found in this study, should be cross-checked in advance, and considered when interpreting results from impact assessment model chains. They should be particularly acknowledged in (topographically complex) regions where also the GRID data was created with sparse station density. A related discussion on limitations of bias correction due to restricted location representativeness can be found in Maraun and Widmann (2015).

Problems arising from bias-correcting climate variables independently have been acknowledged by other researchers (e.g., Meyer et al., 2019; Chen et al., 2018), and the issue of hydrologically relevant remaining biases after bias correction was pointed out in the works of Addor and Seibert (2014), Hakala et al. (2018) and Maraun et al. (2019). For a general discussion on the benefits and limitations of bias correction we refer to the works of Ehret et al. (2012) and Maraun (2016).

4.3. Ensemble member selection and cautionary remarks

Our results do not allow us to give a uniform recommendation for preferred models to use, because most of the models perform better in one region than in the other. In terms of discharge characteristics, however, CNRM-CM5 CCLM, MPI-ESM CCLM and EC-EARTH CCLM performed reasonably well for the period of 1961–2005 in both (alpine and pre-alpine) catchments. HadGEM CCLM

is not able to capture the annual precipitation cycle, especially in the southeastern pre-alpine catchment, underestimating precipitation by up to 50%. However, this scarcely affected multi-model median discharge indicators in our study. The CNRM-CM5 ALADIN simulations did not stand out either in our analyses, but were found to be erroneous at a later stage (after the ÖKS15 dataset had already been released) (Chimani et al., 2019). Furthermore, since the original publication of the EURO-CORDEX data, errors regarding an unrealistic accumulation of snow (also referred to as the "snow tower issue") have been discovered for the GCM-RCM combinations EC-EARTH RACMO and EC-EARTH HIRHAM (EURO-CORDEX Errata, 2021). Frei et al. (2018) showed that this unrealistic accumulation of snow can dampen the climate change signal of temperature at the locations involved. We found that this issue only affects high-altitude grid cells in the western part of Austria and thus determined it as not relevant for our study region. However, projections concerned should be applied with great caution and removed from the analyzed ensemble where necessary. As suggested by Hakala et al. (2018), both future and past periods should be considered in the decision on omitting individual GCM-RCM realizations.

4.4. Selection of the analysis period

Although the results for ensemble median-simulated discharges and indicators for the shorter reference period (1971–2000) did not stand out in our analyses, the potential lack of overlap between the analysis period and the bias-correction reference period of 45 years (1961–2005) should not be neglected. Discharge time series dating back to 1971 or even 1961 are rare, particularly for small and medium-sized catchments. Furthermore, since five out of thirteen ÖKS15 models are available only from 1971 and on, the user can either choose a shorter analysis period (the full ensemble available for 1971–2005) and accept some of the resulting discrepancies or use a reduced ensemble. The idea of establishing a "default-database" that considers the longest records possible neglects the fact that, for many applications, observational data of 40 years or longer simply do not exist. Consequently, user-oriented evaluation studies like the one presented here can provide further valuable insights for the climate modelling community.

5. Conclusions

In this study, we assessed the value of the high-resolution climate dataset ÖKS15 for hydrological impact studies. To achieve this purpose, impacts on hydrological indicators were analyzed along different spatial scales and sources of uncertainty, using an alpine and a pre-alpine catchment in southeastern Austria as examples. Clearly, some of our results are specific to the Austrian ÖKS15 dataset, but others are common for similar high-resolution climate model data in general.

In order to quantify the effect of uncertainty propagation from meteorological driving data to driven hydrologic indicators, we used the hydrological model WaSiM. We found that the observed hydro-climatic conditions could generally be reproduced effectively when driving WaSiM with bias-corrected climate model data. Contrary to the uncertainties noted when RAW EURO-CORDEX models are used, uncertainties arising from the use of the bias-corrected ÖKS15 are comparable to those in the observed data for most of the hydrological indicators analyzed. Taking due account of the limitations and assumptions inherent in bias-corrected data, this robustness affirms that the ÖKS15 data are basically fit for purpose for hydrological applications. Our results particularly support the specific recommendation to use ÖKS15 data in long-term analyses of mean hydrological conditions. At the same time, hydrologically relevant limitations of the ÖKS15 dataset do exist. Even for the bias-corrected data, some inconsistencies in timing, magnitude and location persist, partially leading to deviations in hydrological signatures.

We found that HadGEM CCLM was particularly striking and not able to capture the annual precipitation cycle. Thus this model should be applied with great caution, especially for the southeast of Austria. However, multi-model median discharge indicators analyzed within this study were scarcely affected. With regard to the precipitation overestimation in the reference dataset, a bias of almost 20% remains for discharge in the alpine catchment. Nonetheless, as the temperature and precipitation biases of uncorrected RAW models are particularly high in complex terrain, the bias correction adds value in these settings. Still, the uncorrected RAW models perform reasonably well with respect to some features, leaving them as practicable options for impact studies (e.g., related to low flows).

As a further cautionary remark, we note that the univariate bias correction method, which does not consider the combined occurrence of temperature and precipitation, affects the representation of snow-related processes. This should be acknowledged by end-users but might be of less interest in pre-alpine (not snow-dominated) settings. Another finding is that differences in the bias correction reference period and some of the models' temporal coverage also impact meteorological signatures and confine the recommended use of ÖKS15 data to basins with a sufficiently extensive gauging history, which allows users to run an initial check for remaining biases.

We acknowledge uncertainties and limitations of our hydrological model setup and parameters, which we tried to circumvent by partly confining our analysis to the model world. Comparing GRID data to WaSiM-internal STATION interpolation as a reference should not suggest that the latter represents the truth. Measurement, structural, parameter and interpolation uncertainty are inherent in them as well. For example, no precipitation correction was carried out to avoid obscuring the comparison between the GRID and STATION data, even if undercatch can be considerable, particularly in the alpine catchment. The fact that input differences from the lack of overlap between the analysis period and the bias-correction reference period do not clearly propagate to discharges as well as mismatches in high flow indicators point to limitations in the models used, which need to be addressed in future work. Uncertainty in

the hydrological models also affect low flows for which our results indicate a good agreement among all datasets. Vidal et al. (2016), for example, found diverging low-flow responses from different hydrological models in a changing climate. Ideally the multi-model approach should thus not only be considered using an ensemble of climate models, but applying multiple hydrological models (e.g., Horton et al., 2021), particularly with a view to the simulation of snow-related processes in a warmer future climate (e.g. Troin et al., 2016). The share of the hydrological models' part in overall climate change impact uncertainty has been discussed in Dobler et al. (2012), Bosshard et al. (2013) and Addor et al. (2014).

As a further constraint of our approach, we note that vegetation and land use changes, which have had considerable, regionally occurring impacts over the past decades, were not included in our models. Together with the consideration of changes due to other human impacts, land use changes should be addressed in subsequent studies, particularly when focusing on future climate change (e.g., Sivapalan and Blöschl, 2015).

Finally, focusing on just two example catchments represents another limitation of our analysis and the results might somewhat differ when using the ÖKS15 data for other regions in Austria.

The approach taken in this study, however, is considered an important step in the interdisciplinary community effort to further develop climate analysis and simulation-based, high-resolution hydrological research in Austria. We believe that our findings help to improve the usage of climate model datasets for hydrological applications in general. While identifying the ÖKS15 dataset generally fit for purpose in hydrological applications, describing its strengths and limitations will also help users of ÖKS15 and corresponding datasets to design and interpret hydrological impact studies more effectively.

CRediT authorship contribution statement

Stefanie Peßenteiner: Conceptualization, Methodology, Data curation, Software, Validation, Formal analysis, Writing – original draft, Writing – review & editing, Visualization. **Clara Hohmann:** Software, Validation, Visualization, Writing – review & editing. **Wolfgang Schöner:** Writing – review & editing, Supervision, Project administration, Funding acquisition. **Gottfried Kirchengast:** Writing – review & editing, Supervision, Funding acquisition.

Declaration of Competing Interest

The authors declare that they have no known competing financial interests or personal relationships that could have appeared to influence the work reported in this paper.

Acknowledgements

This research has been supported by the Austrian Climate and Energy Fund (Project RunSed-CC, ACRP grant no. KR16AC0K13305), the Austrian Science Fund (FWF) Doctoral Programme Climate Change—Uncertainties, Thresholds and Coping Strategies (grant no. W1256) and the University of Graz. We thank Armin Leuprecht and Sebastian Scher for valuable discussions. Furthermore, we thank the Austrian Central Institution for Meteorology and Geodynamics (ZAMG) and the Austrian Hydrographic Service (AHYD) for the provision of data. Finally, we would also like to thank the two anonymous reviewers for their constructive comments, which have helped to improve the manuscript.

Appendix

See Fig. A.1 and Fig. A.2.

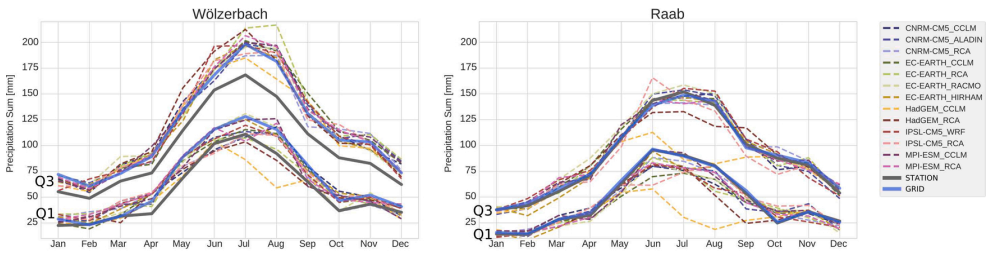


Fig. A.1. Annual cycle of the 0.25 quantile (Q1) and the 0.75 quantile (Q3) of catchment average monthly precipitation from bias-corrected RCM simulations (ÖKS15) as compared to observations (GRID and STATION). Left: For the Wölzerbach catchment. Right: For the Raab catchment. In July and August, the Wölzerbach Q3 STATION sums are more strongly underestimated than in other months. This is probably related to local convective precipitation not captured by the STATION interpolation. The low performance of the HadGEM CCLM model is clearly visible for both catchments and is extremely pronounced in the pre-alpine Raab catchment.

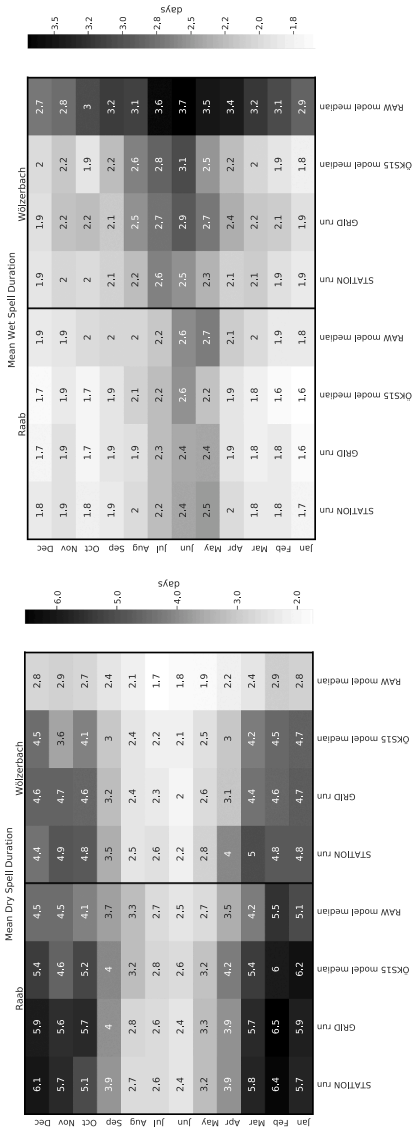


Fig. A.2. Mean monthly dry spell duration (right) and wet spell (left) duration for the Wölzerbach and the Raab catchment in the reference period of 1961–2005.

See Table A.1.

Table A.1
Underlying models and realizations of the ÖKS15 dataset. Letters r, i and p refer to realization, initialization method and physics used for the GCM.

Period	1961–2005	1961–2005	1961–2005	1961–2005	1961–2005	1971–2005
GCM/RCM	**ALADIN**	**CCLM**	**RACMO**	**HIRHAM5**	**WRF**	**RCA**
CNRM-CM5	r1i1p1	r1i1p1				r1i1p1
EC-EARTH		r12i1p1	r1i1p1	r3i1p1		r12i1p1
HadGEM2-ES		r1i1p1				r1i1p1
IPSL-CM5A-MR					r1i1p1	r1i1p1
MPI-ESM-LR		r1i1p1				r1i1p1

See Table A.2.

Table A.2
Performance of the hydrological model WaSiM in the Wölzerbach and the Raab catchment, calibrated with SCE-UA (Duan et al., 1994) in a split-sample approach.

Catchment	Gauge	Meteorological input used for parameter calibration	Period	NSE	NSElog
Wölzerbach	Niederwölz	GRID	Calibration 2004–2007	0.7	0.71
Wölzerbach	Niederwölz	GRID	Validation 2008–2010	0.68	0.69
Raab	St. Ruprecht	STATION	Calibration 2003–2009	0.66	0.73
Raab	St. Ruprecht	STATION	Validation 1995–2001	0.78	0.8
Raab	Takern II	STATION	Calibration 2003–2009	0.75	0.79
Raab	Takern II	STATION	Validation 1995–2001	0.61	0.77
Raab	Neumarkt	STATION	Calibration 2003–2009	0.74	0.79
Raab	Neumarkt	STATION	Validation 1995–2001	0.62	0.65

See Table A.3.

Table A.3
Statistics of temperature differences (GRID minus STATION) for the Wölzerbach and Raab catchments over the period of 1961–2005.

Wölzerbach							Raab						
Station	BIAS (°C)	CORR	MAE (°C)	Height (m a.s. l.)	Duration (Years)	Operator	Station	BIAS (°C)	CORR	MAE (°C)	Height (m a.s. l.)	Duration (Years)	Operator
12800	0	0.98	1.03	1005	25	Z	13300	-0.1	1	0.23	489	24	Z
13010	0.9	0.99	1.28	1070	28	Z	13301	0	1	0.17	480	20	Z
15900	-0.3	0.99	0.82	810	41	Z	13305	-0.1	1	0.47	505	9	Z
15910	-0.8	0.99	0.97	1305	39	Z	13510	-0.5	0.99	0.89	1020	15	Z
15911	0.3	1	0.47	1215	5	Z	13515	-0.4	0.99	0.76	1034	11	Z
15920	0.1	0.99	0.76	816	17	Z	16400	0.2	1	0.41	340	45	Z
16000	0.2	0.99	0.93	842	15	Z	16402	0.2	1	0.24	366	28	Z
16001	-0.3	0.99	0.8	881	11	Z	16410	-1.1	0.99	1.31	725	15	Z
16003	-1.4	0.99	1.48	1125	15	Z	16411	-0.7	0.98	1.08	726	20	Z
16015	0.2	0.99	0.67	869	13	Z	16412	-0.1	1	0.13	367	18	Z
106005	1.4	0.96	1.94	1120	35	H	16420	-0.1	1	0.26	1436	32	Z
106500	1.8	0.98	2.08	985	1	H	16421	-0.2	1	0.36	1443	14	Z
106567	0.8	0.98	1.41	1605	7	H	16500	0.2	1	0.24	375	45	Z
111674	1.9	0.97	2.14	900	45	H	16510	-1.1	0.99	1.35	543	20	Z
111732	1.5	0.95	2.11	1260	8	H	16511	-0.7	0.99	1.01	530	16	Z
123158	0.7	0.98	1.28	810	5	H	19200	0	1	0.16	303	25	Z
1065001	1.4	0.97	1.96	980	8	H	19201	-0.1	1	0.4	303	16	Z
							19204	0.1	1	0.08	269	3	Z
							19205	0.1	1	0.39	323	8	Z
							110890	1.1	0.99	1.28	306	8	H
							111294	0.6	0.99	1.17	260	8	H
							111369	1.2	0.99	1.49	702	8	H
							111401	-0.1	0.99	0.88	1070	8	H

See Table A.4.

Table A.4
Statistics of precipitation differences (GRID minus STATION) for the Wölzerbach and Raab catchments over the period of 1961–2005.

Wölzerbach							Raab						
Station	PBIAS (%)	CORR	MAE (mm/day)	Height(m a.s.l.)	Duration (Years)	Operator	Station	PBIAS (%)	CORR	MAE (mm/day)	Height(m a.s.l.)	Duration (Years)	Operator
12800	-15.77	0.9	1.16	1005	25	Z	13300	0.5	0.99	0.3	489	24	Z
13010	1.71	0.88	1.22	1070	28	Z	13301	-2.43	0.98	0.36	480	20	Z
15900	11.7	0.89	0.99	810	40	Z	13305	16.49	0.92	0.82	505	8	Z
15910	-3.79	0.87	1.2	1305	39	Z	13510	2.52	0.9	1.13	1020	15	Z
15911	12.08	0.87	1.39	1215	5	Z	13515	-1.13	0.89	1.13	1034	9	Z
15920	6.75	0.91	1	816	17	Z	16400	0.64	0.99	0.3	340	45	Z
16000	6.06	0.99	0.41	842	15	Z	16402	0.28	0.99	0.32	366	27	Z
16001	-0.56	0.98	0.42	881	11	Z	16410	-8.16	0.93	0.86	725	14	Z
16003	0.92	0.98	0.45	1125	15	Z	16411	8.67	0.88	0.97	726	14	Z
16015	7.15	0.93	0.59	869	13	Z	16412	1.89	0.98	0.33	367	17	Z
106005	-1.56	0.99	0.32	1120	35	H	16420	1.55	0.98	0.42	1436	31	Z
106567	-29.32	0.89	2.05	1605	18	H	16421	1.25	0.98	0.44	1443	12	Z
111674	35.72	0.87	1.36	900	35	H	16500	-0.55	0.99	0.27	375	45	Z
111682	7.16	0.98	0.4	1070	35	H	16510	-1.19	0.91	0.78	543	19	Z
111708	19.74	0.99	0.47	745	35	H	16511	2.2	0.92	0.78	530	15	Z
111724	5.71	0.99	0.4	1050	35	H	19200	-1.57	0.91	0.89	303	23	Z
111732	4.74	0.88	1.4	1260	35	H	19201	0.25	0.92	0.88	303	14	Z
112508	3.84	0.87	1.14	950	32	H	19204	-1.38	0.92	0.69	269	2	Z
123158	13.5	0.89	0.99	810	31	H	19205	-1.46	0.9	0.76	323	7	Z
1065001	-7.02	0.91	1.1	980	8	H	101063	2.55	0.97	0.46	350	6	H
1231581	17.12	0.93	0.89	810	5	H	105080	-4.27	0.67	1.08	228	1	H
							110890	-1.2	0.9	0.8	306	35	H
							110908	2.87	0.86	0.95	240	35	H
							110916	2.83	0.98	0.48	922	35	H
							110932	1.74	0.98	0.41	690	35	H
							110999	0.81	0.99	0.3	350	35	H
							111005	-0.02	0.99	0.28	285	35	H
							111054	0.62	0.99	0.29	450	35	H
							111062	1.01	0.99	0.25	330	35	H
							111088	6.36	0.88	0.88	240	35	H
							111187	4.32	0.85	0.95	374	35	H
							111195	4.93	0.98	0.31	250	35	H
							111203	1.17	0.98	0.34	260	35	H
							111229	14.92	0.84	1.02	200	35	H
							111294	-1.93	0.89	0.85	260	31	H
							111302	5.89	0.9	0.87	350	31	H
							111310	5.64	0.88	0.89	420	31	H
							111328	8.64	0.89	1.17	1038	31	H
							111344	-1.68	0.93	0.63	275	29	H
							111369	10.51	0.89	1.04	702	25	H
							111393	0.88	0.9	0.89	525	22	H
							111401	9.39	0.89	1.18	1070	18	H
							111419	2.22	0.9	0.79	303	16	H
							111435	-1.25	0.91	1.13	1020	16	H
							111443	7.53	0.93	0.62	355	14	H
							111450	3.33	0.91	0.71	230	13	H
							111476	0.77	0.86	0.93	415	9	H

(*continued on next page*)

Table A.4 (*continued*)

Wölzerbach						Raab					
Station	PBIAS (%)	CORR	MAE (mm/day)	Height(m a.s.l.)	Duration (Years)	Operator	Station	PBIAS (%)	CORR	MAE (mm/day)	Height(m a.s.l.)	Duration (Years)	Operator
							111484	5.4	0.89	0.74	265	9	H
							112003	1.12	0.99	0.27	560	35	H
							112037	0.98	0.99	0.26	420	32	H
							112045	0.97	0.9	0.95	670	34	H
							112078	0.52	0.91	0.85	386	35	H
							112086	-0.6	0.98	0.35	360	35	H
							112383	1.45	0.9	0.92	350	35	H
							112391	-0.1	0.99	0.24	270	35	H
							112409	1.33	0.95	0.64	220	35	H
							112425	1.9	0.98	0.32	360	35	H
							112433	3.18	0.91	0.84	380	31	H
							112441	0.84	0.98	0.34	200	35	H
							112466	1.35	0.82	1.18	370	35	H
							112516	4.63	0.94	0.79	256	31	H
							112540	11.48	0.89	1.04	648	28	H
							112565	31.31	0.88	1.26	665	28	H
							112664	-4.5	0.95	0.6	288	25	H
							112847	3.11	0.92	0.75	460	15	H
							112862	2.47	0.94	0.67	390	15	H
							123042	11.26	0.92	0.83	610	12	H
							123075	4.76	0.89	1.01	520	10	H
							123083	5.57	0.93	0.71	400	10	H
							123117	1.54	0.9	0.96	680	9	H

References

Addor, N., Rössler, O., Köplin, N., Huss, M., Weingartner, R., Seibert, J., 2014. Robust changes and sources of uncertainty in the projected hydrological regimes of Swiss catchments. Water Resour. Res. 50, 7541–7562. https://doi.org/10.1002/2014WR015549.

Addor, N., Seibert, J., 2014. Bias correction for hydrological impact studies – beyond the daily perspective. Hydrol. Processes 28, 4823–4828. https://doi.org/10.1002/hyp.10238.

Beyer, M., Wallner, M., Bahlmann, L., Thiemig, V., Dietrich, J., Billib, M., 2016. Rainfall characteristics and their implications for rain-fed agriculture: a case study in the Upper Zambezi River Basin. Hydrol. Sci. J. 61, 321–343. https://doi.org/10.1080/02626667.2014.983519.

Bosshard, T., Carambia, M., Goergen, K., Kotlarski, S., Krahe, P., Zappa, M., Schär, C., 2013. Quantifying uncertainty sources in an ensemble of hydrological climate-impact projections. Water Resour. Res. 49, 1523–1536. https://doi.org/10.1029/2011WR011533.

CH2011, 2011, Swiss Climate Change Scenarios CH2011, published by C2SM, MeteoSwiss, ETH, NCCR Climate, and OcCC, Zurich, Switzerland, 88 pp. ISBN: 978–3-033–03065-7.

CH2018, 2018, CH2018 – Climate Scenarios for Switzerland, Technical Report, National Centre for Climate Services, Zurich, 271 pp. ISBN: 978–3-9525031–4-0.

Chen, J., Li, C., Brissette, F.P., Chen, H., Wang, M., Essou, G.R.C., 2018. Impacts of correcting the inter-variable correlation of climate model outputs on hydrological modeling. J. Hydrol. 560, 326–341. https://doi.org/10.1016/j.jhydrol.2018.03.040.

Chimani, B., Heinrich, G., Hofstätter, M., Kerschbaumer, M., Kienberger, S., Leuprecht, A., Lexer, A., Peßenteiner, S., Poetsch, M., Salzmann, M., Spiekermann, R., Switanek, M., Truhetz, H., 2016. ÖKS15 – Klimaszenarien für Österreich. Daten, Methoden und Klimaanalyse. (Project report, in German). Wien. https://hdl.handle.net/20.500.11756/06edd0c9.

Chimani, B., Matulla, C., Eitzinger, J., Hofstätter, M., Kubu, G., Maraun, D., Mendlik, T., Schellander-Gorgas, T., Thaler, S., 2019. Guideline zur Nutzung der ÖKS15-Klimawandelsimulationen sowie der entsprechenden gegitterten Beobachtungsdatensätze (Report in German). https://hdl.handle.net/20.500.11756/e3232e36.

Dobler, C., Hagemann, S., Wilby, R.L., Stötter, J., 2012. Quantifying different sources of uncertainty in hydrological projections in an Alpine watershed. Hydrol. Earth System Sci. 16, 4343–4360. https://doi.org/10.5194/hess-16-4343-2012.

Duan, Q., Sorooshian, S., Gupta, V.K., 1994. Optimal use of the SCE-UA global optimization method for calibrating watershed models. J. Hydrol. 158, 265–284. https://doi.org/10.1016/0022-1694(94)90057-4.

Ehret, U., Zehe, E., Wulfmeyer, V., Warrach-Sagi, K., Liebert, J., 2012. HESS opinions "should we apply bias correction to global and regional climate model data?". Hydrol. Earth System Sci. 16, 3391–3404. https://doi.org/10.5194/hess-16-3391-2012.

Ekström, M., Gutmann, E.D., Wilby, R.L., Tye, M.R., Kirono, D.G.C., 2018. Robustness of hydroclimate metrics for climate change impact research. WIREs Water 5, e1288. https://doi.org/10.1002/wat2.1288.

EURO-CORDEX Errata, 2021. EURO-CORDEX Errata Table. https://docs.google.com/spreadsheets/d/1Vcob7VlE4H98g0IdMzdy5Ae4Y-WU0lRktI1mPneibXM/edit#gid=0 (Accessed 16 September 2021).

Frei, P., Kotlarski, S., Liniger, M.A., Schär, C., 2018. Future snowfall in the Alps: projections based on the EURO-CORDEX regional climate models. Cryosphere 12, 1–24. https://doi.org/10.5194/tc-12-1-2018.

Gädeke, A., Hölzel, H., Koch, H., Pohle, I., Grünewald, U., 2014. Analysis of uncertainties in the hydrological response of a model-based climate change impact assessment in a subcatchment of the Spree River, Germany. Hydrol. Process. 28, 3978–3998. https://doi.org/10.1002/hyp.9933.

Gampe, D., Schmid, J., Ludwig, R., 2019. Impact of reference dataset selection on RCM evaluation, bias correction, and resulting climate change signals of precipitation. J. Hydrometeorol. 20, 1813–1828. https://doi.org/10.1175/JHM-D-18-0108.1.

Hakala, K., Addor, N., Seibert, J., 2018. Hydrological modeling to evaluate climate model simulations and their bias correction. J. Hydrometeorol. 19, 1321–1337. https://doi.org/10.1175/JHM-D-17-0189.1.

Hakala, K., Addor, N., Teutschbein, C., Vis, M., Dakhlaoui, H. Seibert, J., 2019. Hydrological Modeling of Climate Change Impacts, in P. Maurice (Ed.), Encyclopedia of Water. https://doi.org/10.1002/9781119300762.wsts0062.

Hamon, W.R., 1961. Estimating potential evapotranspiration. J. Hydraul. Div.n 87, 107–120. https://doi.org/10.1061/JYCEAJ.0000599.

Hiebl, J., Frei, C., 2016. Daily temperature grids for Austria since 1961– concept, creation and applicability. Theor. Appl. Climatol. 124, 161–178. https://doi.org/10.1007/s00704-015-1411-4.

Hofstätter, M., Jacobeit, J., Homann, M., Lexer, A., Chimani, B., Beck, C., Ganekind, M., 2015. WETRAX – Weather Patterns, Cyclone Tracks and related Precipitation Extremes. Großflächige Starkniederschläge im Klimawandel in Mitteleuropa. Project report (in German). (No. 19), Geographica Augustana.

Hohmann, C., Kirchengast, G., Birk, S., 2018. Alpine foreland running drier? Sensitivity of a drought vulnerable catchment to changes in climate, land use, and water management. Clim. Chang. 147, 179–193. https://doi.org/10.1007/s10584-017-2121-y.

Hohmann, C., Kirchengast, G., O, S., Rieger, W., Foelsche, U., 2021. Small catchment runoff sensitivity to station density and spatial interpolation: hydrological modeling of heavy rainfall using a dense rain gauge network. Water 13, 1381. https://doi.org/10.3390/w13101381.

Horton, P., Schaefli, B., Kauzlaric, M., 2021. Why do we have so many different hydrological models? A review based on the case of Switzerland. EarthArXiv. https://doi.org/10.31223/X5CK5K.

Huang, S., Krysanova, V., Hattermann, F., 2015. Projections of climate change impacts on floods and droughts in Germany using an ensemble of climate change scenarios. Reg. Environ. Chang. 15, 461–473. https://doi.org/10.1007/s10113-014-0606-z.

Iizumi, T., Takikawa, H., Hirabayashi, Y., Hanasaki, N., Nishimori, M., 2017. Contributions of different bias-correction methods and reference meteorological forcing data sets to uncertainty in projected temperature and precipitation extremes. J. Geophys. Res. Atmosph. 122, 7800–7819. https://doi.org/10.1002/2017JD026613.

Jacob, D., Petersen, J., Eggert, B., Alias, A., Christensen, O.B., Bouwer, L.M., Braun, A., Colette, A., Déqué, M., Georgievski, G., Georgopoulou, E., Gobiet, A., Menut, L., Nikulin, G., Haensler, A., Hempelmann, N., Jones, C., Keuler, K., Kovats, S., Kröner, N., Kotlarski, S., Kriegsmann, A., Martin, E., van Meijgaard, E., Moseley, C., Pfeifer, S., Preuschmann, S., Radermacher, C., Radtke, K., Rechid, D., Rounsevell, M., Samuelsson, P., Somot, S., Soussana, J.-F., Teichmann, C., Valentini, R., Vautard, R., Weber, B., Yiou, P., 2014. EURO-CORDEX: new high-resolution climate change projections for European impact research. Reg. Environ. Chang. 14, 563–578. https://doi.org/10.1007/s10113-013-0499-2.

Jacob, D., Teichmann, C., Sobolowski, S., Katragkou, E., Anders, I., Belda, M., Benestad, R., Boberg, F., Buonomo, E., Cardoso, R.M., Casanueva, A., Christensen, O.B., Christensen, J.H., Coppola, E., De Cruz, L., Davin, E.L., Dobler, A., Domínguez, M., Fealy, R., Fernandez, J., Gaertner, M.A., García-Díez, M., Giorgi, F., Gobiet, A., Goergen, K., Gómez-Navarro, J.J., Alemán, J.J.G., Gutiérrez, C., Gutiérrez, J.M., Güttler, I., Haensler, A., Halenka, T., Jerez, S., Jiménez-Guerrero, P., Jones, R.G., Keuler, K., Kjellström, E., Knist, S., Kotlarski, S., Maraun, D., van Meijgaard, E., Mercogliano, P., Montávez, J.P., Navarra, A., Ni kulin, G., Noblet-Ducoudré, N., Panitz, H.J., Pfeifer, S., Piazza, M., Pichelli, E., Pietikäinen, J.P., Prein, A.F., Preuschmann, S., Rechid, D., Rockel, B., Romera, R., Sánchez, E., Sieck, K., Soares, P. M.M., Somot, S., Srnec, L., Sørland, S.L., Termonia, P., Truhetz, H., Vautard, R., Warrach-Sagi, K., Wulfmeyer, V., 2020. Regional climate downscaling over Europe: perspectives from the EURO-CORDEX community. Reg. Environ. Chang. 20, 51. https://doi.org/10.1007/s10113-020-01606-9.

Kabas, T., Foelsche, U., Kirchengast, G., 2011. Seasonal and annual trends of temperature and precipitation within 1951/1971–2007 in South-Eastern Styria, Austria. Meteorol. Z. 20, 277–289. https://doi.org/10.1127/0941-2948/2011/0233.

Krause, P., Boyle, D.P., Bäse, F., 2005. Comparison of different efficiency criteria for hydrological model assessment. Adv. Geosci. 5, 89–97. https://doi.org/10.5194/adgeo-5-89-2005.

Leuprecht A., Chimani,B., Heinrich, G., Hofstätter, M., Kerschbaumer, M., Kienberger, S., Lexer, A., Peßenteiner, S., Poetsch, M., Salzmann, M., Spiekermann, R., Switanek, M., Truhetz, H., 2017: ÖKS15 bias corrected EURO-CORDEX models, Version 2, 2017. Vienna, Austria. CCCA Data Centre. https://data.ccca.ac.at/group/oks15 (Accessed 7 June, 2021).

Liersch, S., Tecklenburg, J., Rust, H., Dobler, A., Fischer, M., Kruschke, T., Koch, H., Hattermann, F.F., 2018. Are we using the right fuel to drive hydrological models? A climate impact study in the Upper Blue Nile. Hydrol. Earth System Sci. 22, 2163–2185. https://doi.org/10.5194/hess-22-2163-2018.

Lowe, J.A., Bernie, D., 2018. UKCP18 science overview report. Met Office Hadley Centre. https://www.metoffice.gov.uk/pub/data/weather/uk/ukcp18/science-reports/UKCP18-Overview-report.pdf.

4 Sensitivity and uncertainty analysis

Mader, H., Steidl, T., Wimmer, R., 1996. Abflußregime österreichischer Fließgewässer. Beitrag zu einer bundesweiten Fließgewässertypologie. Austrian Federal Environment Agency (FEA), Vienna. (Report in German). https://www.umweltbundesamt.at/fileadmin/site/publikationen/M082z.pdf.
Maraun, D., Mendlik, T., Truhetz, H., Chimani, B., Matulla, C., Hiebl, J., Schellander-Gorgas, T., Thaler, S., Kubu, G., 2019. Supporting the Austrian Research Community in using recent Climate Change Projections for Climate Impact Studies. Final Report. ACRP Project No. KR15AC8K12604.
Maraun, D., 2016. Bias correcting climate change simulations - a critical review. Curr. Clim. Chang. Rep. 2, 211–220. https://doi.org/10.1007/s40641-016-0050-x.
Maraun, D., Wetterhall, F., Ireson, A.M., Chandler, R.E., Kendon, E.J., Widmann, M., Brienen, S., Rust, H.W., Sauter, T., Themeßl, M., Venema, V.K.C., Chun, K.P., Goodess, C.M., Jones, R.G., Onof, C., Vrac, M., Thiele, Eich, I., 2010. Precipitation downscaling under climate change: Recent developments to bridge the gap between dynamical models and the end user. Rev. Geophys. 48. https://doi.org/10.1029/2009RG000314.
Maraun, D., Widmann, M., 2015. The representation of location by a regional climate model in complex terrain. Hydrol. Earth System Sci. 19, 3449–3456. https://doi.org/10.5194/hess-19-3449-2015.
Mendlik, T., Gobiet, A., 2016. Selecting climate simulations for impact studies based on multivariate patterns of climate change. Clim. Change 135, 381–393. https://doi.org/10.1007/s10584-015-1582-0.
Meyer, J., Kohn, I., Stahl, K., Hakala, K., Seibert, J., Cannon, A.J., 2019. Effects of univariate and multivariate bias correction on hydrological impact projections in alpine catchments. Hydrol. Earth System Sci. 23, 1339–1354. https://doi.org/10.5194/hess-23-1339-2019.
Moriasi, D.N., Arnold, J.G., Van Liew, M.W., Bingner, R.L., Harmel, R.D., Veith, T.L., 2007. Model evaluation guidelines for systematic quantification of accuracy in watershed simulations. Trans. ASABE 50, 885–900. https://doi.org/10.13031/2013.23153.
Nash, J.E., Sutcliffe, J.V., 1970. River flow forecasting through conceptual models part I — a discussion of principles. J. Hydrol. 10, 282–290. https://doi.org/10.1016/0022-1694(70)90255-6.
Olsson, J., Arheimer, B., Borris, M., Donnelly, C., Foster, K., Nikulin, G., Persson, M., Perttu, A.-M., Uvo, C.B., Viklander, M., Yang, W., 2016. Hydrological climate change impact assessment at small and large scales: key messages from recent progress in Sweden. Climate 4, 39. https://doi.org/10.3390/cli4030039.
Pastén-Zapata, E., Jones, J.M., Moggridge, H., Widmann, M., 2020. Evaluation of the performance of Euro-CORDEX Regional Climate Models for assessing hydrological climate change impacts in Great Britain: A comparison of different spatial resolutions and quantile mapping bias correction methods. J. Hydrol. 584, 124653 https://doi.org/10.1016/j.jhydrol.2020.124653.
Pennino, M.J., McDonald, R.I., Jaffe, P.R., 2016. Watershed-scale impacts of stormwater green infrastructure on hydrology, nutrient fluxes, and combined sewer overflows in the mid-Atlantic region. Sci. Total Environ. 565, 1044–1053. https://doi.org/10.1016/j.scitotenv.2016.05.101.
Piringer, M., Knauder, W., Anders, I., Andre, K., Zollitsch, W., Hörtenhuber, S.J., Baumgartner, J., Niebuhr, K., Hennig-Pauka, I., Schönhart, M., Schauberger, G., 2019. Climate change impact on the dispersion of airborne emissions and the resulting separation distances to avoid odour annoyance. Atmosph. Environ. X 2, 100021. https://doi.org/10.1016/j.aeaoa.2019.100021.
Prein, A.F., Gobiet, A., 2017. Impacts of uncertainties in European gridded precipitation observations on regional climate analysis. Int. J. Climatol. 37, 305–327. https://doi.org/10.1002/joc.4706.
Prettenthaler, F., Podesser, A., Pilger, H. (Eds.), 2010. Klimaatlas Steiermark. Austrian Academy of Sciences, Vienna. (In German). ISBN 978-3-7001-6754-9.
Reifen, C., Toumi, R., 2009. Climate projections: past performance no guarantee of future skill? Geophys. Res. Lett. 36. https://doi.org/10.1029/2009GL038082.
Reszler, C., Switanek, M.B., Truhetz, H., 2018. Convection-permitting regional climate simulations for representing floods in small- and medium-sized catchments in the Eastern Alps. Nat. Hazards Earth System Sci. 18, 2653–2674. https://doi.org/10.5194/nhess-18-2653-2018.
Ridolfi, E., Kumar, H., Bárdossy, A., 2020. A methodology to estimate flow duration curves at partially ungauged basins. Hydrol. Earth System Sci. 24, 2043–2060. https://doi.org/10.5194/hess-24-2043-2020.
Rössler, O., Kotlarski, S., Fischer, A.M., Keller, D., Liniger, M., Weingartner, R., 2019. Evaluating the added value of the new Swiss climate scenarios for hydrology: an example from the Thur catchment. Clim. Serv. 13, 1–13. https://doi.org/10.1016/j.cliser.2019.01.001.
Schulla, J., 2017. Model Description WaSiM. (Technical report). Zurich. www.wasim.ch. (Accessed 7 June 2021).
Schürz, C., Hollosi, B., Matulla, C., Pressl, A., Ertl, T., Schulz, K., Mehdi, B., 2019. A comprehensive sensitivity and uncertainty analysis for discharge and nitrate-nitrogen loads involving multiple discrete model inputs under future changing conditions. Hydrol. Earth System Sci. 23, 1211–1244. https://doi.org/10.5194/hess-23-1211-2019.
Sivapalan, M., Blöschl, G., 2015. Time scale interactions and the coevolution of humans and water. Water Resour. Res. 51, 6988–7022. https://doi.org/10.1002/2015WR017896.
Smiatek, G., Kunstmann, H., 2019. Simulating future runoff in a complex terrain alpine catchment with EURO-CORDEX data. J. Hydrometeorol. 20, 1925–1940. https://doi.org/10.1175/JHM-D-18-0214.1.
Switanek, M.B., Troch, P.A., Castro, C.L., Leuprecht, A., Chang, H.-I., Mukherjee, R., Demaria, E.M.C., 2017. Scaled distribution mapping: a bias correction method that preserves raw climate model projected changes. Hydrol. Earth System Sci. 21, 2649–2666. https://doi.org/10.5194/hess-21-2649-2017.
Teutschbein, C., Seibert, J., 2010. Regional climate models for hydrological impact studies at the catchment scale: a review of recent modeling strategies. Geogr. Compass 4, 834–860. https://doi.org/10.1111/j.1749-8198.2010.00357.x.
Troin, M., Poulin, A., Baraer, M., Brissette, F., 2016. Comparing snow models under current and future climates: Uncertainties and implications for hydrological impact studies. J. Hydrol. 540, 588–602. https://doi.org/10.1016/j.jhydrol.2016.06.055.
Vidal, J.P., Hingray, B., Magand, C., Sauquet, E., Ducharne, A., 2016. Hierarchy of climate and hydrological uncertainties in transient low-flow projections. Hydrol. Earth System Sci. 20, 3651–3672. https://doi.org/10.5194/hess-20-3651-2016.
Wenger, S.J., Luce, C.H., Hamlet, A.F., Isaak, D.J., Neville, H.M., 2010. Macroscale hydrologic modeling of ecologically relevant flow metrics. Water Resources Research 46 (9), W09513. https://doi.org/10.1029/2009WR008839.
Willkofer, F., Schmid, F.-J., Komischke, H., Korck, J., Braun, M., Ludwig, R., 2018. The impact of bias correcting regional climate model results on hydrological indicators for Bavarian catchments. J. Hydrol. Reg. Stud. 19, 25–41. https://doi.org/10.1016/j.ejrh.2018.06.010.
Wong, W.K., Haddeland, I., Lawrence, D., Beldring, S. Gridded 1×1 km climate and hydrological projectionsfor Norway. Report 59, 2016. Norwegian Water Resources and Energy Directorate. https://publikasjoner.nve.no/rapport/2016/rapport2016_59.pdf.
Zhang, Y., Shao, Q., Zhang, S., Zhai, X., She, D., 2016. Multi-metric calibration of hydrological model to capture overall flow regimes. J. Hydrol. 539, 525–538. https://doi.org/10.1016/j.jhydrol.2016.05.053.

5 Summary and conclusions

Climate change is an increasing challenge at the current time. The hydrological community also sees an urgent need to conduct further research in this area (*Blöschl et al.*, 2019). The Austrian Raab catchment in the southern alpine forelands is an interesting study area in this context, since the region has a good data availability and is strongly influenced by climate change and extreme events (*Kabas et al.*, 2011; *Schroeer and Kirchengast*, 2018).

In this thesis, we performed three hydrological modeling studies to analyze aspects of sensitivity and uncertainty from different angles. First, we examined the effects of low flow and changes in precipitation, temperature, land use, and irrigation. Second, we analyzed the precipitation station density and interpolation schemes in the context of extreme precipitation events. And, third, we investigated the usability of high-resolution climate data sets, ÖKS15 in hydrological impact studies.

In Section 5.1, the main results of all three research articles are summarized in tabular form and briefly for each article. Section 5.2 closes the thesis by providing a synthesis of the conclusions and prospects.

5.1 Main results of the three research articles

Table 5.1 summarizes main results of each of the three articles in a convenient overview. This is followed by short subsections providing summaries and conclusions specifically for each article.

Table 5.1: Summarized main results of the three research articles.

Publication	**Main results**
Research Article 1 *Hohmann et al.* (2018)	• climate drivers (temperature and precipitation) dominate summer-time runoff changes • land use and irrigation have a smaller impact than climate drivers, but are still important since they may compensate for or amplify changes • the southeastern alpine forelands are vulnerable to summer dryness under climate change
Research Article 2 *Hohmann et al.* (2021)	• modeling performance improved by increasing station density up to a certain resolution (mean nearest-neighbor distance of about 6 km/2.5 km for long-/short-duration heavy rainfall events • such a sufficient station density is often not available in small catchments (10–30 km^2) • sufficient station density clearly depends on catchment, event pattern, and station distribution • given a dense network (< 1.7 km spacing), any reasonable interpolation scheme is suitable • station density is generally more important than the interpolation scheme
Research Article 3 *Peßenteiner et al.* (2021)	• generally the ÖKS15 high-resolution climate data sets are suitable for hydrological applications and reproduce hydro-climatic conditions effectively • hydrologically relevant limitations exist • differences in timing, magnitude, and location of patterns lead to deviations in the annual water cycle • bias-corrected data still contain some biases due to imperfect reference data and correction methods

Summary and conclusions for Research Article 1

In Research Article 1 by *Hohmann et al.* (2018), we studied how summer runoff and evapotranspiration respond to moderate and strong changes in climate (temperature +2 K/+4 K and precipitation −15%/−30%), land use (more dry and sealed areas), and water management (use of irrigation). The main findings are: (1) Climate change and especially precipitation changes dominate the summer time runoff; (2) land use and irrigation changes have a smaller influence than the climate change drivers, but are still relevant, especially in distinctly dry or wet years; (3) the strongest averaged runoff decrease of nearly 80% was calculated with all changes together; and (4) land use changes might help to reduce the overall tendency toward summer low flow. The actual evapotranspiration shows less distinct responses to changes as compared to the river runoff. Here, the dominant driver is the temperature change, but also water availability, a factor which is not negligible in a drought vulnerable region. The irrigation helps to increase the actual evapotranspiration when water availability is the limiting factor. The study underlined the vulnerability of the southern alpine foreland to summer dryness under climate change conditions.

Since Research Article 1 was an initial study, further research (e.g., with a more detailed scenario-based approach) is needed to further investigate the drought risk in the southern alpine forelands. This study also supported the use of the approach to include non-climatic aspects in climate change studies due to the interaction and possible compensation or amplification effects of other environmental changes. Results clearly show that the non-climatic drivers are not negligible and should also be considered in climate change studies, as well as in other regions worldwide. The study also reveals the importance of this type of initial studies, as they can help us to get an initial overview of important aspects that deserve further and more detailed analysis.

Summary and conclusions for Research Article 2

Precipitation is the most important input in hydrological models and, as seen above, is the dominant driver of runoff response under climate change. Hence, in Research Article 2 by *Hohmann et al.* (2021), we additionally studied the response of precipitation station density and interpolation schemes to runoff. Here, we focused on extreme precipitation events and small catchments to analyze how

many stations are needed to reliably model runoff for such events. We analyzed three short-duration, convective-type events and three long-duration, stratiform-types events in the lower Raab catchment and its subcatchments with basin areas of 10 km^2 to 30 km^2. We performed model simulations with a set of 16 subnetworks with varying station density and two interpolation schemes, respectively.

The results show that a sufficient station density is clearly dependent on the catchment, the event pattern, and the station distribution. Generally, the model performance improved by increasing station density until a sufficient one with a mean nearest-neighbor distance of around 6 km for long-duration events and around 2.5 km for short-duration events, respectively, was found. Such a threshold is not always seen in small subcatchments (of order 10 km^2 size). The station density has a stronger effect on the runoff than the interpolation scheme. If a dense station network (< 1.7 km nearest-neighbor distance) is present, the choice of interpolation scheme does not affect the runoff results significantly (e.g., any reasonable scheme may be suitable).

The findings underline the strong influence that precipitation station density has on simulated runoff. Since most catchment areas worldwide do not have a suitably dense station network, this aspect has to be kept in mind, and the ground-based station data may best be supplemented with other data sources. Here, calibrated high-quality radars might be a good option. When only a sparse network is available, the choice of interpolation scheme plays an important role and needs to be done with due care. Since it is not always possible to reduce this aspect of uncertainty arising from the meteorological input in hydrological modeling, awareness of the related limitations is important, especially when using such modeling for climate change impact studies.

Summary and conclusions for Research Article 3

In 2016, an ensemble of high-resolution climate data sets was released for Austria, ÖKS15 (*Chimani et al.*, 2016). The usability of these ÖKS15 data sets for hydrological applications is discussed in Research Article 3 by *Peßenteiner et al.* (2021). We analyzed different sources of uncertainty and spatial scales, as well as the impact on hydrological indicators. The hydro-meteorological characteristics of the data sets for the recent climate period (1961–2005), as well as the data used for its bias correction and downscaling of the GCMs-RCMs, were examined. Different spatial and temporal scales were analyzed, and the data sets were also compared to

raw EURO-CORDEX model data sets. The focus of the examination was directed toward the meteorological parameters of precipitation and temperature as input for a hydrological model, and their influence on simulated river runoff was examined. Two catchments, an alpine (Wölzerbach) and a prealpine catchment (Raab) were studied.

The results suggest that the ÖKS15 data sets generally reproduce hydro-climatic conditions accurately under the recent climate conditions. However, hydrological relevant limitations exist if the ÖKS15 data sets are used. Still, by using bias-corrected data, some differences occur in the timing, magnitude, and location of patterns, which lead to deviations in the hydrological (runoff) signatures at different scales. In general, the bias correction provides added value to the hydrological use of the ÖKS15 data sets compared to the uncorrected ones, especially in the complex terrain of the alpine Wölzerbach catchment. Regarding low flow in the prealpine Raab catchment, the raw uncorrected models are an option as well, since they performed reasonably well without bias correction in this specific case. Snow related processes, which are important in the alpine catchment, must be considered with caution, due to the use of the univariate ÖKS15 bias correction method, which cannot be used to consider the combined effects of temperature and precipitation. Some remaining biases, despite the bias-correction due to imperfect reference data and correction methods, were mentioned.

Overall, the study results show that the high-resolution climate data sets ÖKS15 may be used for hydrological impact studies. However, we recommend checking a sufficient runoff gauging history for the catchment of interest, as this allows the users to become aware of any remaining biases. Generally this approach is suitable for use by members of the interdisciplinary community and can be applied to support further developments in climate-hydrological analysis in Austria.

5.2 Synthesis, conclusions, and prospects

As seen in this thesis and as has been strongly underlined by the recently published Sixth Assessment Report of the IPCC on the physical science basis of climate change (*IPCC*, 2021), climate change is a very important topic. However, a number of uncertainties arise when predicting or projecting future changes. Under climate change conditions, the extreme events will occur more frequently and more intensely. Therefore, extreme events like heavy precipitation are important to

study to determine their uncertainty and sensitivity to change. Furthermore, when dealing with climate change, the non-climatic drivers are also not negligible but rather important factor as well.

Precipitation is the most important driver for runoff and, as such, it is strongly influenced by climate change. This importance is clearly visible and is underpinned in the findings reported in all three research articles in this thesis. Regarding precipitation, the uncertainty in future projections is especially high, and the past trends are not very distinct. However, heavy precipitation events can trigger severe damages such as flooding and landslides, indicating the importance of the knowledge about possible uncertainties. In this context, uncertainties related to future projections are a particularly crucial topic, as mentioned in Research Article 1. The uncertainty with regard to station data (including its own measuring uncertainty) and the spatially distributed rainfall has to be addressed as well, and this was described in Research Articles 2 and 3. In addition, the uncertainty arising from the use of gridded data sets based on (bias-corrected) regional climate models has to be evaluated, which we did as part of the study reported in Research Article 3. Furthermore, the relevance of non-climatic drivers, like land use changes, and water management options, was investigated as part of the study described in Research Article 1.

Extreme precipitation should be studied in combination with runoff modeling, since the hazard is mostly not the heavy precipitation event itself, but rather its effects, such as floods or landslides. In particular, not all heavy precipitation events result in the same hazards and many other factors like pre-event soil moisture, exposure, or groundwater level play important roles. These aspects underscore the event dependency of the hydrological impacts. For example, the study results described in Research Article 2 highlighted the strong event dependency of the precipitation station density and the interpolation scheme. Analyzing more events may help to see the overall tendency more clearly, but each individual event is somewhat unique, especially for extreme events, and may be quite different from others in terms of the hydrological impacts.

Looking beyond the southeastern alpine foreland study region, precipitation is an important aspect worldwide. Especially convective events, which are common in the study region, strongly affect the whole mid-latitude land regions. While the uncertainty and sensitivity analyses performed with the WegenerNet data helped us substantially to study such precipitation events, the findings also can be

helpful for less-instrumented regions. The vulnerability to summer dryness under climate change conditions, described in Research Article 1, applies to the whole southeastern alpine foreland due to its geographical position between the Alps, the Mediterranean, and the eastern European lowlands (i.e., in Hungary). Hungary is already now being affected by the hot summer dryness seen in the Pannonian steppe/Puszta (*Gavrilov et al.*, 2020).

High-resolution national climate data sets, like the Austrian ÖKS15 data sets, are already set up for other countries like UK, Norway, or Switzerland (*Wong et al.*, 2016; *Rössler et al.*, 2019; *Kay et al.*, 2020). In the future, other countries might also prepare such data sets for their focal regions. In this respect, Research Article 3 helps to be aware of potential pitfalls and uncertainty resulting from the hydrological use of such data sets. These results indicate the important efforts to combine climate change and hydrological research. In fact, all three research articles presented in this thesis include approaches that combine these two communities. First, Research Article 1 describes a study on the climate, land use, and water management change impacts on runoff. Second, Research Article 2 reports the outcome of an uncertainty and sensitivity analysis of runoff in response to extreme precipitation. And, third, Research Article 3 includes an assessment of the value of high-resolution climate data sets for hydrological impact studies.

Considering further research, the Austrian ÖKS15 high-resolution climate data sets or similar data sets might be used in other regions, either alone or in combination with non-climatic drivers like land use and water management changes for driving hydrological models in the context of climate change impact studies. With such approaches, possible future scenarios can be analyzed, and the effects on the hydrological cycle and related extremes and impacts can be studied. This will also help to adjust future climate change adaptation strategies and to be better prepared for possible future changes in runoff and other water balance components.

Regarding observations, deepening the understanding of the extreme precipitation events and including high-resolution radar data sets and high-resolution runoff data of small subcatchments would be of substantial benefit in further studies. Options to conduct further crucial climate-hydrology studies related to small vulnerable catchments are continually opening up. The increasing climate change is creating an increasingly more pressing need in many land regions worldwide. It is hoped that the results presented in this thesis can serve as an important and valuable scientific basis for such valuable future studies.

List of Figures

3.1 Overview maps of the study areas, Raab catchment and Wölzerbach catchment. 20

3.2 Input data maps for the Raab catchment with the coarse- and the fine-resolution grids. 28

4.1 Figures Research Article 1, *Hohmann et al.* (2018)
Fig 1: Study area and temperature and precipitation trend in south-eastern Austria.
Fig 2: WaSiM model structure.
Fig 3: Runoff time series at station Neumarkt for specific dry and wet years.
Fig 4: Average summertime runoff changes for the stations Feldbach and Neumarkt.
Fig 5: Severity and direction of average summertime changes of the input variables and response variables. 43

4.2 Figures Research Article 2, *Hohmann et al.* (2021)
Fig 1: Map of the Raab catchment, station subnetworks, and subcatchments.
Fig 2: WaSiM model setup, including modules and input data sets.
Fig 3: Overview of the study design.
Fig 4: Evolution of precipitation time series and spatial distribution.
Fig 5: Precipitation maps using the WaSiM interpolation schemes and the corresponding time series of runoff and precipitation.
Fig 6: Precipitation and associated runoff time series for a short- and a long-duration event.
Fig 7: Peak flow deviation from the reference case as a grid-cell plot.
Fig 8: Peak flow deviation between the reference case and the mean across all (sub)catchments for all subnetwork cases. 69

4.3 Figures Research Article 3, *Peßenteiner et al.* (2021)
Fig 1: Location of study areas in Styria, Austria.
Fig 2: Methodological approach applied within this study.
Fig 3: Modeled versus observed distributions (CDFs) of temperature for historic and future periods.
Fig 4: Annual cycle of catchment average monthly precipitation.
Fig 5: Annual cycle of percentual differences of precipitation between the GRID reference data set and the ÖKS15 models.
Fig 6: Flow duration curves of WaSiM-simulated discharges driven either with STATION, GRID or ÖKS15 data.
Fig 7: Flow regimes simulated by WaSiM in the period 1971–2000.
Fig 8: Overview of uncertainties for different meteorological and hydrological indicators. 99

List of Tables

2.1 Comparison of the scenario-neutral and the scenario-based approaches. 9

3.1 Hydro-meteorological data sets used in this thesis. 25

3.2 Elevation model, land use, and soil data, which are used in this thesis for process-based hydrological modeling. 27

3.3 WaSiM setups used, with input and modules for the two setups in the Raab catchment and for the setup in the Wölzerbach catchment. 32

3.4 Calibration parameter of WaSiM used in this thesis. 34

3.5 Model efficiency metrics used in this thesis. 35

3.6 Summarized study design characteristics of the three research articles, including the overall research questions of this thesis. 40

4.1 Tables Research Article 1 *Hohmann et al.* (2018)
Tab 1: Environmental change cases simulated and investigated in the low flow sensitivity analysis. 43

4.2 Tables Research Article 2, *Hohmann et al.* (2021)
Tab 1: Characteristics of the study catchment area and representative subcatchment areas.
Tab 2: Catchment attributes and hydrometeorological data used for hydrological modeling in this study.
Tab 3: Precipitation stations of the operational, the primary, the complementary, and the reference subnetwork cases.
Tab 4: Precipitation events selected for this study and associated key characteristics.
Tab 5: Calculated differences in the timing of the runoff peak. . . . 69

4.3 Tables Research Article 3, *Peßenteiner et al.* (2021)
Tab 1: Meteorological and hydrological data used in the study.
Tab 2: Data sets, indicators, and variables used for evaluating meteorological and hydrological variables.
Tab 3: List of hydro-meteorological indicators used for comparing and evaluating different input data sets.
Tab 4: Catchment-wide seasonal mean temperature differences between GRID and STATION, ÖKS15 and RAW data sets, respectively.
Tab 5: Performance of the hydrological model WaSiM in the Wölzerbach and the Raab catchments.
Tab 6: Discharge indicators for the gauges Niederwölz (Wölzerbach) and Feldbach (Raab). 99

5.1 Summarized main results of the three research articles. 126

References

AghaKouchak, A., A. Mirchi, K. Madani, G. Di Baldassarre, A. Nazemi, A. Alborzi, H. Anjileli, M. Azarderakhsh, F. Chiang, E. Hassanzadeh, L. S. Huning, I. Mallakpour, A. Martinez, O. Mazdiyasni, H. Moftakhari, H. Norouzi, M. Sadegh, D. Sadeqi, A. F. Van Loon, and N. Wanders (2021), Anthropogenic drought: Definition, challenges, and opportunities, *Reviews of Geophysics*, *59*, e2019RG000683, doi:10.1029/2019rg000683.

Alaoui, A., E. Willimann, K. Jasper, G. Felder, F. Herger, J. Magnusson, and R. Weingartner (2014), Modelling the effects of land use and climate changes on hydrology in the Ursern Valley, Switzerland, *Hydrological Processes*, *28*, 3602–3614, doi:10.1002/hyp.9895.

Andréassian, V., C. Perrin, C. Michel, I. Usart-Sanchez, and J. Lavabre (2001), Impact of imperfect rainfall knowledge on the efficiency and the parameters of watershed models, *Journal of Hydrology*, *250*, 206–223, doi:10.1016/S0022-1694(01)00437-1.

APCC (2014), *Österreichischer Sachstandsbericht Klimawandel 2014 (AAR14). Austrian Panel on Climate Change (APCC)*, 1096 pp., Verlag der Österreichischen Akademie der Wissenschaften, Vienna, Austria.

Ashraf, S., A. AghaKouchak, A. Nazemi, A. Mirchi, M. Sadegh, H. R. Moftakhari, E. Hassanzadeh, C. Y. Miao, K. Madani, M. Mousavi Baygi, H. Anjileli, D. R. Arab, H. Norouzi, O. Mazdiyasni, M. Azarderakhsh, A. Alborzi, M. J. Tourian, A. Mehran, A. Farahmand, and I. Mallakpour (2019), Compounding effects of human activities and climatic changes on surface water availability in Iran, *Climatic Change*, *152*, 379–391, doi:10.1007/s10584-018-2336-6.

Avila, F. B., S. Dong, K. P. Menang, J. Rajczak, M. Renom, M. G. Donat, and L. V. Alexander (2015), Systematic investigation of gridding-related scaling effects on annual statistics of daily temperature and precipitation maxima: A

case study for south-east Australia, *Weather and Climate Extremes*, *9*, 6–16, doi:10.1016/j.wace.2015.06.003.

Balin, D., H. Lee, and M. Rode (2010), Is point uncertain rainfall likely to have a great impact on distributed complex hydrological modeling?, *Water Resources Research*, *46*, W11520, doi:10.1029/2009WR007848.

Bárdossy, A., and T. Das (2008), Influence of rainfall observation network on model calibration and application, *Hydrology and Earth System Sciences*, *12*, 77–89, doi:10.5194/hess-12-77-2008.

Beevers, L., L. Collet, G. Aitken, C. Maravat, and A. Visser (2020), The influence of climate model uncertainty on fluvial flood hazard estimation, *Natural Hazards*, *104*, 2489–2510, doi:10.1007/s11069-020-04282-4.

Beven, K. (2011), I believe in climate change but how precautionary do we need to be in planning for the future?, *Hydrological Processes*, *25*, 1517–1520, doi:10.1002/hyp.7939.

Blöschl, G., and A. Montanari (2010), Climate change impacts - throwing the dice?, *Hydrological Processes*, *24*, 374–381, doi:10.1002/hyp.7574.

Blöschl, G., M. F. Bierkens, A. Chambel, C. Cudennec, G. Destouni, A. Fiori, J. W. Kirchner, J. J. McDonnell, H. H. Savenije, M. Sivapalan, C. Stumpp, E. Toth, E. Volpi, G. Carr, C. Lupton, J. Salinas, B. Széles, A. Viglione, H. Aksoy, S. T. Allen, A. Amin, V. Andréassian, B. Arheimer, S. K. Aryal, V. Baker, E. Bardsley, M. H. Barendrecht, A. Bartosova, O. Batelaan, W. R. Berghuijs, K. Beven, T. Blume, T. Bogaard, P. Borges de Amorim, M. E. Böttcher, G. Boulet, K. Breinl, M. Brilly, L. Brocca, W. Buytaert, A. Castellarin, A. Castelletti, X. Chen, Y. Chen, Y. Chen, P. Chifflard, P. Claps, M. P. Clark, A. L. Collins, B. Croke, A. Dathe, P. C. David, F. P. J. de Barros, G. de Rooij, G. Di Baldassarre, J. M. Driscoll, D. Duethmann, R. Dwivedi, E. Eris, W. H. Farmer, J. Feiccabrino, G. Ferguson, E. Ferrari, S. Ferraris, B. Fersch, D. Finger, L. Foglia, K. Fowler, B. Gartsman, S. Gascoin, E. Gaume, A. Gelfan, J. Geris, S. Gharari, T. Gleeson, M. Glendell, A. Gonzalez Bevacqua, M. P. González-Dugo, S. Grimaldi, A. B. Gupta, B. Guse, D. Han, D. Hannah, A. Harpold, S. Haun, K. Heal, K. Helfricht, M. Herrnegger, M. Hipsey, H. Hlaváčiková, C. Hohmann, L. Holko, C. Hopkinson, M. Hrachowitz, T. H. Illangasekare, A. Inam, C. Innocente, E. Istanbulluoglu, B. Jarihani, Z. Kalantari, A. Kalvans, S. Khanal, S. Khatami, J. Kiesel, M. Kirkby, W. Knoben,

K. Kochanek, S. Kohnová, A. Kolechkina, S. Krause, D. Kreamer, H. Kreibich, H. Kunstmann, H. Lange, M. L. R. Liberato, E. Lindquist, T. Link, J. Liu, D. P. Loucks, C. Luce, G. Mahé, O. Makarieva, J. Malard, S. Mashtayeva, S. Maskey, J. Mas-Pla, M. Mavrova-Guirguinova, M. Mazzoleni, S. Mernild, B. D. Misstear, A. Montanari, H. Müller-Thomy, A. Nabizadeh, F. Nardi, C. Neale, N. Nesterova, B. Nurtaev, V. O. Odongo, S. Panda, S. Pande, Z. Pang, G. Papacharalampous, C. Perrin, L. Pfister, R. Pimentel, M. J. Polo, D. Post, C. Prieto Sierra, M.-H. Ramos, M. Renner, J. E. Reynolds, E. Ridolfi, R. Rigon, M. Riva, D. E. Robertson, R. Rosso, T. Roy, J. H. Sá, G. Salvadori, M. Sandells, B. Schaefli, A. Schumann, A. Scolobig, J. Seibert, E. Servat, M. Shafiei, A. Sharma, M. Sidibe, R. C. Sidle, T. Skaugen, H. Smith, S. M. Spiessl, L. Stein, I. Steinsland, U. Strasser, B. Su, J. Szolgay, D. Tarboton, F. Tauro, G. Thirel, F. Tian, R. Tong, K. Tussupova, H. Tyralis, R. Uijlenhoet, R. van Beek, R. J. van der Ent, M. van der Ploeg, A. F. Van Loon, I. van Meerveld, R. van Nooijen, P. R. van Oel, J.-P. Vidal, J. von Freyberg, S. Vorogushyn, P. Wachniew, A. J. Wade, P. Ward, I. K. Westerberg, C. White, E. F. Wood, R. Woods, Z. Xu, K. K. Yilmaz, and Y. Zhang (2019), Twenty-three unsolved problems in hydrology (UPH) - a community perspective, *Hydrological Sciences Journal*, *64*, 1141–1158, doi:10.1080/02626667.2019.1620507.

Bosshard, T., M. Carambia, K. Goergen, S. Kotlarski, P. Krahe, M. Zappa, and C. Schär (2013), Quantifying uncertainty sources in an ensemble of hydrological climate-impact projections, *Water Resources Research*, *49*, 1523–1536, doi:10.1029/2011WR011533.

Breinl, K., H. Müller-Thomy, and G. Blöschl (2020), Space-time characteristics of areal reduction factors and rainfall processes, *Journal of Hydrometeorology*, *21*, 671–689, doi:10.1175/JHM-D-19-0228.1.

Bronstert, A., V. Kolokotronis, D. Schwandt, and H. Straub (2007), Comparison and evaluation of regional climate scenarios for hydrological impact analysis: General scheme and application example, *International Journal of Climatology*, *27*, 1579–1594, doi:10.1002/joc.1621.

Brown, C., and R. L. Wilby (2012), An alternate approach to assessing climate risks, *Eos - Transactions American Geophysical Union*, *93*, 401–412, doi:10.1029/2012EO410001.

Brown, C., W. Werick, W. Leger, and D. Fay (2011), A decision-analytic approach

to managing climate risks: Application to the Upper Great Lakes, *Journal of the American Water Resources Association*, *47*, 524–534, doi:10.1111/j.1752-1688.2011.00552.x.

Bürger, G., J. Schulla, and A. T. Werner (2011), Estimates of future flow, including extremes, of the Columbia River headwaters, *Water Resources Research*, *47*, W10520, doi:10.1029/2010WR009716.

Chen, C., J. O. Haerter, S. Hagemann, and C. Piani (2011), On the contribution of statistical bias correction to the uncertainty in the projected hydrological cycle, *Geophysical Research Letters*, *38*, L20403, doi:10.1029/2011GL049318.

Chen, H., J. Sun, X. Chen, and W. Zhou (2012), CGCM projections of heavy rainfall events in China, *International Journal of Climatology*, *32*, 441–450, doi:10.1002/joc.2278.

Chimani, B., G. Heinrich, M. Hofstätter, M. Kerschbaumer, S. Kienberger, A. Leuprecht, A. Lexer, S. Peßenteiner, M. Poetsch, M. Salzmann, R. Spiekermann, M. Switanek, and H. Truhetz (2016), *ÖKS15 – Klimaszenarien für Österreich. Daten, Methoden und Klimaanalyse. (Project report in German)*, 353 pp., ZAMG, Vienna, Austria, https://hdl. handle.net/20.500.11756/06edd0c9.

Cook, B. I., J. S. Mankin, and K. J. Anchukaitis (2018), Climate change and drought: From past to future, *Current Climate Change Reports*, *4*, 164–179, doi:10.1007/s40641-018-0093-2.

Cullmann, J., V. Mishra, and R. Peters (2006), Flow analysis with WaSiM-ETH – model parameter sensitivity at different scales, *Advances in Geosciences*, *9*, 73–77, doi:10.5194/adgeo-9-73-2006.

Cullmann, J., T. Krausse, and P. Saile (2011), Parameterising hydrological models – Comparing optimisation and robust parameter estimation, *Journal of Hydrology*, *404*, 323–331, doi:10.1016/j.jhydrol.2011.05.003.

Dirks, K. N., J. E. Hay, C. D. Stow, and D. Harris (1998), High-resolution studies of rainfall on Norfolk Island Part II: Interpolation of rainfall data, *Journal of Hydrology*, *208*, 187–193, doi:10.1016/S0022-1694(98)00155-3.

Dong, X., C. M. Dohmen-Janssen, and M. J. Booij (2005), Appropriate spatial sampling of rainfall or flow simulation, *Hydrological Sciences Journal*, *50*, 279–298, doi:10.1623/hysj.50.2.279.61801.

Duan, Q., S. Sorooshian, and V. Gupta (1992), Effective and efficient global optimization for conceptual rainfall-runoff models, *Water Resources Research*, *28*, 1015–1031, doi:10.1029/91WR02985.

Duan, Q., S. Sorooshian, and V. K. Gupta (1994), Optimal use of the SCE-UA global optimization method for calibrating watershed models, *Journal of Hydrology*, *158*, 265–284, doi:10.1016/0022-1694(94)90057-4.

Elfert, S., and H. Bormann (2010), Simulated impact of past and possible future land use changes on the hydrological response of the Northern German lowland 'Hunte' catchment, *Journal of Hydrology*, *383*, 245–255, doi:10.1016/j.jhydrol.2009.12.040.

Fischer, E. M., and R. Knutti (2016), Observed heavy precipitation increase confirms theory and early models, *Nature Climate Change*, *6*, 986–991, doi:10.1038/nclimate3110.

Fuchsberger, J., G. Kirchengast, C. Bichler, A. Leuprecht, and T. Kabas (2021), WegenerNet climate station network Level 2 data version 7.1 (2007 - 2020), Wegener Center for Climate and Global Change, University of Graz, Austria, doi:10.25364/WEGC/WPS7.1:2021.1.

Gädeke, A., H. Hölzel, H. Koch, I. Pohle, and U. Grünewald (2014), Analysis of uncertainties in the hydrological response of a model-based climate change impact assessment in a subcatchment of the Spree River, Germany, *Hydrological Processes*, *28*, 3978–3998, doi:10.1002/hyp.9933.

Gavrilov, M. B., M. G. Radaković, G. Sipos, G. Mezősi, G. Gavrilov, T. Lukić, B. Basarin, B. Benyhe, K. Fiala, P. Kozák, Z. M. Perić, D. Govedarica, Y. Song, and S. B. Marković (2020), Aridity in the central and southern Pannonian basin, *Atmosphere*, *11*, 1269, doi:10.3390/atmos11121269.

Gervais, M., L. B. Tremblay, J. R. Gyakum, and E. Atallah (2014), Representing extremes in a daily gridded precipitation analysis over the United States: Impacts of station density, resolution, and gridding methods, *Journal of Climate*, *27*, 5201–5218, doi:10.1175/JCLI-D-13-00319.1.

Gharun, M., R. W. Vervoort, T. L. Turnbull, and M. A. Adams (2014), A test of how coupling of vegetation to the atmosphere and climate spatial variation affects water yield modelling in mountainous catchments, *Journal of Hydrology*, *514*, 202–213, doi:10.1016/j.jhydrol.2014.04.037.

Gilewski, P., and M. Nawalany (2018), Inter-comparison of rain-gauge, radar, and satellite (IMERG GPM) precipitation estimates performance for rainfall-runoff modeling in a mountainous catchment in Poland, *Water*, *10*, 1665, doi: 10.3390/w10111665.

Goodrich, D. C., J.-M. Faurès, D. A. Woolhiser, L. J. Lane, and S. Sorooshian (1995), Measurement and analysis of small-scale convective storm rainfall variability, *Journal of Hydrology*, *173*, 283–308, doi:10.1016/0022-1694(95)02703-R.

Goovaerts, P. (2000), Geostatistical approaches for incorporating elevation into the spatial interpolation of rainfall, *Journal of Hydrology*, *228*, 113–129, doi: 10.1016/S0022-1694(00)00144-X.

Grigoryan, G. V., M. C. Casper, J. Gauer, A. C. Vasconcelos, and P. P. Reiter (2010), Impact of climate change on water balance of forest sites in Rhineland-Palatinate, Germany, *Advances in Geosciences*, *27*, 37–43, doi:10.5194/adgeo-27-37-2010.

Gupta, H. V., S. Sorooshian, and P. O. Yapo (1999), Status of automatic calibration for hydrologic models: Comparison with multilevel expert calibration, *Journal of Hydrologic Engineering*, *4*, 135–143, doi:10.1061/(ASCE)1084-0699(1999)4:2(135).

Gupta, H. V., H. Kling, K. K. Yilmaz, and G. F. Martinez (2009), Decomposition of the mean squared error and NSE performance criteria: Implications for improving hydrological modelling, *Journal of Hydrology*, *377*, 80–91, doi: 10.1016/j.jhydrol.2009.08.003.

Gupta, S. C., A. C. Kessler, M. K. Brown, and F. Zvomuya (2015), Climate and agricultural land use change impacts on streamflow in the upper midwestern United States, *Water Resources Research*, *51*, 5301–5317, doi: 10.1002/2015WR017323.

Hakala, K., N. Addor, and J. Seibert (2018), Hydrological modeling to evaluate climate model simulations and their bias correction, *Journal of Hydrometeorology*, *19*, 1321–1337, doi:10.1175/JHM-D-17-0189.1.

Hamon, W. R. (1961), Estimating potential evapotranspiration, *Journal of the Hydraulics Division*, *87*, 107–120, doi:10.1061/JYCEAJ.0000599.

Hattermann, F. F., T. Vetter, L. Breuer, B. Su, P. Daggupati, C. Donnelly, B. Fekete, F. Florke, S. N. Gosling, P. Hoffmann, S. Liersch, Y. Masaki, Y. Motovilov, C. Muller, L. Samaniego, T. Stacke, Y. Wada, T. Yang, and V. Krysnaova (2018), Sources of uncertainty in hydrological climate impact assessment: A cross-scale study, *Environmental Research Letters*, *13*, 015006, doi:10.1088/1748-9326/aa9938.

Haude, W. (1955), *Zur Bestimmung der Verdunstung auf möglichst einfache Weise*, vol. 11, Deutscher Wetterdienst, Bad Kissingen, Germany.

Herrera, S., S. Kotlarski, P. M. M. Soares, R. M. Cardoso, A. Jaczewski, J. M. Gutiérrez, and D. Maraun (2018), Uncertainty in gridded precipitation products: Influence of station density, interpolation method and grid resolution, *International Journal of Climatology*, *39*, 3717–3729, doi:10.1002/joc.5878.

Hiebl, J., and C. Frei (2016), Daily temperature grids for Austria since 1961 - concept, creation and applicability, *Theoretical and Applied Climatology*, *124*, 161–178, doi:10.1007/s00704-015-1411-4.

Hofstätter, M., J. Jacobeit, M. Homann, A. Lexer, B. Chimani, A. Philipp, C. Beck, and M. Ganekind (2015), *WETRAX – Weather Patterns, Cyclone Tracks and related Precipitation Extremes. Großflächige Starkniederschläge im Klimawandel in Mitteleuropa. (Projekt report in German)*, 239 pp., Geographica Augustana 19, Augsburg, Germany.

Hohmann, C., G. Kirchengast, and S. Birk (2018), Alpine foreland running drier? Sensitivity of a drought vulnerable catchment to changes in climate, land use, and water management, *Climatic Change*, *147*, 179–193, doi:10.1007/s10584-017-2121-y.

Hohmann, C., G. Kirchengast, O. Sungmin, W. Rieger, and U. Foelsche (2021), Small catchment runoff sensitivity to station density and spatial interpolation: Hydrological modeling of heavy rainfall using a dense rain gauge network, *Water*, *13*, 1381, doi:10.3390/w13101381.

Huang, S., V. Krysanova, and F. Hattermann (2015), Projections of climate change impacts on floods and droughts in Germany using an ensemble of climate change scenarios, *Regional Environmental Change*, *15*, 461–473, doi:10.1007/s10113-014-0606-z.

Huang, Y., A. Bárdossy, and K. Zhang (2019), Sensitivity of hydrological models to temporal and spatial resolutions of rainfall data, *Hydrology and Earth System Sciences*, *23*, 2647–2663, doi:10.5194/hess-23-2647-2019.

IPCC (2021), *Climate change 2021: The physical science basis. Contribution of working group I to the sixth assessment report of the intergovernmental panel on climate change*, Cambridge University Press, (in press), Cambridge, United Kingdom.

Jacob, D., J. Petersen, B. Eggert, A. Alias, O. B. Christensen, L. M. Bouwer, A. Braun, A. Colette, M. Déqué, G. Georgievski, E. Georgopoulou, A. Gobiet, L. Menut, G. Nikulin, A. Haensler, N. Hempelmann, C. Jones, K. Keuler, S. Kovats, N. Kröner, S. Kotlarski, A. Kriegsmann, E. Martin, E. van Meijgaard, C. Moseley, S. Pfeifer, S. Preuschmann, C. Radermacher, K. Radtke, D. Rechid, M. Rounsevell, P. Samuelsson, S. Somot, J. F. Soussana, C. Teichmann, R. Valentini, R. Vautard, B. Weber, and P. Yiou (2014), EURO-CORDEX: New high-resolution climate change projections for European impact research, *Regional Environmental Change*, *14*, 563–578, doi:10.1007/s10113-013-0499-2.

Joseph, J., S. Ghosh, A. Pathak, and A. K. Sahai (2018), Hydrologic impacts of climate change: Comparisons between hydrological parameter uncertainty and climate model uncertainty, *Journal of Hydrology*, *566*, 1–22, doi:10.1016/j.jhydrol.2018.08.080.

Kabas, T., U. Foelsche, and G. Kirchengast (2011), Seasonal and annual trends of temperature and precipitation within 1951/1971-2007 in south-eastern Styria, Austria, *Meteorologische Zeitschrift*, *20*, 277–289, doi:10.1127/0941-2948/2011/0233.

Kay, A. L. (2021), Simulation of river flow in Britain under climate change: Baseline performance and future seasonal changes, *Hydrological Processes*, *35*, e14137, doi:10.1002/hyp.14137.

Kay, A. L., G. Watts, S. C. Wells, and S. Allen (2020), The impact of climate change on U. K. river flows: A preliminary comparison of two generations of probabilistic climate projections, *Hydrological Processes*, *34*, 1081–1088, doi:10.1002/hyp.13644.

Keller, L., O. Rössler, O. Martius, and R. Weingartner (2019), Comparison of

scenario-neutral approaches for estimation of climate change impacts on flood characteristics, *Hydrological Processes*, *33*, 535–550, doi:10.1002/hyp.13341.

Kharin, V. V., F. W. Zwiers, X. Zhang, and G. C. Hegerl (2007), Changes in temperature and precipitation extremes in the IPCC ensemble of global coupled model simulations, *Journal of Climate*, *20*, 1419–1444, doi:10.1175/JCLI4066.1.

Kidd, C., and G. Huffman (2011), Global precipitation measurement, *Meteorological Applications*, *18*, 334–353, doi:10.1002/met.284.

Kim, D., J. A. Chun, and C. M. Aikins (2018), An hourly-scale scenario-neutral flood risk assessment in a mesoscale catchment under climate change, *Hydrological Processes*, *32*, 3416–3430, doi:10.1002/hyp.13273.

Kirchengast, G., T. Kabas, A. Leuprecht, C. Bichler, and H. Truhetz (2014), WegenerNet: A pioneering high-resolution network for monitoring weather and climate, *Bulletin of the American Meteorological Society*, *95*, 227–242, doi:10.1175/BAMS-D-11-00161.1.

Kirstetter, P.-E., Y. Hong, J. J. Gourley, S. Chen, Z. Flamig, J. Zhang, M. Schwaller, W. Petersen, and E. Amitai (2012), Toward a framework for systematic error modeling of spaceborne precipitation radar with NOAA/NSSL ground radar-based National Mosaic QPE, *Journal of Hydrometeorology*, *13*, 1285–1300, doi:10.1175/JHM-D-11-0139.1.

Klebinder, K., B. Sotier, V. Lechner, and P. Strauss (2017), *Hydrologische und hydropedologische Kenndaten Raabgebiet und Region Südoststeiermark (Project report in German)*, 30 pp., Department of Natural Hazards; Austrian Research Center for Forests (BFW), Innsbruck; Austria.

Kleinn, J., C. Frei, J. Gurtz, D. Lüthi, P. L. Vidale, and C. Schär (2005), Hydrologic simulations in the Rhine basin driven by a regional climate model, *Journal of Geophysical Research: Atmospheres*, *110*, D04102, doi:10.1029/2004JD005143.

Knoben, W. J., J. E. Freer, and R. A. Woods (2019), Technical note: Inherent benchmark or not? Comparing Nash-Sutcliffe and Kling-Gupta efficiency scores, *Hydrology and Earth System Sciences*, *23*, 4323–4331, doi:10.5194/hess-23-4323-2019.

Knutti, R., and J. Sedláček (2013), Robustness and uncertainties in the new CMIP5 climate model projections, *Nature Climate Change*, *3*, 369–373, doi: 10.1038/nclimate1716.

Kobold, M., and M. Brilly (2006), The use of HBV model for flash flood forecasting, *Natural Hazards and Earth System Science*, *6*, 407–417, doi:10.5194/nhess-6-407-2006.

Korck, J., J. Danneberg, and W. Willems (2012), Impacts of climate change on the water regime of the Inn River basin - extracting adaptation-relevant information from climate model ensembles and impact modelling, *Advances in Geosciences*, *32*, 99–107, doi:10.5194/adgeo-32-99-2012.

Kotlarski, S., P. Szabó, S. Herrera, O. Räty, K. Keuler, P. M. Soares, R. M. Cardoso, T. Bosshard, C. Pagé, F. Boberg, J. M. Gutiérrez, F. A. Isotta, A. Jaczewski, F. Kreienkamp, M. A. Liniger, C. Lussana, and K. Pianko-Kluczyńska (2017), Observational uncertainty and regional climate model evaluation: A pan-European perspective, *International Journal of Climatology*, *39*, 3730–3749, doi:10.1002/joc.5249.

Krammer, C., K. Klebinder, A. Eder, B. Sotier, P. Strauss, and T. Bauer (2016), HYDROBOD: Obtaining a GIS-based hydrological soil database and a runoff coefficient calculator for Lower Austria, *Forum geografic*, *XV*, 100–104, doi: 10.5775/fg.2016.123.s.

Kunstmann, H., and C. Stadler (2005), High resolution distributed atmospheric-hydrological modelling for Alpine catchments, *Journal of Hydrology*, *314*, 105–124, doi:10.1016/j.jhydrol.2005.03.033.

Kunstmann, H., J. Krause, and S. Mayr (2006), Inverse distributed hydrological modelling of Alpine catchments, *Hydrology and Earth System Sciences*, *10*, 395–412, doi:10.5194/hess-10-395-2006.

Laaha, G., J. Parajka, A. Viglione, D. Koffler, K. Haslinger, W. Schöner, J. Zehetgruber, and G. Blöschl (2016), A three-pillar approach to assessing climate impacts on low flows, *Hydrology and Earth System Sciences*, *20*, 3967–3985, doi:10.5194/hess-20-3967-2016.

Lasser, M., S. O, and U. Foelsche (2019), Evaluation of GPM-DPR precipitation estimates with WegenerNet gauge data, *Atmospheric Measurement Techniques*, *12*, 5055–5070, doi:10.5194/amt-12-5055-2019.

Liersch, S., J. Tecklenburg, H. Rust, A. Dobler, M. Fischer, T. Kruschke, H. Koch, and F. F. Hattermann (2018), Are we using the right fuel to drive hydrological models? A climate impact study in the Upper Blue Nile, *Hydrology and Earth System Sciences*, *22*, 2163–2185, doi:10.5194/hess-22-2163-2018.

Lopez, M. G., H. Wennerström, L. Nordén, and J. Seibert (2015), Location and density of rain gauges for the estimation of spatial varying precipitation, *Geografiska Annaler: Series A, Physical Geography*, *97*, 167–179, doi:10.1111/geoa.12094.

Ly, S., C. Charles, and A. Degré (2013), Different methods for spatial interpolation of rainfall data for operational hydrology and hydrological modeling at watershed scale. A review, *Biotechnologie, Agronomie, Société et Environnement*, *17*, 392–406.

Mader, H., T. Steidl, and R. Wimmer (1996), *Abflussregime Österrreichischer Fließgewässer. Beitrag zu einer bundesweiten Fließgewässertypologie (Project report in German)*, 192 pp., Umweltbundesamt, Vienna, Austria.

Maier, R., G. Krebs, M. Pichler, D. Muschalla, and G. Gruber (2020), Spatial rainfall variability in urban environments – high-density precipitation measurements on a city-scale, *Water*, *12*, 1157, doi:10.3390/w12041157.

Maraun, D., and M. Widmann (2018), *Statistical downscaling and bias correction for climate research*, Cambridge University Press, Cambridge, United Kingdom, doi:10.1017/9781107588783.

Maraun, D., F. Wetterhall, A. M. Ireson, R. E. Chandler, E. J. Kendon, M. Widmann, S. Brienen, H. W. Rust, T. Sauter, M. Themel, V. K. Venema, K. P. Chun, C. M. Goodess, R. G. Jones, C. Onof, M. Vrac, and I. Thiele-Eich (2010), Precipitation downscaling under climate change: Recent developments to bridge the gap between dynamical models and the end user, *Reviews of Geophysics*, *48*, RG3003, doi:10.1029/2009RG000314.

McMillan, H., T. Krueger, and J. Freer (2012), Benchmarking observational uncertainties for hydrology: Rainfall, river discharge and water quality, *Hydrological Processes*, *26*, 4078–4111, doi:10.1002/hyp.9384.

McMillan, H., A. Montanari, C. Cudennec, H. Savenije, H. Kreibich, T. Krueger, J. Liu, A. Mejia, A. Van Loon, H. Aksoy, G. Di Baldassarre, Y. Huang, D. Mazvimavi, M. Rogger, B. Sivakumar, T. Bibikova, A. Castellarin, Y. Chen, D. Finger,

A. Gelfan, D. M. Hannah, A. Y. Hoekstra, H. Li, S. Maskey, T. Mathevet, A. Mijic, A. P. Acuña, M. J. Polo, V. Rosales, P. Smith, A. Viglione, V. Srinivasan, E. Toth, R. van Nooyen, and J. Xia (2016), Panta Rhei 2013-2015: Global perspectives on hydrology, society and change, *Hydrological Sciences Journal*, *61*, 1174–1191, doi:10.1080/02626667.2016.1159308.

McMillan, H. K. (2012), Effect of spatial variability and seasonality in soil moisture on drainage thresholds and fluxes in a conceptual hydrological model, *Hydrological Processes*, *26*, 2838–2844, doi:10.1002/hyp.9396.

Mendlik, T., and A. Gobiet (2016), Selecting climate simulations for impact studies based on multivariate patterns of climate change, *Climatic Change*, *135*, 381–393, doi:10.1007/s10584-015-1582-0.

Meselhe, E. A., E. H. Habib, O. C. Oche, and S. Gautam (2009), Sensitivity of conceptual and physically based hydrologic models to temporal and spatial rainfall sampling, *Journal of Hydrologic Engineering*, *14*, 711–720, doi:10.1061/(ASCE)1084-0699(2009)14:7(711).

Montanari, A., G. Young, H. H. G. Savenije, D. Hughes, T. Wagener, L. L. Ren, D. Koutsoyiannis, C. Cudennec, E. Toth, S. Grimaldi, G. Blöschl, M. Sivapalan, K. Beven, H. Gupta, M. Hipsey, B. Schaefli, B. Arheimer, E. Boegh, S. J. Schymanski, G. D. Baldassarre, B. Yu, P. Hubert, Y. Huang, A. Schumann, D. A. Post, V. Srinivasan, C. Harman, S. Thompson, M. Rogger, A. Viglione, H. McMillan, G. Characklis, Z. Pang, V. Belyaev, Montanari, G. Di Baldassarre, B. Yu, P. Hubert, Y. Huang, A. Schumann, D. A. Post, V. Srinivasan, C. Harman, S. Thompson, M. Rogger, A. Viglione, H. McMillan, G. Characklis, Z. Pang, and V. Belyaev (2013), "Panta Rhei – Everything Flows": Change in hydrology and society – The IAHS Scientific Decade 2013-2022, *Hydrological Sciences Journal*, *58*, 1256–1275, doi:10.1080/02626667.2013.809088.

Montheith, J. (1975), *Vegetation and the atmosphere*, 298 pp., London, United Kingdom.

Moriasi, D. N., J. G. Arnold, M. W. Van Liew, R. L. Bingner, R. Harmel, and T. L. Veith (2007), Model evaluation guidelines for systematic quantification of accuracy in watershed simulations, *Transactions of the ASABE*, *50*, 885–900, doi:10.13031/2013.23153.

Mote, P., L. Brekke, P. B. Duffy, and E. Maurer (2011), Guidelines for constructing climate scenarios, *Eos, Transactions American Geophysical Union*, *92*, 257–258, doi:10.1029/2011EO310001.

Muerth, M. J., B. Gauvin St-Denis, S. Ricard, J. A. Velázquez, J. Schmid, M. Minville, D. Caya, D. Chaumont, R. Ludwig, and R. Turcotte (2013), On the need for bias correction in regional climate scenarios to assess climate change impacts on river runoff, *Hydrology and Earth System Sciences*, *17*, 1189–1204, doi:10.5194/hess-17-1189-2013.

Nash, J., and J. Sutcliffe (1970), River flow forecasting through conceptual models part I – A discussion of principles, *Journal of Hydrology*, *10*, 282–290, doi: 10.1016/0022-1694(70)90255-6.

Nathan, R. J., T. A. McMahon, M. C. Peel, and A. Horne (2019), Assessing the degree of hydrologic stress due to climate change, *Climatic Change*, *156*, 87–104, doi:10.1007/s10584-019-02497-4.

Nazemi, A. A., and H. S. Wheater (2014), Assessing the vulnerability of water supply to changing streamflow conditions, *Eos, Transactions American Geophysical Union*, *95*, 288–289, doi:10.1002/2014EO320007.

Niehoff, D., U. Fritsch, and A. Bronstert (2002), Land-use impacts on storm-runoff generation: Scenarios of land-use change and simulation of hydrological response in a meso-scale catchment in SW-Germany, *Journal of Hydrology*, *267*, 80–93, doi:10.1016/S0022-1694(02)00142-7.

O, S., and U. Foelsche (2019), Assessment of spatial uncertainty of heavy rainfall at catchment scale using a dense gauge network, *Hydrology and Earth System Sciences*, *23*, 2863–2875, doi:10.5194/hess-23-2863-2019.

O, S., U. Foelsche, G. Kirchengast, J. Fuchsberger, J. Tan, and W. A. Petersen (2017), Evaluation of GPM IMERG Early, Late, and Final rainfall estimates using WegenerNet gauge data in southeastern Austria, *Hydrology and Earth System Sciences*, *21*, 6559–6572, doi:10.5194/hess-21-6559-2017.

Obled, C., J. Wendling, and K. J. Beven (1994), The sensitivity of hydrological models to spatial rainfall patterns: An evaluation using observed data, *Journal of Hydrology*, *159*, 305–333, doi:10.1111/j.1474-919X.1892.tb00320.x.

Olsson, J., B. Arheimer, M. Borris, C. Donnelly, K. Foster, G. Nikulin, M. Persson, A. M. Perttu, C. B. Uvo, M. Viklander, and W. Yang (2016), Hydrological climate change impact assessment at small and large scales: Key messages from recent progress in Sweden, *Climate*, *4*, 39, doi:10.3390/cli4030039.

Oudin, L., V. Andréassian, T. Mathevet, C. Perrin, and C. Michel (2006), Dynamic averaging of rainfall-runoff model simulations from complementary model parameterizations, *Water Resources Research*, *42*, W07410, doi:10.1029/2005WR004636.

Pastén-Zapata, E., J. M. Jones, H. Moggridge, and M. Widmann (2020), Evaluation of the performance of Euro-CORDEX Regional Climate Models for assessing hydrological climate change impacts in Great Britain: A comparison of different spatial resolutions and quantile mapping bias correction methods, *Journal of Hydrology*, *584*, 124653, doi:10.1016/j.jhydrol.2020.124653.

Peßenteiner, S., C. Hohmann, G. Kirchengast, and W. Schöner (2021), High-resolution climate datasets in hydrological impact studies: Assessing their value in alpine and prealpine catchments in southeastern Austria, *Journal of Hydrology: Regional Studies*, *38*, 100962, doi:10.1016/j.ejrh.2021.100962.

Pielke, R. A., and R. L. Wilby (2012), Regional climate downscaling: What's the point?, *Eos, Transactions American Geophysical Union*, *93*, 52–53, doi:10.1029/2012EO050008.

Piringer, M., W. Knauder, I. Anders, K. Andre, W. Zollitsch, S. J. Hörtenhuber, J. Baumgartner, K. Niebuhr, I. Hennig-Pauka, M. Schönhart, and G. Schauberger (2019), Climate change impact on the dispersion of airborne emissions and the resulting separation distances to avoid odour annoyance, *Atmospheric Environment: X*, *2*, 100021, doi:10.1016/j.aeaoa.2019.100021.

Pollock, M. D., G. O'Donnell, P. Quinn, M. Dutton, A. Black, M. E. Wilkinson, M. Colli, M. Stagnaro, L. G. Lanza, E. Lewis, C. G. Kilsby, and P. E. O'Connell (2018), Quantifying and mitigating wind-induced undercatch in rainfall measurements, *Water Resources Research*, *54*, 3863–3875, doi:10.1029/2017WR022421.

Prein, A. F., R. M. Rasmussen, K. Ikeda, C. Liu, M. P. Clark, and G. J. Holland (2016), The future intensification of hourly precipitation extremes, *Nature Climate Change*, *7*, 48–52, doi:10.1038/nclimate3168.

Price, K., S. T. Purucker, S. R. Kraemer, J. E. Babendreier, and C. D. Knightes (2014), Comparison of radar and gauge precipitation data in watershed models across varying spatial and temporal scales, *Hydrological Processes*, *28*, 3505–3520, doi:10.1002/hyp.9890.

Prudhomme, C., R. Wilby, S. Crooks, A. Kay, and N. Reynard (2010), Scenario-neutral approach to climate change impact studies: Application to flood risk, *Journal of Hydrology*, *390*, 198–209, doi:10.1016/j.jhydrol.2010.06.043.

Reifen, C., and R. Toumi (2009), Climate projections: Past performance no guarantee of future skill?, *Geophysical Research Letters*, *36*, L13704, doi:10.1029/2009GL038082.

Reszler, C., M. B. Switanek, and H. Truhetz (2018), Convection-permitting regional climate simulations for representing floods in small-and medium-sized catchments in the Eastern Alps, *Natural Hazards and Earth System Sciences*, *18*, 2653–2674, doi:10.5194/nhess-18-2653-2018.

Rössler, O., B. Diekkrüger, and J. Löffler (2012), Potential drought stress in a Swiss mountain catchment – Ensemble forecasting of high mountain soil moisture reveals a drastic decrease, despite major uncertainties, *Water Resources Research*, *48*, W04521, doi:10.1029/2011WR011188.

Rössler, O., S. Kotlarski, A. M. Fischer, D. Keller, M. Liniger, and R. Weingartner (2019), Evaluating the added value of the new Swiss climate scenarios for hydrology: An example from the Thur catchment, *Climate Services*, *13*, 1–13, doi:10.1016/j.cliser.2019.01.001.

Schewe, J., J. Heinke, D. Gerten, I. Haddeland, N. W. Arnell, D. B. Clark, R. Dankers, S. Eisner, B. M. Fekete, F. J. Colón-González, S. N. Gosling, H. Kim, X. Liu, Y. Masaki, F. T. Portmann, Y. Satoh, T. Stacke, Q. Tang, Y. Wada, D. Wisser, T. Albrecht, K. Frieler, F. Piontek, L. Warszawski, and P. Kabat (2014), Multimodel assessment of water scarcity under climate change, *Proceedings of the National Academy of Sciences of the United States of America*, *111*, 3245–3250, doi:10.1073/pnas.1222460110.

Schroeer, K., and G. Kirchengast (2018), Sensitivity of extreme precipitation to temperature: The variability of scaling factors from a regional to local perspective, *Climate Dynamics*, *50*, 3981–3994, doi:10.1007/s00382-017-3857-9.

Schulla, J. (1997), Hydrologische Modellierung von Flussgebieten zur Abschätzung der Folgen von Klimaänderungen, Dissertation, Eidgenössische Technische Hochschule Zürich (ETH), Zurich, Switzerland.

Schulla, J. (2019), *Model Description WaSiM (Technical report)*, 376 pp., www.wasim.ch (last access on 2021-07-13), Zurich, Switzerland.

Schürz, C., B. Hollosi, C. Matulla, A. Pressl, T. Ertl, K. Schulz, and B. Mehdi (2019), A comprehensive sensitivity and uncertainty analysis for discharge and nitrate-nitrogen loads involving multiple discrete model inputs under future changing conditions, *Hydrology and Earth System Sciences*, *23*, 1211–1244, doi: 10.5194/hess-23-1211-2019.

Schwarzak, S., S. Hänsel, and J. Matschullat (2015), Projected changes in extreme precipitation characteristics for Central Eastern Germany (21st century, model-based analysis), *International Journal of Climatology*, *35*, 2724–2734, doi:10. 1002/joc.4166.

Seibert, P., A. Frank, and H. Formayer (2007), Synoptic and regional patterns of heavy precipitation in Austria, *Theoretical and Applied Climatology*, *87*, 139–153, doi:10.1007/s00704-006-0198-8.

Sevruk, B., M. Ondrás, and B. Chvíla (2009), The WMO precipitation measurement intercomparisons, *Atmospheric Research*, *92*, 376–380, doi:10.1016/j. atmosres.2009.01.016.

Sharma, T., H. Vittal, S. Chhabra, K. Salvi, S. Ghosh, and S. Karmakar (2018), Understanding the cascade of GCM and downscaling uncertainties in hydro-climatic projections over India, *International Journal of Climatology*, *38*, e178–e190, doi:10.1002/joc.5361.

Singh, R., T. Wagener, R. Crane, M. E. Mann, and L. Ning (2014), A vulnerability driven approach to identify adverse climate and land use change combinations for critical hydrologic indicator thresholds: Application to a watershed in Pennsylvania, USA, *Water Resources Research*, *50*, 3409–3427, doi: 10.1002/2013WR014988.

Singh, S. K., J. Liang, and A. Bárdossy (2012), Improving the calibration strategy of the physically-based model WaSiM-ETH using critical events, *Hydrological Sciences Journal*, *57*, 1487–1505, doi:10.1080/02626667.2012.727091.

Smiatek, G., and H. Kunstmann (2019), Simulating future runoff in a complex terrain alpine catchment with EURO-CORDEX data, *Journal of Hydrometeorology*, *20*, 1925–1940, doi:10.1175/JHM-D-18-0214.1.

Sotier, B., K. Klebinder, A. Eder, P. Strauss, G. Markart, and J. Dorner (2010), Erstellung einer Landnutzungskarte als Grundlage hydrologischer Bewertung, in *Tagungsband: Angewandte Geoinformatik 2010*, p. 9, Salzburg, Austria.

St-Hilaire, A., T. B. M. J. Ouarda, M. Lachance, B. Bobée, J. Gaudet, and C. Gignac (2003), Assessment of the impact of meteorological network density on the estimation of basin precipitation and runoff: A case study, *Hydrological Processes*, *17*, 3561–3580, doi:10.1002/hyp.1350.

Steinschneider, S., S. Wi, and C. Brown (2015), The integrated effects of climate and hydrologic uncertainty on future flood risk assessments, *Hydrological Processes*, *29*, 2823–2839, doi:10.1002/hyp.10409.

Sun, X., R. G. Mein, T. D. Keenan, and J. F. Elliott (2000), Flood estimation using radar and raingauge data, *Journal of Hydrology*, *239*, 4–18, doi:10.1016/S0022-1694(00)00350-4.

Switanek, M. B., P. A. Troch, C. L. Castro, A. Leuprecht, H.-I. Chang, R. Mukherjee, and E. M. C. Demaria (2017), Scaled distribution mapping: A bias correction method that preserves raw climate model projected changes, *Hydrology and Earth System Sciences*, *21*, 2649–2666, doi:10.5194/hess-21-2649-2017.

Syed, K. H., D. C. Goodrich, D. E. Myers, and S. Sorooshian (2003), Spatial characteristics of thunderstorm rainfall fields and their relation to runoff, *Journal of Hydrology*, *271*, 1–21, doi:10.1016/S0022-1694(02)00311-6.

Szcześniak, M., and M. Piniewski (2015), Improvement of hydrological simulations by applying daily precipitation interpolation schemes in meso-scale catchments, *Water*, *7*, 747–779, doi:10.3390/w7020747.

Tetzlaff, D., and S. Uhlenbrook (2005), Significance of spatial variability in precipitation for process-oriented modelling: results from two nested catchments using radar and ground station data, *Hydrology and Earth System Sciences*, *9*, 29–41, doi:10.5194/hess-9-29-2005.

Teutschbein, C., and J. Seibert (2010), Regional climate models for hydrological impact studies at the catchment scale: A review of recent modeling strategies, *Geography Compass*, *4*, 834–860, doi:10.1111/j.1749-8198.2010.00357.x.

Teutschbein, C., and J. Seibert (2012), Bias correction of regional climate model simulations for hydrological climate-change impact studies: Review and evaluation of different methods, *Journal of Hydrology*, *456-457*, 12–29, doi:10.1016/j.jhydrol.2012.05.052.

Tian, Y., and C. D. Peters-Lidard (2010), A global map of uncertainties in satellite-based precipitation measurements, *Geophysical Research Letters*, *37*, L24407, doi:10.1029/2010GL046008.

van Genuchten, M. (1980), A closed-form equation for pre- dicting the hydraulic conductivity of unsaturated soils, *Soil Science Society of America Journal*, *44*, 892–898, doi:10.2136/sssaj1980.03615995004400050002x.

Van Loon, A. F., T. Gleeson, J. Clark, A. I. J. M. Van Dijk, K. Stahl, J. Hannaford, G. Di Baldassarre, A. J. Teuling, L. M. Tallaksen, R. Uijlenhoet, D. M. Hannah, J. Sheffield, M. Svoboda, B. Verbeiren, T. Wagener, S. Rangecroft, N. Wanders, and H. A. J. Van Lanen (2016), Drought in the Anthropocene, *Nature Geoscience*, *9*, 89–91, doi:10.1038/ngeo2646.

Vereecken, H. (1989), Estimating the soil moisture retention characteristic from texture, bulk density, and carbon content, *Soil Science*, *148*, 389–403.

Verworn, A., and U. Haberlandt (2011), Spatial interpolation of hourly rainfall-effect of additional information, variogram inference and storm properties, *Hydrology and Earth System Sciences*, *15*, 569–584, doi:10.5194/hess-15-569-2011.

Vormoor, K., O. Rössler, G. Bürger, A. Bronstert, and R. Weingartner (2017), When timing matters-considering changing temporal structures in runoff response surfaces, *Climatic Change*, *142*, 213–226, doi:10.1007/s10584-017-1940-1.

Wang, H., J. Chen, C. Xu, J. Zhang, and H. Chen (2020), A framework to quantify the uncertainty contribution of GCMs over multiple sources in hydrological impacts of climate change, *Earth's Future*, *8*, e2020EF001602, doi:10.1029/2020EF001602.

Weiß, M. M. (2011), Future water availability in selected european catchments: A probabilistic assessment of seasonal flows under the IPCC A1B emission scenario

using response surfaces, *Natural Hazards and Earth System Sciences*, *11*, 2163–2171, doi:10.5194/nhess-11-2163-2011.

Wilby, R. L. (2010), Evaluating climate model outputs for hydrological applications, *Hydrological Sciences Journal*, *55*, 1090–1093, doi:10.1080/02626667.2010.513212.

Wilby, R. L., and I. Harris (2006), A framework for assessing uncertainties in climate change impacts: Low-flow scenarios for the River Thames, UK, *Water Resources Research*, *42*, W02419, doi:10.1029/2005WR004065.

Willkofer, F., F.-J. Schmid, H. Komischke, J. Korck, M. Braun, and R. Ludwig (2018), The impact of bias correcting regional climate model results on hydrological indicators for Bavarian catchments, *Journal of Hydrology: Regional Studies*, *19*, 25–41, doi:10.1016/J.EJRH.2018.06.010.

Wong, W. K., I. Haddeland, D. Lawrence, and S. Beldring (2016), *Gridded 1 x 1 km climate and hydrological projections for Norway (Report No 59)*, 26 pp., Norwegian Water Resources and Energy Directorate, Oslo, Norway.

Xu, H., C.-Y. Xu, H. Chen, Z. Zhang, and L. Li (2013), Assessing the influence of rain gauge density and distribution on hydrological model performance in a humid region of China, *Journal of Hydrology*, *505*, 1–12, doi:10.1016/J.JHYDROL.2013.09.004.

Yira, Y., B. Diekkrüger, G. Steup, and A. Bossa (2016), Modeling land use change impacts on water resources in a tropical West African catchment (Dano, Burkina Faso), *Journal of Hydrology*, *537*, 187–199, doi:10.1016/j.jhydrol.2016.03.052.

Yuan, X., M. Zhang, L. Wang, and T. Zhou (2017), Understanding and seasonal forecasting of hydrological drought in the Anthropocene, *Hydrology and Earth System Sciences*, *21*, 5477–5492, doi:10.5194/hess-21-5477-2017.

Zeng, Q., H. Chen, C.-Y. Xu, M.-X. Jie, J. Chen, S.-L. Guo, and J. Liu (2018), The effect of rain gauge density and distribution on runoff simulation using a lumped hydrological modelling approach, *Journal of Hydrology*, *563*, 106–122, doi:10.1016/J.JHYDROL.2018.05.058.

Zhang, X., and R. Srinivasan (2009), Gis-based spatial precipitation estimation: A comparison of geostatistical approaches, *Journal of the American Water Resources Association*, *45*, 894–906, doi:10.1111/j.1752-1688.2009.00335.x.

Research on catchment hydrology related to climate change improves the understanding of changes and their impacts on environment and society. Under climate change, extreme events like heavy precipitation events and droughts tend to increase in frequency and intensity. I studied sensitivities and uncertainties of hydro-climatic changes in response to runoff and other water-balance quantities with the hydrological model WaSiM. The thesis work involved: 1) Simulating hydrological responses to changes in climate, land use, and water management (low-flow focus); 2) examining the influence of precipitation station density and interpolation schemes on runoff during heavy rainfall events; and 3) assessing the value of high-resolution climate data sets (ÖKS15) in hydrological impact studies.
The prealpine Raab catchment in southeastern Austria served as the main focal area (complemented by an alpine catchment). The area is well-known for heavy precipitation events and summer dryness, and has a good data availability.
The comprehensive sensitivity and uncertainty analyses yielded the following results: The Raab catchment will be vulnerable to summer dryness in the future. Non-climatic drivers have lower impacts on the water balance than climate drivers, but can counteract other changes. The reliable precipitation station density depends strongly on the event, catchment, and station distribution in heavy precipitation events. The evaluated Austrian ÖKS15 high-resolution climate data sets are suitable for hydrological impact studies with some limitations.
Overall, I could clearly identify how uncertainty affects assessments of climate change and precipitation events. Climate change is a key driver in hydrological changes, but other non-climatic drivers (i.e., land use or water management changes) should also be analyzed. Extreme precipitation events should be studied together with runoff to evaluate the impacts of such events on the environment and society more effectively.

Wissenschaftliche Forschung im Bereich von Hydrologie und Klimawandel trägt zu einem besseren Verständnis von möglichen Veränderungen und deren Einfluss auf Umwelt und Gesellschaft bei. Extremereignisse wie Starkregen und Dürren nehmen im Zuge des Klimawandel tendenziell an Häufigkeit und Intensität zu. Die Sensitivitäten und Unsicherheiten von hydro-klimatischen Veränderungen des Abflusses und anderen Wasserbilanzgliedern untersuchte ich mit Hilfe des hydrologischen Modells WaSiM. Die Schwerpunkte dieser Arbeit wurden gelegt auf: 1) Simulation von Klima-, Landnutzungs- und Wassermanagementänderungen bei Niedrigwasser; 2) Einfluss von Niederschlagsstationsdichte und -Interpolationsverfahren auf den Abfluss bei Starkregen; und 3) der Wert hochaufgelöster Klimadatensätze (ÖKS15) für hydrologische Studien.
Schwerpunktregion ist das voralpine Raab Einzugsgebiet im Südosten Österreichs (ergänzt durch ein alpines Einzugsgebiet). Diese Region ist bekannt für Starkregen und sommerliche Trockenheit und bietet eine gute Datenlage. Die Ergebnisse dieser Sensitivitäts- und Unsicherheitsanalysen beinhalten, dass das Raabtal in Zukunft besonders Trockenheitsgefährdet ist. Auch wenn nichtklimatische Faktoren einen geringeren Einfluss auf die Wasserbilanz haben, sind diese Faktoren auf Grund von Wechselwirkungen nicht zu vernachlässigen. Die notwendige Niederschlagsstationsdichte ist bei Starkregenereignissen stark ereignis-, einzugsgebiets- und stationsabhängig. Die ausgewerteten ÖKS15 Klimadatensätze sind für hydrologische Impaktstudien mit einigen Einschränkungen geeignet.
Insgesamt wurde die Bedeutung von Unsicherheiten in Bezug auf Klimawandel und Niederschlag deutlich. Im Kontext der Hydrologie sollten die klimatischen und nicht klimatischen Treiber (u.a. Landnutzungsänderungen) des Klimawandels zusammen analysiert werden. Extremniederschläge sollten zusammen mit Abflüssen untersucht werden, um deren Auswirkungen auf Umwelt und Gesellschaft besser einschätzen zu können-

SR 99 | 2023 Sensitivity and uncertainty analysis of hydro-climatic changes in south-east Alpine foreland catchments
Wegener Center Verlag, University of Graz, Austria. ISBN 978-3-9504700-8-6